DANISH
TECHNOLOGICAL
INSTITUTE

Test of PowerShades and calibration of models of PowerShades

Technological Insitute

Test of PowerShades and calibration of models of PowerShades

Søren Østergaard Jensen
Centre for Refrigeration and Heat Pump Technology
Technological Institute

November 2008

Preface

This report describes the results from measurements in two test rooms – one with PowerShades in the windows, the results from calibration of a computer model of the test rooms and the results from simulation of the thermal performance of a real building with PowerShades. The work performed is part of the project "PowerShades – Development and pilot demonstration of new transparent photo voltaic module" project no. 2006-1-6322 financed by Energinet.dk.

The following persons have participated in this part of the project:

Søren Østergaard Jensen, M.Sc., Danish Technological Institute
Alicia Johanson, M.Sc., PhotoSolar Aps
Eik Bezzel, M.Sc., PhotoSolar Aps

Test of PowerShades and calibration of models of PowerShades
1st printing, 1st edition, 2008

Industry and Energy division

ISBN: 87-7756-770-6
ISSN: 1600-3780

List of contents

1. Introduction

PowerShades consist of an opaque solar cell material with holes which partly let the solar radiation through. Dependent on the design of the holes direct solar radiation from specific incidence angles can be screened off while solar radiation from other directions are allowed to pass as shown in figure 1.1. The PowerShades are aimed to be installed in the glazing of traditional windows.

PowerShades will typically be designed to shade off the direct solar radiation during midday when the sun is high in the sky and when the risk of overheating of the building due to solar radiation is high. Figure 1.2 shows an example of the progressive shading due to PowerShades.

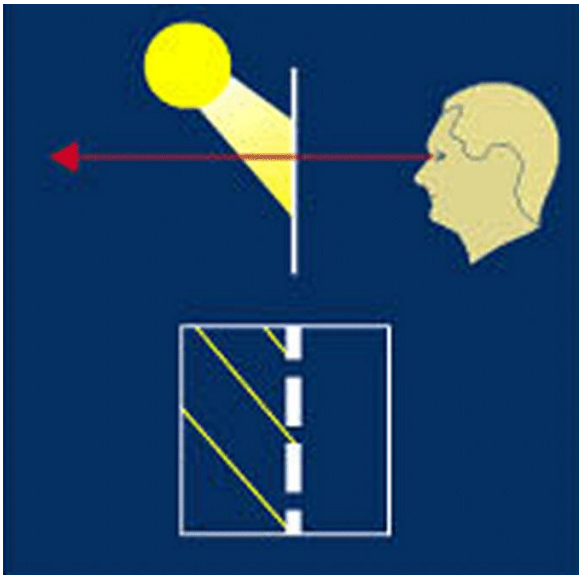

Figure 1.1 The principle of the solar shading feature of PowerShades.

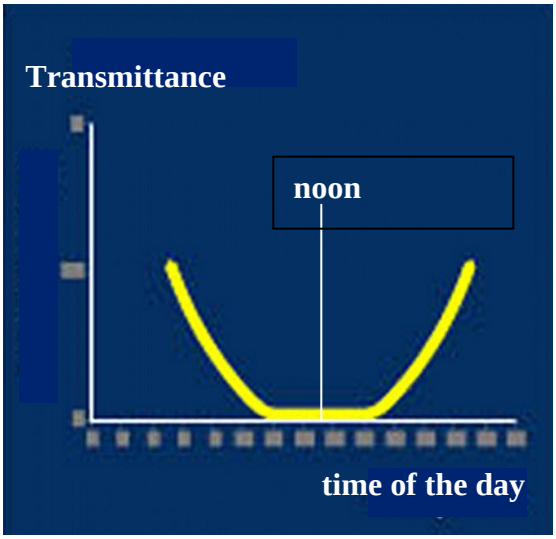

Figure 1.2 Progressive solar shading of direct solar radiation over the day due to the angle selectivity of the PowerShades.

PowerShades were theoretically investigated in the project "Transparent solar cells – the electricity producing solar shading of the future" (Technological Institut, 2005). The thermal behaviour of PowerShades was investigated using the simulation program ESP-r (ESRU, 2001). A new module for dealing with the angle selectivity of PowerShades was developed for ESP-r. ESP-r was used to investigate different designs of PowerShades and to compare the thermal behaviour of PowerShades with traditional forms of solar shading. A building with PowerShades in the south facing windows was modelled. Further the simulations were carried out for three locations in Europe: Copenhagen (DK), Munich (D) and Palermo (I).

The conclusion from the simulations was that PowerShades perform better than solar shading glass (with a g-value of 0.35) and as well as a highly efficient external shading (with an overall g-value of 0.17). However, these results are based on simulations using a novel module of ESP-r including calculated optical properties of the PowerShades. There was, therefore, a need for verification of the simulation model using measurements from a building with PowerShades mounted in the windows and exposed to real weather conditions.

Simulations and measurements could be compared with PowerShades mounted in real buildings. This will give a good subjective impression of the performance of PowerShades – and has been done as part of the project (Powershades have been installed in a meeting room at PhotoSolar and in the laboratory containing the test rooms where the thermal performance of PowerShades is measured). But for purpose of verification of a computer model real buildings are too undefined and uncontrolled. The uncertainty of the measurements is far too high to be used for verification of a model. There is a need for a much more well defined, well controlled yet realistic environment for test of the PowerShades.

Based on the experience from the PASSYS project (Jensen et al, 1994) it was decided to go for side-by-side comparison using test rooms. (Jensen, 2008a) describes in details the two almost identical test rooms which has been erected at the Danish Technological Institute for the purpose of obtaining high quality data for the purpose of calibrating a ESP-r model of the test rooms including PowerShades.

1.1. Test rooms

This section only contains a brief description of the test rooms. For at more thorough description please see (Jensen, 2008a) where details on the thermo-physical properties of the test room and on the measuring system are given.

The two test rooms are located in a laboratory at the Danish Technological Institute in Taastrup a little West of Copenhagen. Figure 1.1 shows a plan over the Danish Technical Institute with the building hosting the test rooms and an indication of the location of the test rooms within the building. Figure 1.1 shows that the facades of the test rooms are facing nearly south – more precisely 13° from south towards west.

Figure 1.2 shows a principle sketch of the test rooms situated in the laboratory. Test room B shares as shown a wall with the room besides the laboratory hosting the test rooms. Figure 1.3 shows a picture of the laboratory before erection of the test rooms. The door at the back walls (the shared wall of test room B) has been removed, and the doorway closed by materials almost identical to the existing wall.

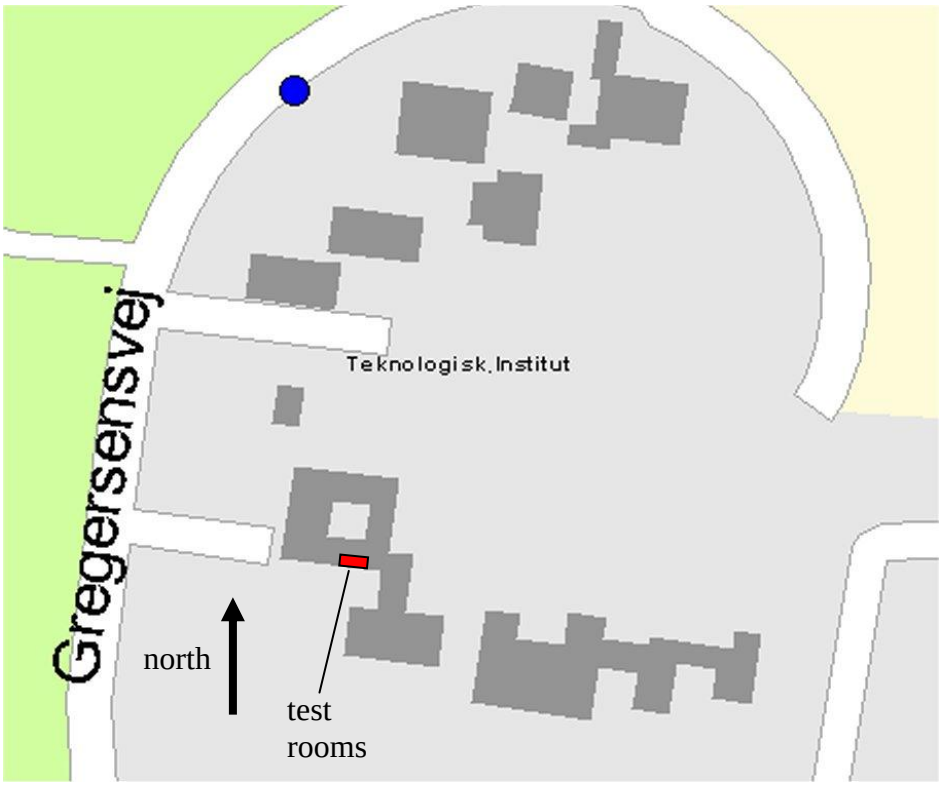

Figure 1.1. The location of the test rooms at the Technological Institute.

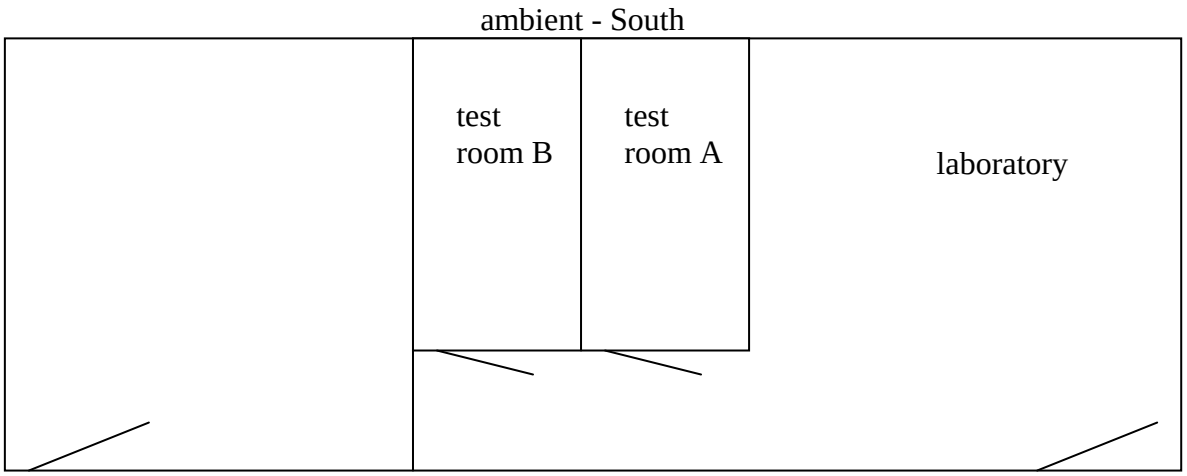

Figure 1.2. Principle sketch of the location of the test rooms within the laboratory.

The aim was to make the two test rooms as identical as possible, and they are except for the following things:

1) the east wall in room B. This wall is slightly different from the other walls of the test rooms. All internal walls are made of sectional bars giving a space of 70 mm with mineral wool in between and gypsum plates on both sides. The east wall has two gypsum plates on both sides while the others only have one. The east wall only have 50 mm of

mineral wool in the gap between the gypsum plates instead of 70 mm as the other walls. This gives a slight difference in air temperature as discussed in (Jensen, 2008a).

2) the rooms are inverted with respect to the façade as shown in figure 1.4. The two windows are identical for the two test rooms, but while in test room A the smallest window which can open is located to the west it is located to the east in test room B. Further the column between the windows (figure 1.5) will create shading in the morning in test room A and in the afternoon in test room B.
3) due to the building situated to the east of the building with the test rooms - see figures 1.1 and 1.4 - the shading on the facades of the two test rooms is different in the morning at low sun angles.

The above differences will create differences in the measurements for the two rooms, however, the same discrepancies can be created in the simulations, so this should not give raise to major difficulties. When looking solemnly at the measured data the physical differences should be remembered as the observed discrepancies else may give rise to confusion.

Figure 1.3. The laboratory before the two test rooms was installed.

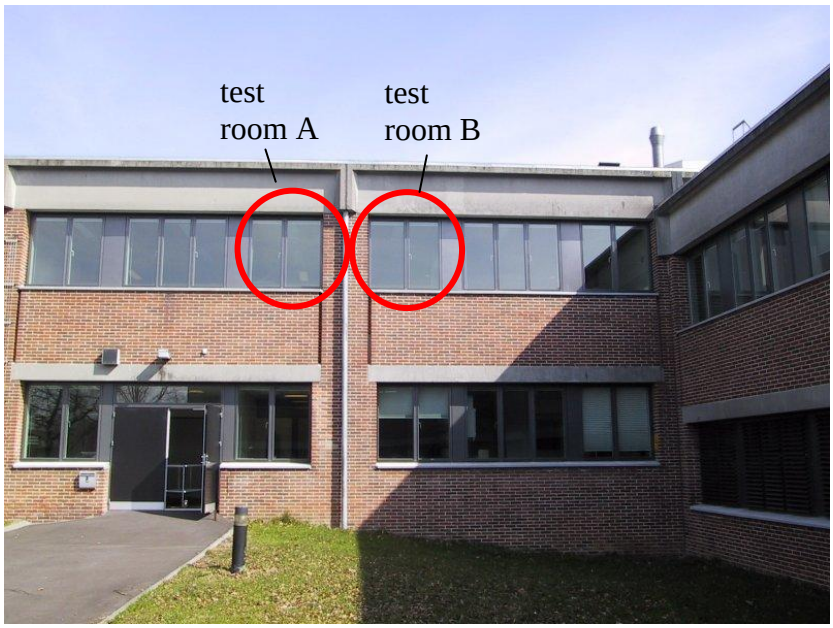

Figure 1.4. Façade of the rest rooms. The red circles show the windows of the two test rooms.

Figure 1.5. The column in the façade between the two test rooms.

1.1.1. The dimensions of the test room

The dimensions of the two test rooms are almost identical. Figure 1.6 shows the dimensions of the test cells. The internal floor area and volume of the test cells are thus:

	area	volume
Test room A	6.83 m²	16.70 m³
Test room B	6.85 m²	16.76 m³

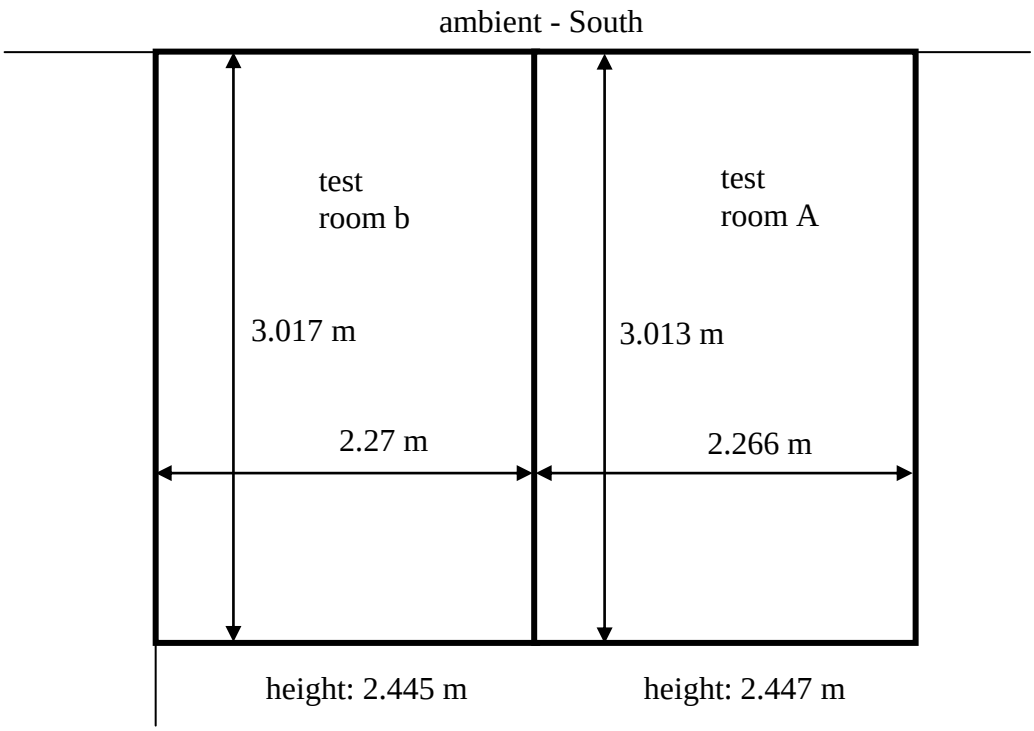

Figure 1.6. The dimensions of the test rooms.

The test rooms are as seen in figure 1.6 almost identical with regards to the dimensions.

1.1.2. Windows of the test rooms

The most important feature of the test rooms is of course the windows.

The windows from the 70'ies were in 2005 replaced with new windows from the Danish firm Velfac. As the products at Velfac are traceable it was easy to obtain the properties of the windows

The windows in the two test rooms are identical. The windows consist in each test room of two slightly different window panes mounted in a common frame with a bar between the two window pans as seen in figure 2.1. The smaller of the windows can be opened while the large is fixed. The hole in the wall is 1.57 x 1.58 = 2.48 m², while the total transparent area is 1.98 m²

Velfac gives the following properties for the windows (Velfac sun 1/clear):

Outside 6 mm glass with low e-coating, cavity of 14 mm filled with Argon and inside 4 mm glass one with sun screening coating.

Centre U-value for the glazing:	1.1 W/m²K
U-value for the framing:	3.1 W/m²K
Edge loss coefficient between glazing and framing:	0.058 W/mK

Optical properties of the glazing:

Light transmission:	67 %
Light reflectance	
outside:	11 %
inside:	12 %
UV-transmittance:	5 %
Solar direct transmittance:	34 %
Solar direct reflectance:	31 %
Solar direct absorptance	
outside pane:	34 %
inside pane:	1 %
Solar factor (g-value):	37 % - ie the window has a solar screening coating

1.1.3. PowerShades vs MicroShades

PowerShades are as explained earlier semi transparent solar cells with an intelligent micro structure which is designed to screen off the direct solar radiation at certain incidence angles. MicroShades have the same micro structure as PowerShades but are not coated with solar cells. So there is no real difference between the two products with regard to the transmission of solar radiation and daylight. The only difference being the part of the screened off solar radiation which is transformed to electricity in PowerShades. Approximately 5% of the solar radiation hitting a window with PowerShades will be transformed to electricity. This means that the PowerShades themselves will be a little less warm than MicroShades.

However, due to the fact that PowerShades and MicroShades may get rather hot (up to 70°C) they have to be installed in the outer layer of a low energy window. If they were installed in the inner layer of the window they would lead to tremendous indoor climate problems.

As PowerShades and MicroShades have to be installed in the outer layer of a low energy window the difference in heating of the two products will have no noticeable influence on the indoor climate behind the window as shown in (Jensen, 2008b).

As PowerShades at this moment hasn't been developed to a stage where production of prototypes is possible and due to the fact that it makes no difference for the indoor climate MicroShades have been tested in the test room instead of PowerShades. However, due to the name of the project the tested MicroShades will in this report be referred to as PowerShades.

2. Tests

The test rooms and the measuring system were erected/installed during the summer and autumn of 2006. The measuring system was only fully operational by the end of 2006. During the period September 2006 – April 2008 several window systems have been tested.

Period	test room A	test room B
Until October 11, 2006	Velfac sun 1/clear	Velfac sun 1/clear
October 11, 2006 – October 22, 2007	PS4060	- Velfac sun 1/clear - Velfac sun 1/clear + external solar screening from Faber - Velfac sun 1/clear + computer curtains
October 22, 2007 ->	Prototype 1	Velfac sun 1/clear

Table 2.1. The window systems tested in the windows of the two test rooms.

2.1. Velfac sun 1/clear

The original windows from Velfac is already described in details in section 1.1.2. Figure 2.1 shows a picture of this window.

Figure 2.1. The original Velfac sun 1/clear window.

During several periods in 2007 a solar screening system from Faber was mounted in front of the Velfac window in test room B – mainly for daylight measuring purposes. The Faber solar screening system consists of external lamellas with a width of 80 mm, tilted 44° and installed with at distance of 75 mm. A picture of this system is shown in figure 2.2.

Figure 2.2. The Faber solar screening system.

Due to the fact that the Faber system screens off most of the light, which is shown in the following chapter tests were carried out where each second of the lamellas were removed as seen in figure 2.3.

Figure 2.3. The Faber solar screening system with only half the number of lamellas.

2.2. PS4060

On October 11, 2006 the original windows of test room A were replaced with windows with PowerShade foil between two glasses forming the outer layer of a low energy window as seen in figure 2.4.

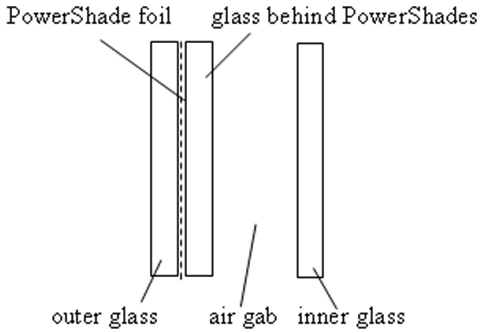

Figure 2.4. The design of the PowerShade window.

Optical properties at an incidence angle of 0°:

Transparent area of the PowerShade foil:	52%
Total transmittance through PowerShades incl. glasses:	26%
Solar height where the direct solar radiation is totally cut off:	64.4°
The centre U-value of the window is as for the Velfac window:	1.1 W/m²K
The framing and edge losses is identical to the Velfac window	

The PowerShade foil were produced as approx. A4 sized pieces and mounted between two layers of glass.

Figure 2.5 shows a photo of the window with PS4060.

Figure 2.5. The PS4060 PowerShade.

Compared to the computer curtain and the Faber solar shading system the outlook though PS4060 is much better as it is easier to recognize objects outside the window. The outlook is more like the outlook through the original Velfac window – figure 2.1 but somewhat misty compared to the Velfac window.

2.3. Prototype 1

On October 22, 2007 the windows with PS4060 of test room A were replaced with windows with a new PowerShade foil again between two glasses forming the outer layer of a low energy window.

Optical properties at an incidence angle of 0°:

Transparent area of the PowerShade foil:	64%
Total transmittance through PowerShades incl. glasses:	35%
Solar height where the direct solar radiation is totally cut off:	68°
The centre U-value of the window is as for the Velfac window:	1.1 W/m²K
The framing and edge losses is identical to the Velfac window	

Figure 2.6 shows a picture of Prototype 1. These PowerShades are made of stripes of foil where 56.5 mm is PowerShades and 3.5 mm is opaque foil for mounting purposes. The PowerShade is mounted between two layers of glass. The above transparent area and total transmittance are including the opaque areas. So the PowerShades in Prototype 1 is of a more open structure than PS4060 allowing more solar radiation and daylight getting into the room.

Figure 2.6. The Prototype 1 PowerShade.

Prototype 1 has almost the same screening effect as the Faber solar screening with half the number of lamellas – figure 2.3 – see the next chapter. However, there is a much better out-

look through Prototype 1. The outlook is as for PS4060 somewhat similar to the outlook through the original window – figure 2.1 - but a bit misty.

2.4. Prototype 2

On March 6, 2008 the original windows in the laboratory containing the test rooms were replaced with windows with a new PowerShade foil again between two glasses forming the outer layer of a low energy window.

Optical properties at an incidence angle of 0°:

Transparent area of the PowerShade foil:	66%
Total transmittance through PowerShades incl. glasses:	36%
Solar height where the direct solar radiation is totally cut off:	68°
The centre U-value of the window is as for the Velfac window:	1.1 W/m²K
The framing and edge losses is identical to the Velfac window	

Figure 2.7 shows a picture of Prototype 2. The main difference between prototype 1 and 2 is that the distance between the opaque areas of the foil now is 137 mm and the width of the opaque stripes is 3 mm. The PowerShade is mounted between two layers of glass.

Figure 2.7. The Prototype 2 PowerShade.

3. Daylight factors

One of the purposes of installing the PowerShades in rooms of real room size was to be able to evaluate the influence of the PowerShades on the daylight conditions within a room behind the powerShades.

The dimensions of the test rooms are given in figure 1.6. The colour of the walls except the façade is light grey while the colour of the façade internally, the ceiling and the entrance door is white. The colour of the floor is brown. For more details please refer to (Jensen, 2008a).

Daylight factors are obtained in the following way: the horizontal Lux is measured in the room at a height of 0.7 m. At the same time the horizontal Lux on the roof without shading is measured. The measurements have to be conducted during cloudy conditions without any direct solar radiation. The daylight factor is the Lux in the room divided by the Lux at the roof and multiplied with 100. The unit is %.

Further the Lux meter in the room has been traversed through the room from the window to the back of the room.

The following daylight measurements have been conducted:

Daylight measurements	test room A	test room B
1	PS4060	Velfac sun 1/clear
2	PS4060	Computer curtains
3	PS4060	Velfac sun 1/clear + external solar screening from Faber
4	PS4060	Velfac sun 1/clear + external solar screening from Faber with half number of lamellas
5	Prototype 1	Velfac sun 1/clear

Table 3.1. The daylight measurements conducted in the test rooms.

The daylight factors may vary due to different sky conditions between the measurements and can, therefore, not be compared directly. Instead the daylight factors for the different measurements have been normalized based on measurement number 1 in table 3.1. The result is shown in figure 3.1.

- the Velfac window with computer curtain and with full Faber solar shading have the lowest and identical daylight factors
- PS4060 has the second lowest daylight factors
- Prototype 1 and Velfac window with half Faber solar shading have the second highest and almost identical daylight factors – this was anticipated as these two systems have similar screening effect
- the Velfac window without screening has the highest daylight factors

The daylight factor should preferably be above 2%. This is only achieved all through the room by the Velfac window, however, with a very high daylight factor at the window. The other windows lead to a more even daylight factor throughout the room. Two of them have daylight factor above 2% during half of the room. The two systems with the lowest daylight

factors will lead to a high electricity demand for artificial lightning – however, this will often not be the case with computer curtains, as they are pulled up when no direct sunlight is disturbing screen work.

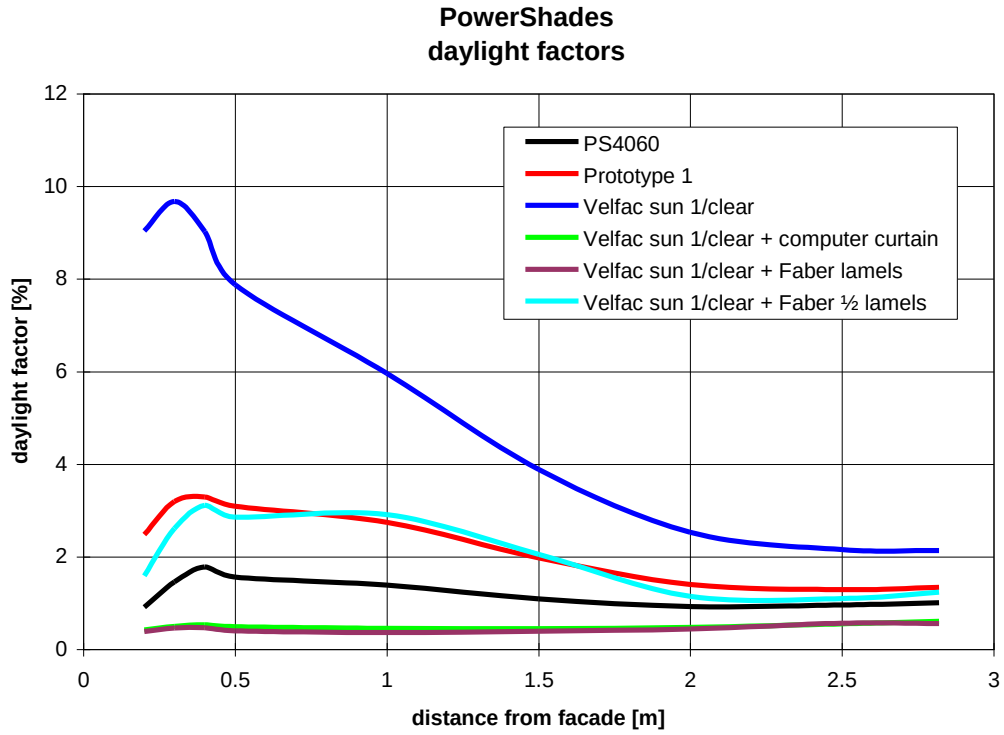

Figure 3.1. Daylight factors in the test rooms with different screening systems.

4. Measurements

The measuring system was gradually put into operation during the autumn of 2006. The temperature sensors were already in operation in august 2006 while the solar measuring station at the top of the building first was fully operational by the end of 2006. 2006 was mainly utilized for calibration of the measuring system.

Some difficulties have of course been experienced which is natural for such large measuring system. It took e.g. a while to stabilize the Lux meters – the measuring system made the hang. After a while this was solved by putting a small capacity in parallel with the Lux meters. Some temperatures have for shorter periods been malfunctioning and shorter power cuts have been experienced – however, the measuring system has an auto boot function and will thus restart when the power is back so the latter has only given reason to minor lack of data in the measurements. All in all these problems has not led to loss of important data.

The measuring system has run without major problems from the start in august 2006 until now – end of 2008 and is foreseen to run until spring 2010 as the present project has a successor.

The PS4060 PowerShades were as seen in table 2.1 installed in room A on October 11, 2006 and replaced with Prototype 1 on October 22, 2007. 2006 was thus dedicated to obtain measurements for calibration of the computer model with the model of PS4060. Extensive calibration exercises were carried out on the collected data from 2006. However, it was impossible to obtain agreement between measurements and calculations no matter which changes were introduced to the model. At the end it was concluded that it was not possible to create a model of PS4060 due to too large uncertainties in the manufacturing of the solar screening foil of PS4060. PS4060 was one of the first batches of PowerShades and the etching technique was at that stage not sufficiently precise. For that reason the calibration using PS4060 was stopped. The calibration of the model has instead been carried out using measurements with Prototype 1 – this is described in the following chapter.

However, the measurements from PS4060 are not wasted. They cannot be used for calibration but may still be used to show the difference between PowerShades and the original Velfac sun 1/clear windows with and without external shading. This is done in the following. But firstly there is a need to determine how well the two test rooms are matched – ie do they perform identical with identical windows in the façade.

4.1. Matching the test rooms

The two test rooms are as described in section 1.1 almost identical except for the mirroring and that one of the internal walls of test room B is different from the other internal wall of both test rooms. So before comparing the performance of the test rooms with different shading systems it is important to know how the differences influence the air temperatures in the two test rooms. This has been done in (Jensen, 2008a). In (Jensen, 2008a) is also investigated all 10 air temperatures of the two test rooms so here will only the mean air temperature of the test rooms be shown. For more details please refer to (Jensen, 2008a).

Figure 4.1 shows the mean air temperatures of the two test rooms for at sunny period in September 2006 (September 12-18).

Figure 4.2 shows the solar radiation on the windows and the ambient temperature.

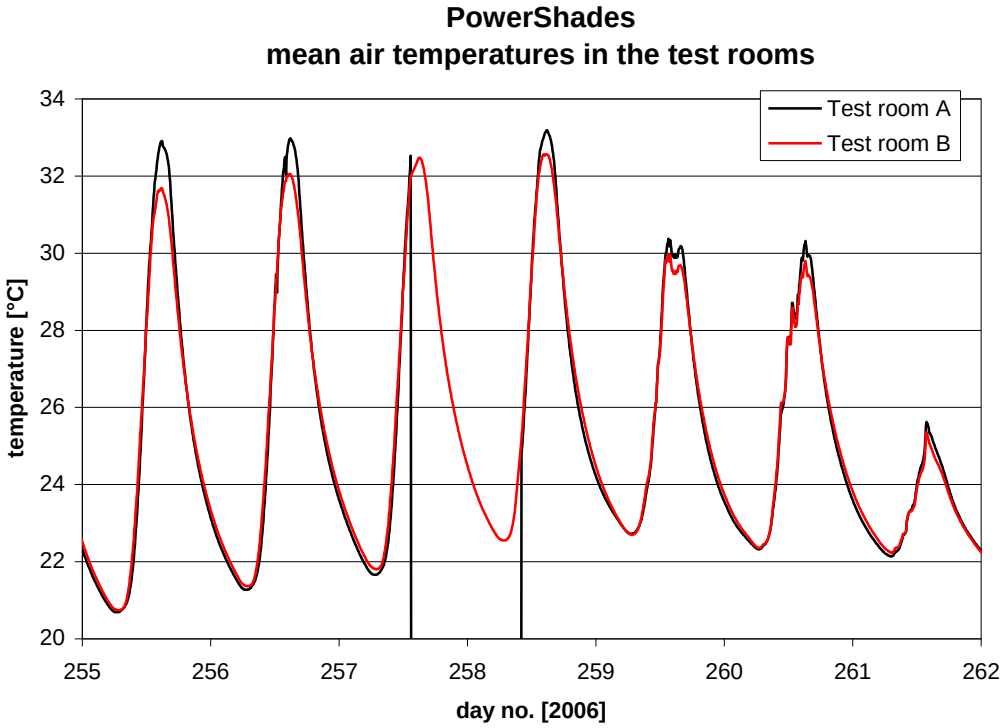

Figure 4.1. The mean air temperature of the two test rooms – September 12-18, 2006. There were unfortunately losses of data for room A for a period of approx. one day.

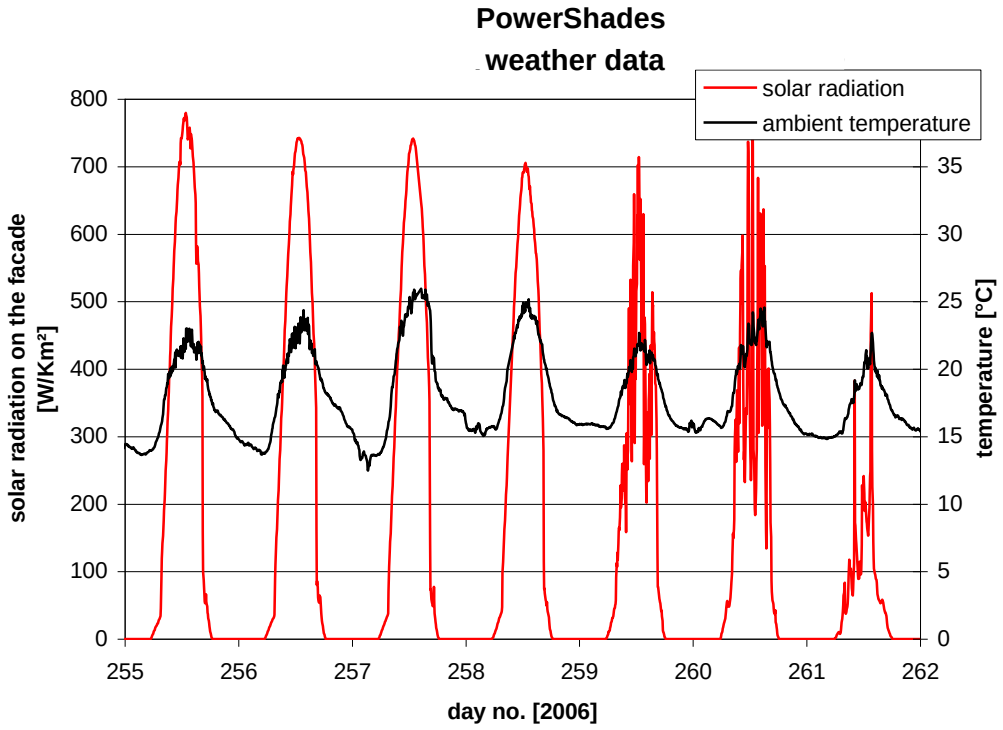

Figure 4.2. The ambient temperature and solar radiation on the façade – September 12-18, 2006.

Figure 4.1 shows that there is a good match between the two mean air temperatures during the nights and during periods with low solar radiation, while there is a difference between 0,5-1,3 K during periods with high solar radiation. In (Jensen, 2008a) it is shown that the solar radiation to the two rooms are identical during main part of the day – except for some differences regarding shading during the morning and evening. This latter is, however, of minor importance.

Except for being inverted the main differences between the two test cells is the wall of room B facing the room next to the laboratory containing the two test cells. This wall has two layers of gypsum plates and less insulation than the rest of the internal walls of the test rooms. This effect has been evaluated using the model of the test rooms developed in the simulation program ESP-r (ESRU, 2001). The evaluation can, however, not be done for the period shown in figure 4.1-2 as the solar measuring station for measuring global and horizontal diffuse radiation was not installed during this period. Instead a period in March 2007 (March 22-28) with almost the same solar height as for figure 4.1-2 was chosen – here, however, the air temperatures cannot be compared, as PowerShades were installed in test room A. Simulations were performed with one and two gypsum plates in the diverging wall of test room B. The simulations showed (Jensen, 2008a) that the extra gypsum plate reduces the peak in the mean air temperature in room B with approx 0.5 K.

So the difference in the test rooms can mostly be accounted for in the simulations, but looking at the measurements the difference in mean air temperature from figure 4.1 should be remembered and accounted for.

4.2. PS4060 vs. Velfac sun 1/clear

Two periods have been chosen for display of the function of the PS4060 PowerShades:

Season	period	solar height °
Spring	21/3-3/4 2007	34.8-40.3
Summer	8/6-18/6 2007	57.2-57.8

Table 4.1. Shown periods with PS4060 in test room A and Velfac sun 1/clear in test room B.

The reason why only a spring and summer period is shown is that the temperature in the test rooms was kept at approx. 21°C using the heaters in the test room – as seen in figure 4.4. During the winter the sun was not able to rise the temperature of the test room above 21°C.

Figure 4.3 shows the weather conditions during March 21-April 3, 2007. Figure 4.3 shows a very sunny period with ambient temperatures varying between 2 and 21°C. Figure 4.4 shows the mean air temperatures in the two test rooms for the considered period.

From figure 4.4.it is seen that during night time the temperatures of the test rooms are kept around 21°C. During overcast conditions the air temperatures stays at around 21°C, while during sunny conditions the solar radiation is able to increase the air temperature with up to 10 K. Figure 4.4 further shows that PS4060 decreases the peak temperature level with approx. 2 K which with the findings from sections 4.1 actually means a reduction of around 3 K.

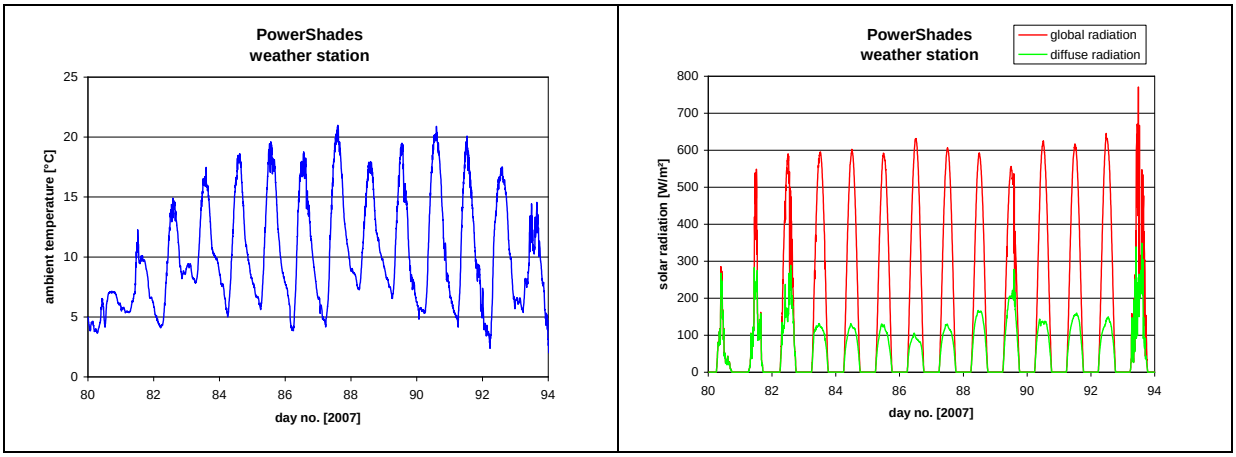

Figure 4.3. The weather conditions during the spring period - March 21-April 3, 2007.

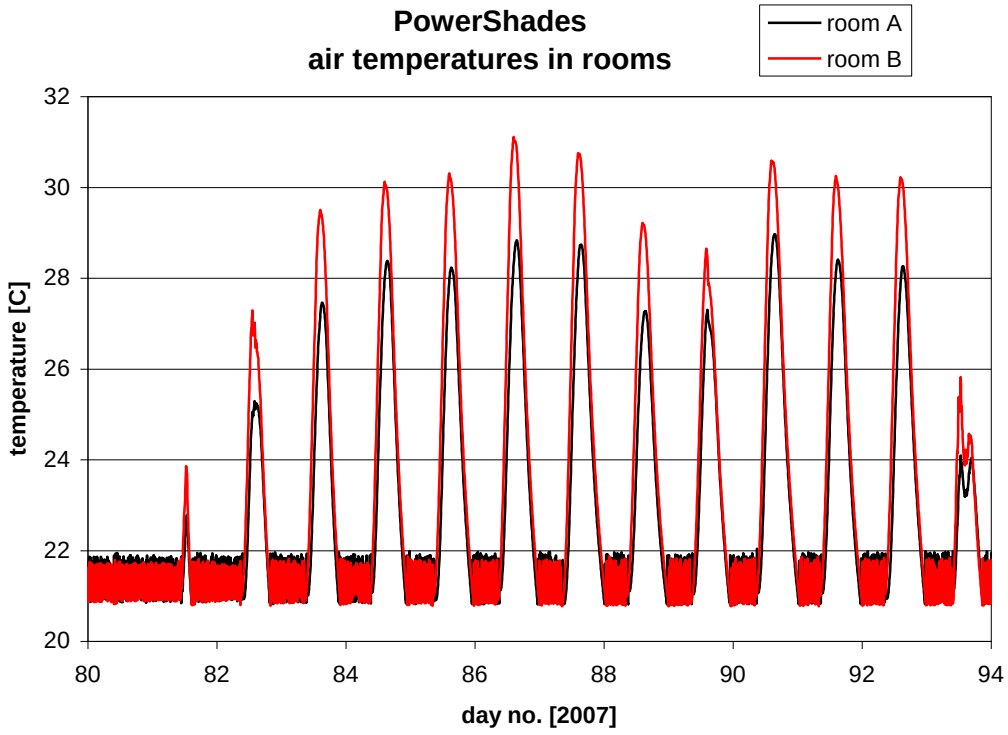

Figure 4.4. The measured mean air temperature of the two test rooms - March 21-April 3, 2007.

The higher peak air temperature of test room B is due to more incoming solar radiation to this room as shown in figure 4.5. At peak the Velfac windows lets up to 140 W or 130 % more solar radiation into the room than PS4060.

Figure 4.6 shows the weather conditions during June 8-18, 2007. Figure 4.6 shows a very sunny period with ambient temperatures varying between 12 and 35°C. Figure 4.7 shows the mean air temperatures in the two test rooms for the considered period, while figure 4.8 shows the solar radiation entering the two test rooms.

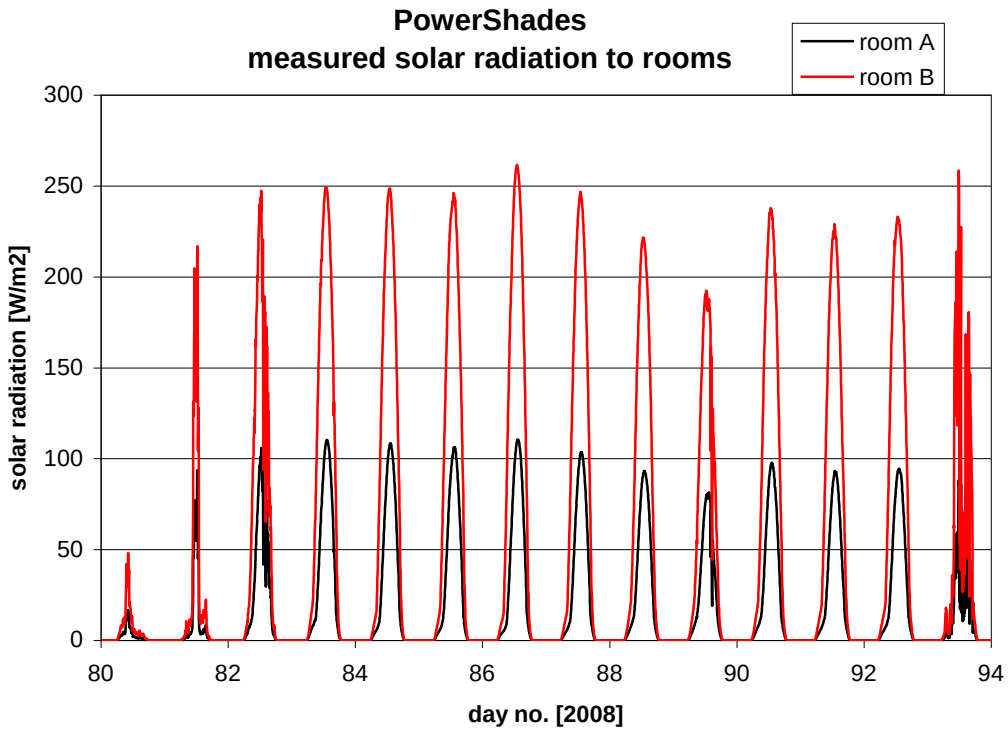

Figure 4.5. Measured solar radiation entering the two test rooms - March 21-April 3, 2007.

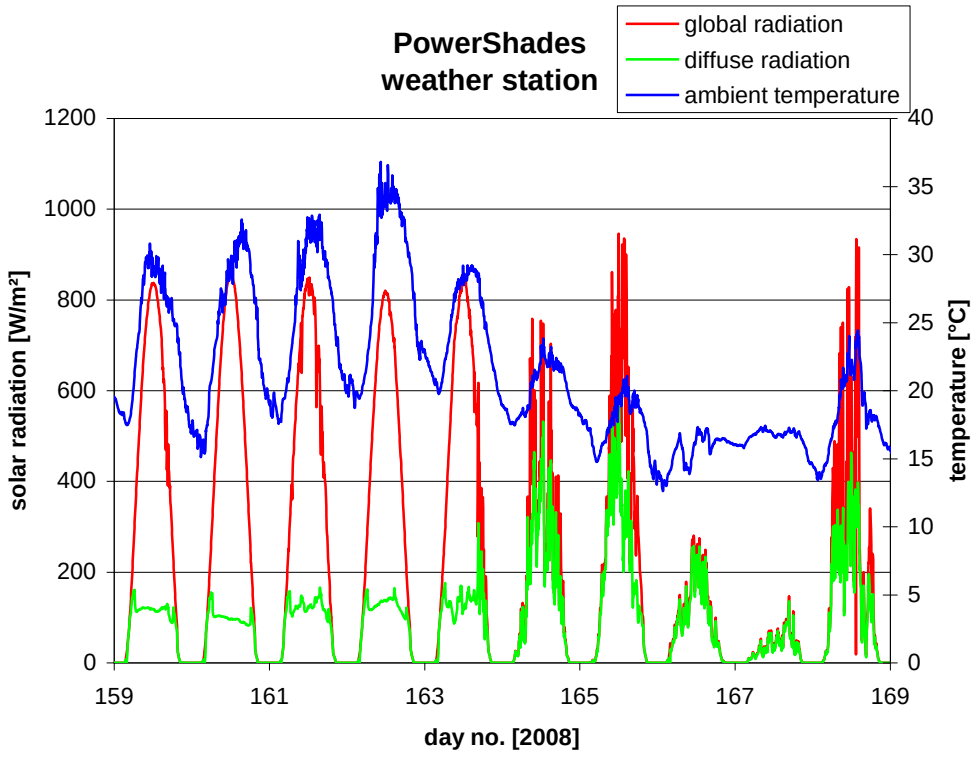

Figure 4.6. The weather conditions during the spring period – June 8-18, 2007.

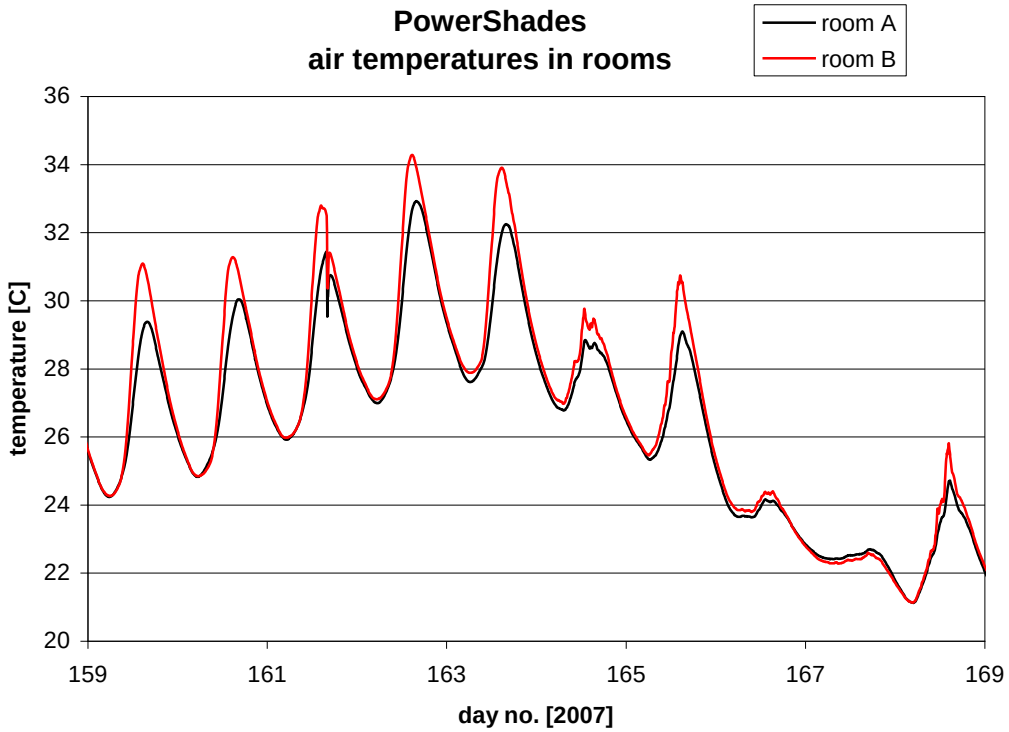

Figure 4.7. The measured mean air temperature of the two test rooms – June 8-18, 2007.

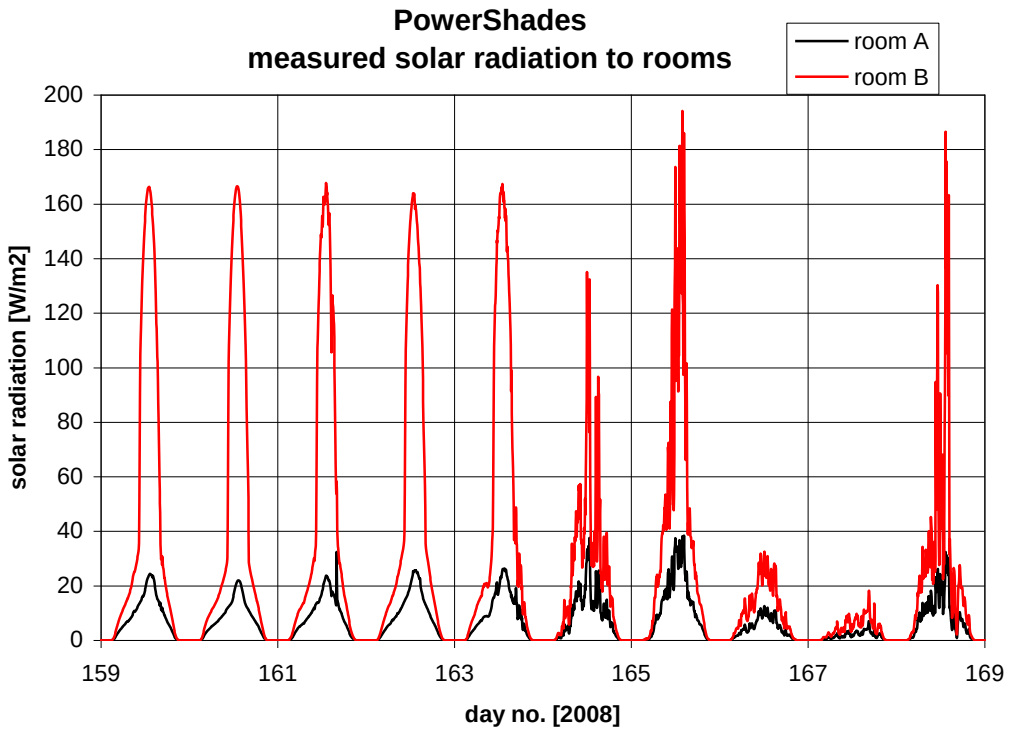

Figure 4.8. Measured solar radiation entering the two test rooms – June 8-18, 2007.

Again PS4060 reduces the peak room air temperature with up to around 2 K, which again with the findings from sections 4.1 actually means a reduction of around 3 K.

The 2 K difference in both spring and summer is as seen when comparing figure 4.5 and 4.8 obtained with a difference in peak solar radiation through the two windows of approx. 140 W/m².

The peak value of solar radiation entering room B is due to the larger solar height reduced from 250 W/m² in figure 4.5 to 170 W/m² in figure 4.8 – i.e. a reduction of 33%. However, the peak solar radiation through PS4060 has been reduced from 110 W/m² to 25 W/m² - ie a reduction of 77%. This clearly illustrates the selective screening effect of PowerShades: increased screening at larger solar heights.

4.3. PS4060 vs. solar shading from Faber

In the following will PS4060 be compared to the original Velfac window with external shading from Faber – figures 2.2-3.

Season	period	solar height °	external shading system
Spring	11/4-20/4 2007	42.9-46.1	full Faber
Summer	21/8-27/8 2007	46.2-44.2	½ Faber

Table 4.2. Shown periods with PS4060 and Velfac sun 1/clear + external solar shading in the test rooms.

The two chosen periods have almost the same solar height which eases the comparison.

Figures 4.9-10 shows the weather condition during the considered periods. Figures 4.11-12 shows the mean air temperature in the two test rooms. The measured incoming solar radiation is not shown as this gives no meaning as it due to the macro structure of the Faber solar shading isn't possible to measure the incoming solar radiation to test room B with the applied pyranometers.

Figures 4.9-10 unfortunately show that the weather conditions during the two considered periods aren't very similar. However, for some of the days the radiation level is rather similar.

Figure 4.11 shows peak differences of up to 5 K with the mean air temperature level in test room B now being the lowest. Due to the peak temperature of below 22°C it is assumed, that the extra thermal mass of test room B has only insignificant influence on the comparison. So the full Faber shading system has a much larger screening effect than PS4060 which also was expected when looking at figures 2.2, 2.4 and 3.2.

Figure 4.12 shows peak differences of up to 2 K. The temperature level in figure 4.12 is higher than in figure 4.11. Here the extra mass of test room B influence the comparison, meaning that the air temperature of test room B for direct comparison may be up to 0.5 K higher than shown in figure 4.12. This means that reducing the Faber system to half the number of lamellas decreases the temperature difference with more than half the difference shown in figure 4.11.

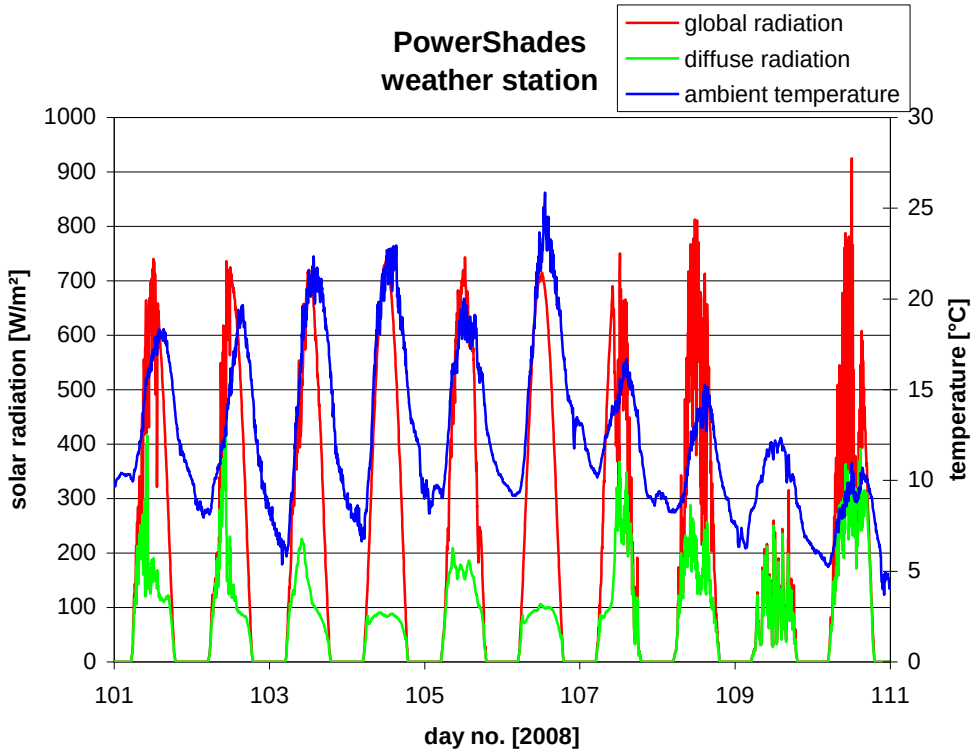

Figure 4.9. The weather conditions during the spring period – April 11-20, 2007.

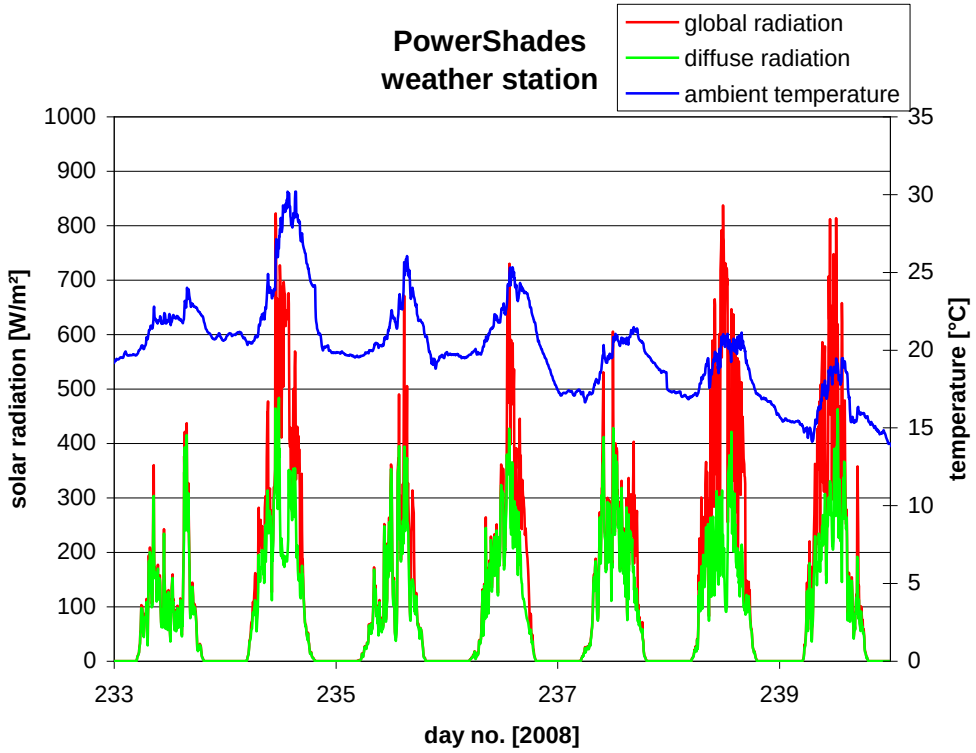

Figure 4.10. The weather conditions during the summer period – August 21-27, 2007.

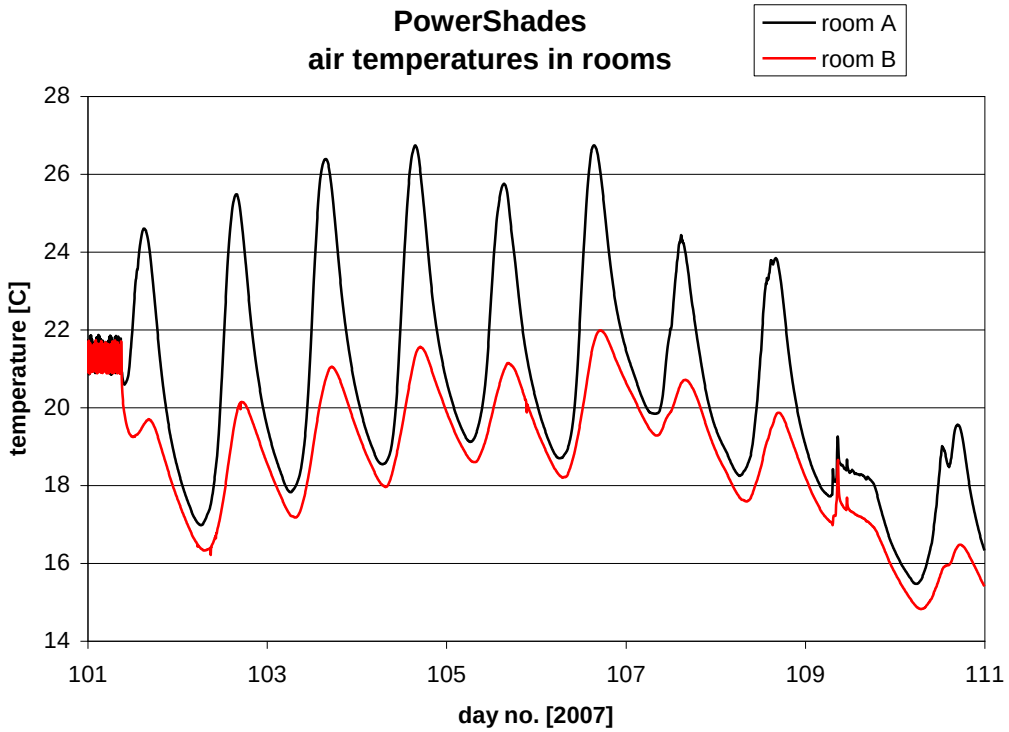

Figure 4.11. The measured mean air temperature of the two test rooms – April 11-20, 2007. Test room B had full external shading from Faber.

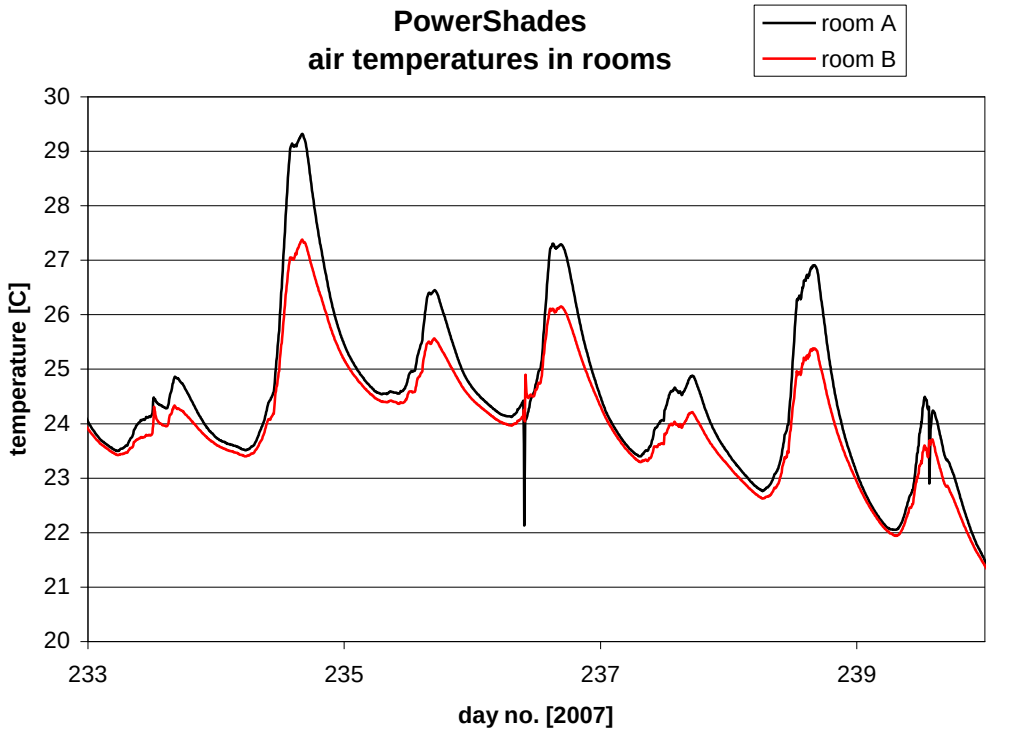

Figure 4.12. The measured mean air temperature of the two test rooms – August 21-27, 2007. Test room B had ½ external shading from Faber.

In figure 3.2 it is seen that the Velfac windows with ½ Faber external shading lets more daylight into the room than PS4060. This seems to be in contradiction with figure 4.12. Figure 4.12 shows that the Velfac windows with ½ Faber external shading lead to lower peak values than PS4060. This is because there is a screening film in the Velfac window which is not present in the PowerShade window. The solar screening film lets in a higher percentage of light than solar heat. The light transmittance of the Velfac window is 67% while the g-value is 37%.

The computer curtain together with the original windows from Velfac was tested – for daylighting purposes – during the winter without much sunlight and with heating so this shading system will not be evaluated here as no measured data for doing such are available.

4.4. Conclusions

It was unfortunately not possible to develop a model of PS4060 for ESP-r due to too large uncertainties concerning the holes in the foil of these PowerShades. However, the measurements may still be utilized to illustrate the effect of PowerShades.

The measurements showed that PS4060 reduced the peak values of the mean air temperature in test room A with about 3 K (if the test rooms were fully identical) compared to test room B with the original Velfac sun 1/clear with at g-value of 0.37 – ie with at solar screening coating. This reduction is seen both for a spring and a summer period.

However, the reduction of 3 K is only for the considered test rooms with their specific thermal capacity and close to zero infiltration. Different thermal capacity, different air change rates and different designs of the PowerShades will change the reduction of the indoor air temperature that PowerShades will result in. This is why it is so important to be able to calibrate the model of the PowerShades. Calibration of a model of PowerShades is dealt with in the following chapter.

The measurements further show the selective behaviour of PowerShades. While the reduction of the incoming solar radiation at sunny days through the Velfac windows at noon was 33% between spring and summer it was 77% for PS4060.

5. Calibration of the model

The main purpose of the test rooms is to be able to deliver high quality data for calibration of models of PowerShades. But why is it important to have a calibrated model of PowerShades? The reason is that it is much cheaper, faster and easier to perform simulations than to perform measurements – especially when one want to perform parametric studies in order to study the effect of changes to the PowerShades. Further when confidence in the model is reached it is easy to scale the model of the PowerShades to real buildings and study their performance under different climate conditions.

The present chapter describes the finding from comparisons between measurements and calculations using the model of the test rooms with Prototype 1 installed in the window of test room A.

The model of the test rooms has been developed in the simulation program ESP-r (ESRU, 2001). The model consists of 28 zones. The two test rooms has been divided in 10 equal zones – 5 on top of each others close to the window and 5 on top of each other close to the backend of the test rooms. The zones are identical to the air volumes surrounding each of the 10 temperature sensors in the test room (Jensen, 2008a). To the east of test room A and to the west of test room B + above, behind and below each test room are located zones which are given the measured air temperature besides, above, behind and below the test rooms as air temperatures. The zones are shown in figure 5.1 (however, one cannot see the 5 zones at the backend of the test rooms). The thermo-physical properties of the materials of the test rooms are as given in (Jensen, 2008a).

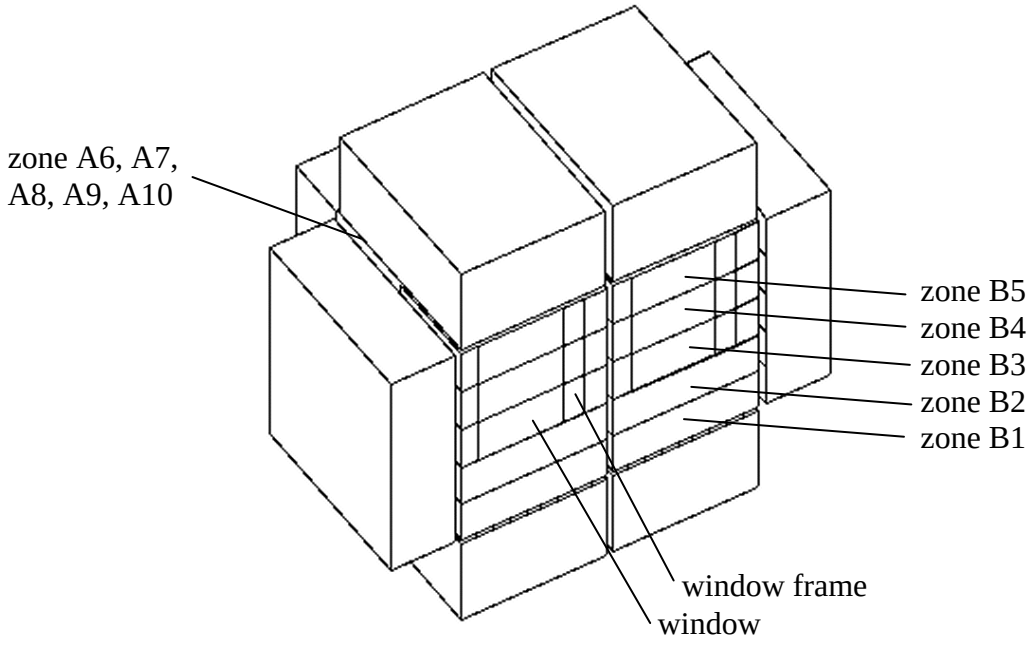

Figure 5.1. The zones of the test rooms and the surrounding zones.

The shading from the building situated to the east of the test rooms, the column between the windows of the test rooms and the overhang above the windows of the test rooms has been introduced in the form of external obstructions as seen in figure 5.2.

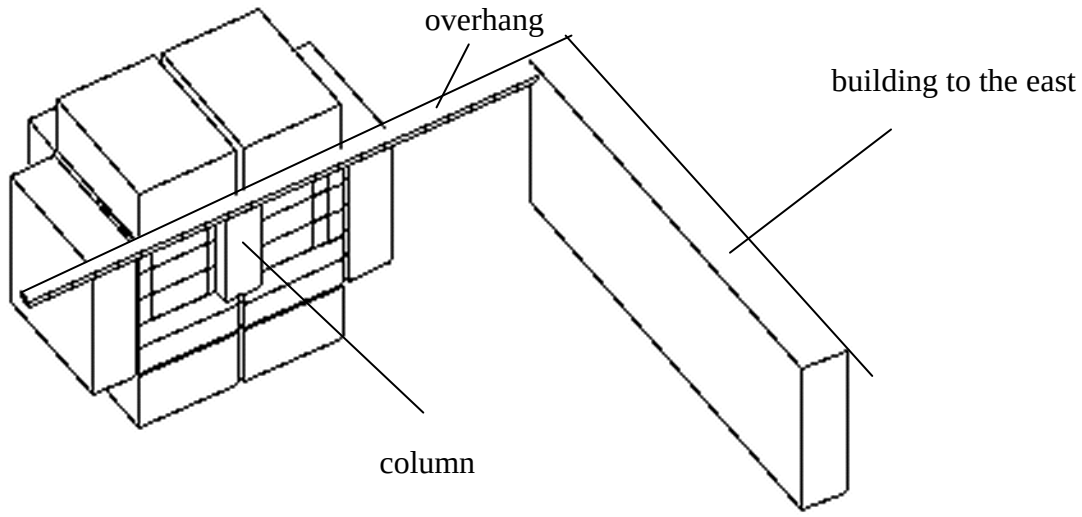

Figure 5.2. The obstruction blocks used for creation of shading.

The function of PowerShades are similar to Venetian blinds, however, PowerShades are a microstructure of small holes embedded in a metal foil with a thickness of less than one mm. This means that PowerShades cannot be treated the same way as traditional windows as the transmission, absorption and reflection changes with the combinations of the two components of the incidence angle for the sun: horizontal and vertical incidence angle.

PowerShades have been modelled using a novel module in ESP-r for modelling bidirectional transmission through transparent multilayered constructions. The module contains a matrix where the total direct transmission, the absorption in each layer of the window and the enhancement in incoming diffuse radiation due to the scattering of direct radiation in the PowerShades are listed for combinations of the horizontal and vertical incidence angle at steps of 5^{o} – see section 5.2.2.2.2..

The model of the PowerShades has previous been calibrated based on measurements obtained in the goniosspectrometer of the Building Division at the Technological University of Denmark [Schultz, 2008).

The solar height at Taastup varies over the year between 10.9° and 57.8°. As PowerShades perform differently over the year due to different performance at different solar heights three periods of measurements during 2008 have been chosen for the calibration of the model - see table 5.1. However, the three periods has not be chosen arbitrarily - both clear sky and overcast conditions should preferably be present and no special purpose experiments should have been performed in the test rooms. For all three periods PowerShades Prototype 1 has been installed in test room A, while the original Velfac windows without any shading devices were installed in test room B.

Season	period	solar height °
Winter	21/1-17/2 2008	14.4-22.7
Spring (autumn)	25/3-26/4 2008	36.1-47.8
Summer	1-28/6 2008	56.5-57.8

Table 5.1. The periods considered for the calibration.

5.1. Weather conditions

Figure 5.3 shows the weather conditions during the chosen winter period. The ambient temperature varies between -4°C and just below 14°C. There is of course many days with fully cloudy conditions but also some days with clear sky conditions. The global radiation in figure 5.3 is measured, while the horizontal diffuse radiation is calculated based on measurements as described in (Jensen, 2008a). The global and horizontal diffuse radiation have been used as input to the simulation model.

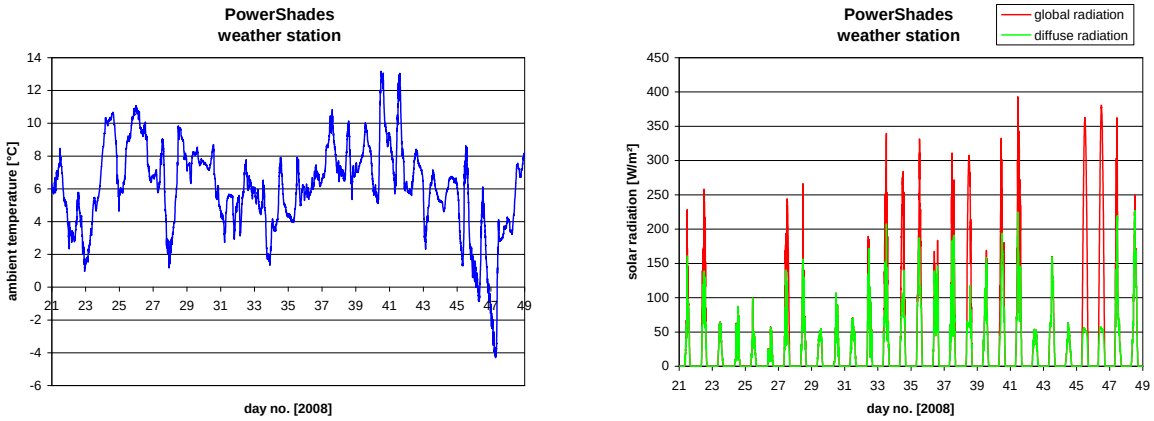

Figure 5.3. The weather conditions during the winter period – 21/1-17/2, 2008.

Figure 5.4 shows the weather conditions during the chosen spring period. The ambient temperature varies between -3°C and 20°C. There is only one day with fully overcast conditions while four days with clear sky conditions. The rest of the days had drifting clouds.

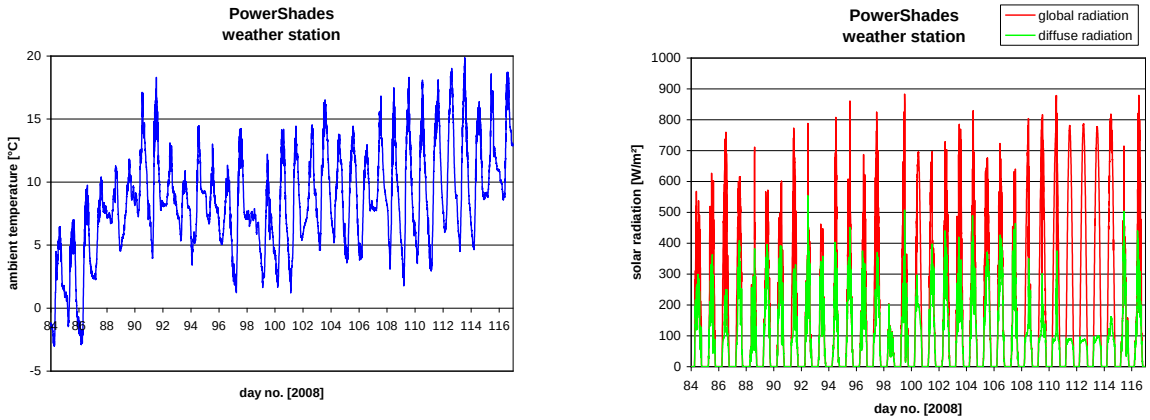

Figure 5.4. The weather conditions during the spring period – 25/3-26/4, 2008.

Figure 5.5 shows the weather conditions during the chosen summer period. The ambient temperature varies between 8°C and 32°C. There are no days with fully overcast but a few days with partly overcast conditions and many days with clear sky or drifting clouds.

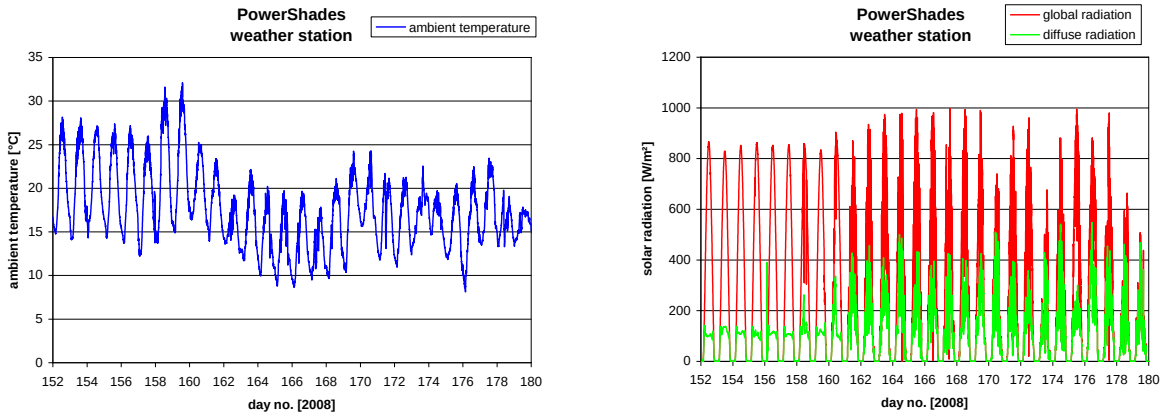

Figure 5.5. The weather conditions during the summer period – 1-28/6, 2008.

5.2. Calibration of the model

A step by step calibration of the model has been carried out and will in the following be described:

- first the model for calculation of the solar radiation hitting the façade has been calibrated,
- then the models for calculating the solar radiation entering the test rooms has been calibrated and
- finally the model for calculating the air temperatures in the test rooms has been calibrated.

5.2.1. Solar radiation hitting the facade

The measured global and horizontal diffuse radiation has been used as input to ESP-r. However, in order to calculate the radiation hitting the façade ESP-r also need to consider the reflection of solar radiation from the surroundings. The latter is done by giving a reflection coefficient (or albedo). The reflected radiation is then calculated as:

$$G_r = ½\ \rho_r\ G_g$$

where: G_r is the reflected solar radiation hitting the façade,
ρ_r is the reflection coefficient and
G_g is the global radiation.

The normal value for the reflection coefficient used in simulations models is 0.2 (often referred to as the ASHREA value). However, the windows of the test rooms are facing a courtyard as seen in figure 2.6 which most often is in shade. The façade of the opposite building facing the façade of the test rooms will most of the day be fully shaded. It was, therefore, anticipated that the value of the reflection coefficient would be less than 0.2.

Figures 5.6-5.8 show a comparison between measured and calculated solar radiation on the façade using a reflection coefficient of 0.2, 0.08 and 0.05 for five sunny days in June. Using a reflection coefficient of 0.2 gives a far too high calculated solar radiation on the façade. 0.08

gives the best result, but for the winter situation an even lower reflection coefficient is needed. So a compromise of 0.05 was chosen.

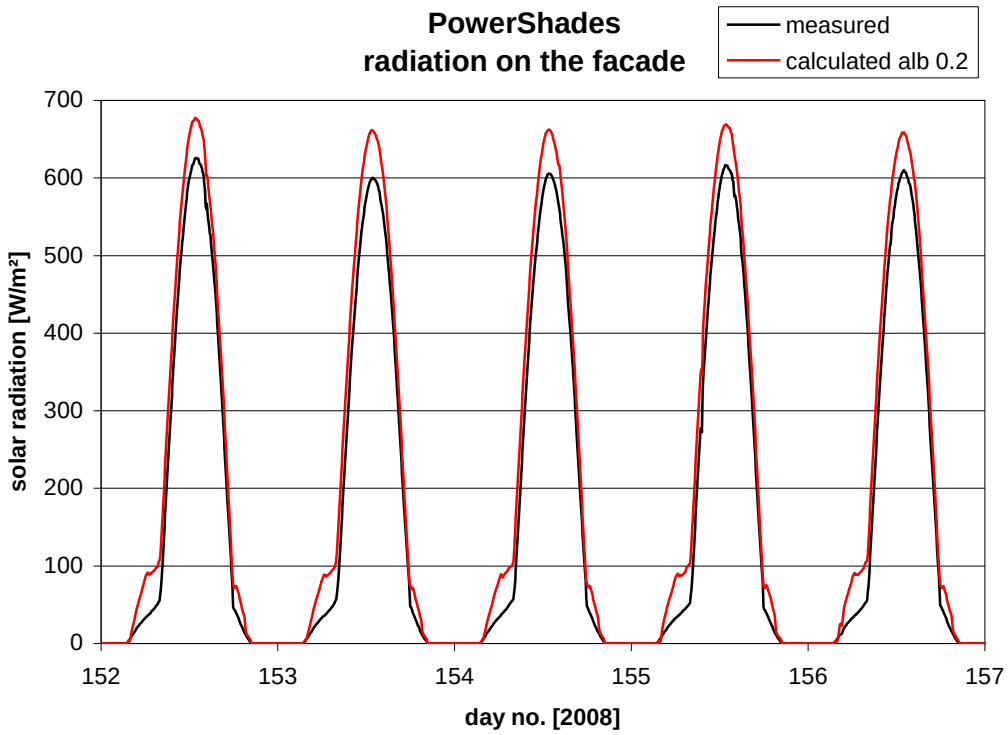

Figure 5.6. Measured and calculated solar radiation hitting the façade when using a reflection coefficient of 0.2 – 1-5/6, 2008.

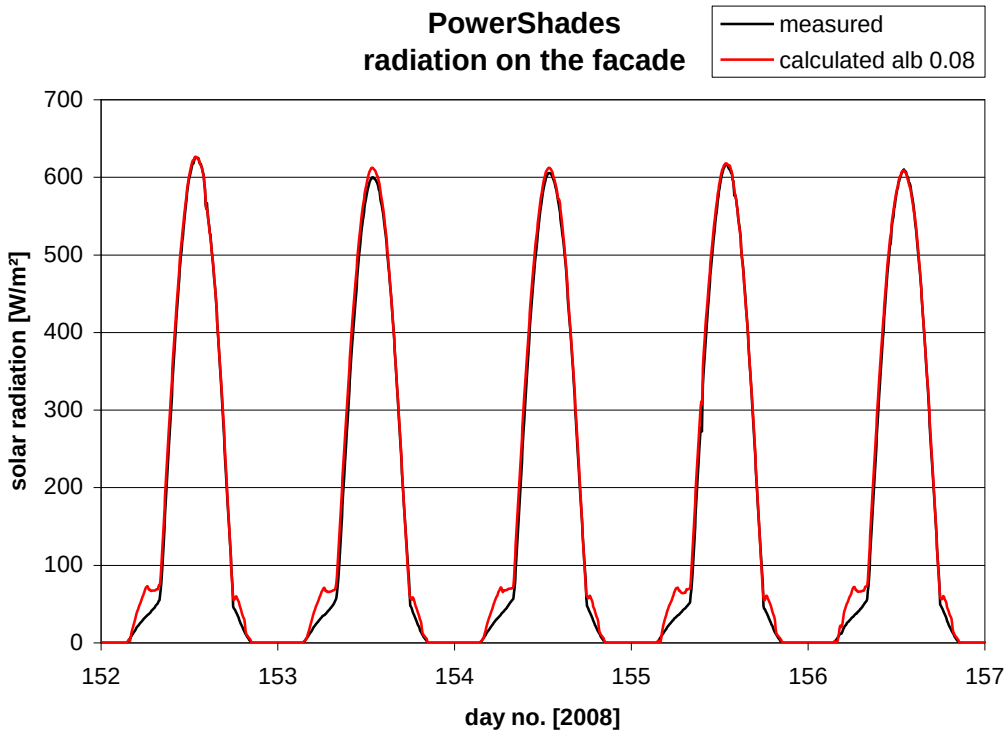

Figure 5.7. Measured and calculated solar radiation hitting the façade when using a reflection coefficient of 0.08 – 1-5/6, 2008.

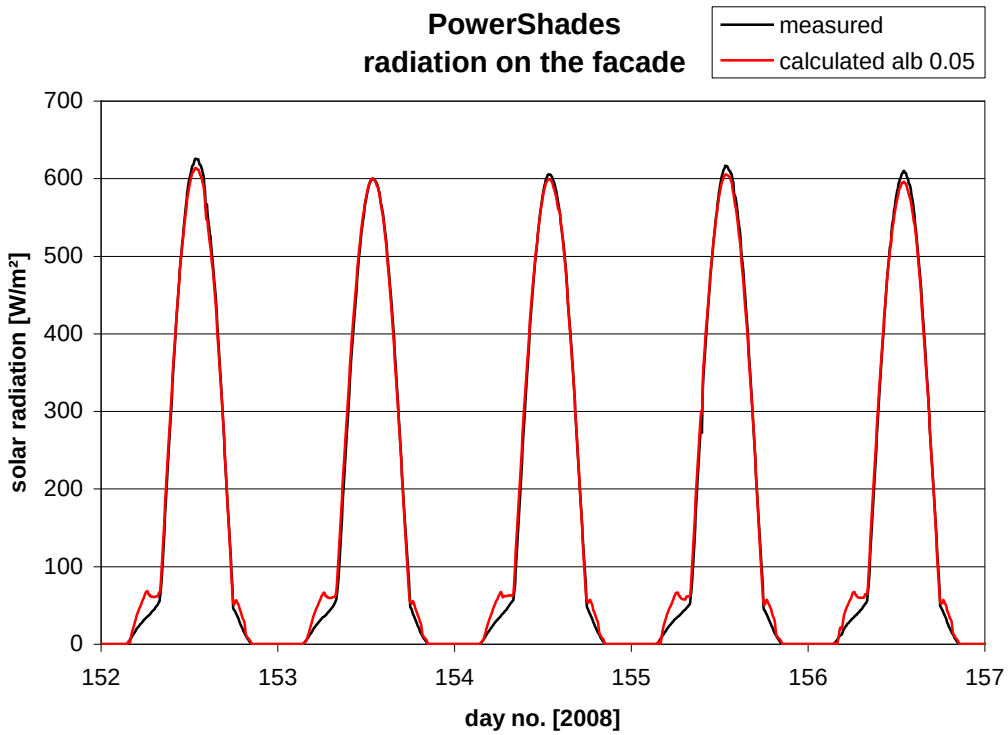

Figure 5.8. Measured and calculated solar radiation hitting the façade when using a reflection coefficient of 0.05 – 1-5/6, 2008.

In the early morning the calculated solar radiation hitting the façade is in figure 5.6-8 too high. It is assumed that this is caused by the uncertainty on the measured/calculated diffuse horizontal radiation in the morning. Peaks in the diffuse radiation are seen in the morning in figure 5.5. The higher calculated morning values will most properly not be present when using test reference years and will, therefore, not be investigated further here.

Figures 5.9-5.17 compare the calculated solar radiation hitting the façade using a reflection coefficient of 0.05 to the measured solar radiation for the three periods: winter, spring and summer. Further two smaller periods are displayed for the three seasons. Be aware of the different y-axis.

Figures 5.9-5.17 show a very good agreement between measured and calculated solar radiation hitting the façade. A better agreement can hardly be expected.

A reflection coefficient of 0.05 will, therefore, be used in the following calibration exercises.

5.2.1.1. Winter 2008

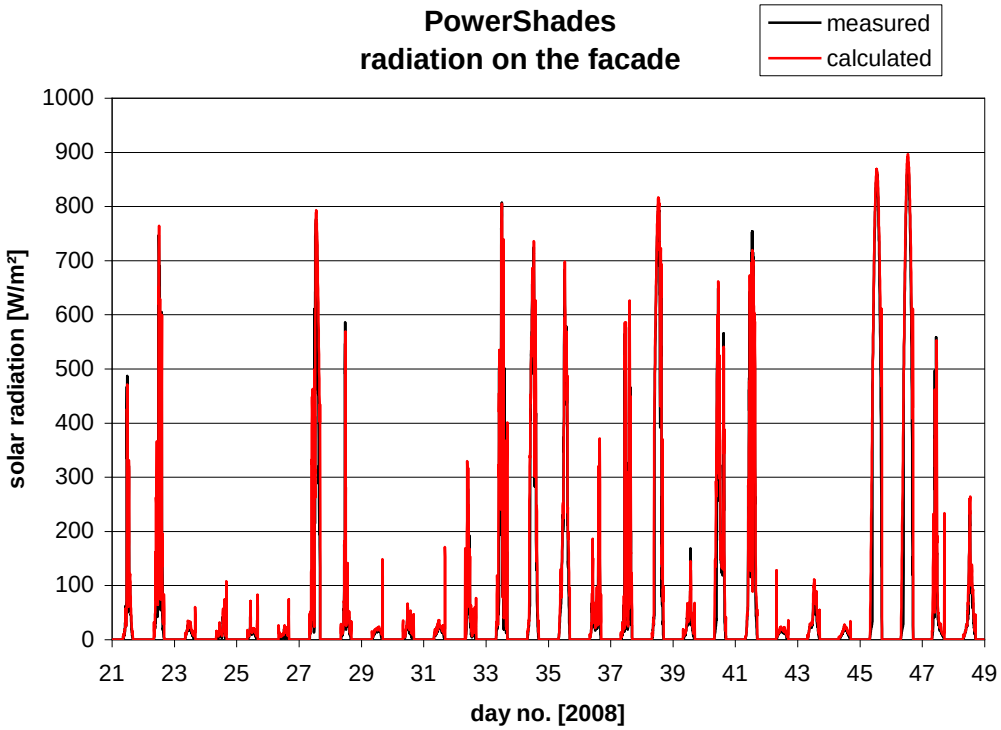

Figure 5.9. Measured and calculated solar radiation hitting the façade when using a reflection coefficient of 0.05 – 21/1-17/2, 2008.

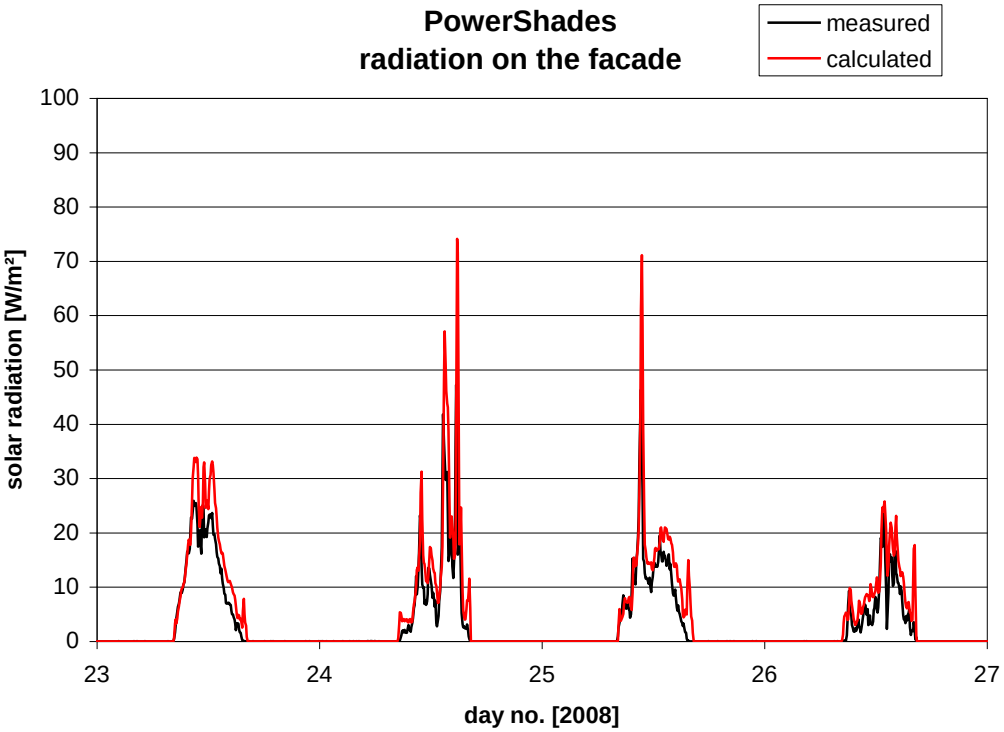

Figure 5.10. Measured and calculated solar radiation hitting the façade when using a reflection coefficient of 0.05 – 23-26/1, 2008.

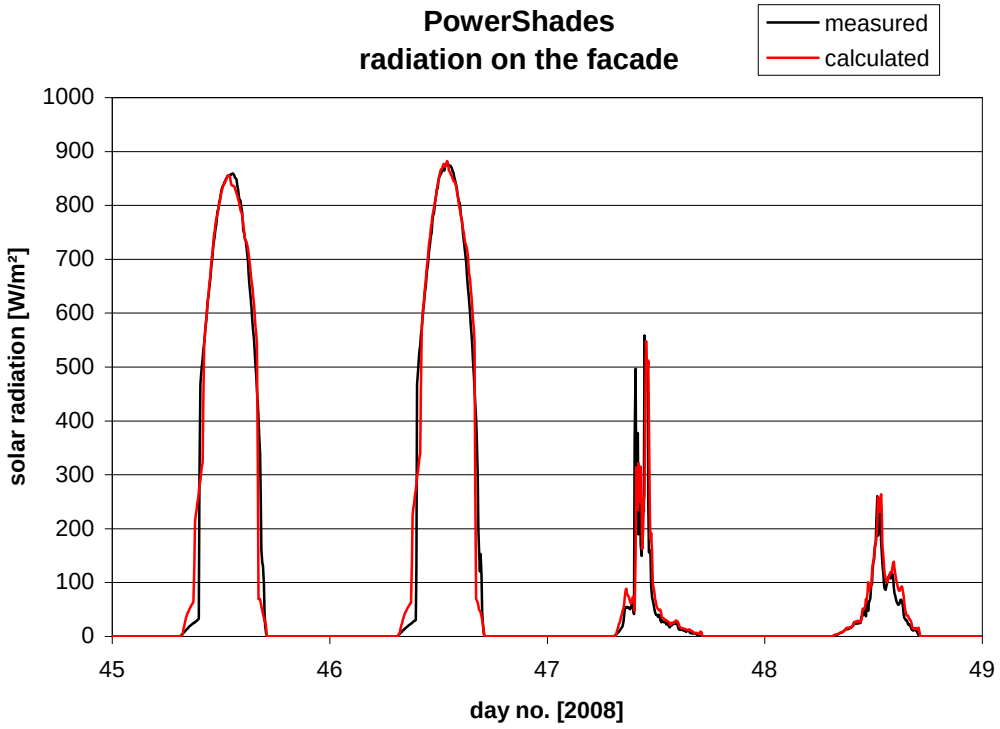

Figure 5.11. Measured and calculated solar radiation hitting the façade when using a reflection coefficient of 0.05 – 14-17/2, 2008.

5.2.1.2. Spring 2008

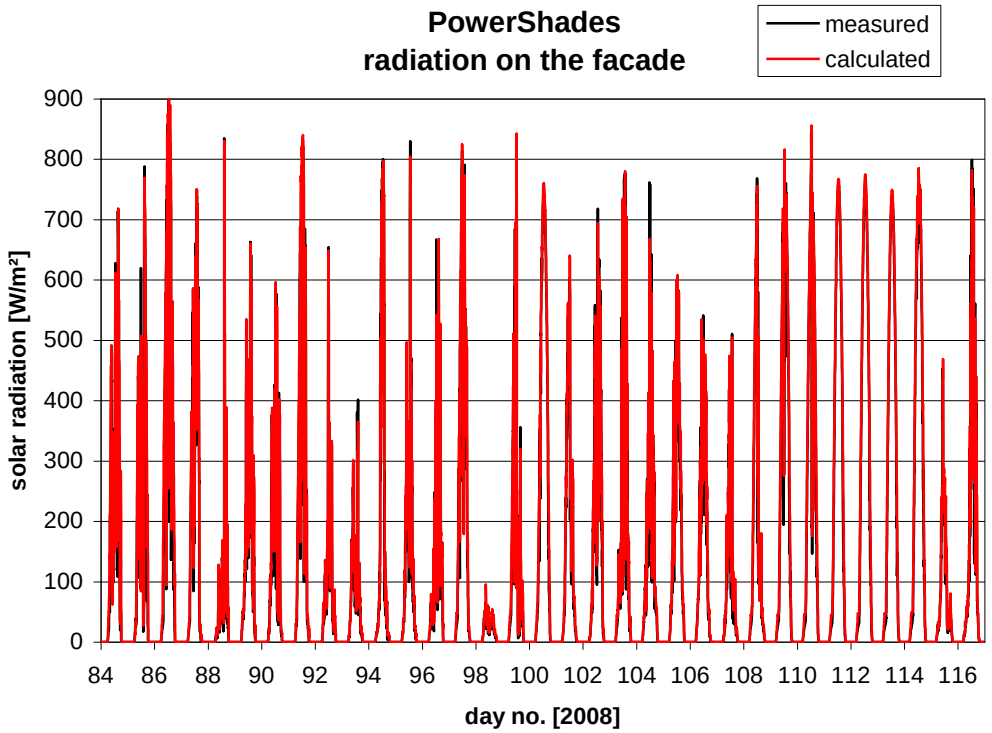

Figure 5.12. Measured and calculated solar radiation hitting the façade when using a reflection coefficient of 0.05 – 25/3-26/4, 2008.

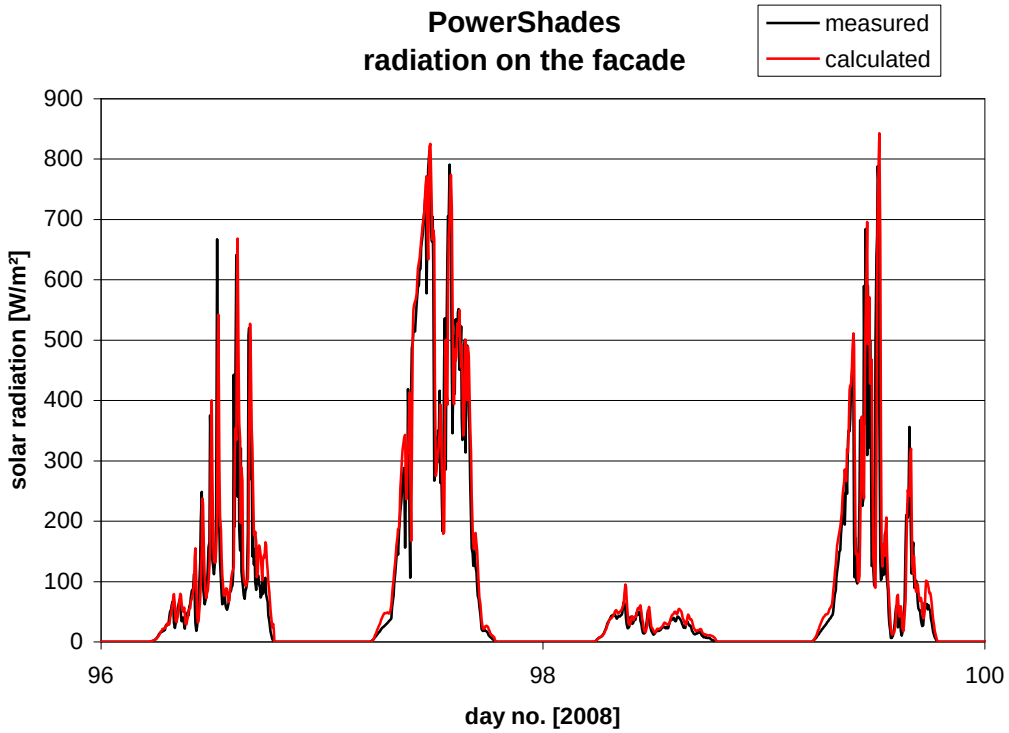

Figure 5.13. Measured and calculated solar radiation hitting the façade when using a reflection coefficient of 0.05 – 6-9/4, 2008.

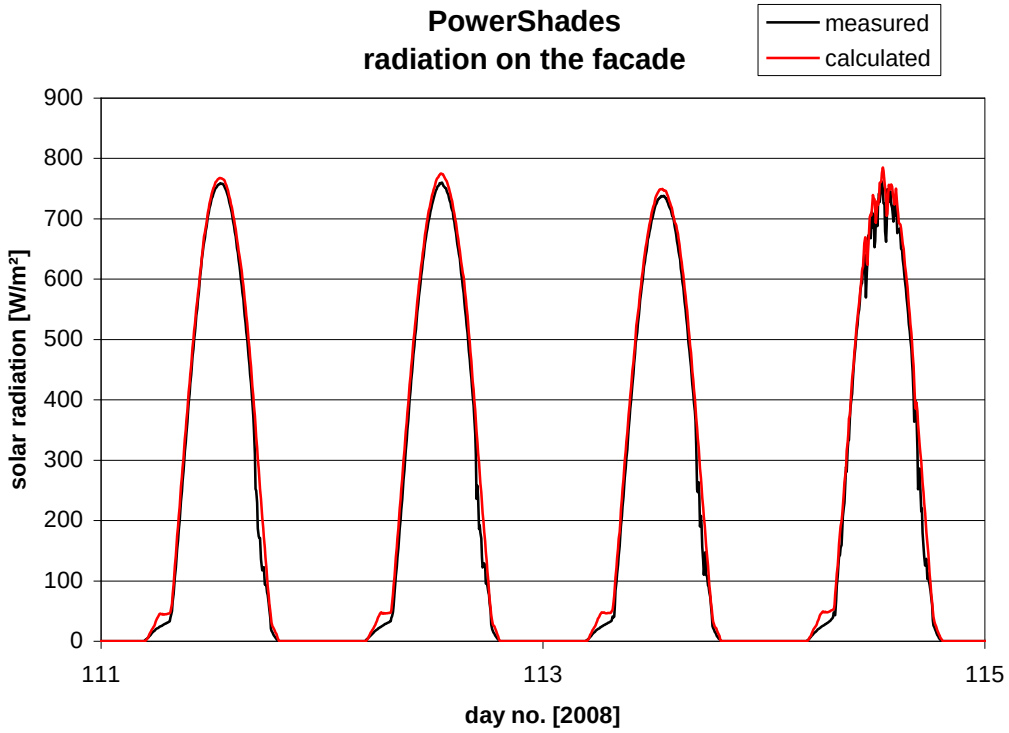

Figure 5.14. Measured and calculated solar radiation hitting the façade when using a reflection coefficient of 0.05 – 21-24/4, 2008.

5.2.1.3. Summer 2008

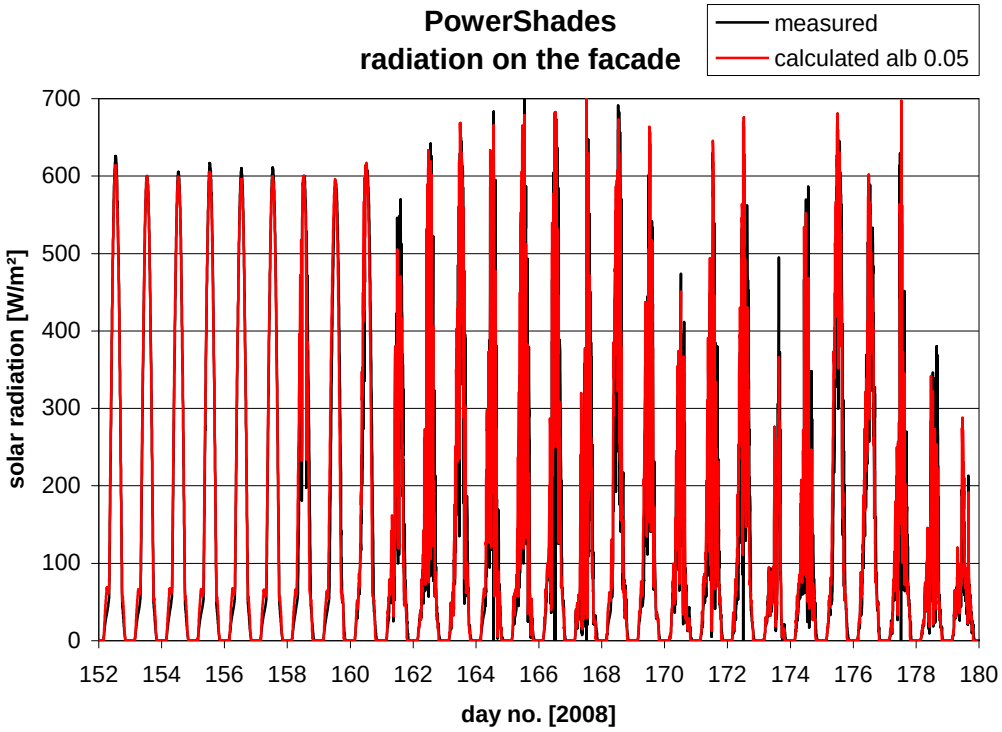

Figure 5.15. Measured and calculated solar radiation hitting the façade when using a reflection coefficient of 0.05 – 1-28/6, 2008.

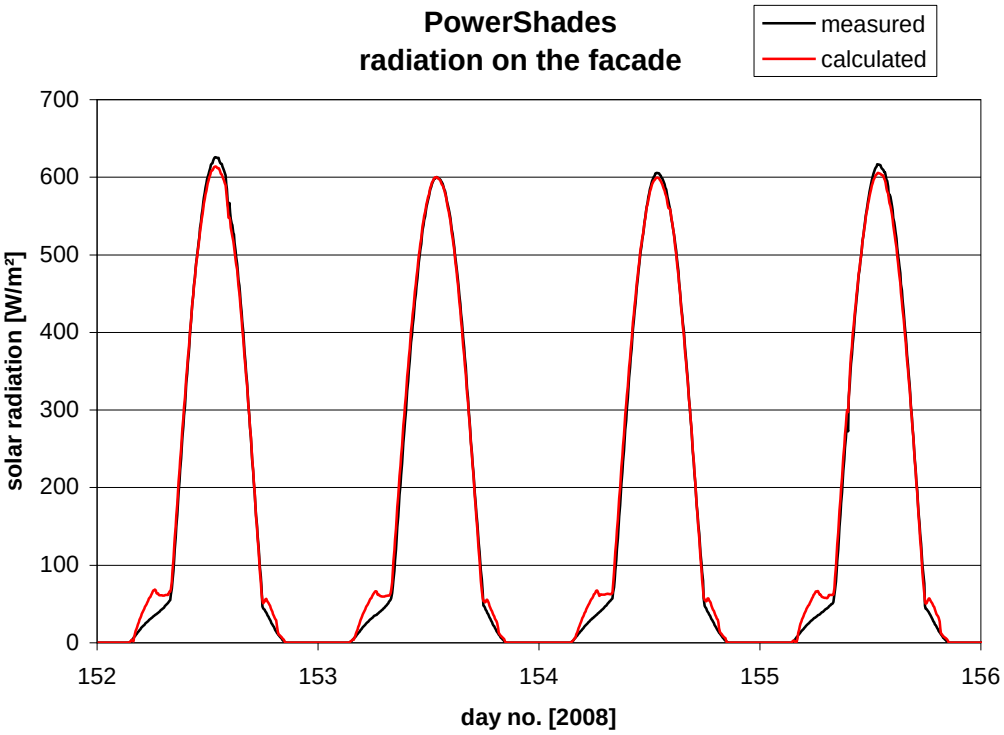

Figure 5.16. Measured and calculated solar radiation hitting the façade when using a reflection coefficient of 0.05 – 1-4/6, 2008.

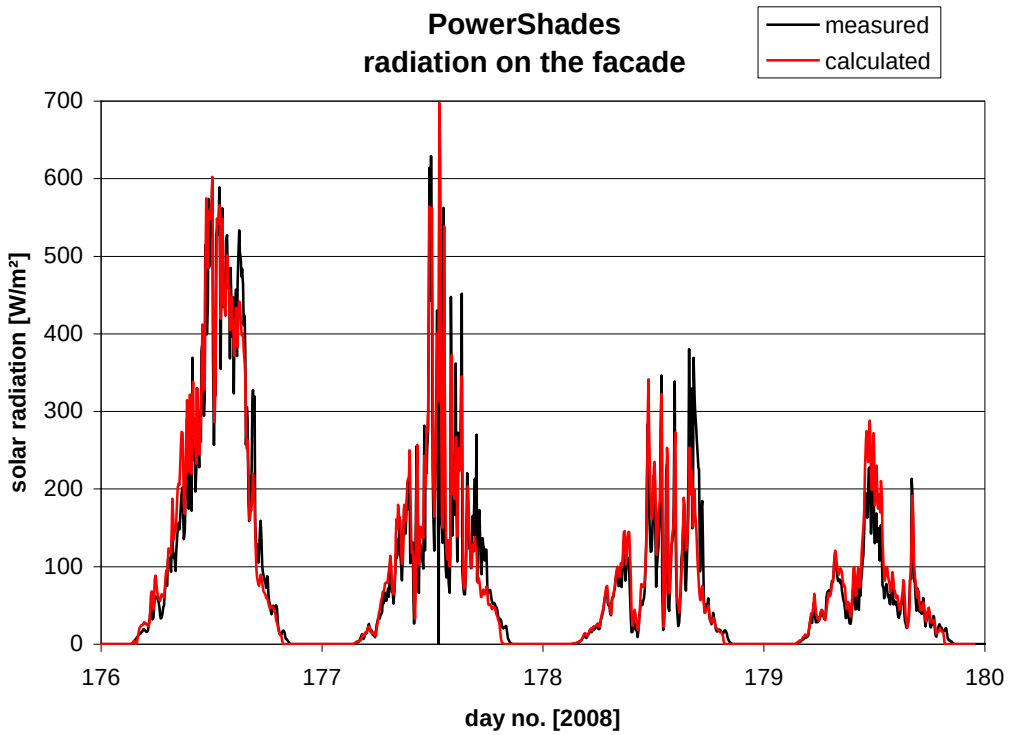

Figure 5.17. Measured and calculated solar radiation hitting the façade when using a reflection coefficient of 0.05 – 25-28/6, 2008.

5.2.2. Solar radiation entering the test rooms

The main objective of the here described calibration exercises is to calibrate the models for calculation of the solar radiation entering through not only the PowerShades but also through the original Velfac window.

As the model of the original Velfac window is much simpler this model will be calibrated first.

5.2.2.1. Calibration of the model of the Velfac window

I (Jensen, 2008a) the optical properties of the original Velfac window were given as:

Layer	incidence angle °				
	0	40	55	70	80
Total transmittance	0.340	0.360	0.332	0.230	0.056
Absorption in outer glass pane	0.340	0.353	0.365	0.387	0.384
Absorption in inner glass pane	0.010	0.012	0.012	0.011	0.005
Total reflectance	0.310	0.275	0.291	0.372	0.555

Table 5.2. Optical properties for the original windows dependent on the incidence angle.

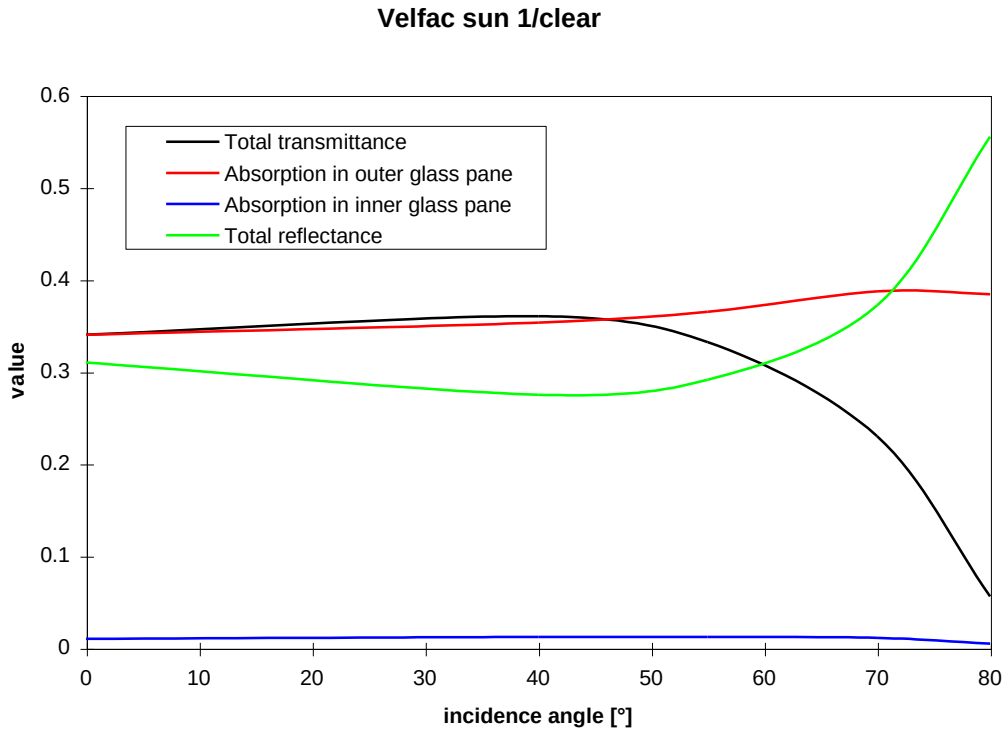

Figure 5.18. Optical properties for the original windows dependent on the incidence angle.

These optical properties were applied in a comparison between the measured and calculated solar radiation entering through the original Velfac window using measurements from 2007. It was found that although rather good agreement was obtained at noon during the winter the model from figure 5.18 gave to high values during spring/fall and summer. Based on the comparison the total transmittance for solar radiation was fitted to obtain a better agreement between measurements and calculations.

Layer	incidence angle °				
	0	40	55	70	80
Total transmittance	0.335	0.307	0.272	0.184	0.085
Absorption in outer glass pane	0.340	0.366	0.387	0.406	0.415
Absorption in inner glass pane	0.010	0.011	0.012	0.013	0.013
Total reflectance	0.315	0.316	0.329	0.397	0.487

Table 5.3. New optical properties for the original windows dependent on the incidence angle.

Figure 5.20 shows that the calibrated value for the total transmittance in figure 5.19 is reduced by up to 20% compared to 5.18. The values for especially the absorption in the outer glass pane have also been changed slightly. These values have only very little influence on the indoor climate, when the U-value of the window is as low as 1.1 W/m²K as shown in (Jensen, 2008b).

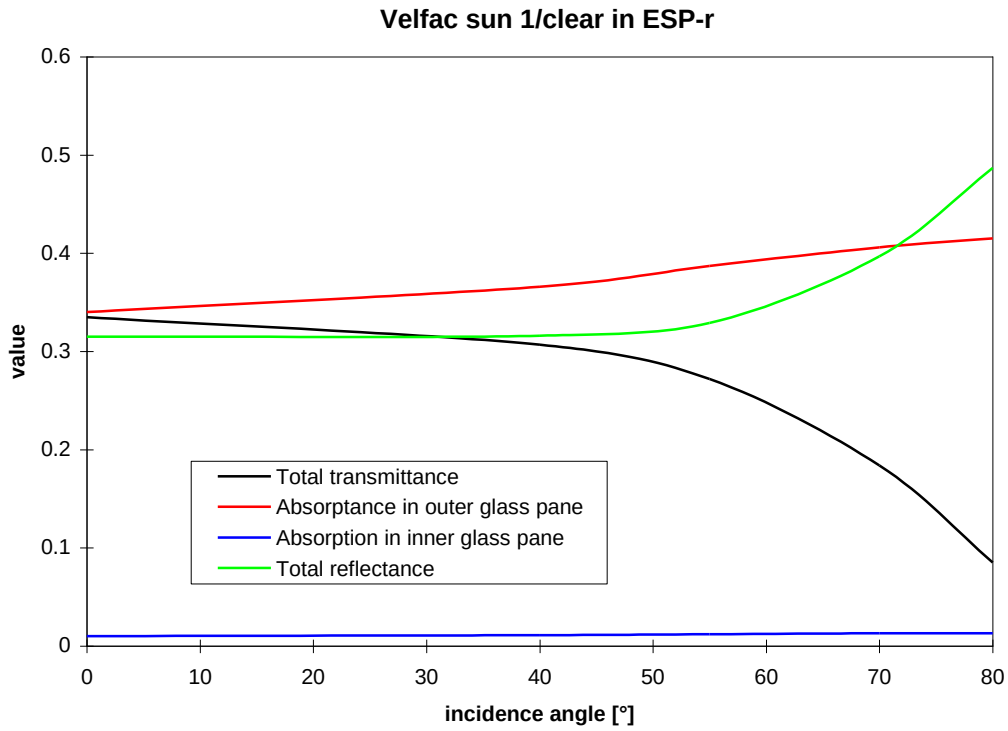

Figure 5.19. New optical properties for the original windows dependent on the incidence angle.

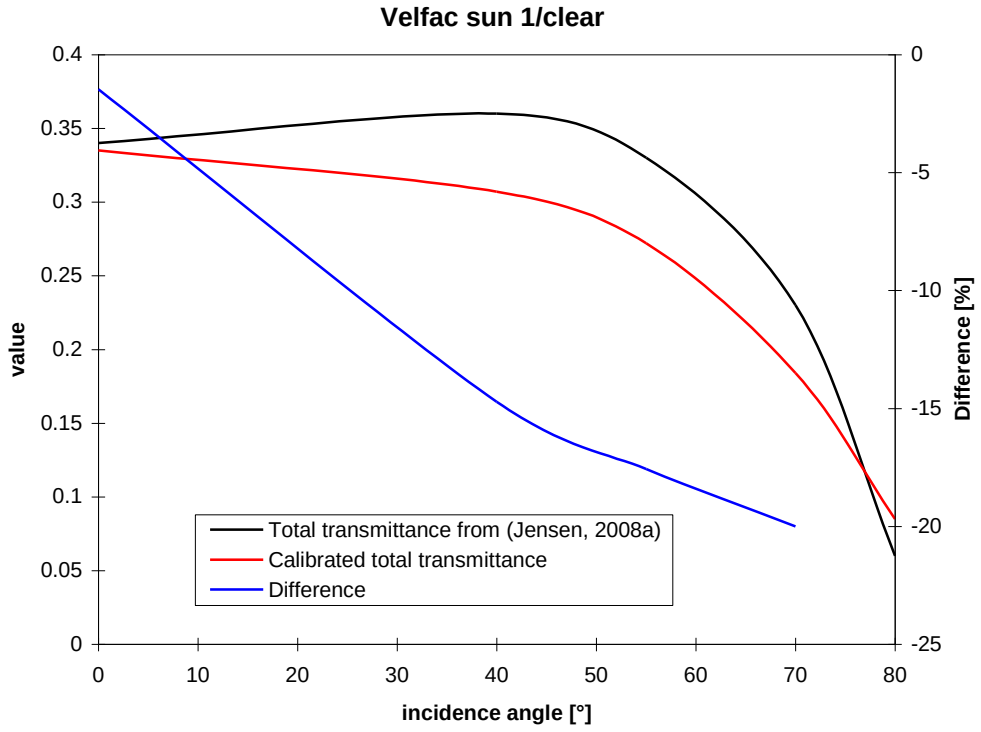

Figure 5.20. The difference in total transmittance between figure 5.18 and 5.19.

The model in table 5.3 was developed based on a calibration using measured values from 2007, but will in the following be tested using measured data from 2008. The same periods as applied in chapter 5.2 will be used.

When comparing calculations with measurements one problem emerge: the pyranometer has a size of 49 x 49 mm^2 and is located 45 mm behind the internal glass, while the window has a width of 640 mm - see figure 3.14 in (Jensen, 2008a). The obstructions shown in figure 5.2 will thus have different influence on the calculated and measured values. This is illustrated in figures 5.21-22. Figure 5.21 shows a comparison between measurements and calculations, where the obstructions in figure 5.2 is considered in the calculations, while figure 5.20 shows almost the same, but here is the obstructions isn't included in the calculations.

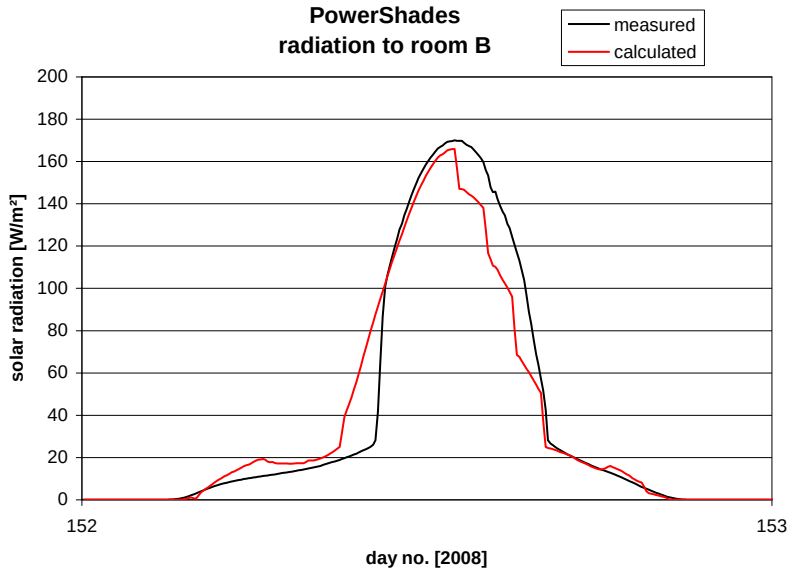

Figure 5.21. Measured and calculated (with shading) solar radiation to room B – 1/6, 2008.

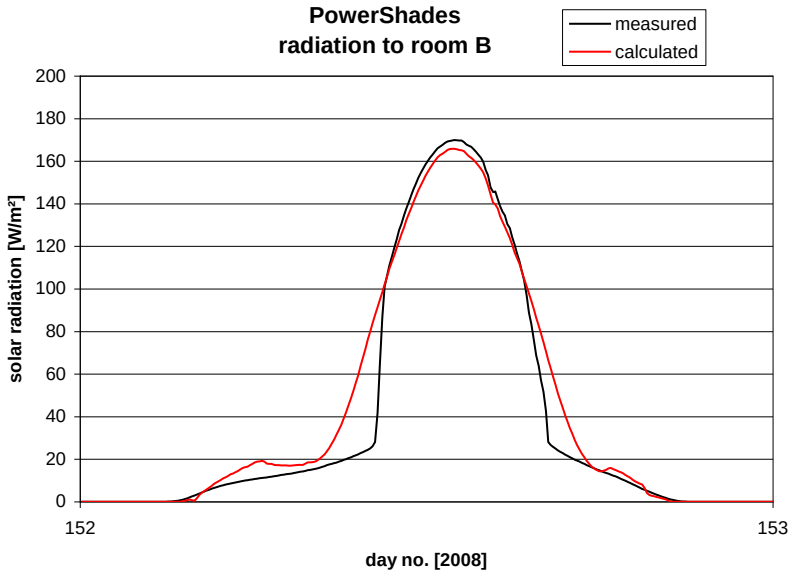

Figure 5.22. Measured and calculated (without shading) solar radiation to room B – 1/6, 2008.

In order to understand figures 5.21-22 it is necessary to take into consideration the location of the pyranometer and how ESP-r handles shading.

In the morning the calculated incoming radiation increases faster than the measured radiation. This is because the pyranometer is located 45 mm behind the inner glass. This means that the frame of the window will shade the pyranometer totally until around 10 am in figures 5.21-22, and then the measured radiation will quickly increase as the shade travels across the 45 mm width of the pyranometer. The calculated radiation will start to increase as soon at the sun starts to hit the façade – here around 9 am due to the orientation of the façade a little to the west.

ESP-r calculates for each hour the percentage of shading on the surfaces of the façade, and use this values for all intermediate simulation time steps between hourly values (in figures 5.21-22 5 minutely time steps). In figure 5.21 this is seen as four steps in the red curve after noon. The first hours after noon when the pyranometer is not shades there is a good agreement between measured and calculated values without shading. This agreement becomes less good when the shading of the column between the two rooms starts to hit the pyranometer. After this there is a good agreement between measured and calculated values with shading.

The above should be remembered when interpreting the following graphs where for clear sky conditions the result will be shown both with and without applying shading in the calculations. This is not done for overcast conditions as the shading has no real effect here.

5.2.2.1.1. Winter

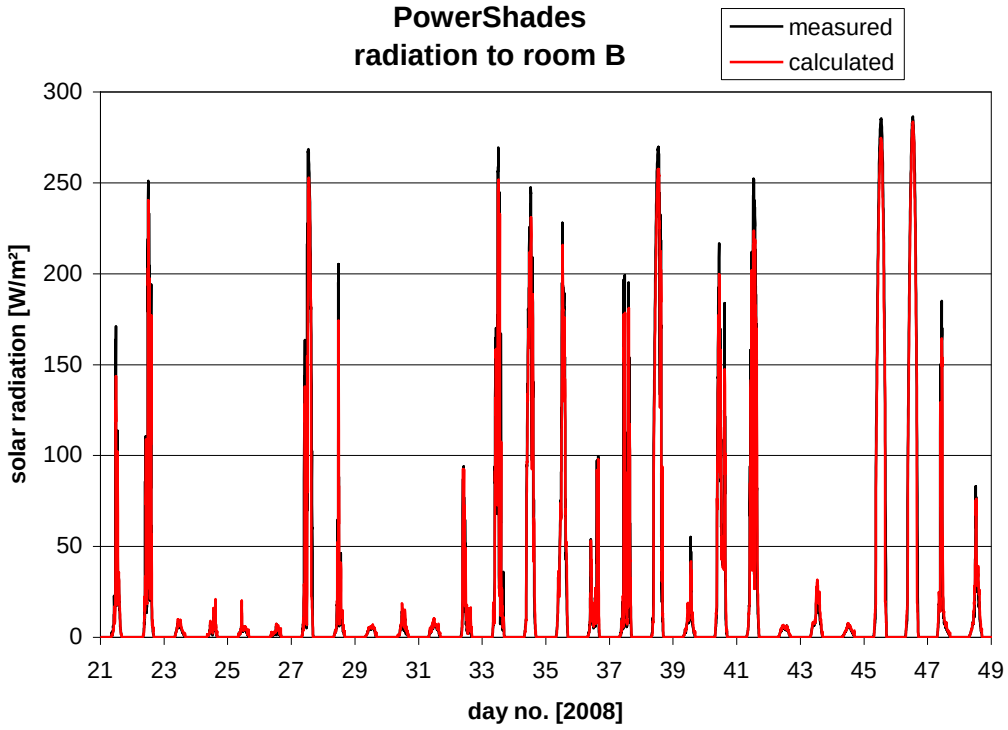

Figure 5.23. Measured and calculated radiation through the Velfac sun 1/clear windows – 21/1-17/2, 2008. With shading.

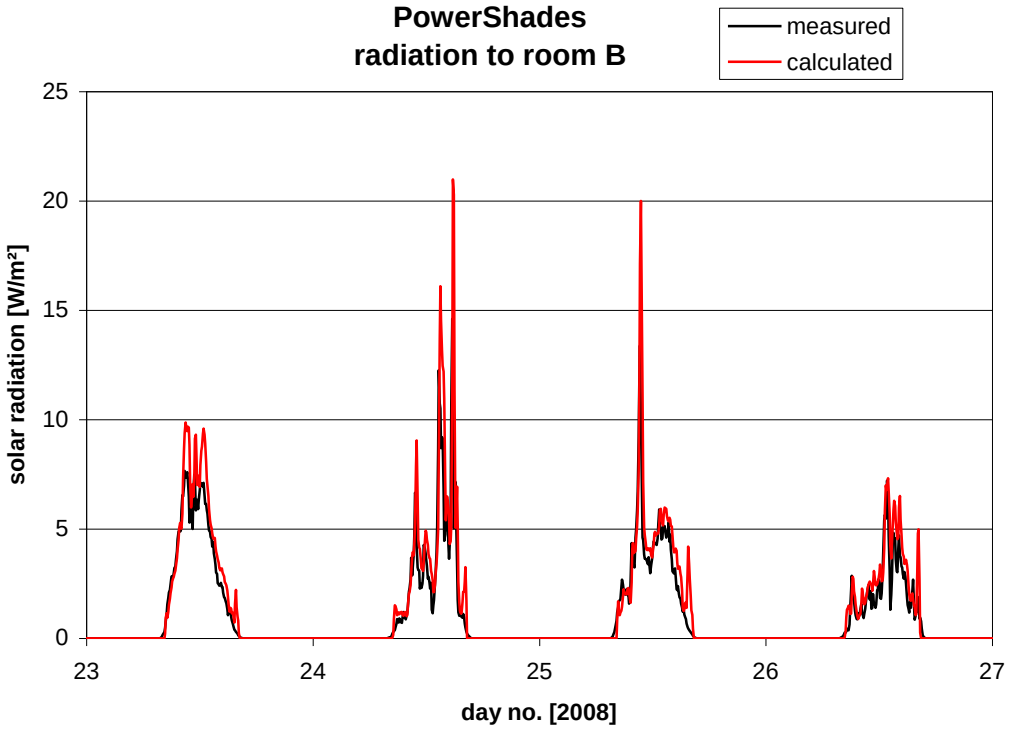

Figure 5.24. Measured and calculated radiation through the Velfac sun 1/clear windows – 23-26/1, 2008. With shading.

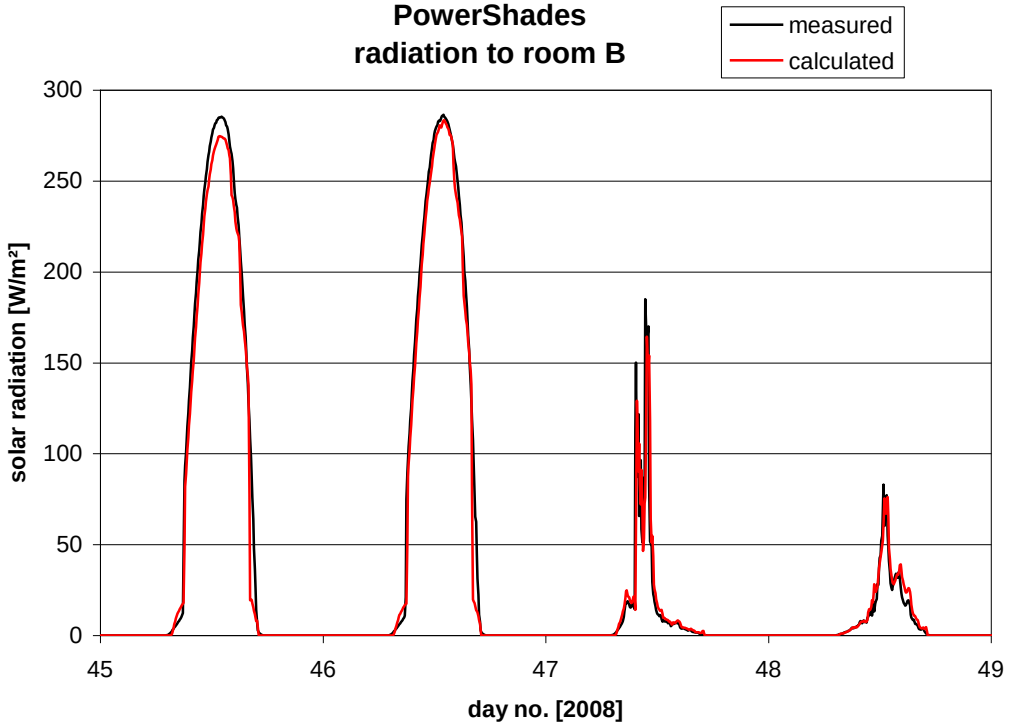

Figure 5.25. Measured and calculated radiation through the Velfac sun 1/clear windows – 14-17/2, 2008. With shading.

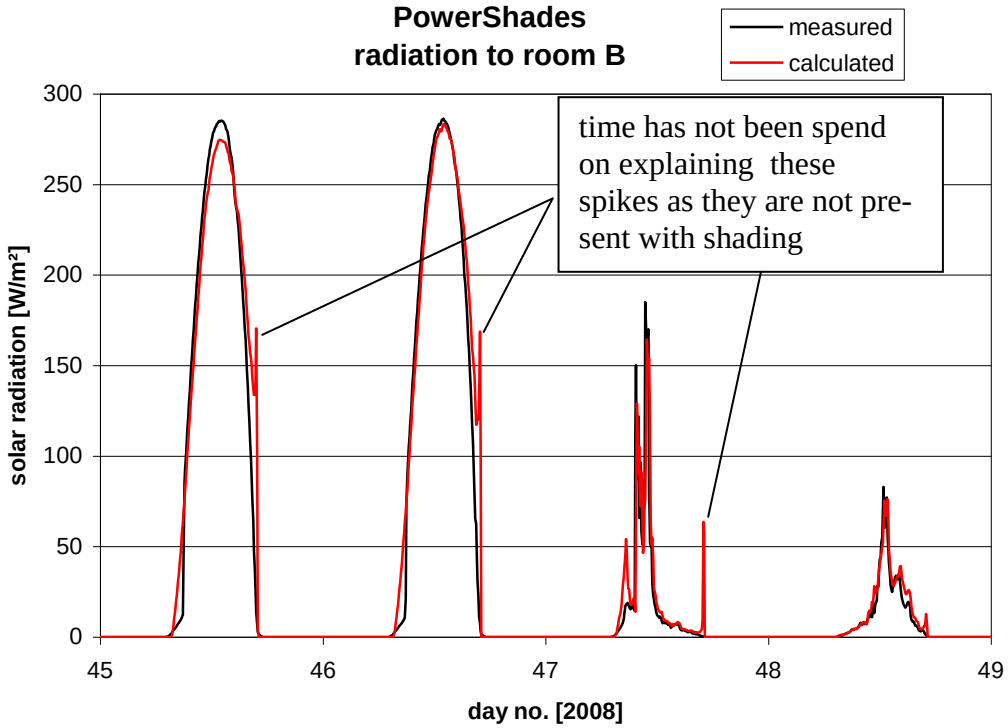

Figure 5.26. Measured and calculated radiation through the Velfac sun 1/clear windows – 14-17/2, 2008. Without shading.

5.2.2.1.1. Spring

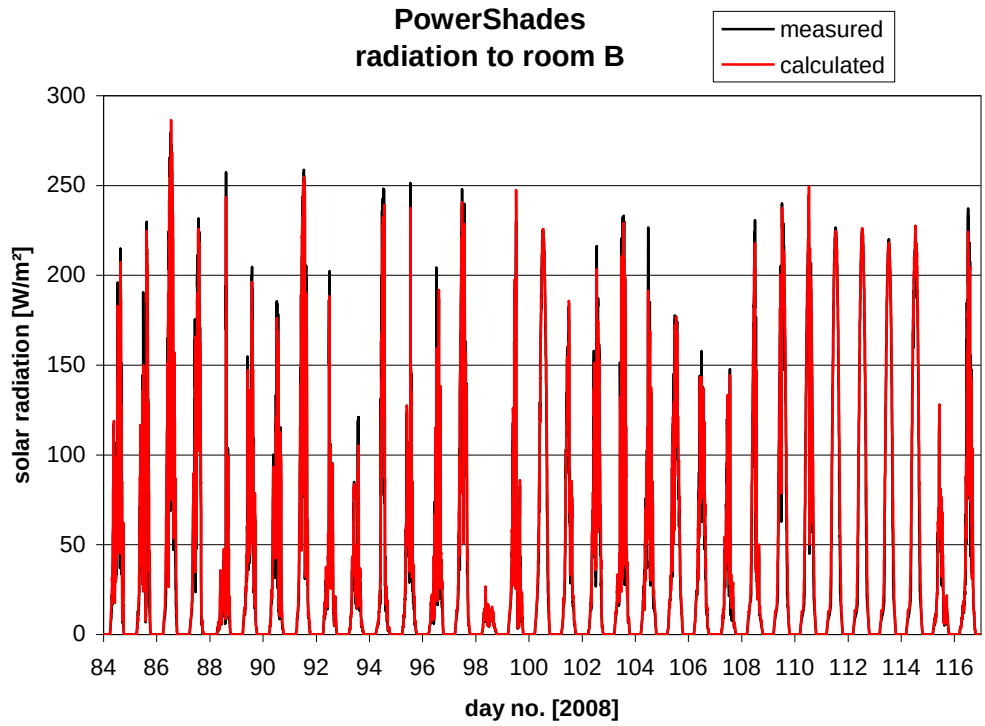

Figure 5.27. Measured and calculated radiation through the Velfac sun 1/clear windows - 25/3-26/4, 2008. Without shading.

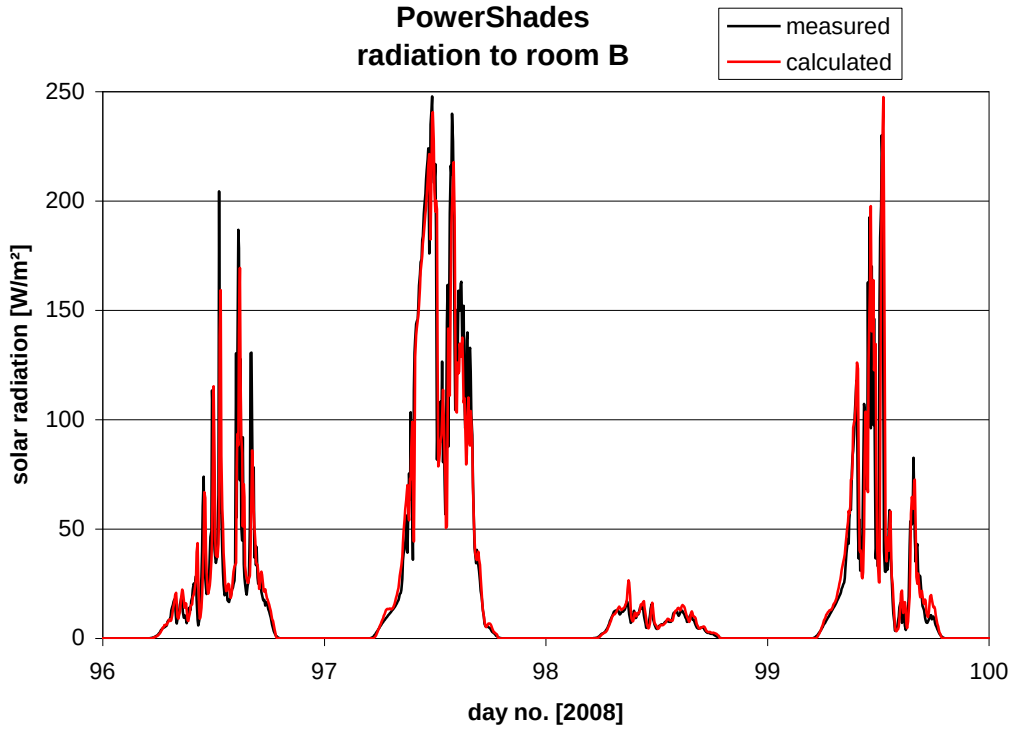

Figure 5.28. Measured and calculated radiation through the Velfac sun 1/clear windows - 6-9/4, 2008. Whit shading.

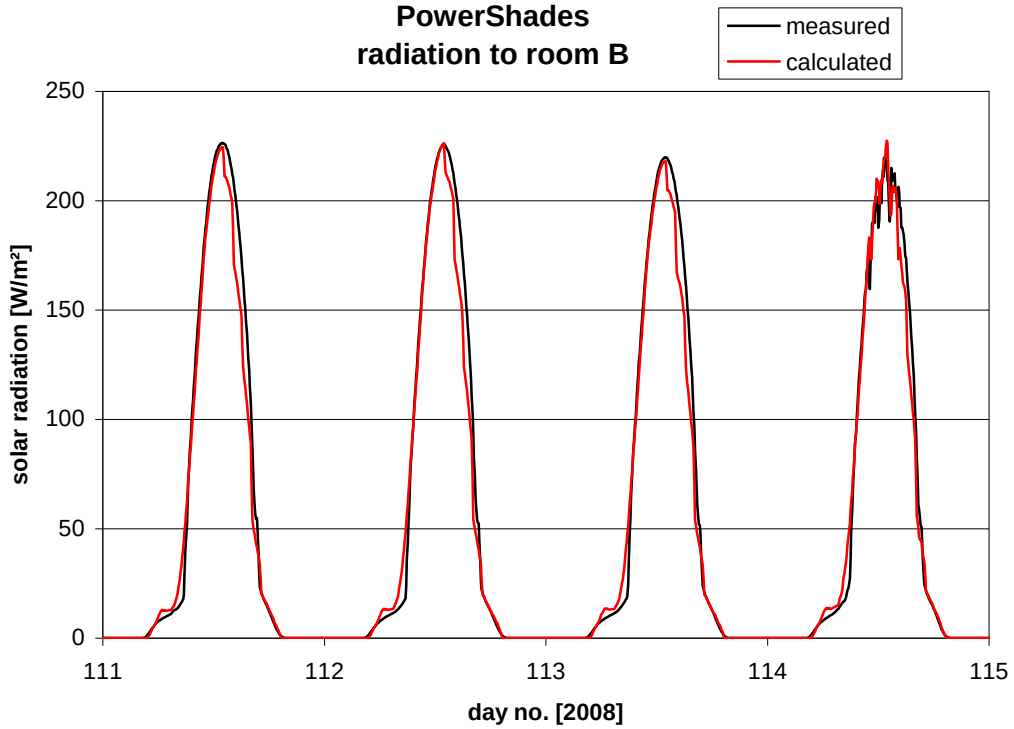

Figure 5.29. Measured and calculated radiation through the Velfac sun 1/clear windows - 21-24/4, 2008. Whit shading.

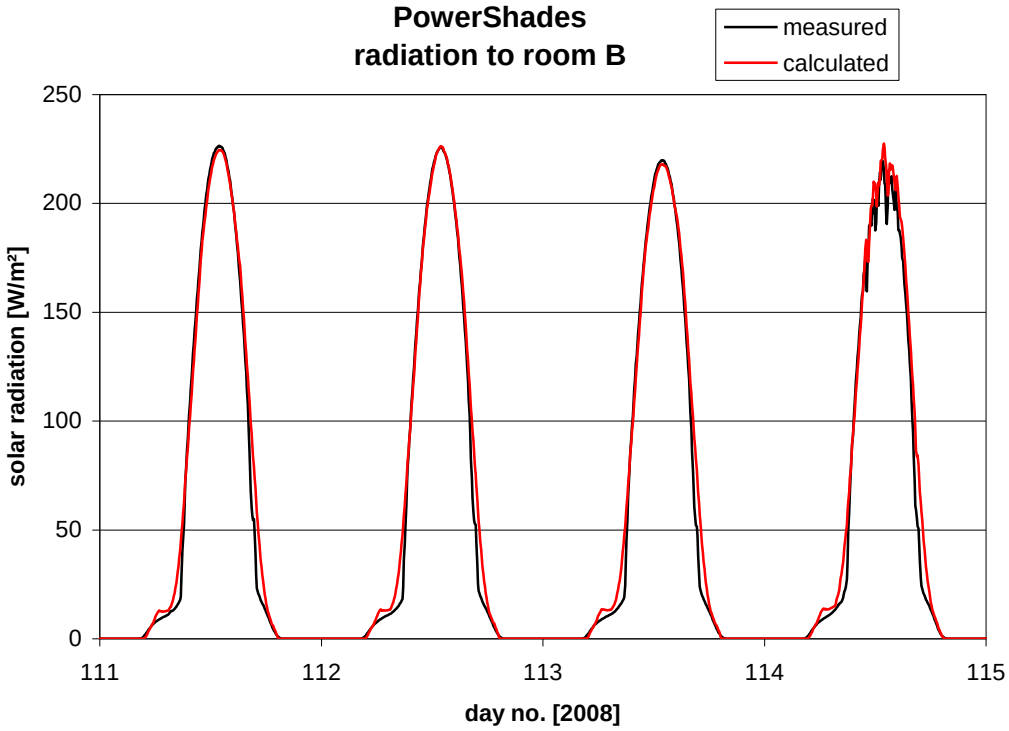

Figure 5.30. Measured and calculated radiation through the Velfac sun 1/clear windows - 21-24/4, 2008. Whit shading.

5.2.2.1.1. Summer

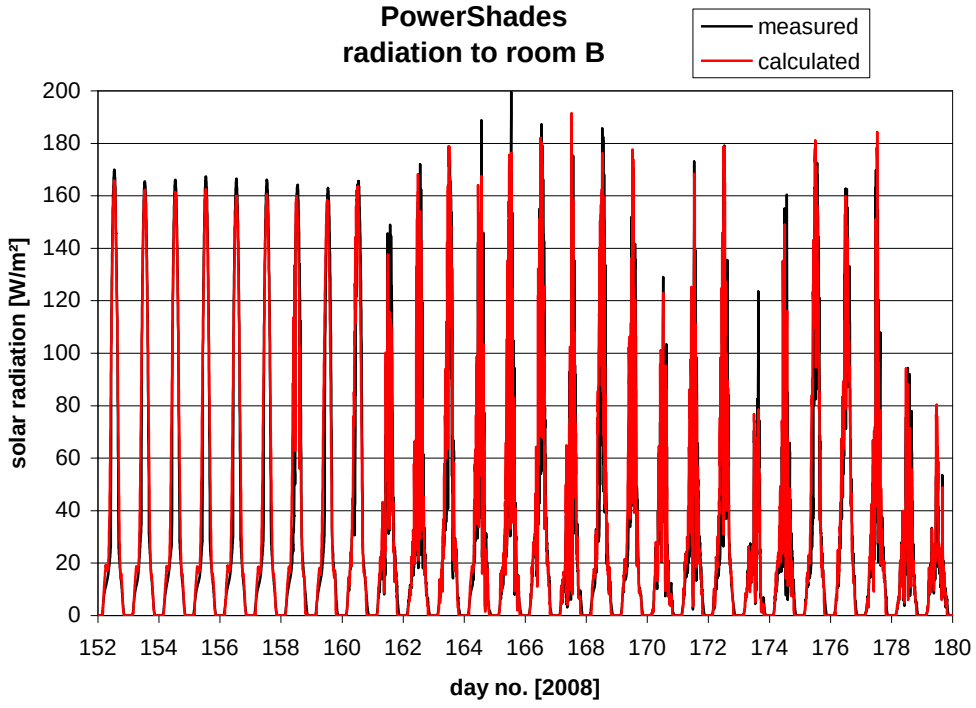

Figure 5.31. Measured and calculated radiation through the Velfac sun 1/clear windows – 1-28/6, 2008. Without shading.

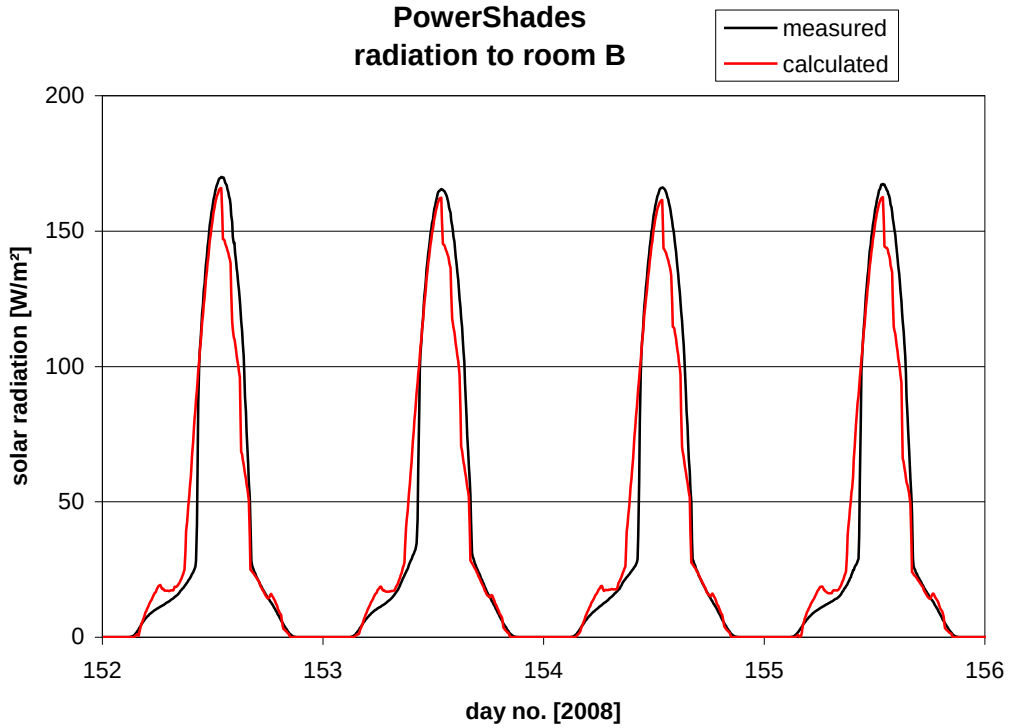

Figure 5.32. Measured and calculated radiation through the Velfac sun 1/clear windows – 1-4/6, 2008. Whit shading.

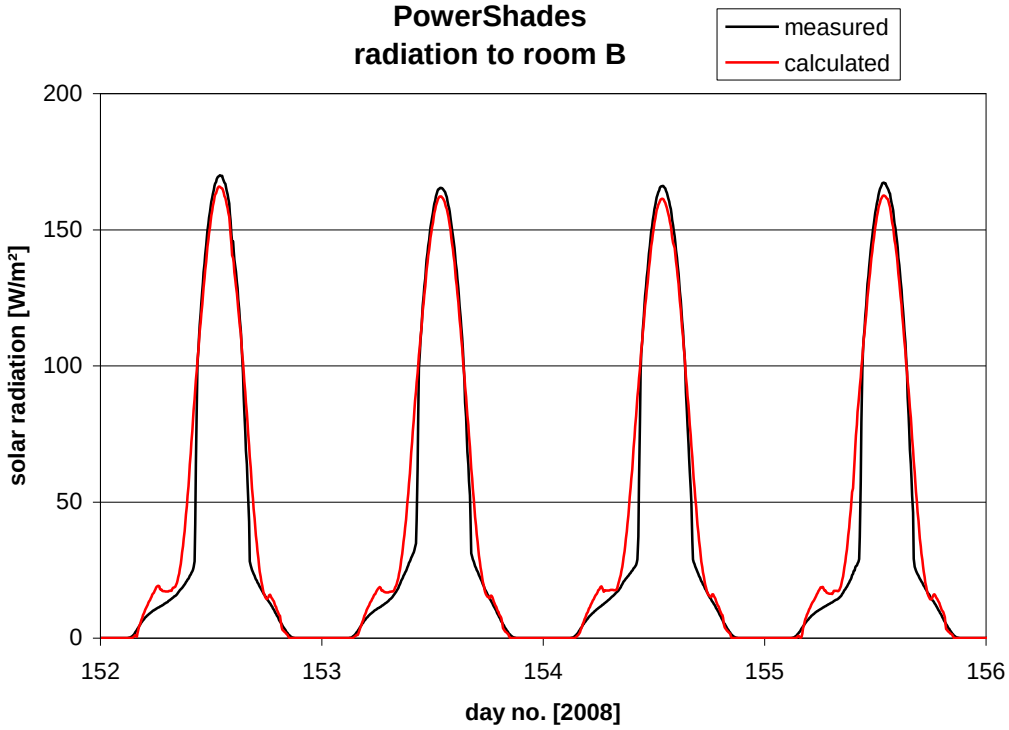

Figure 5.33. Measured and calculated radiation through the Velfac sun 1/clear windows – 1-4/6, 2008. Without shading.

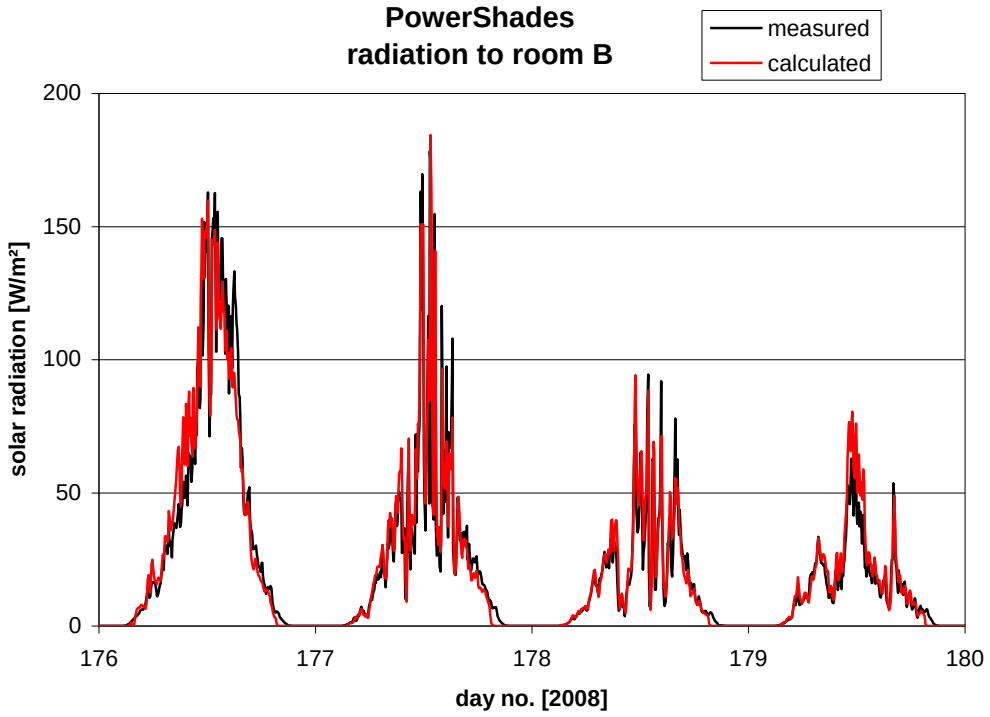

Figure 5.34. Measured and calculated radiation through the Velfac sun 1/clear windows – 25-28/6, 2008. With shading.

Figures 5.23-34 show that there is a very good agreement between measurements and calculations when the differences in shading are taken into consideration as explained for figures 5.21-22. The agreement is good for both clear sky, cloudy and overcast conditions.

The largest shown discrepancy for clear sky conditions is for day 45 (figure 5.25): 3.9 %. Alone for the measurements on the incoming solar radiation there is an uncertainty of around ± 5 %. The often higher discrepancy between measurements and calculations during cloudy and overcast conditions is of course due to the fact that the uncertainty on the calculated radiation hitting the facades is high – see figures 5.10, 5.11, 5.13 and 5.17. However, the energy content of the solar radiation during cloudy/overcast conditions is low so the higher discrepancy wills not here have a large impact on the indoor climate in the rest room. And further – when making parametric studies the same weather data will be applied in all simulations so that uncertainties as shown in figures 5.10, 5.11, 5.13 and 5.17 will not influence the result

Based on the above it is concluded that the model of the original Velfac window shown in table 5.3 and figure 5.19 gives a good description of the optical performance of the Velfac windows although the model is somewhat away from the starting point (table 5.2). However, the optical properties have only been measured for an incidence angle of 0°. The other values in table 5.2 are estimated based on general knowledge on glass – not specific knowledge on the considered window.

The model in table 5.3 and figure 5.19 will, therefore, be used in chapter 5.2.3 when modelling the thermal performance of room B.

5.2.2.2. Calibration of the model of PowerShades

PowerShades are as already mentioned a micro structure of small holes. Figure 5.35 shows an example of PowerShades. PowerShades consists of many small super elliptic shaped holes etched from each side of a thin metal foil. When etching from each side of the foil the holes are vertically displaced a little as seen in figure 5.35. In this way the foil will have more or less the same function as Venetian blinds, however, different appearance and view out as seen in chapter 2. The screening off and view out through PowerShades is determined by the shape of the holes in figure 5.35.

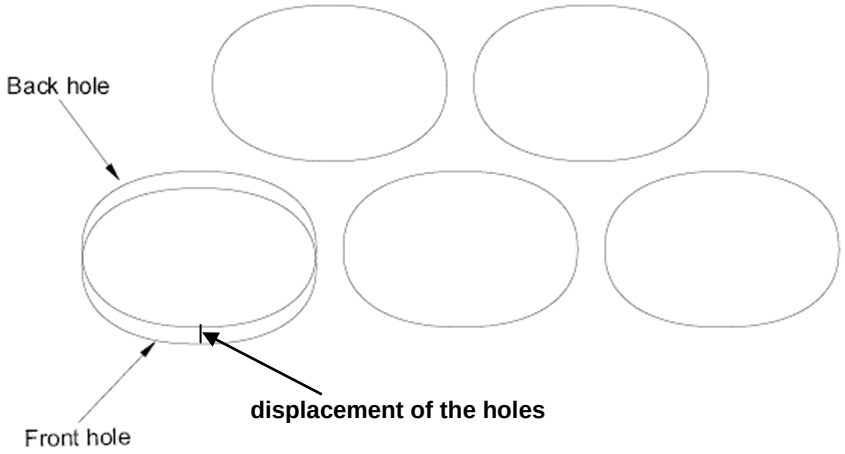

Figure 5.35: Example of the holes in a PowerShade.

The model of PowerShades is a matrix where the total direct transmission, the absorption in each layer of the window and the enhancement in incoming diffuse radiation due to the scattering of direct radiation in the PowerShades are listed for combinations of the horizontal and vertical incidence angle at steps of 5^{o}. The values of the matrix is generated by a spreadsheet where the main parameter is the projected hole area seen by the sun at different incidence angles and optical properties of PowerShades and glass.

The main goal of the calibration of the PowerShade model is to determine if the transmitted solar radiation is in agreement with the measured incoming solar radiation to room A. Normally when simulating the solar radiation through windows the solar radiation is split into direct solar radiation and diffuse solar radiation which are treated separately. For traditional windows the direct solar radiation is treated as shown in e.g. figure 5.19 dependent on the resulting incidence angle (not split into the vertical and horizontal incidence angle as for PowerShades). Diffuse radiation is normally - based on experience - treated also by using the values in figure 5.19 but with a fixed incidence angle of 55-60°. The latter cannot be done for PowerShades. There is no experience for determination of the diffuse radiation through Power Shades, so another approach must be applied.

5.2.2.2.1. Calibration of the model for diffuse radiation through PowerShades

The approach chosen for determination of the transmittance of diffuse radiation is to divide the measured solar radiation to room A with the measured solar radiation on the façade during days with overcast conditions – i.e. days with only diffuse radiation. An example of this is shown in figure 5.36. Figure 5.36 shows the solar radiation on the façade and to room A together with the ration between these two values (= transmittance of diffuse radiation). Unfor-

tunately only few days with overcast conditions were available during the first half year of 2008. The ratio between solar radiation to the room and on the façade for 9 days is shown in figure 5.37 dependent both on the day no. and on the solar height.

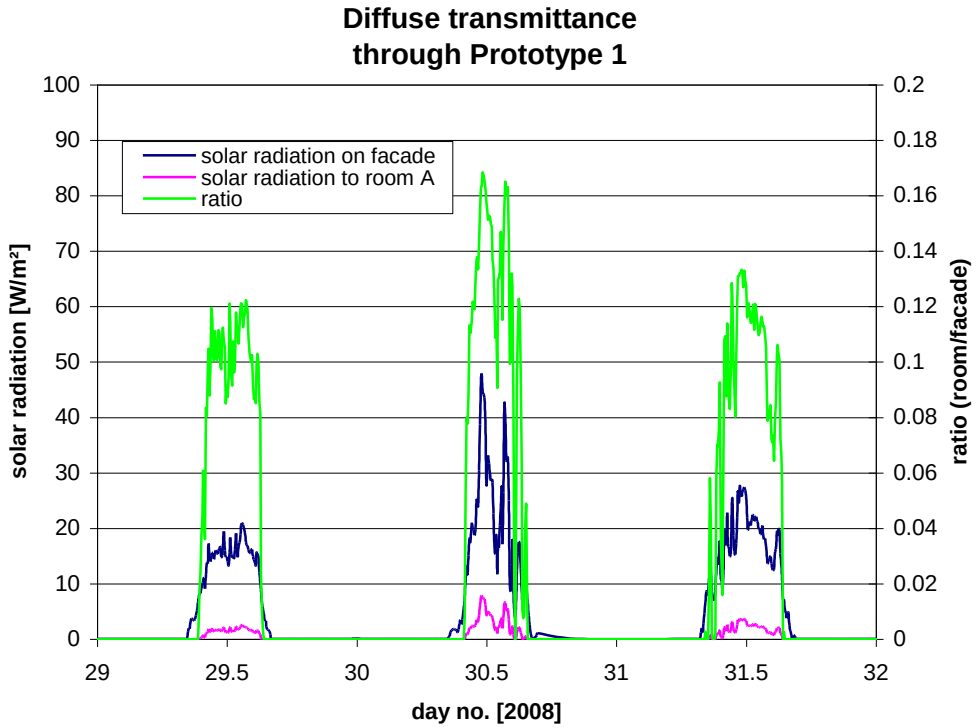

Figure 5.36. The solar radiation on the façade and to room A together with the ratio (= transmittance of diffuse radiation) for three days in January 2008 with overcast conditions – see figure 5.3.

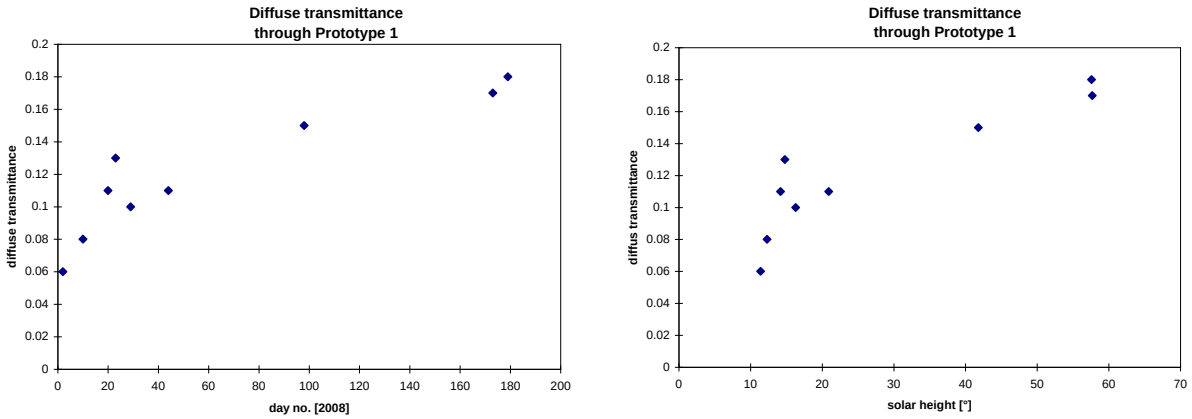

Figure 5.37. The transmittance of diffuse radiation dependent on day no. and solar height.

The transmittance of diffuse radiation increases with the day no. and solar height. It should not be so when knowing the nature of diffuse radiation. However, when looking at figure 5.5 it is seen that day 178 and 179 is not fully overcast. Further the solar radiation to room A is very low during the start of January which makes the calculation of the transmittance very uncertain. Based on this it was decided to use a mean value of 0.12 as the transmittance of diffuse radiation.

A similar investigation for PowerShades PS4060 using data from 2007 reviled that the transmittance of diffuse radiation also was around 0.12 although the opening area of these PowerShades was lower than for Prototype 1. This highlights the need for further research concerning determination of the transmittance of diffuse radiation through PowerShades. There is a need for a method for calculation of the diffuse transmittance without using measurements.

5.2.2.2.2. Calibration of the model of PowerShades – model 121107

The transmittance of diffuse radiation was applied in a model of Prototype 1 called 121107. Table 5.4 shows the top of the matrix of 121107.

```
*BIDIRECTIONAL
*types,1
*item,121107
*layers,5,glass1,shading,glass2,air,glass3
*sets,1 # there is only this set of optical data
*start_set
*diffuse_abs,0.036,0.372,0.013,0.000,0.042
*diffuse_trn,0.12
*direct_angs,37,37
*data
#Incidence angle, Total Glass 1, Shading device, Glass 2, Air, Glass 3, Converted diffuse fraction
#HorizontVertical, Transmittance, Absorb, Absorb, Absorb, Absorb, Absorb, Direct-diffuse
#Degrees, Degrees
-90 -90 0 0 0 0 0 0 0
-90 -85 0 0 0 0 0 0 0
-90 -80 0 0 0 0 0 0 0
-90 -75 0 0 0 0 0 0 0
-90 -70 0 0 0 0 0 0 0
-90 -65 0 0 0 0 0 0 0
-90 -60 0 0 0 0 0 0 0
-90 -55 0 0 0 0 0 0 0
-90 -50 0 0 0 0 0 0 0
-90 -45 0 0 0 0 0 0 0
-90 -40 0 0 0 0 0 0 0
-90 -35 0 0 0 0 0 0 0
-90 -30 0 0 0 0 0 0 0
-90 -25 0 0 0 0 0 0 0
-90 -20 0 0 0 0 0 0 0
-90 -15 0 0 0 0 0 0 0
-90 -10 0 0 0 0 0 0 0
-90 -5 0 0 0 0 0 0 0
-90 0 0 0 0 0 0 0 0
-90 5 0 0 0 0 0 0 0
-90 10 0 0 0 0 0 0 0
-90 15 0 0 0 0 0 0 0
-90 20 0 0 0 0 0 0 0
-90 25 0 0 0 0 0 0 0
-90 30 0 0 0 0 0 0 0
-90 35 0 0 0 0 0 0 0
-90 40 0 0 0 0 0 0 0
-90 45 0 0 0 0 0 0 0
-90 50 0 0 0 0 0 0 0
-90 55 0 0 0 0 0 0 0
-90 60 0 0 0 0 0 0 0
-90 65 0 0 0 0 0 0 0
-90 70 0 0 0 0 0 0 0
-90 75 0 0 0 0 0 0 0
-90 80 0 0 0 0 0 0 0
-90 85 0 0 0 0 0 0 0
-90 90 0 0 0 0 0 0 0
-85 -90 0 0 0 0 0 0 0
-85 -85 0 0.022 0 0 0 0 0
-85 -80 0 0.039 0.003 0 0 0 0
-85 -75 0 0.039 0.02 0 0 0 0.001
-85 -70 0 0.039 0.035 0 0 0 0.002
-85 -65 0 0.039 0.05 0 0 0 0.003
```

diffuse transmittance

1th column: azimuth
2th column: solar height
3th column: total direct transmittance
4th column: absorption in the outer layer of glass
5th column: absorption in the PowerShade foil
6th column: absorption in the in the glass behind the PowerShade foil
7th column: absorption in the air gab of the window
8th column: absorption in the inner layer of glass
9th column: enhancement of diffuse radiation due to scattering of direct radiation in the PowerShade fail

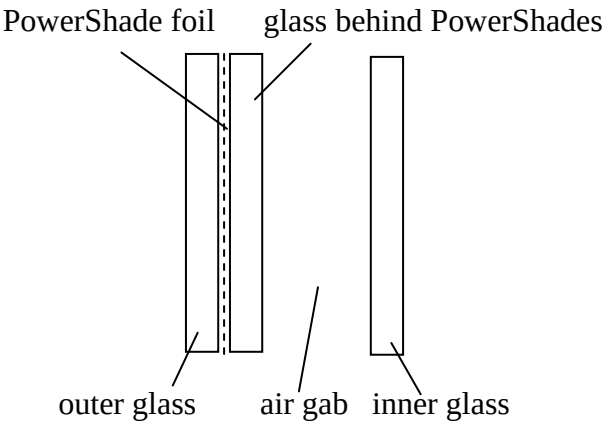

Table 5.4. Example PowerShade matrix. The matrix covers azimuths and solar heights from -90 to 90 ^{o} with steps of 5 ^{o}.

The 9 columns after the starting text contains as described in table 5.4 the total direct transmission, the absorption in each layer of the window and the enhancement of incoming diffuse radiation due to the scattering of direct radiation in the PowerShades, These are listed for combinations of the horizontal and vertical incidence angle at steps of 5^{o}.

Before calibrating the model 121107 it is necessary to discus an uncertainty in the measured solar radiation entering room A due to the fact that Prototype 1 as seen in figure 2.6 is not homogeneous. There are opaque stripes with a height of 3.5 mm for each 56.5 mm. These stripes are not considered in model 111207 but will be introduced later.

The problem is illustrated in figure 5.38. The diameter of the measuring area of the Epply pyranometer is 15 mm while the distance between the opaque stripes of the PowerShades is 56.5 mm. The horizontal distance between the glass with the PowerShades and the measuring area of the Epply pyranometer is 45 mm. The pyranomter is located in such a way, that the opaque stripes don't shade off direct solar radiation on the measuring area of the pyranometer at noon. However the opaque stripes shade off some diffuse radiation (figure 5.38) and some direct radiation at low solar height during the morning and afternoon - the pyranometer was located differently during the three measuring periods in order to obtain no shading on the measuring field of the pyranometer at noon. This should be remembered when inspecting the following graphs.

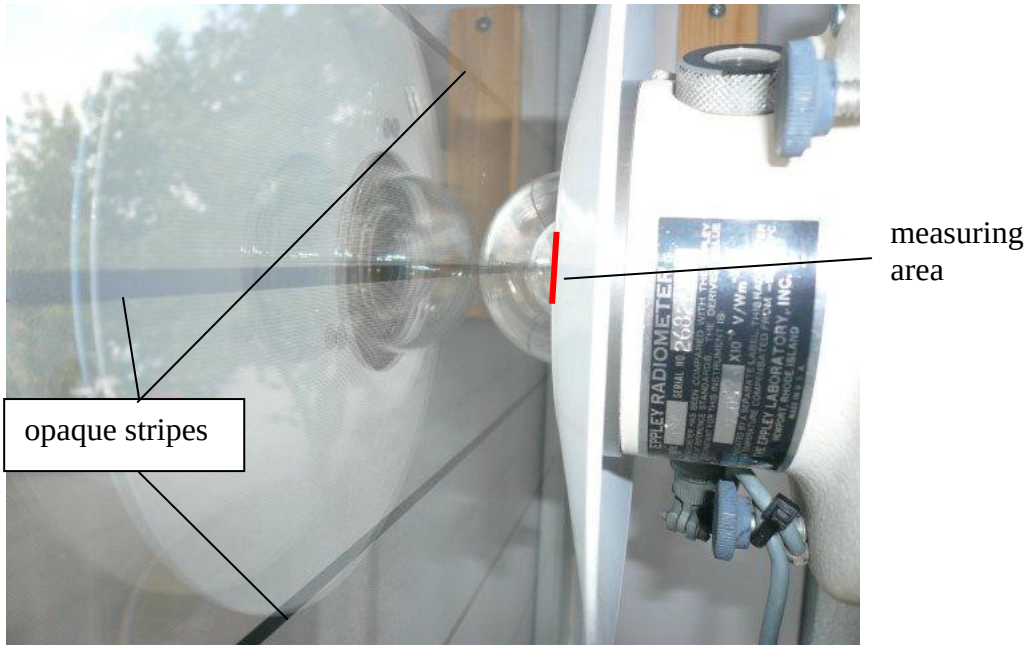

Figure 5.38. The Eppley pyranometer behind Prototype 1 – 22/5, 2008.

Measured date for same periods as in the former chapters will be utilized for the calibration of the model of PowerShades. However, as for the Velfac window the influence of shading will first be evaluated.

Figures 5.39-40 shows a comparison between measured and calculated solar radiation entering room A on a sunny summer day with and without considering shading in the simulations. The calculated results with and without shading is very similar except for a little influence from the column between the test rooms in the morning. For that reason curves without shad-

ing will only be shown in the following as the jagged appearance of the curves with shading confuses a bit the comparison between measured and calculated values. When looking at the measured curve it seems that the opaque stripes of the PowerShades has no obviously influence on the measured values except maybe at the arrows in figure 5.39. It will, therefore, be assumed that the measurements are not influenced for the main part of the measurements – at least not for clear sky conditions. The measured values at overcast may be a little bit too small – based on view factor calculation it is assumed, that the measurements under these conditions is about 3 % too low, which is below the uncertainty of the measurements.

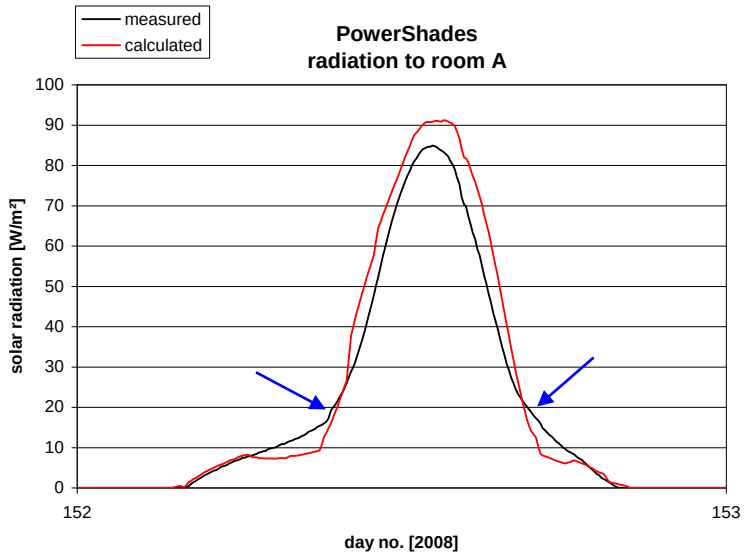

Figure 5.39. Measured and calculated (with shading) solar radiation to room A – 1/6, 2008.

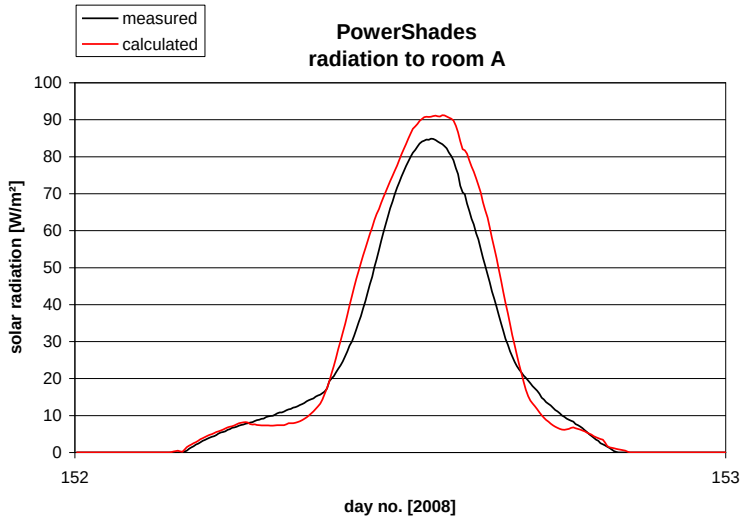

Figure 5.40. Measured and calculated (without shading) solar radiation to room A – 1/6, 2008.

Figures 5.41-50 shows the result from comparison between measured and calculated solar radiation entering room A when using model 121107 for Prototype 1 installed in room A – and with no shading in the model except for the winter period, where the same spikes as in figure 5.26 is seen. For this period comparison with and without shading is shown for clear sky conditions and with shading for overcast conditions.

5.2.2.2.2.1 Winter 2008

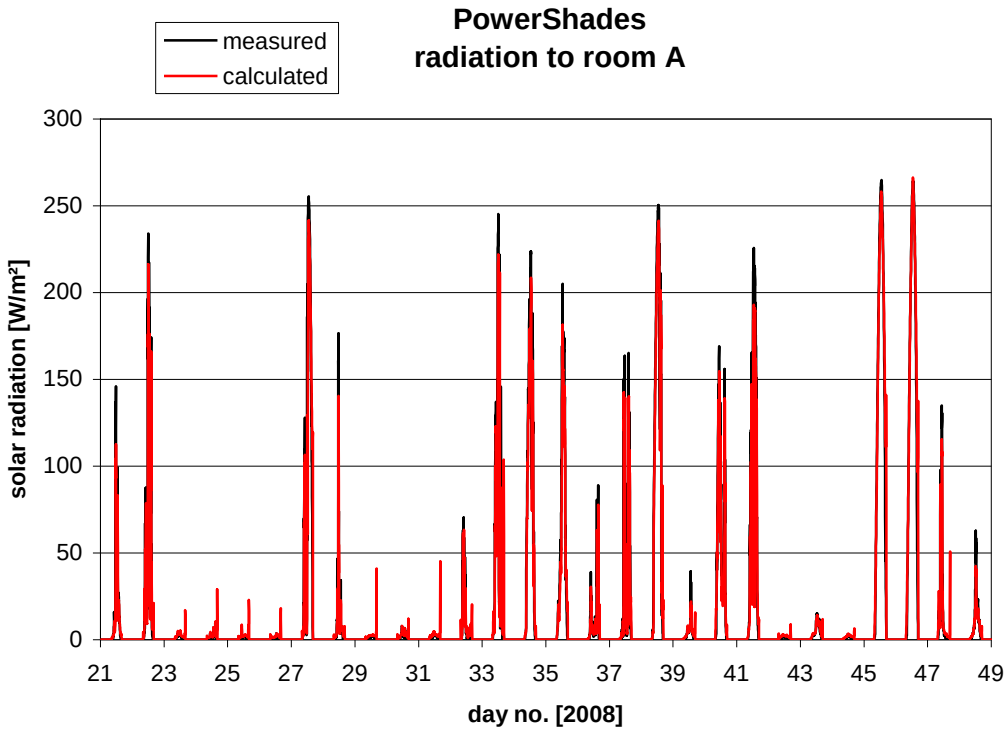

Figure 5.41. Measured and calculated solar radiation to room A – 21/1-17/2, 2008. With PowerShade model 121107 and without shading.

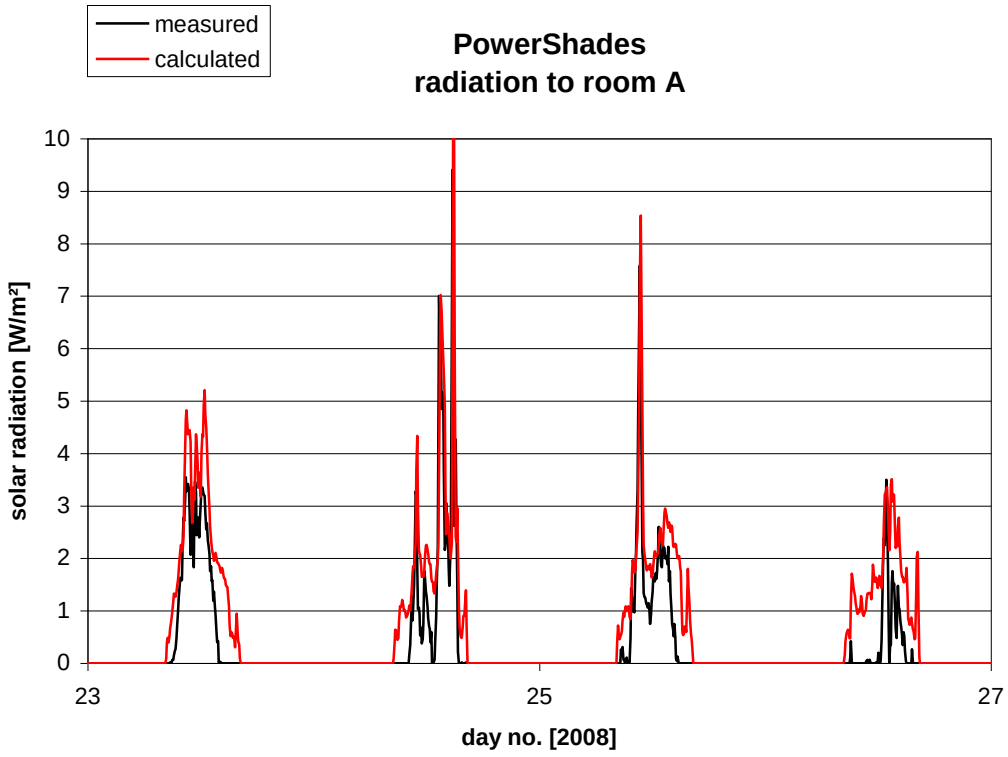

Figure 5.42. Measured and calculated solar radiation to room A – 23-26/1, 2008. With PowerShade model 121107 and with shading.

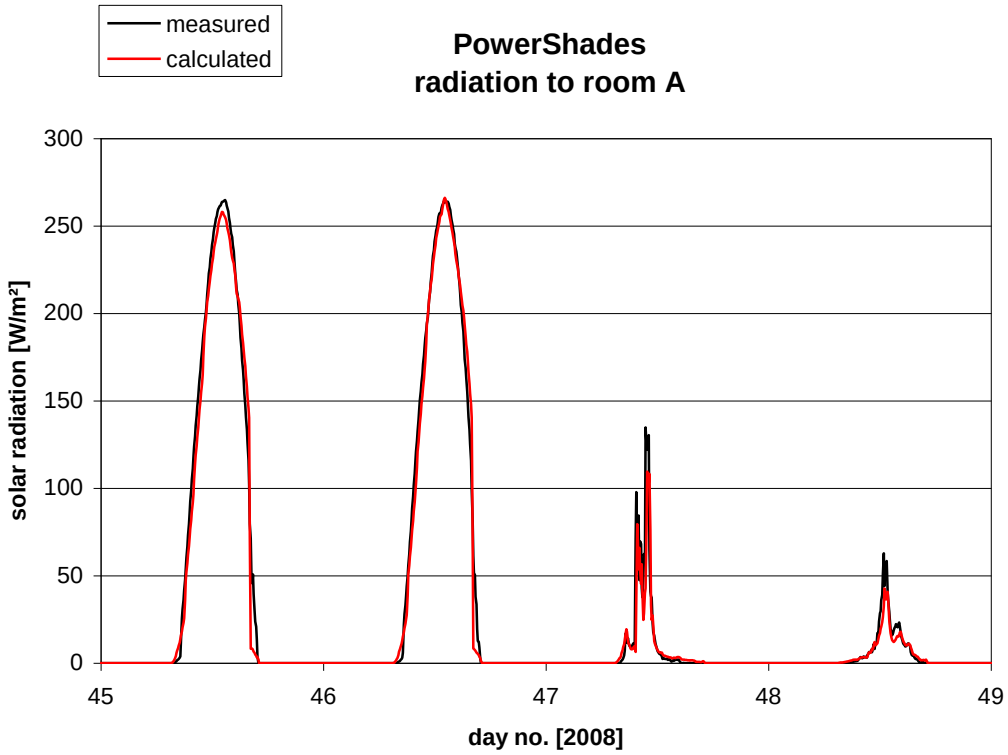

Figure 5.43. Measured and calculated solar radiation to room A – 14-17/2, 2008. With PowerShade model 121107 and with shading.

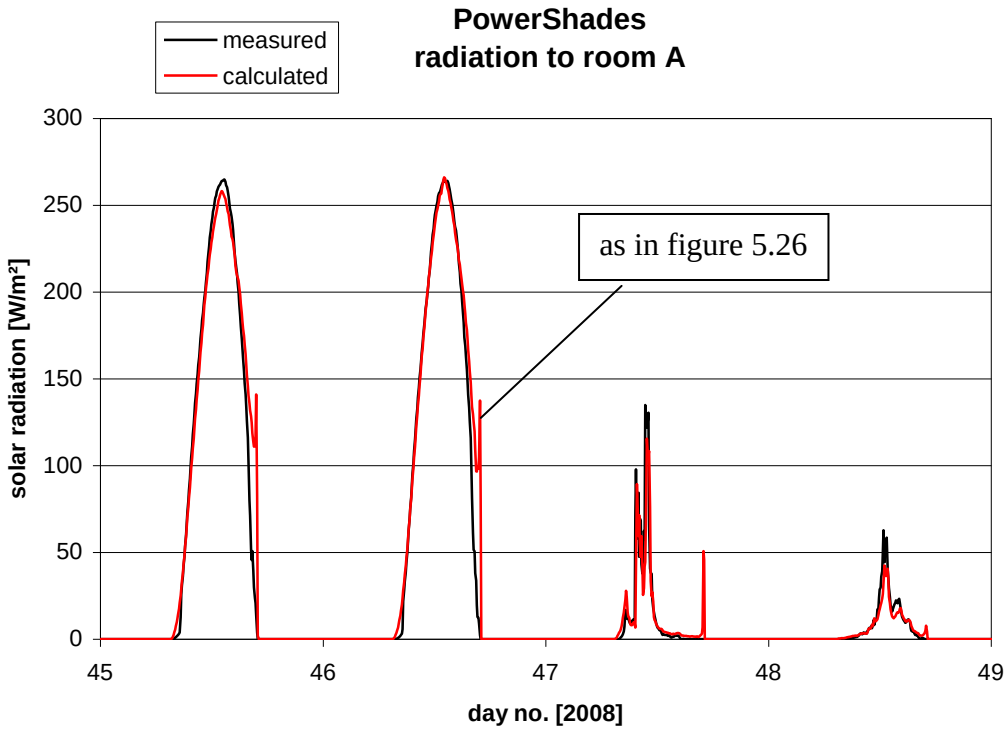

Figure 5.44. Measured and calculated solar radiation to room A – 14-17/2, 2008. With PowerShade model 121107 and without shading.

5.2.2.2.2.2 Spring 2008

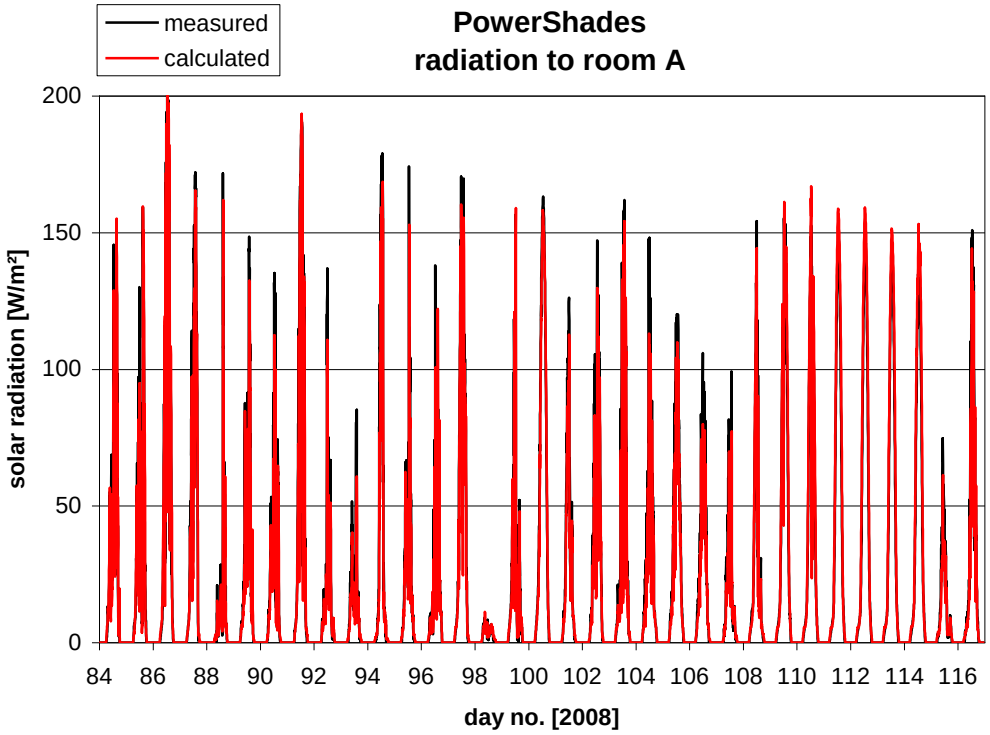

Figure 5.45. Measured and calculated solar radiation to room A – 25/3-26/4, 2008. With PowerShade model 121107 and without shading.

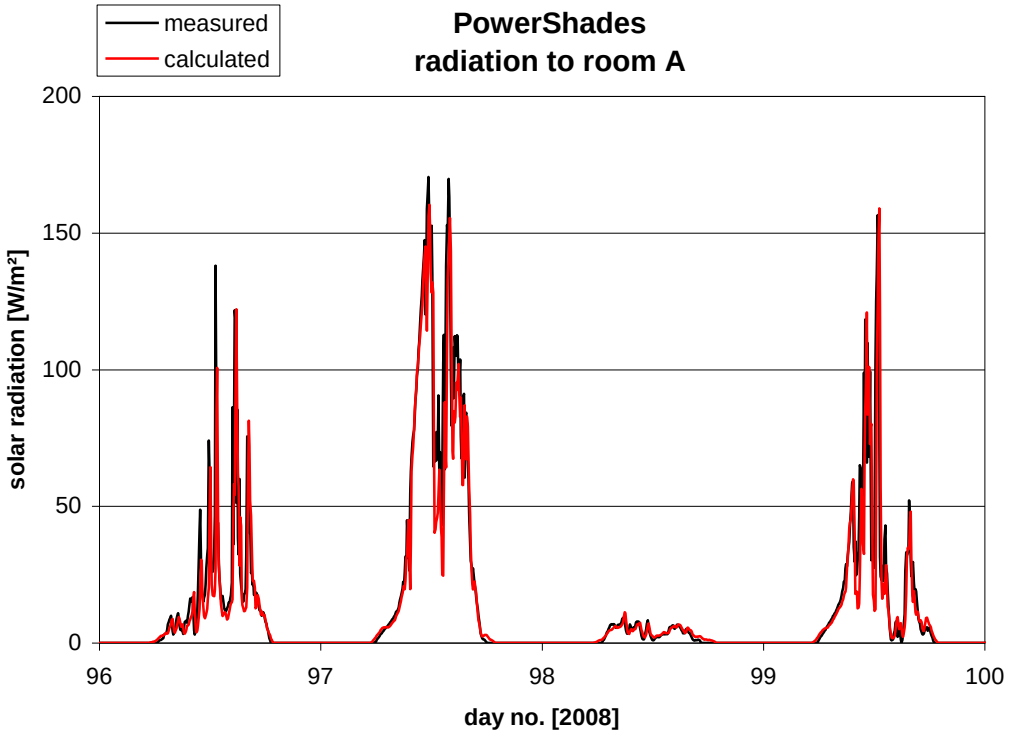

Figure 5.46. Measured and calculated solar radiation to room A – 6-9/4, 2008. With Power-Shade model 121107 and without shading.

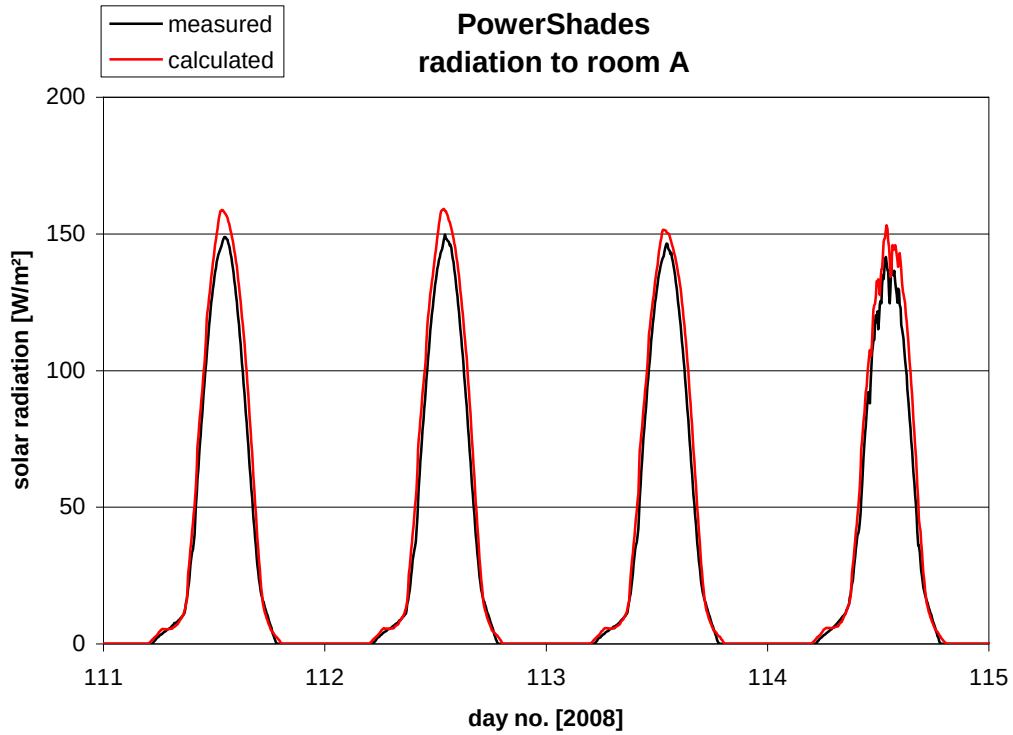

Figure 5.47. Measured and calculated solar radiation to room A – 21-24/4, 2008. With PowerShade model 121107 and without shading.

5.2.2.2.2.3 Summer 2008

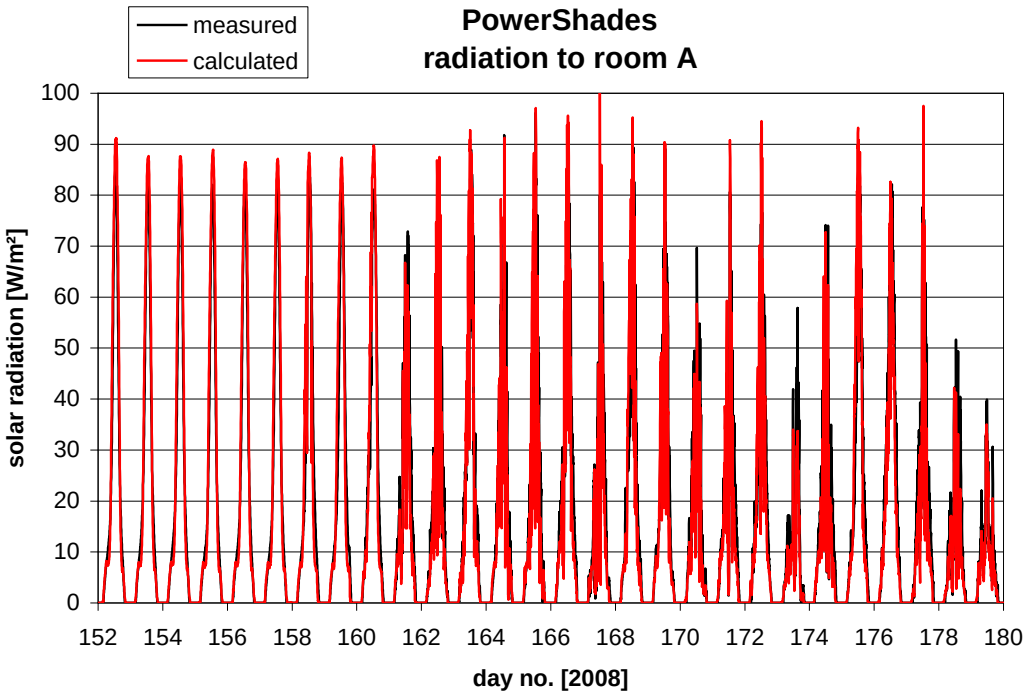

Figure 5.48. Measured and calculated solar radiation to room A – 1-28/6, 2008. With PowerShade model 121107 and without shading.

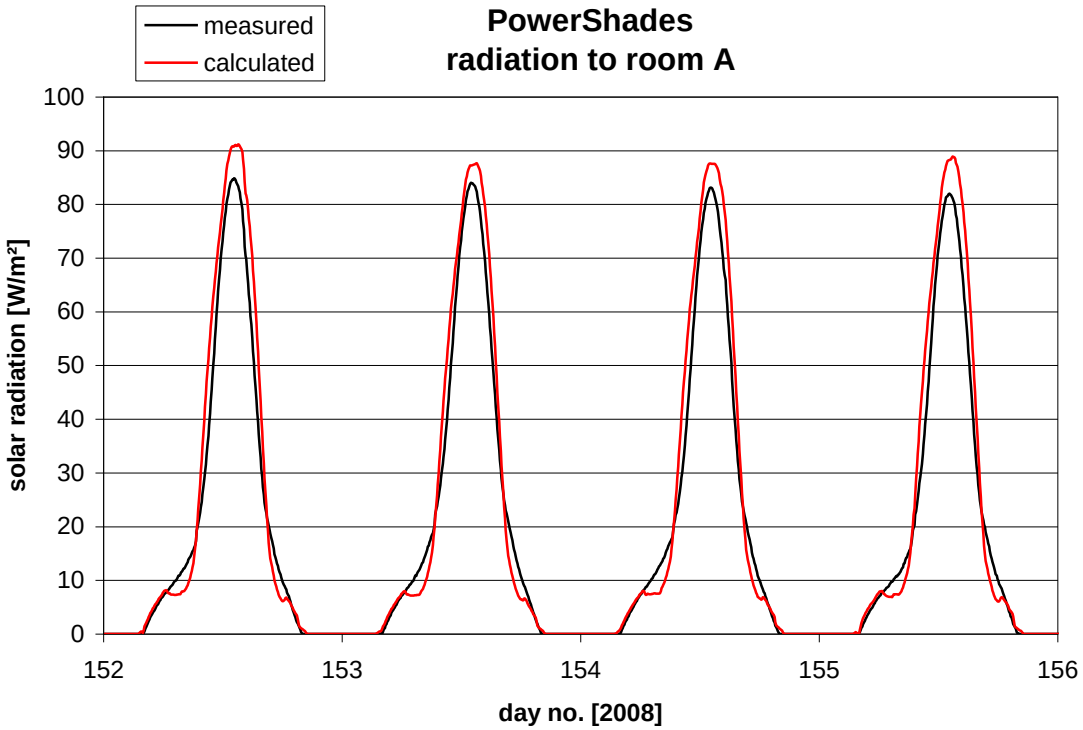

Figure 5.49. Measured and calculated solar radiation to room A – 1-4/6, 2008. With PowerShade model 121107 and without shading.

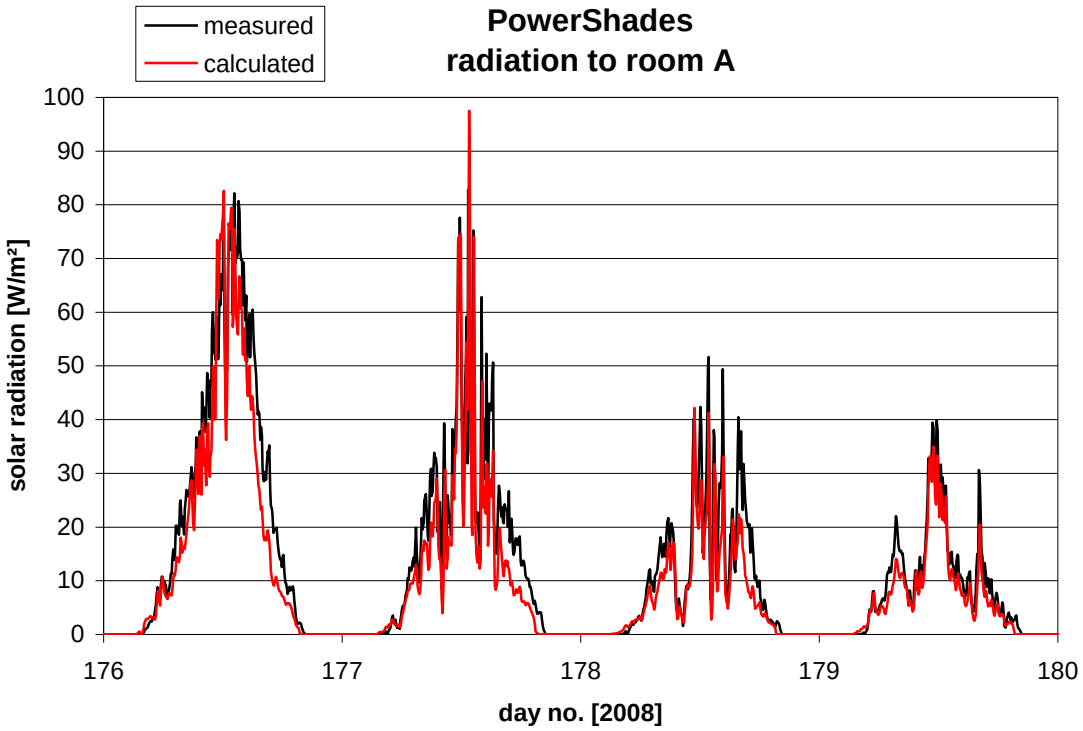

Figure 5.50. Measured and calculated solar radiation to room A – 25-28/6, 2008. With PowerShade model 121107 and without shading.

5.2.2.2.2.4 Conclusions

Winter
Figures 5.43-44 shows a very good agreement between measured and calculated incoming solar radiation during clear sky conditions. The figures also show a good agreement during cloudy conditions.

Figure 5.42, however, shows a less good agreement at totally overcast conditions, but as the power of the incoming solar radiation here is below 10 W and most often below 3 W the high discrepancy doesn't really matter.

Spring
Figure 5.46 shows very good agreement between measurements and calculations at cloudy and overcast conditions. While figure 5.47 shows calculated incoming solar radiation 4-6 % higher than measured at noon. The measured incoming solar radiation is also overestimated a couple of hours before and after noon, but in very good agreement during the early morning and late afternoon.

Summer
Figure 5.49 shows an discrepancy between the measurements and calculations between 5 and 8.4 % at noon and also here an overestimation of the calculated solar radiation around noon. The model, however, underestimate the incoming solar radiation in the early morning and late afternoon, when the first and last direct solar radiation hits the window. This is shown more clearly in figures 5.39-40.

Figure 5.50 shows a scattered agreement between measurements and calculations during cloudy and overcast conditions. However, not that bad when considering figure 5.37, where the diffuse transmittance during these days was found to around 0.18 while 0.12 is used in the model.

Conclusions
The incoming solar radiation is rather well represented in the model at cloudy and overcast conditions.

The model tents to overestimate the incoming solar radiation at high solar heights. During the summer the model underestimates the incoming solar radiation at high azimuts when direct solar radiation is present at the window.

The overestimation at noon is shown in figure 5.51. The right graph in figure 5.51 is transformed to at factor which should be multiplied with the total direct transmission in the matrix. This factor is shown in figure 5.52. The equation of the linearly regression is also shown in figure 5.52.

The equation $y = -0.0021x + 1.0529$ where x is the solar height has been multiplied with the total direct transmittance in the PowerShade model 121107 and a new model called 121107-1 was developed. This model has been used in simulations for the summer 2008 period. The result is shown in the following.

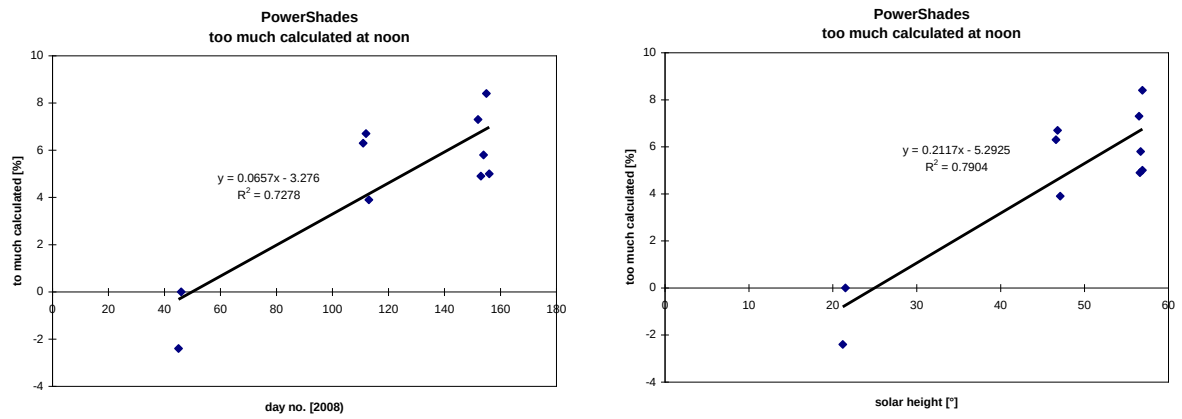

Figure 5.51. The overestimation of the solar radiation at noon dependent on day no. and solar height.

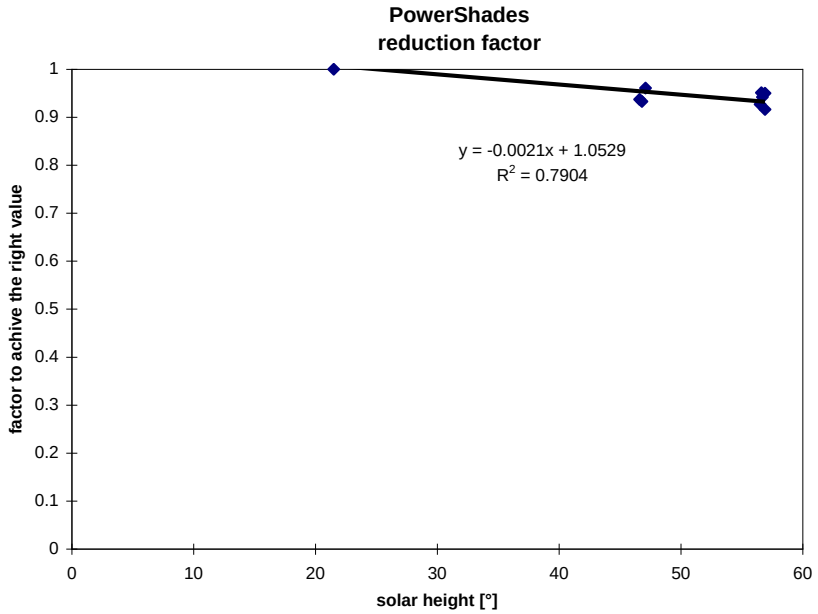

Figure 5.52. The factor for correction of the solar radiation at noon dependent on solar height.

5.2.2.2.3. Calibration of the model of PowerShades – model 121107-1

Figures 5.53-55 show the result of simulations with model 121107-1 for the winter period. Figure 5.53 shows that the calculated solar radiation now is in better agreement with the measured values at noon, however, figures 5.53-54 show that the calculated curve still has "wider shoulder" than the measured curve.

Figure 5.54 show that the calculated incoming radiation at cloudy and overcast conditions is almost unchanged except for at little smaller peak values, which is alright as seen in figure 5.50.

The "wider shoulders" are shown more clearly in figure 5.56 where the calculated values have been divided by the measured values. This is shown more clearly in figure 5.57 where the six days is put together in one day. Figure 5.58 shows the "mean" day of figure 5.57. In figure

5.59 figure 5.58 is transferred to a correction factor dependent of relative azimuth and a regression curve is found.

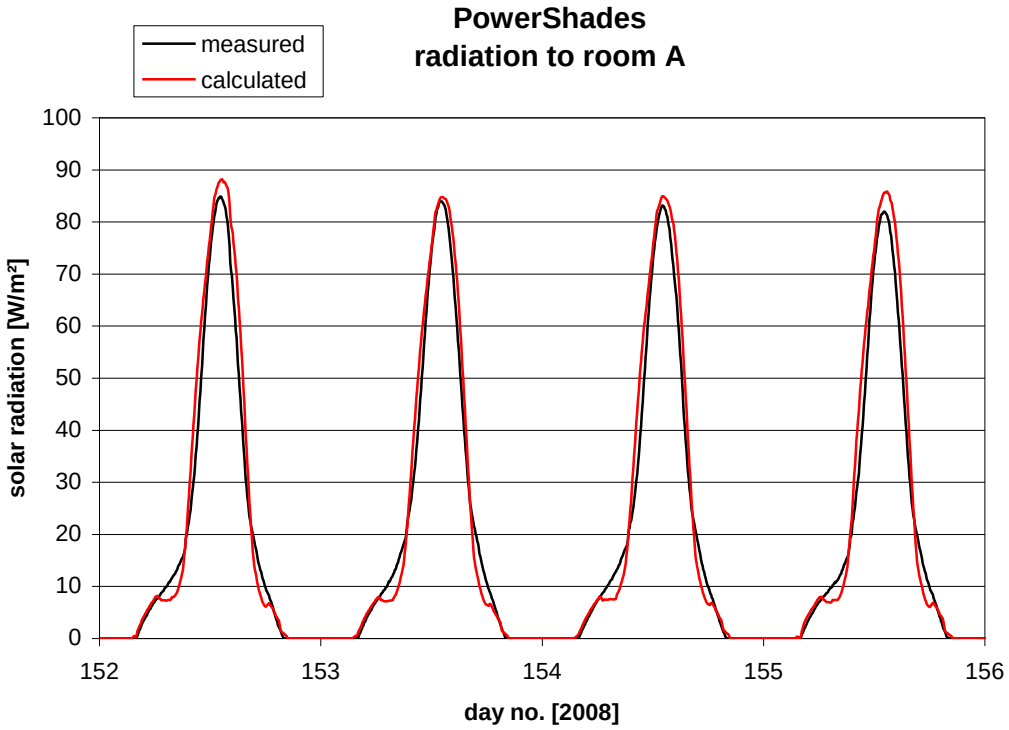

Figure 5.53. Measured and calculated solar radiation to room A – 1-4/6, 2008. With PowerShade model 121107-1 and without shading.

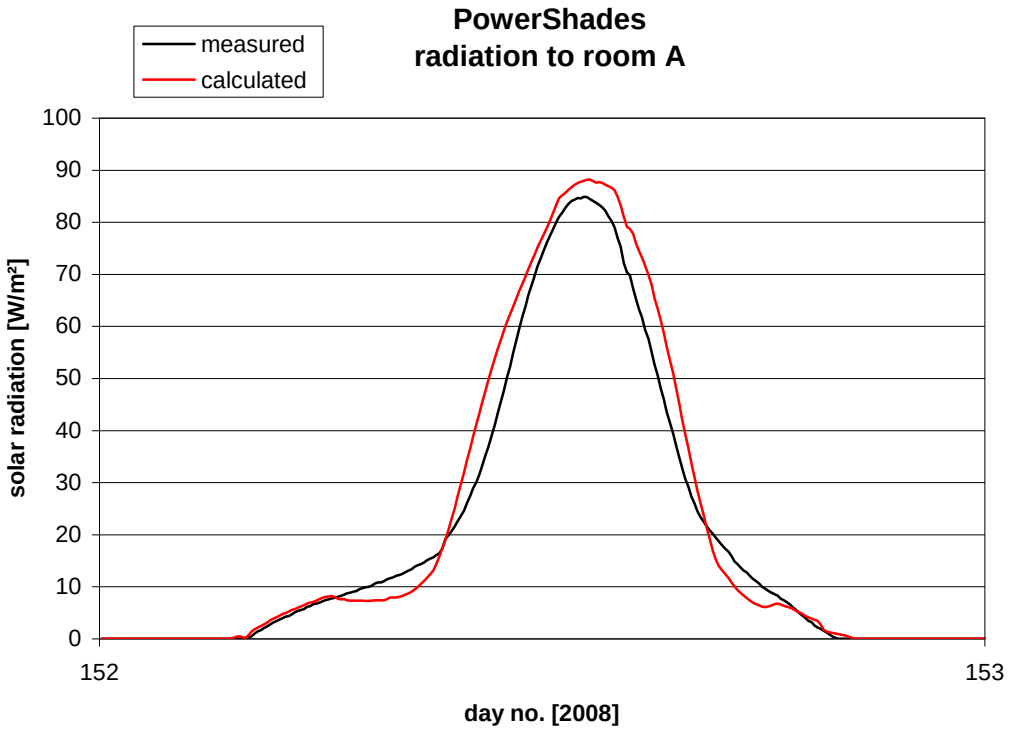

Figure 5.54. Measured and calculated solar radiation to room A – 1/6, 2008. With PowerShade model 121107-1 and without shading.

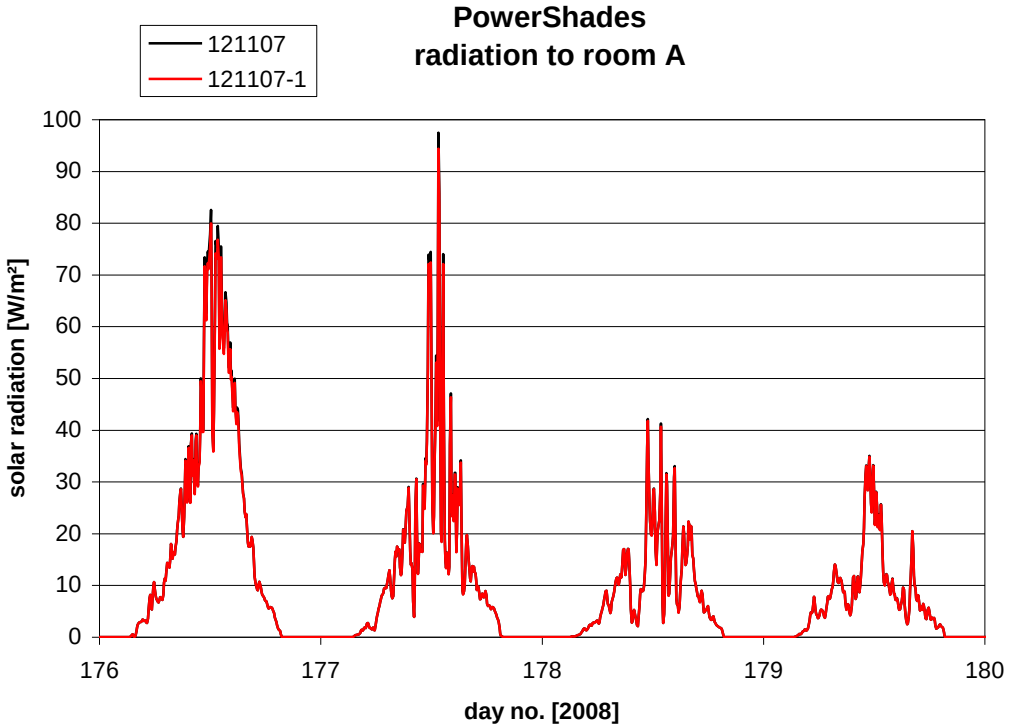

Figure 5.55. Calculated solar radiation to room A – 25-28/6, 2008 with 121107 and 121107-1. Without shading.

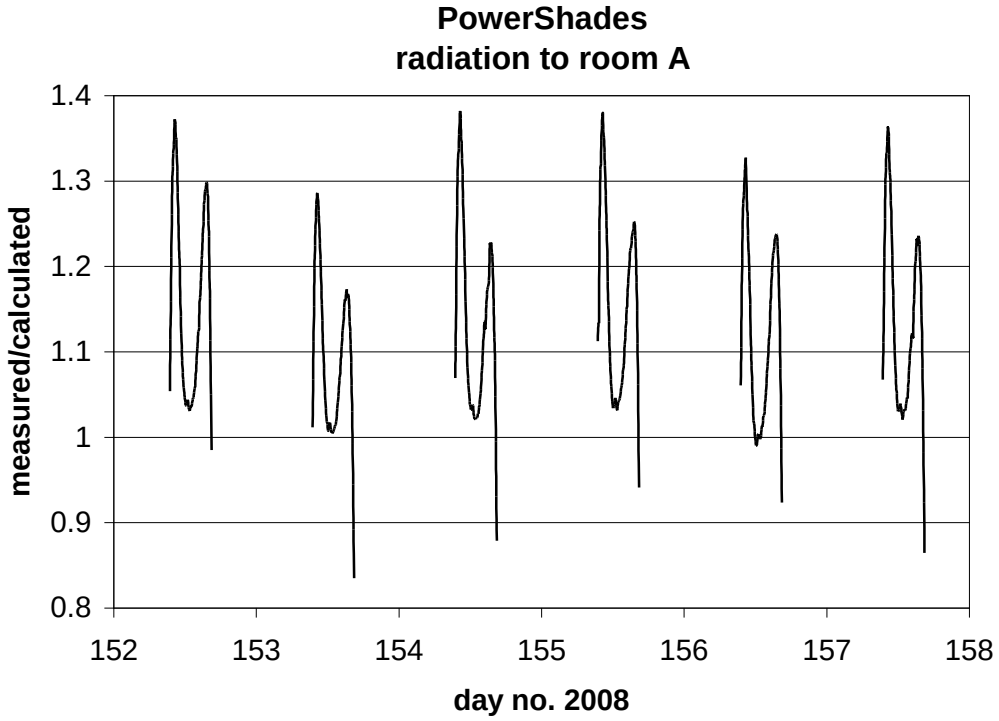

Figure 5.56. Calculated divided by measured solar radiation to room A – 1-6/6, 2008. With PowerShade model 121107-1 and without shading.

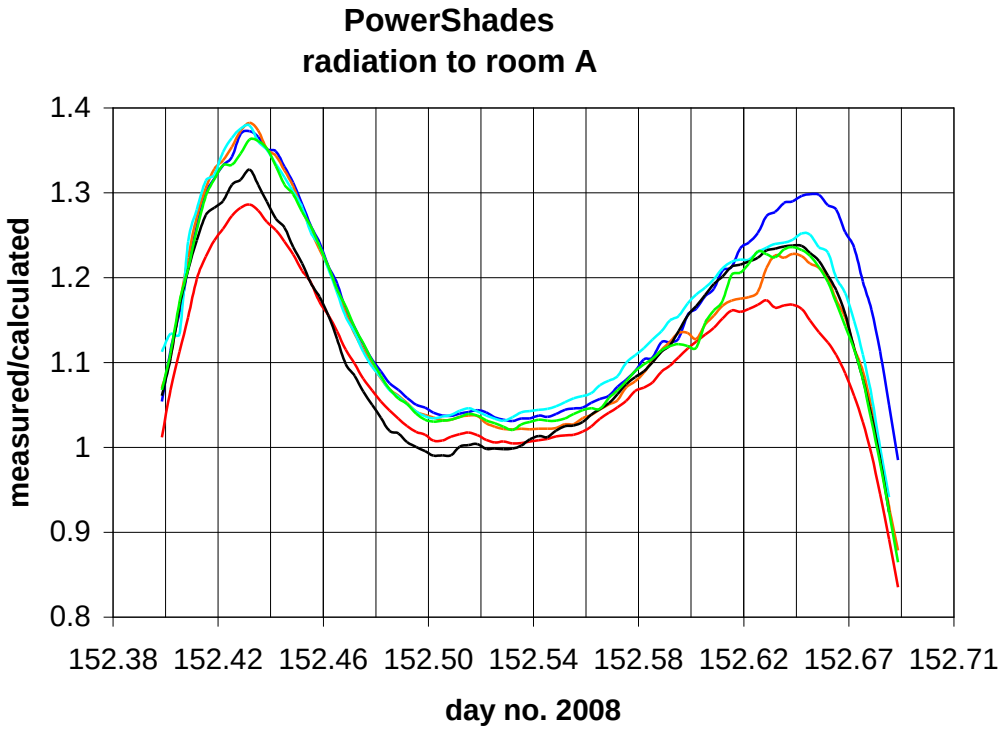

Figure 5.57. Calculated divided by measured solar radiation to room A put together in one day (day no. 152) – 1-6/6, 2008. With PowerShade model 121107-1 and without shading.

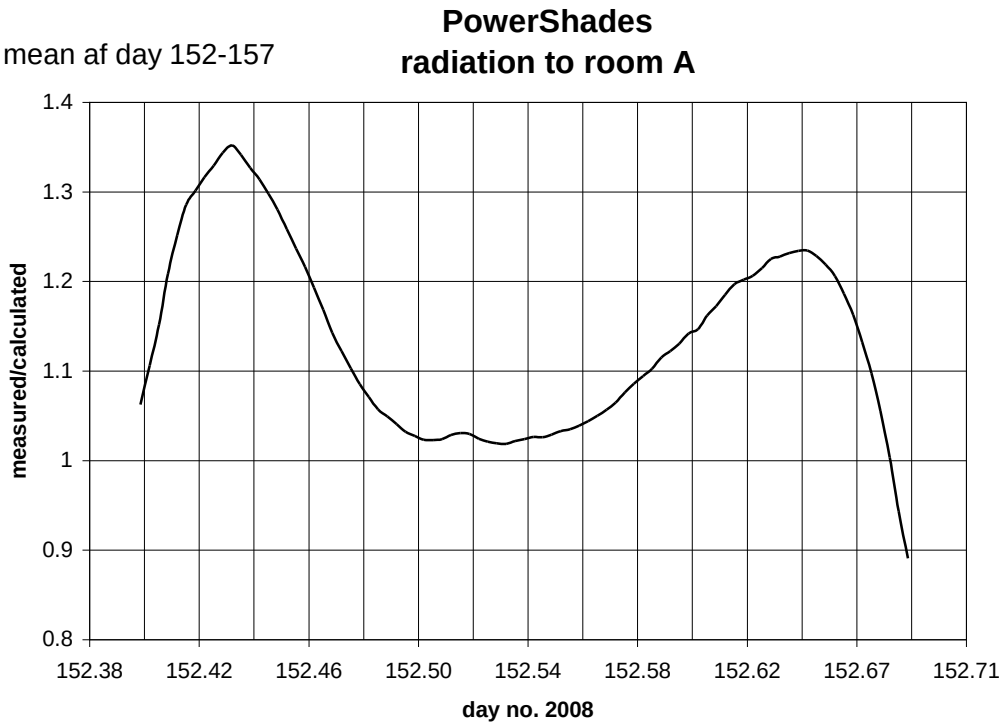

Figure 5.58. Calculated divided by measured solar radiation to room A. Mean values for 1-6/6, 2008. With PowerShade model 121107-1 and without shading.

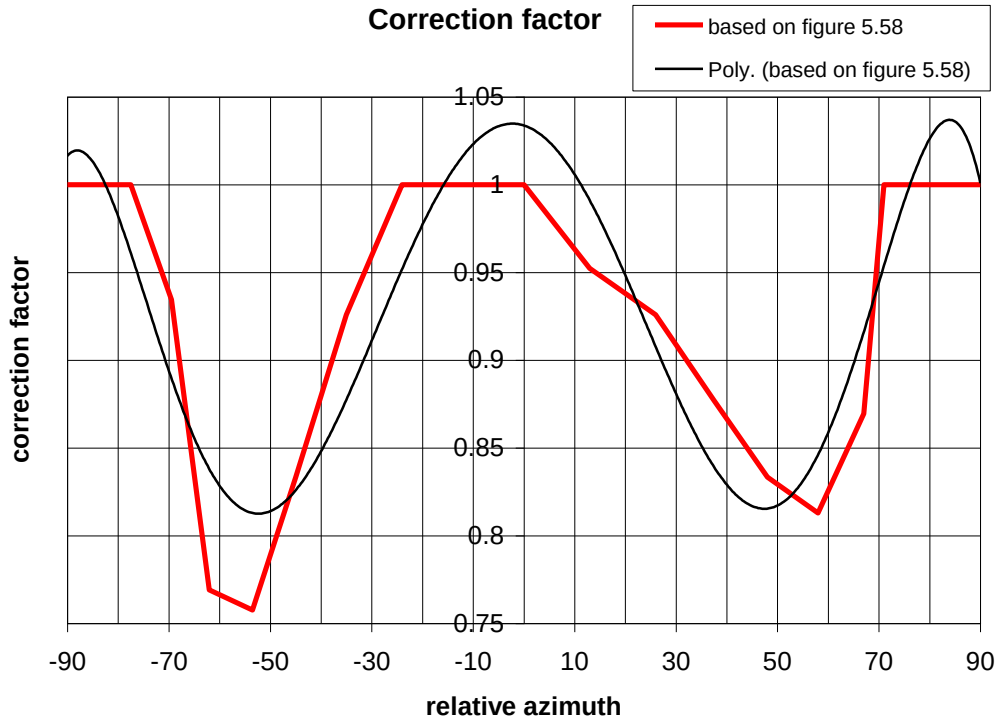

Figure 5.59. Correction factor for model 121107-1. Mean values for 1-6/6, 2008. Without shading.

The regression equation from figure 5.57:

$y = -3.6223*10^{-12}*x^6-4.9168*10^{-11}*x^5+5.343*10^{-8}*x^4+5*10^{-7}*x^3-.982*10^{-4}*x^2-9.108*10^{-4}*x+1.0338$

for $y < 1$, for $y \geq 1$ y is set to 1.

where: x is the relative azimuth. The relative azimuth is zero when the sun vertically is perpendicular to the façade.

has been multiplied with the total direct transmission in model 121107-1. This gives model 121107-2.

5.2.2.2.4. Calibration of the model of PowerShades – model 121107-2

Figures 5.60-62 show the result of simulations with model 121107-2 for the summer period. Figures 5.60-61 show better agreement between measured and calculated values – however, there is still room for improvement.

Figure 5.62 shows as 5.55 that the calculated incoming radiation at cloudy and overcast conditions is almost unchanged except for at little smaller peak values.

Figures 5.63-65 shows results from applying model 121107-2 on the spring period. Figures 5.63-64 shows very good agreement while figure 5.65 again shows that not much have been changed when looking at overcast days.

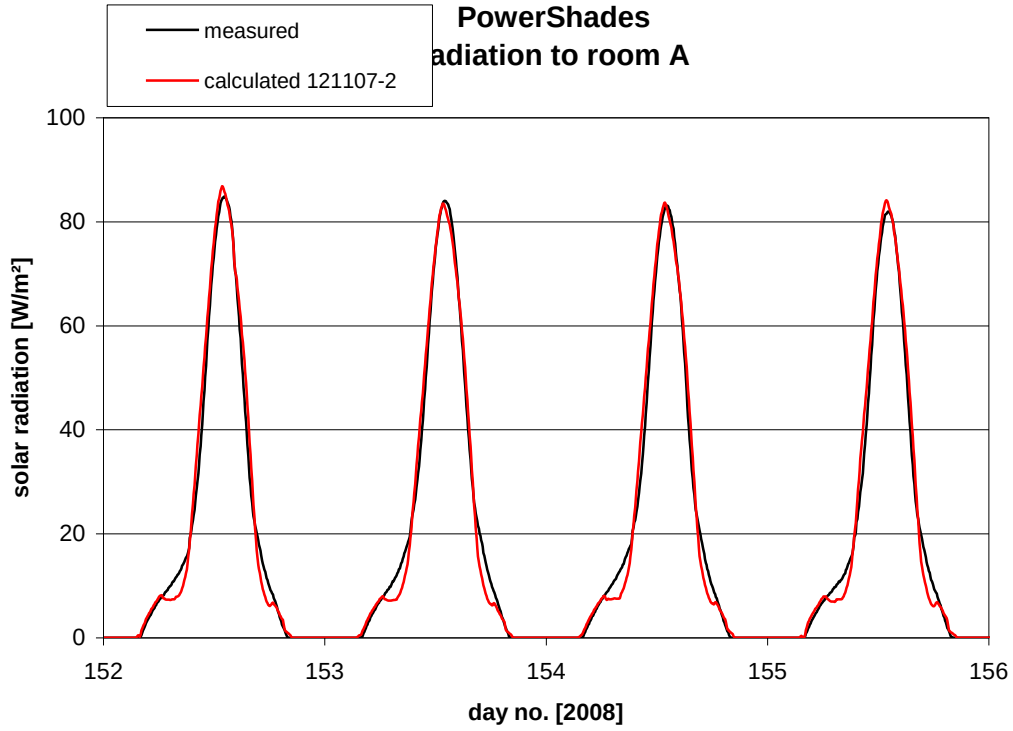

Figure 5.60. Measured and calculated solar radiation to room A – 1-4/6, 2008. With PowerShade model 121107-2 and without shading.

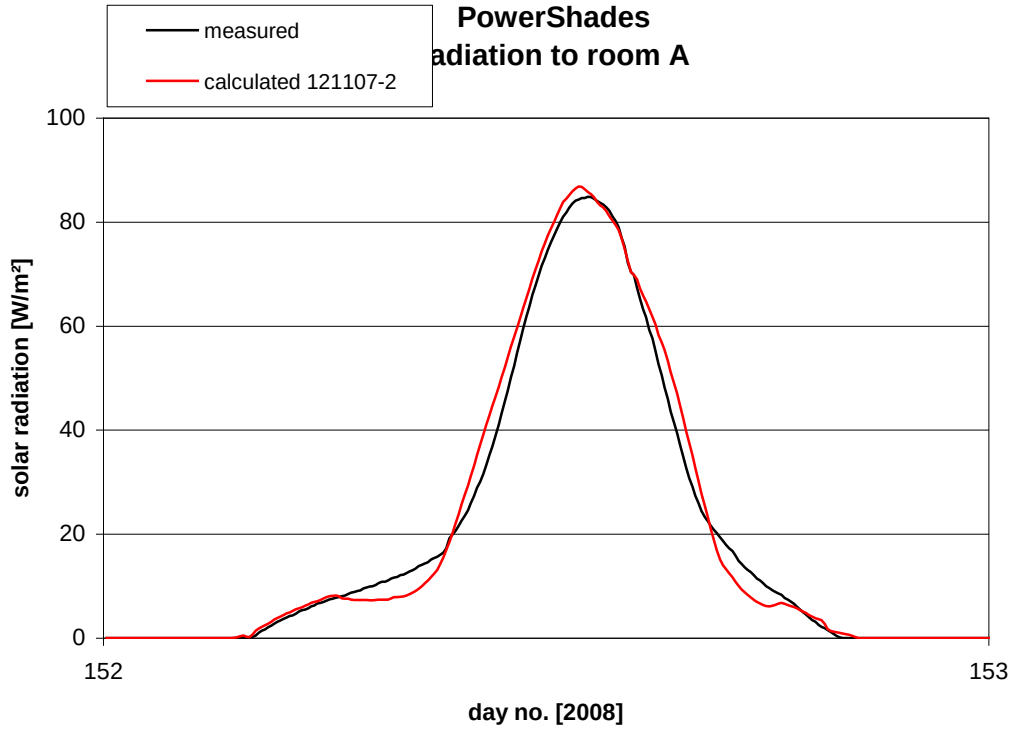

Figure 5.61. Measured and calculated solar radiation to room A – 1/6, 2008. With PowerShade model 121107-2 and without shading.

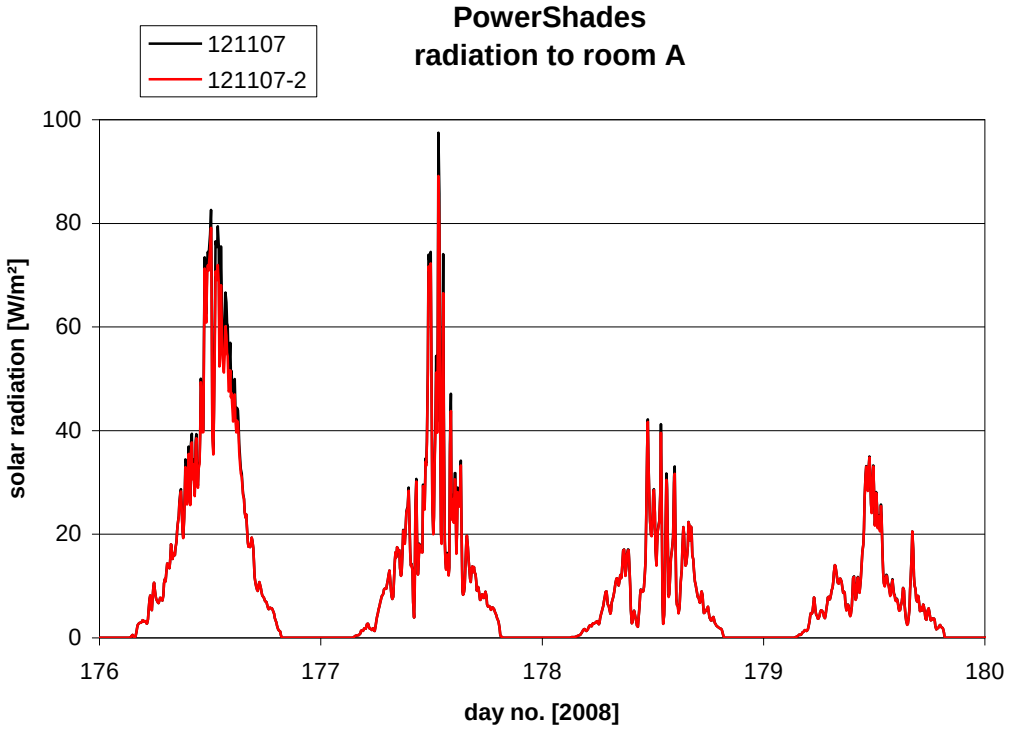

Figure 5.62. Calculated solar radiation to room A – 25-28/6, 2008 with 121107 and 121107-2. Without shading.

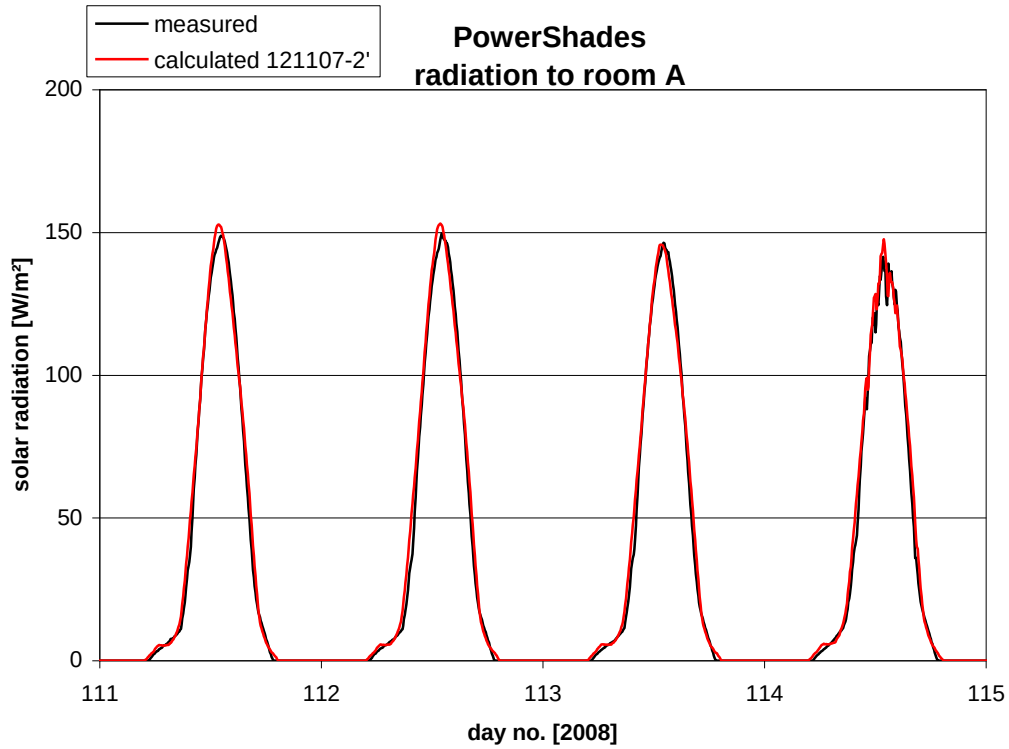

Figure 5.63. Measured and calculated solar radiation to room A – 21-24/4, 2008. With PowerShade model 121107-2 and without shading.

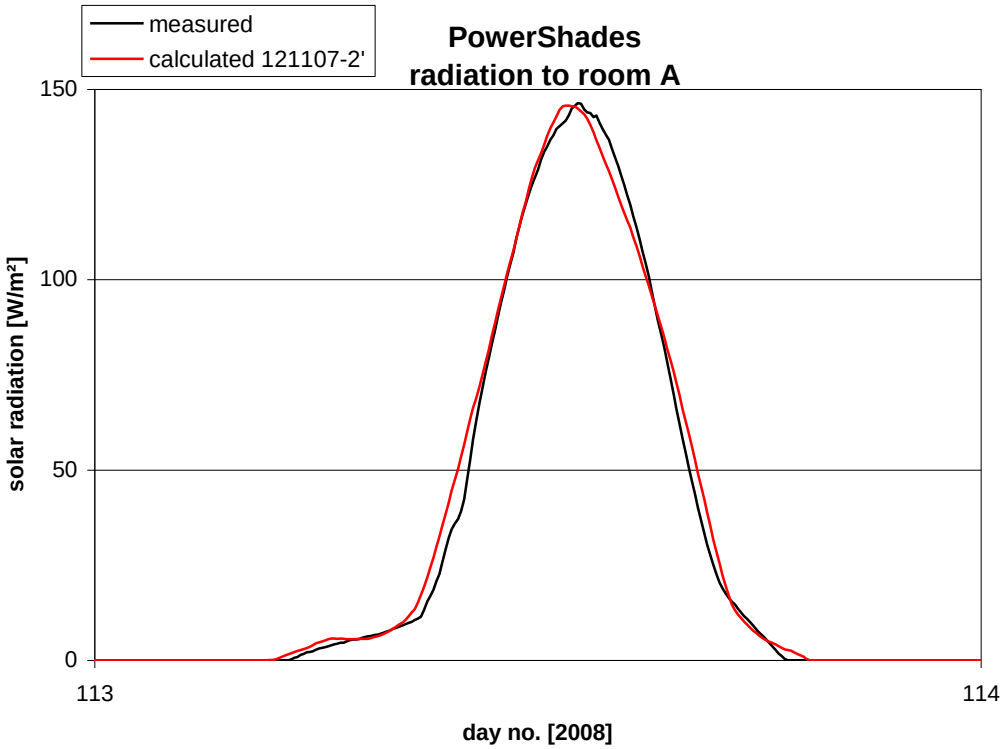

Figure 5.64. Measured and calculated solar radiation to room A – 23/4, 2008. With PowerShade model 121107-2 and without shading.

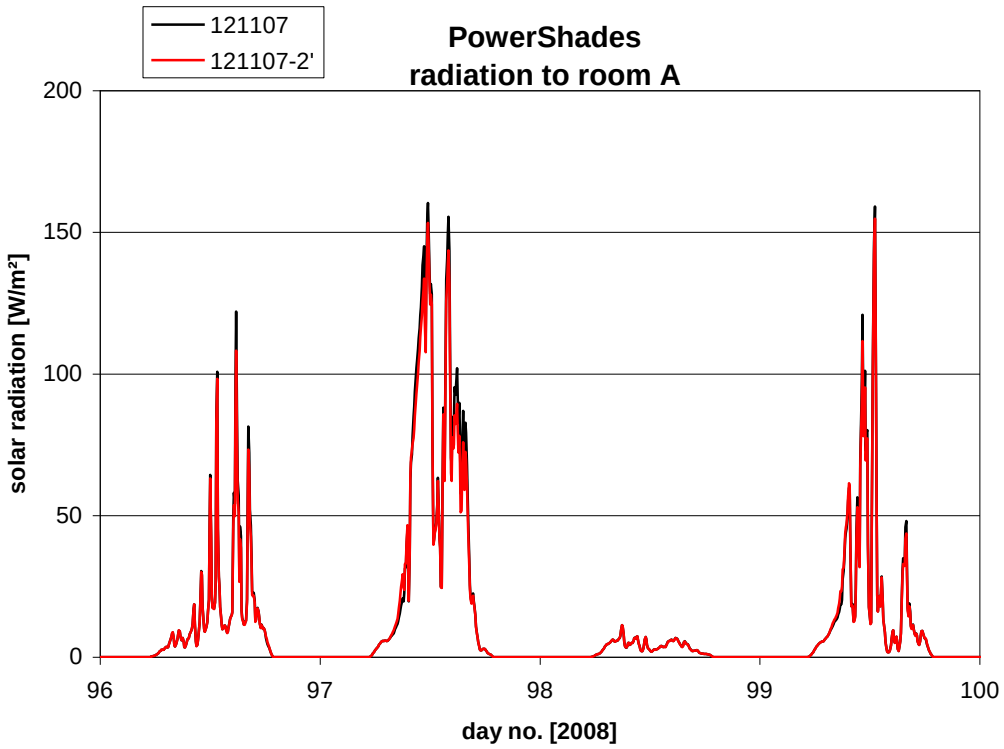

Figure 5.65. Calculated solar radiation to room A – 23-26/1, 2008 with 121107 and 121107-2. Without shading.

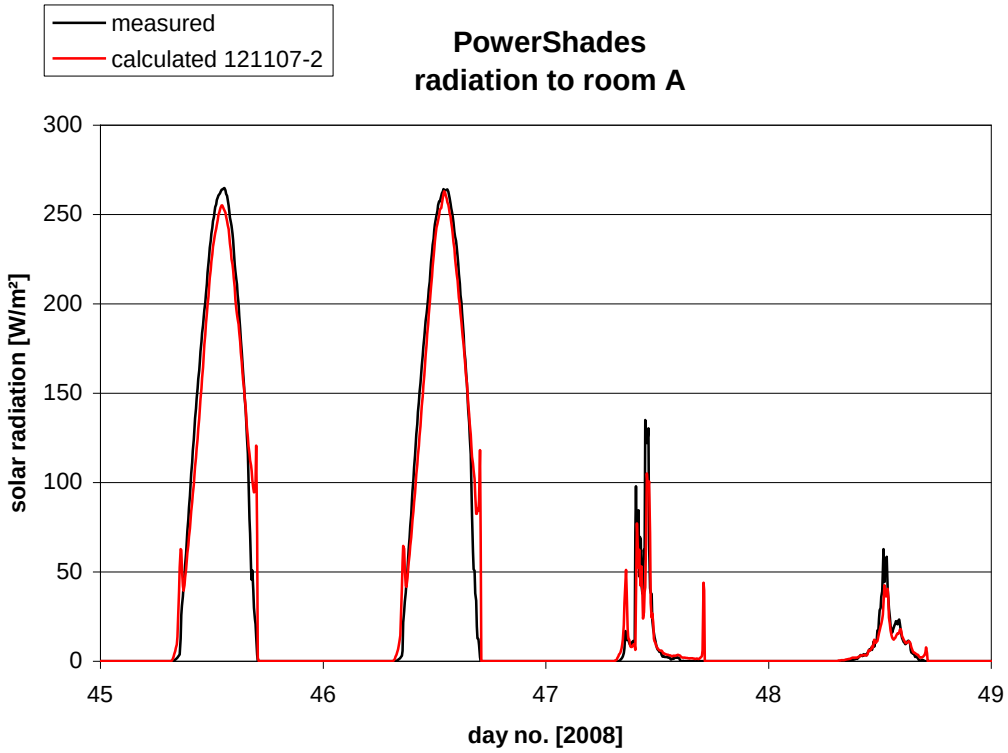

Figure 5.66. Measured and calculated solar radiation to room A – 21/1-17/2, 2008. With PowerShade model 121107-2 and without shading.

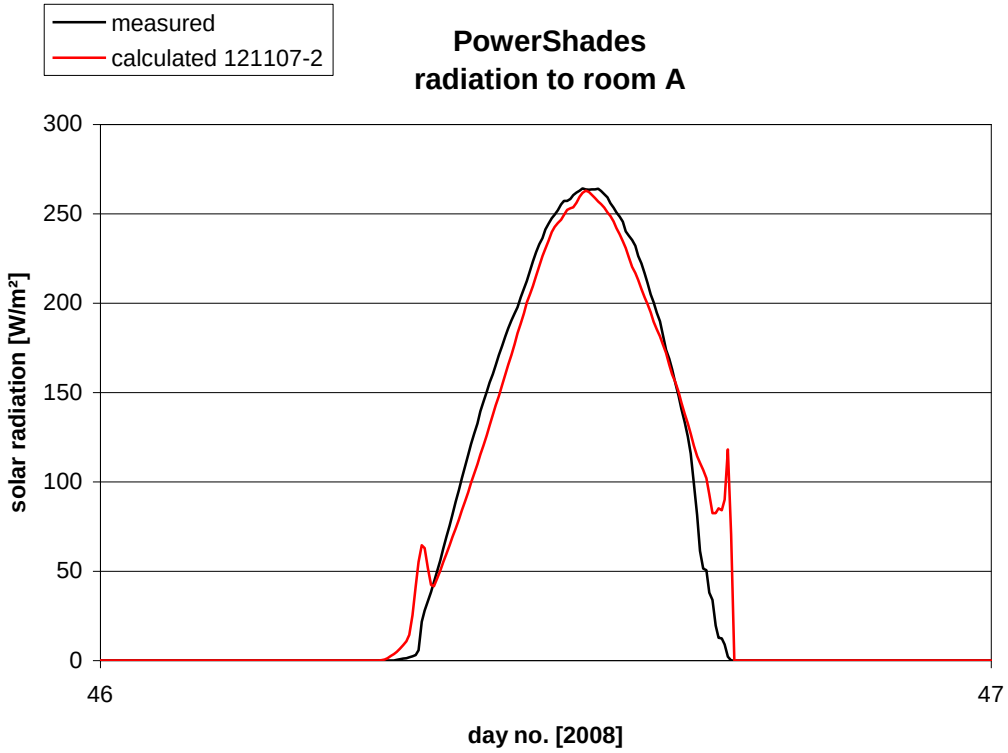

Figure 5.67. Measured and calculated solar radiation to room A – 22/1, 2008. With PowerShade model 121107-2 and without shading.

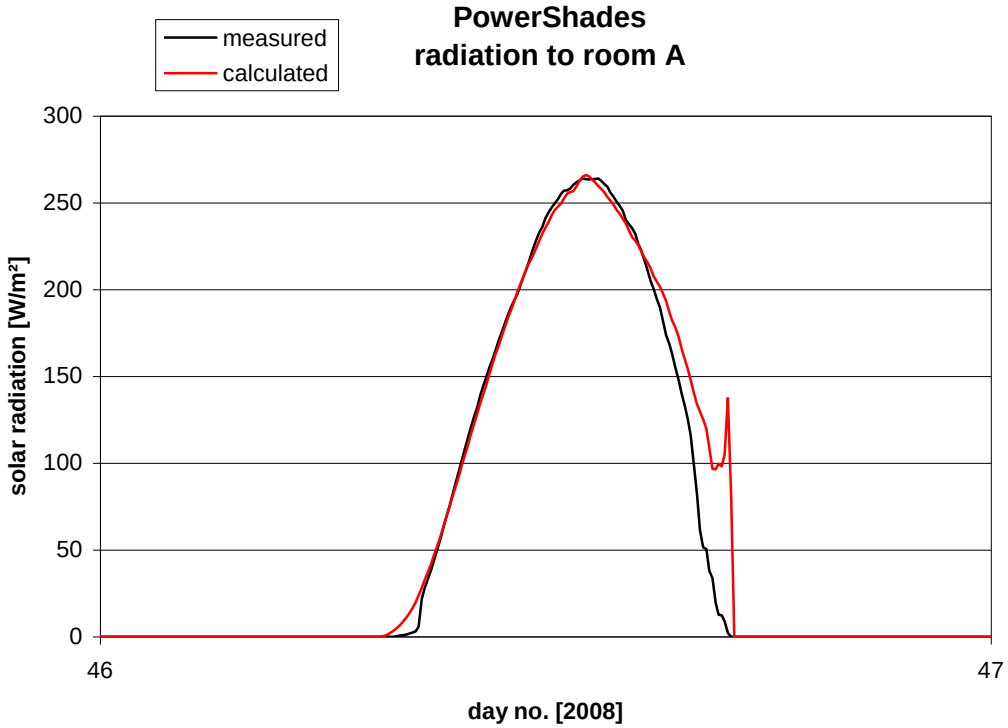

Figure 5.68. Measured and calculated solar radiation to room A – 22/1, 2008. With PowerShade model 121107 and without shading.

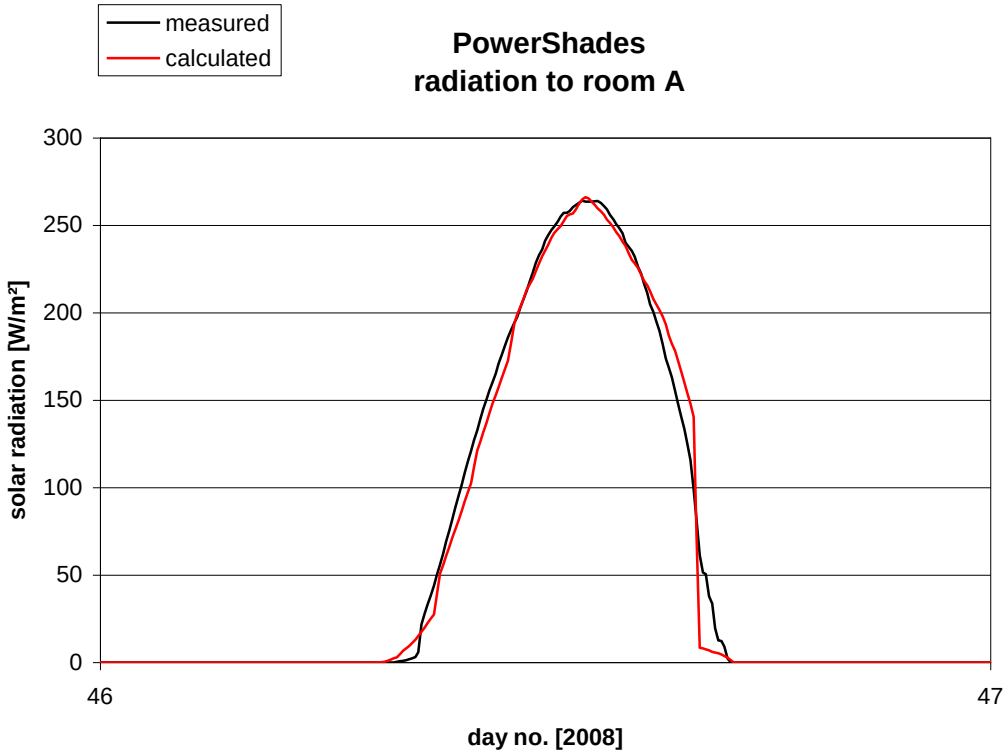

Figure 5.69. Measured and calculated solar radiation to room A – 22/1, 2008. With PowerShade model 121107 and with shading.

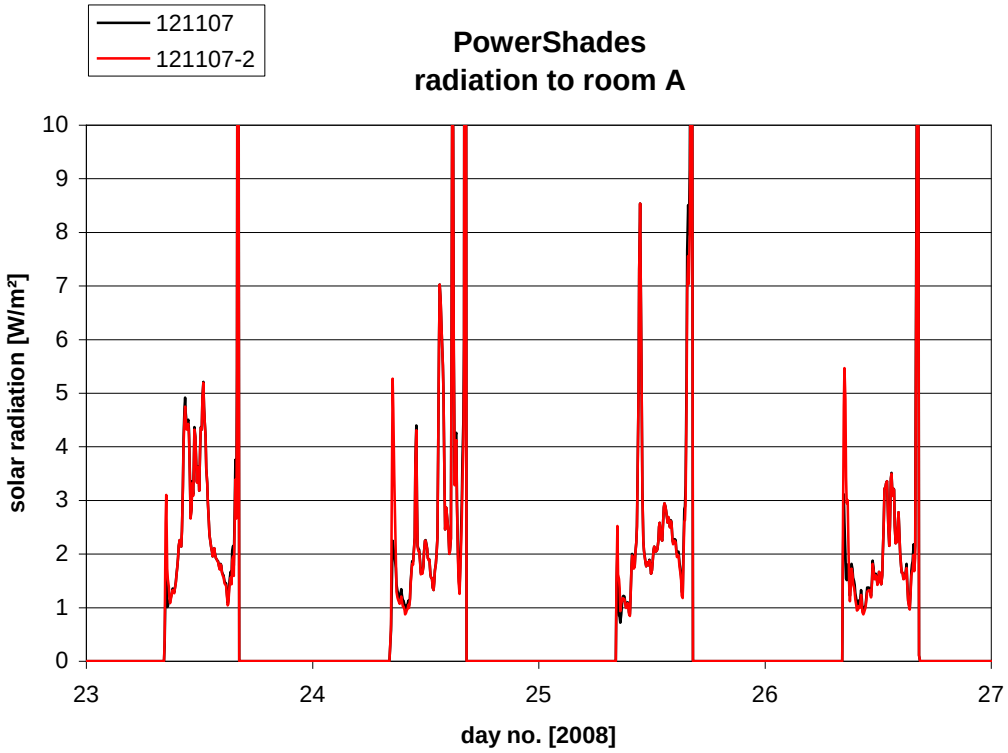

Figure 5.70. Calculated solar radiation to room A – 23-26/1, 2008 with 121107 and 121107-2. Without shading.

Figure 5.66-70 shows the result from applying model 121107-2 on the winter period. Figure 5.43 showed very good agreement when applying model 121107 on the winter period. Using figures 5.67-69 it is possible to compare model 121107-2 with model 121107. The agreement with measurements is less good in the morning when using 121107-2 – and also in the early afternoon, however, later in the afternoon better agreement is obtained with 121107-2 than with 121107. All in all the agreement has been reduced when going to 121107-2, which is not surprising as model 121107-2 is based on corrections found for the summer period, and that the agreement when using 121107 was rather good.

Although not perfect model 121107-2 shows all in all better agreement than model 121107. For figure 5.61 the difference in incoming solar radiation has been calculated. The difference has been calculated both for the area between the two blue vertical in figure 5.71 and between the two green lines in figure 5.71.

difference in incoming radiation between blue lines: 2 %
difference in incoming solar radiation between green lines: 6 %
for both cases: the calculated solar radiation is higher than the measured solar radiation

Model 121107-2 has been developed based on corrections to model 121107. The corrections has been determined using measured data in a not very scientific way – e.g. the corrections for too “wide shoulders” are only based on measurements from the summer period. This correction should off course be dependent on the day of the year as figures 5.67-69 shows.

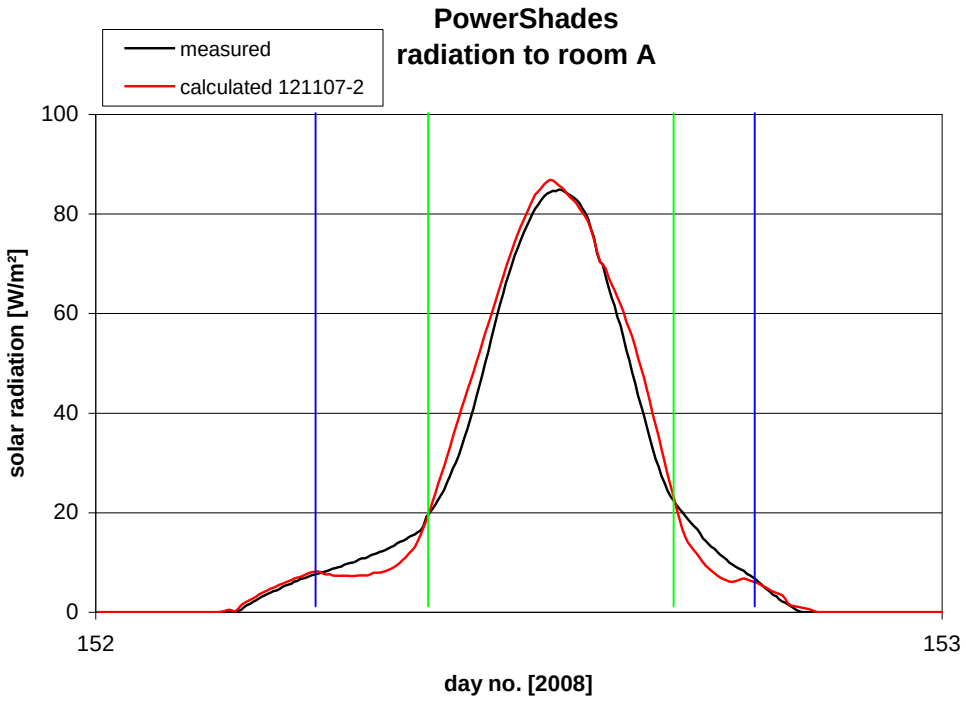

Figure 5.71. Measured and calculated solar radiation to room A – 1/6, 2008. With PowerShade model 121107-2 and without shading.

Based on the above findings the program for creating model 121107 will be modified in order more precisely calculate the projected area of the holes in the PowerShades seen by the sun.

The calibration exercise could stop here as the aim: evaluation of the model for calculation of solar transmittance through PowerShades has been carried out. However, there are rooms behind the windows. It would, therefore, be relevant not only to gain confidence in the modelling of PowerShades but also the modelling of the thermal performance of PowerShades in combination with the room behind the window with PowerShades.

This will be done in the following. But before doing this it has to be stated that it is often rather difficult to obtain as good agreement for the thermal performance of a room as seen in the previous chapters for the models of PowerShades and the Velfac window. This is because a room is often not very well defined although care has been taken in obtaining the thermo physical properties of the materials of the room and in sealing the room. Further it is very complicated processes which occur in a room.

Although not perfect, model 121107-2 will in the following be utilized for a calibration of the test rooms behind the Velfac and PowerShades windows - i.e. the measured and calculated room temperatures will be compared. However, model 121107-2 does as earlier mentioned not consider the stripes of the PowerShades – see figure 2.6. The stripes constitute 5 % of the area of the window. The total direct and diffuse radiation in model 121107-2 has thus been reduced with 5 % in order to obtain a more precise calculation of the total solar radiation through the PowerShade window. The absorptance of the PowerShade foil has been increased accordingly assuming that the absorptance in the PowerShades material is 0.76. The absoptance of the PowerShades foil is as earlier mentioned not that important.

5.2.2.3. Comparison between the Velfac and PowerShades window

However, before calibrating the model of the rooms behind the windows the measured incoming solar radiation through the two window systems will be compared. This is done in figures 5.73-81 where the same periods as earlier shown.

Figures 5.74, 5.77 and 5.81 show that the PowerShades reduce the diffuse radiation with up to 50 % compared to the Velfac window. This was expected. The diffuse transmittance of traditional windows is as already mentioned found in figure 5.19 at 60° which gives a diffuse transmittance of approx 0.25 while the diffuse radiation for the PowerShades in chapter 5.2.2.1.2 was found to be 0.12.

Figures 5.75, 5.78 and 5.80 show that the reduction of the solar radiation compared to the Velfac window at clear sky conditions as designed increases going from winter to summer. This is shown more clearly in figure 5.72

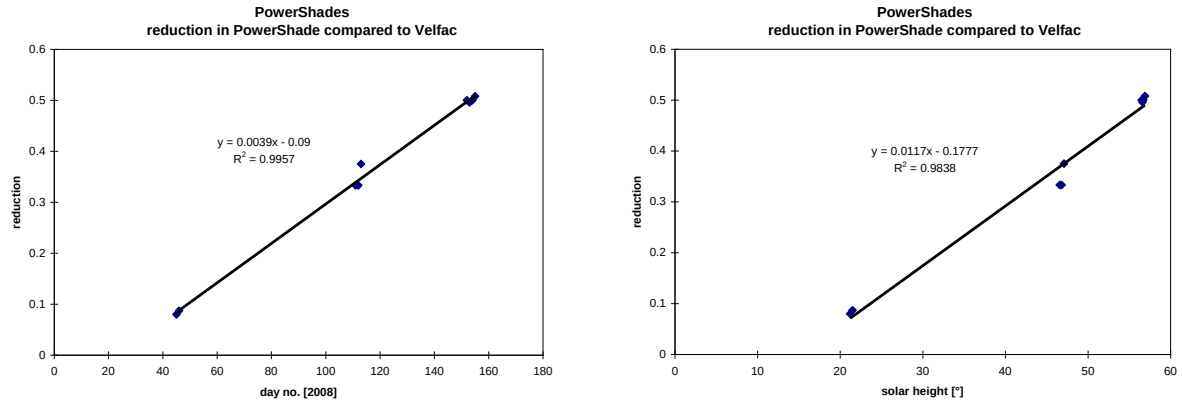

Figure 5.72. The reduction of the transmission of the solar radiation in the PowerShades compared to Velfac window at clear sky conditions dependents on day no. and solar height.

Figure 5.72 shows a linearly reduction as a function of both day no. and solar height. The regression equation for the dependency on the solar height shows that no reduction compared to the Velfac window occurs at a solar height of 15° - i.e. close to the lowest solar height in Denmark, while the figure shows a max reduction of the incoming solar radiation of 50 % at high solar heights.

Based on this it can be concluded that Prototype 1 of PowerShades has almost the same reduction for direct solar radiation as the solar screening film in the Velfac window at mid winter where the incoming solar heat often is useful while Prototype 1 lets 50 % less direct solar radiation into the room at noon during high summer. This means that PowerShades as indented reduces the overheating risks while still letting solar radiation in during periods where the heat from the sun may be useful.

The reduction depending on solar height varies depending on the design of the PowerShades. This is seen when comparing the above with figures 4.5 and 4.8. The reduction obtained by PowerShades PS4060 compared to the Velfac window at noon during clear sky conditions is here already about 57 % by the end of March and around 86 % during high summer.

5.2.2.3.1. Winter

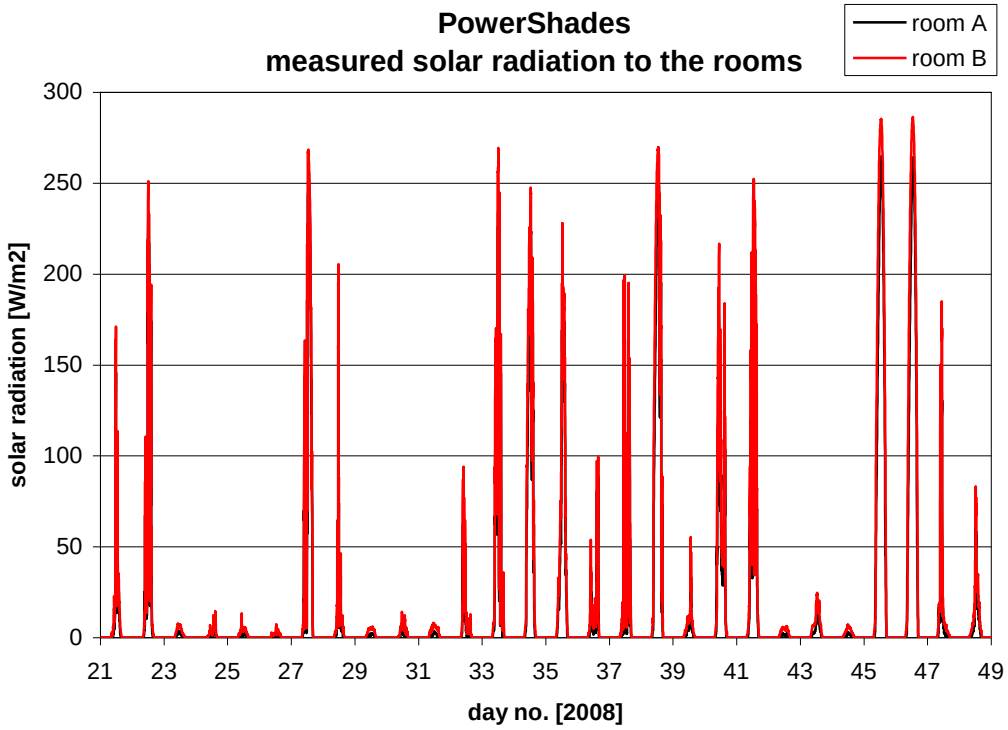

Figure 5.73. Measured solar radiation to the two rooms – 21/1-17/2, 2008.

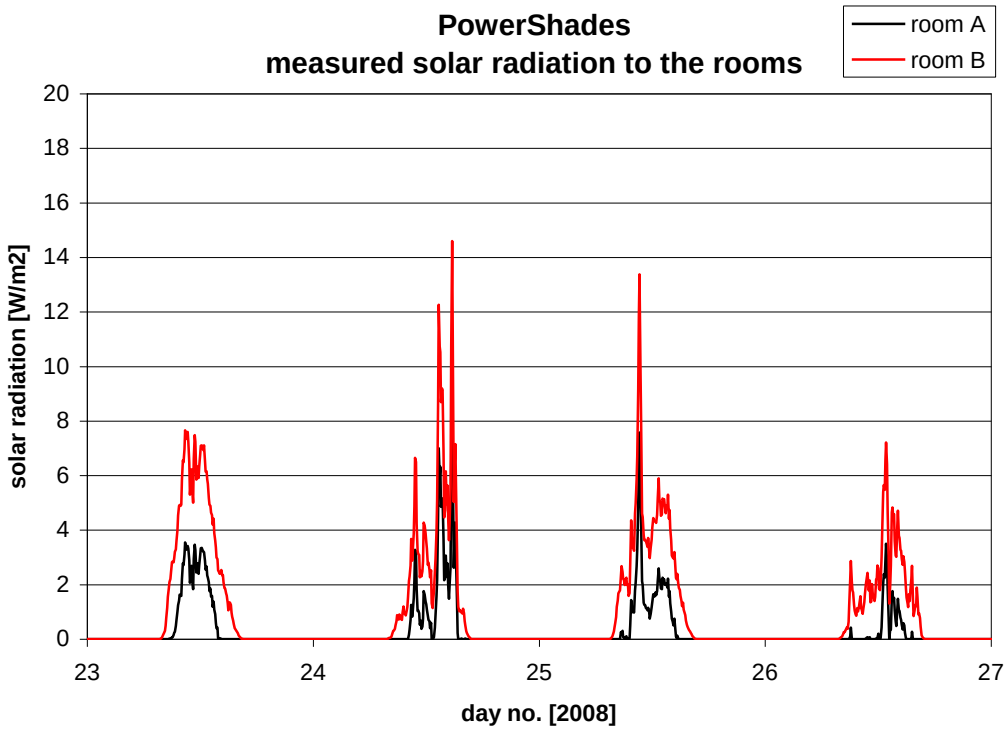

Figure 5.74. Measured solar radiation to the two rooms – 23-26/1, 2008.

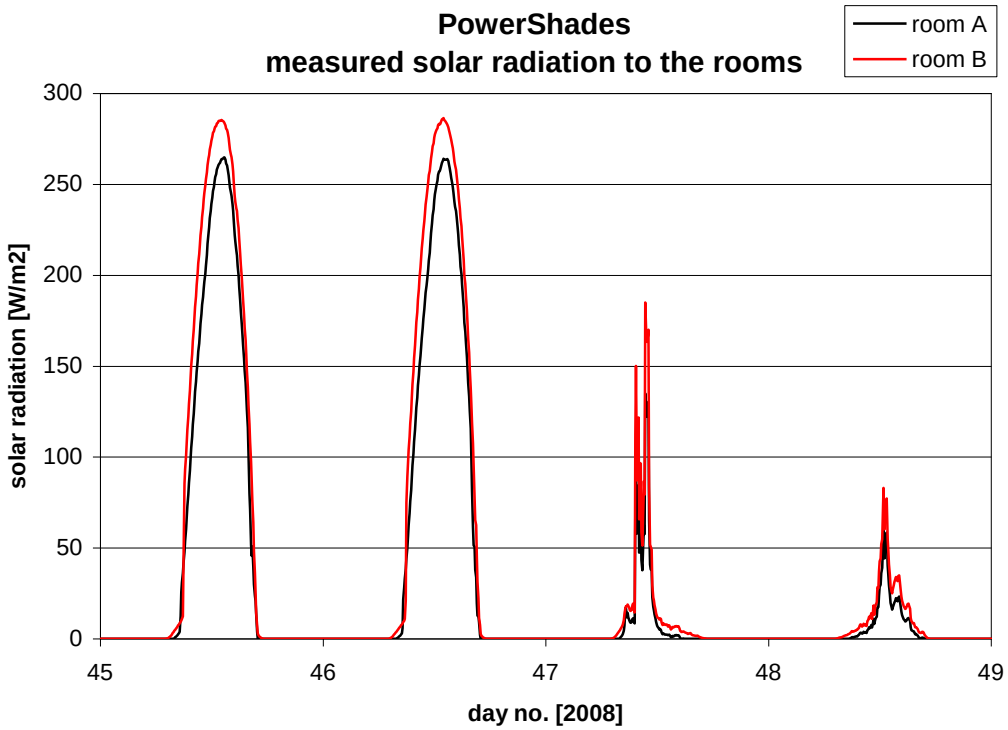

Figure 5.75. Measured solar radiation to the two rooms – 14-17/2, 2008.

5.2.2.3.2. Spring

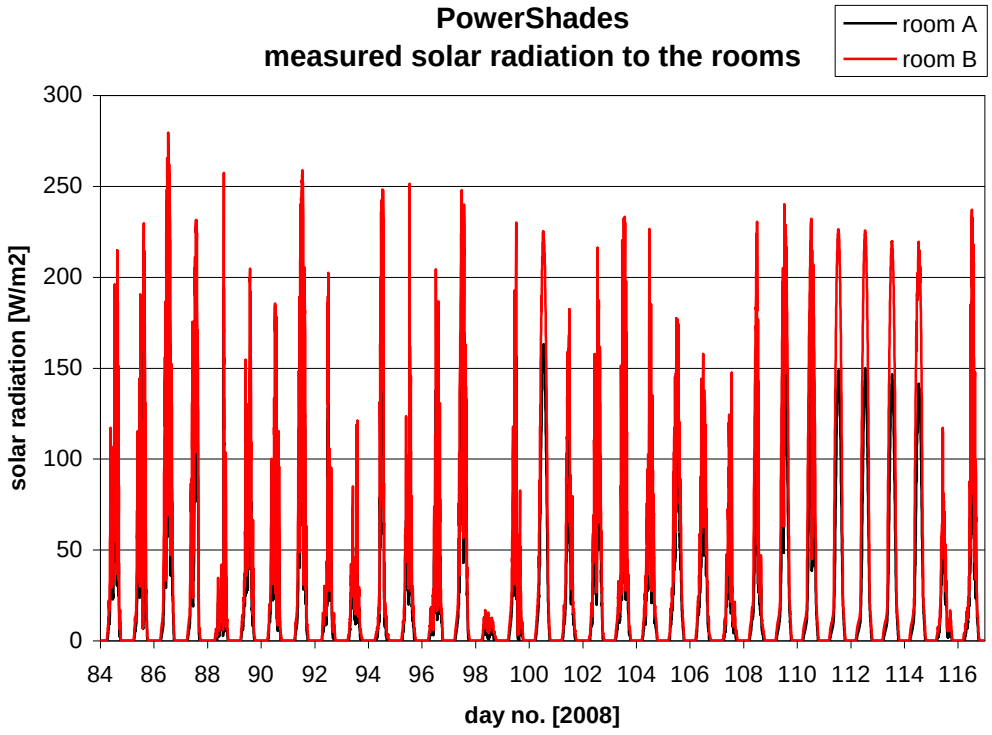

Figure 5.76. Measured solar radiation to the two rooms – 25/3-26/4, 2008.

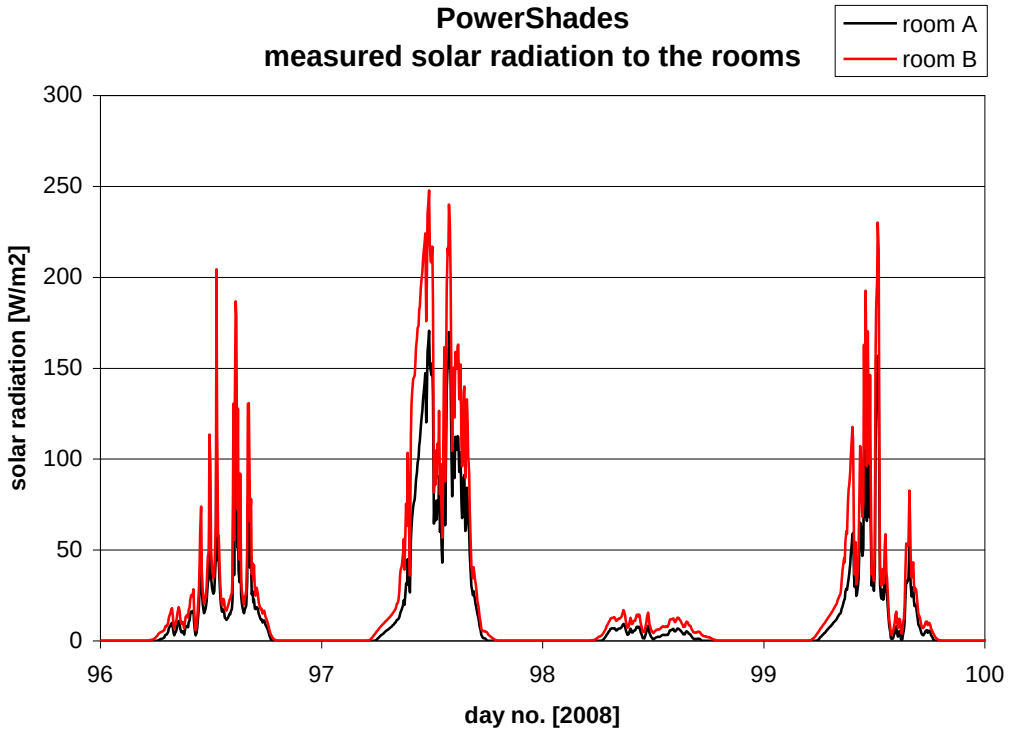

Figure 5.77. Measured solar radiation to the two rooms – 6-9/4, 2008.

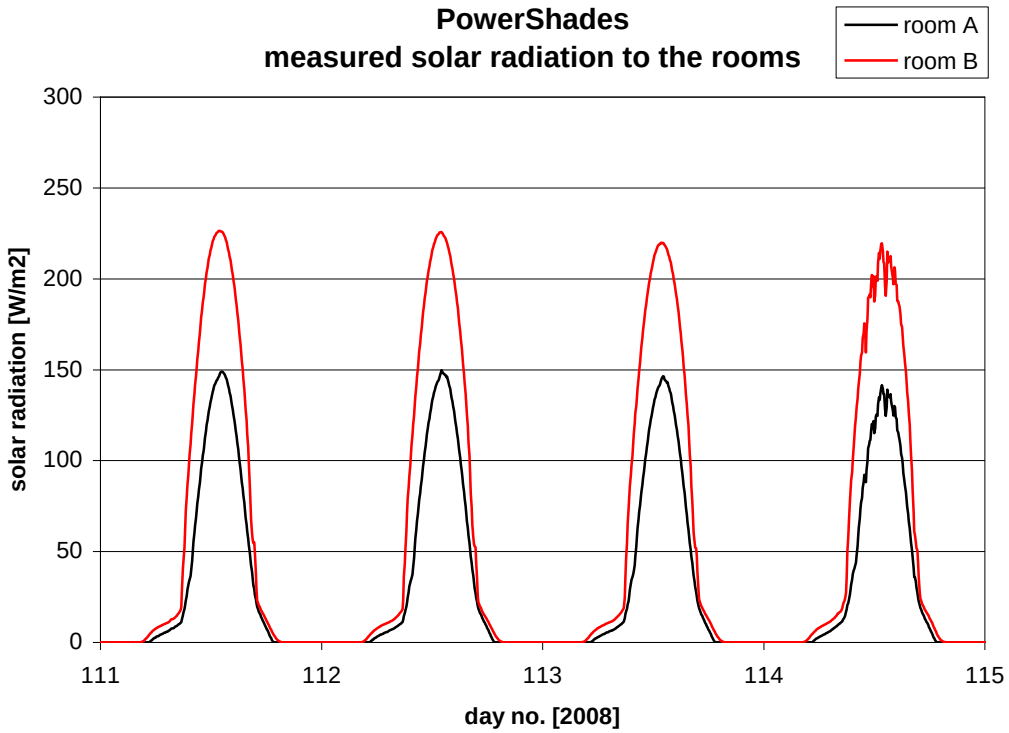

Figure 5.78. Measured solar radiation to the two rooms – 21-24/4, 2008.

5.2.2.3.3. Summer

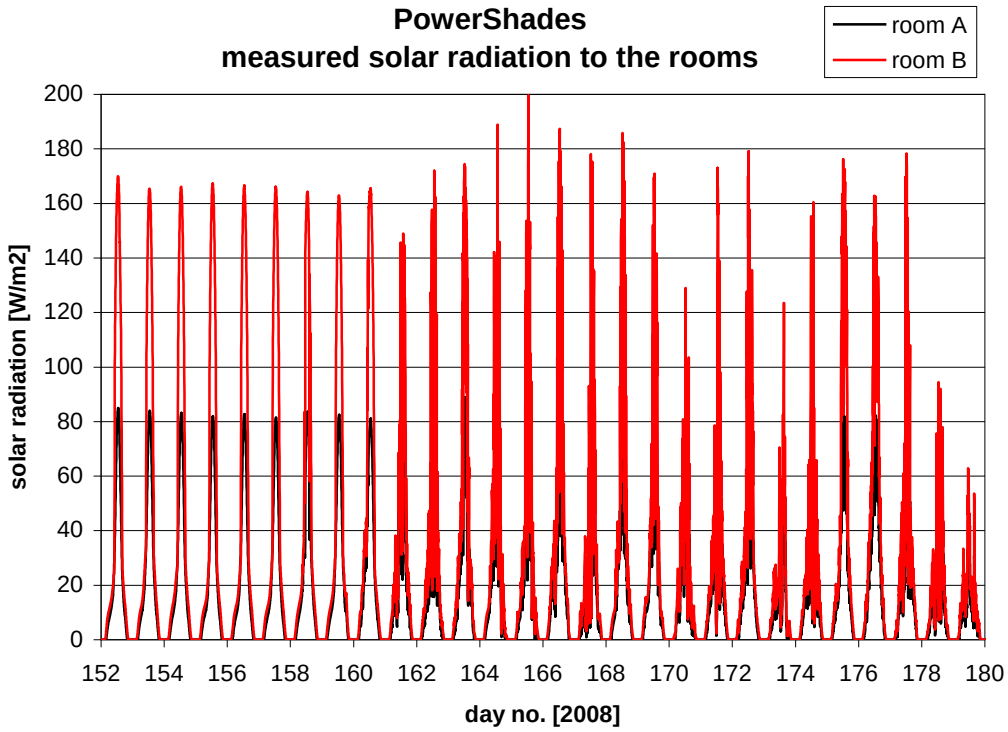

Figure 5.79. Measured solar radiation to the two rooms – 1-28/6, 2008.

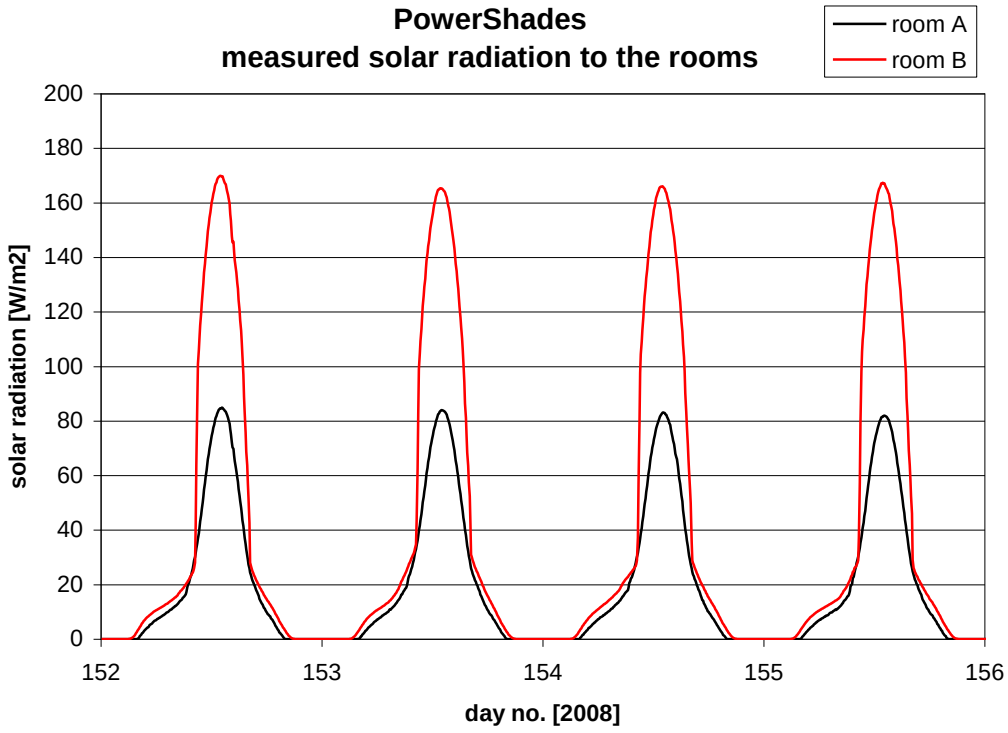

Figure 5.80. Measured solar radiation to the two rooms – 1-4/6, 2008.

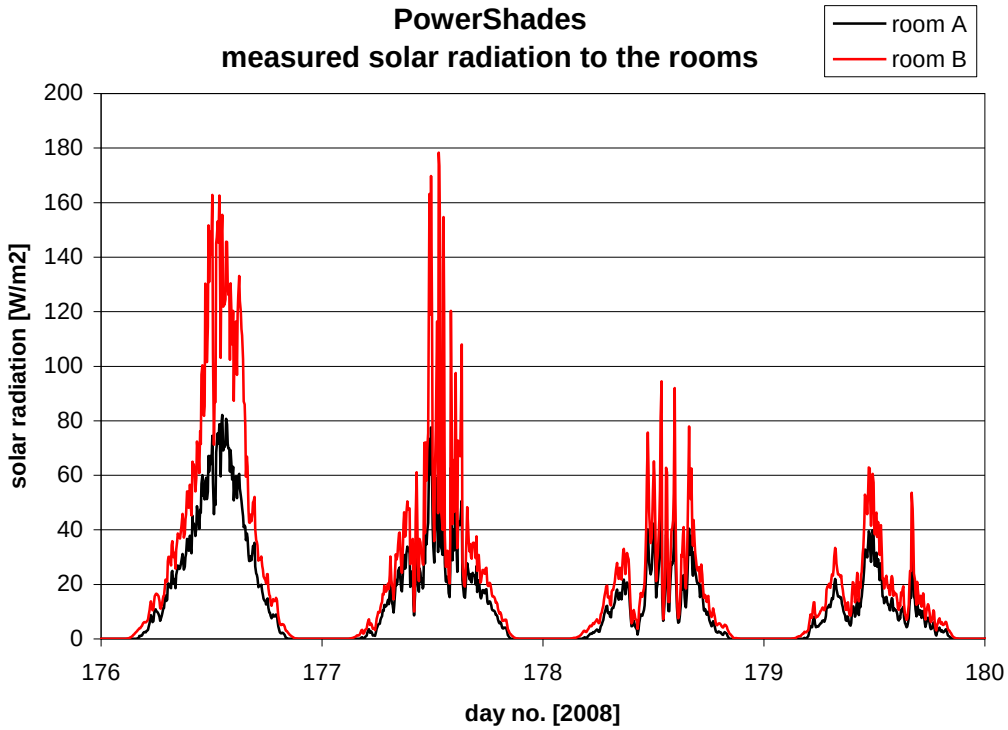

Figure 5.81. Measured solar radiation to the two rooms – 25-28/6, 2008.

5.2.2.4. Comparison between Prototype 1 and 2

Chapter 2.3 and 2.4 describe two rather similar prototypes of PowerShades. The main difference is the distance between the opaque stripes of the PowerShade foil and a little bit more open structure of the PowerShade foil, making Prorotype 2 a bit more transparent than Prototype 1.

Prototype 2 was installed in the windows next to the two test rooms on March 6 and a pyranometer was installed behind on of the windows with Prototype 2 on April 16. It is therefore only possible to compare the two prototypes for the chosen spring and summer periods. However, in order to also include winter conditions measurements from November 16-20 are also shown. These figures 5.82-85 show close ups at clear sky conditions for spring, clear sky and cloudy/drifting clouds conditions during summer and clear sky/overcast for winter.

Figures 5.82-85 show that more solar radiation is let in through Prototype 1 than Prototype 2 – this is shown more clearly in figures 5.86-89. The transmittance was supposed to be almost identical. The difference could be due to wrong readings from the new pyranometer behind Prototype 2. However, the two pyranometers were calibrated with the vertical pyranometer on the façade in (Jensen, 2008a) and an uncertainty of ±3 % was found.

Figure 5.90 shows the differences from figures 5.86-89 during clear sky conditions at noon. It is seen that the difference seems to be slightly solar height dependent. This together with the findings in chapter 5.2.2.2 show that there still lacks knowledge in the understanding of the transmittance through PowerShades. It was not possible to obtain the missing knowledge during the present project. The work regarding the mathematically description of the transmit-

tance through PowerShades will, however, continued in a new project succeeding the present project.

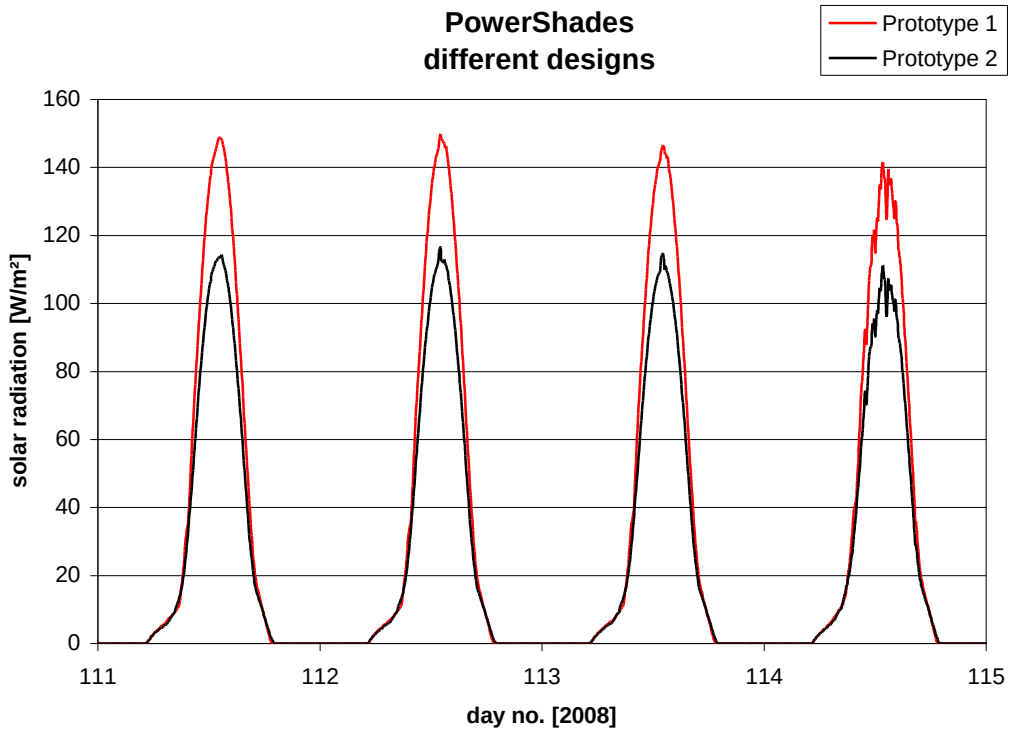

Figure 5.82. Measured solar radiation though Prototype 1 and 2 – 21-24/4, 2008.

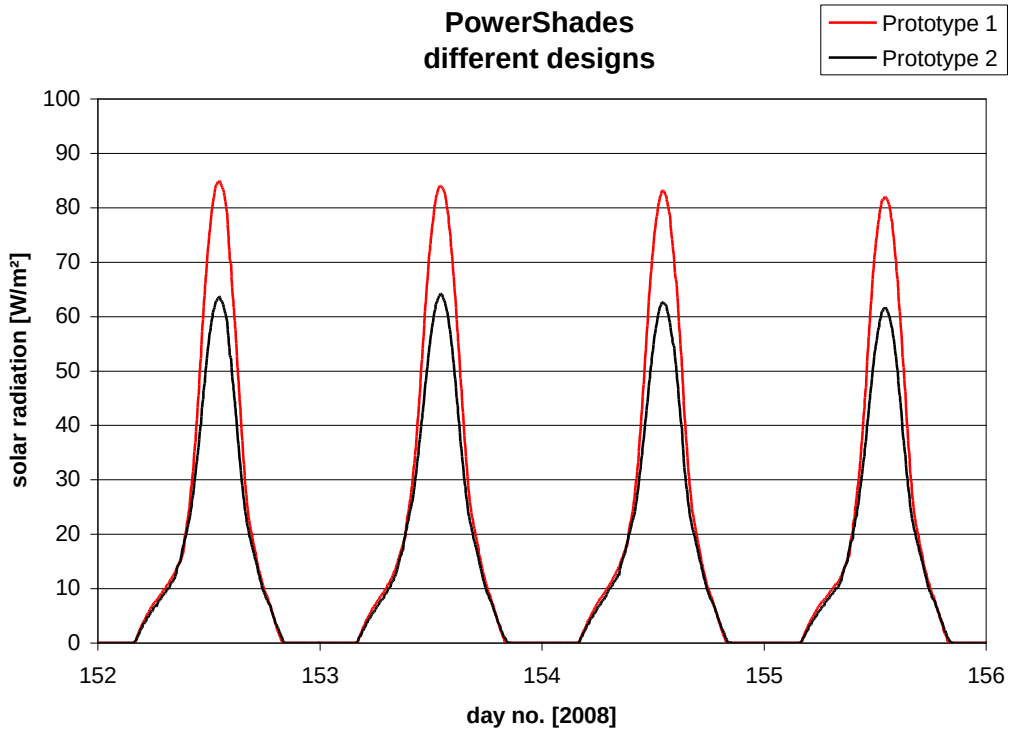

Figure 5.83. Measured solar radiation though Prototype 1 and 2 – 1-4/6, 2008.

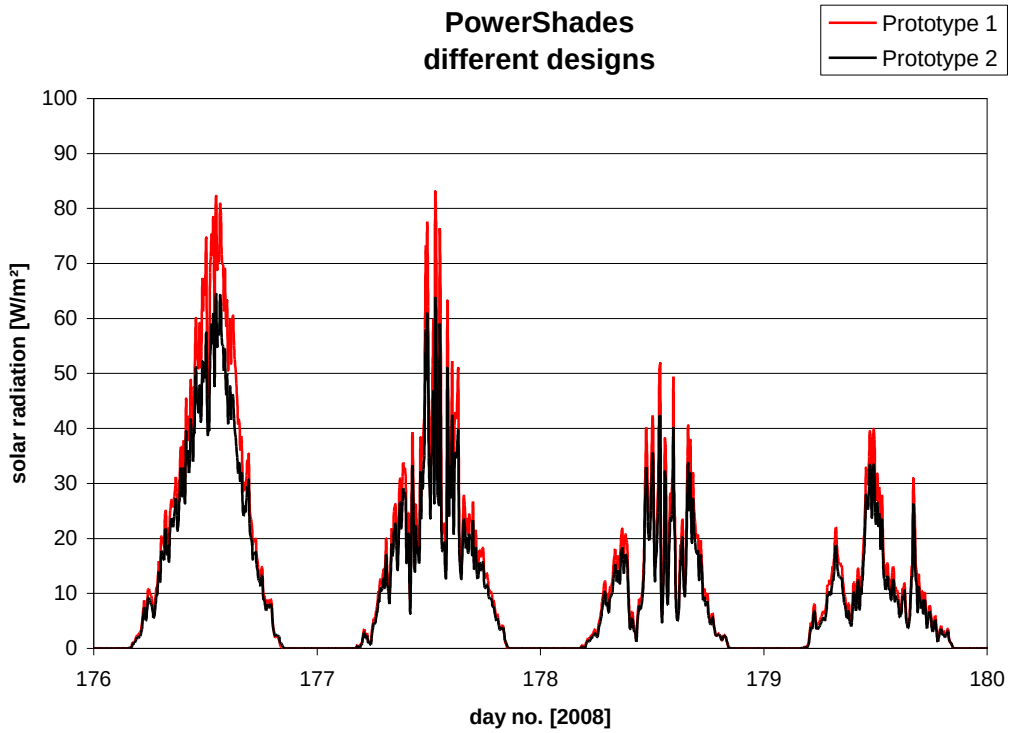

Figure 5.84. Measured solar radiation though Prototype 1 and 2 – 25-28/6, 2008.

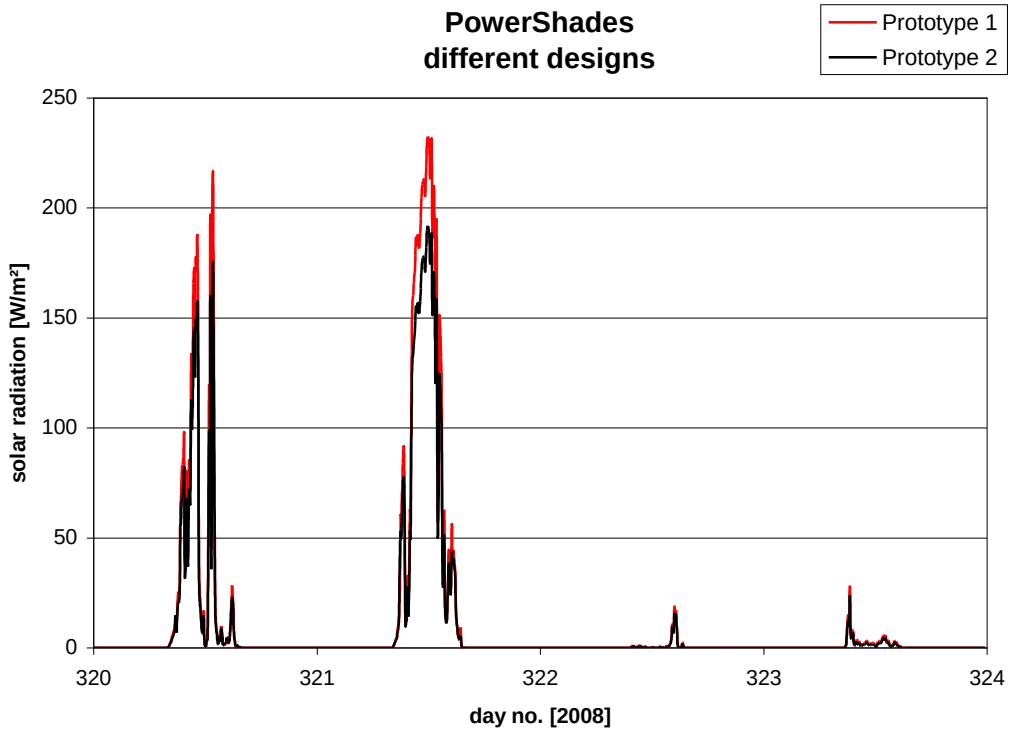

Figure 5.85. Measured solar radiation though Prototype 1 and 2 – 16-20/11, 2008.

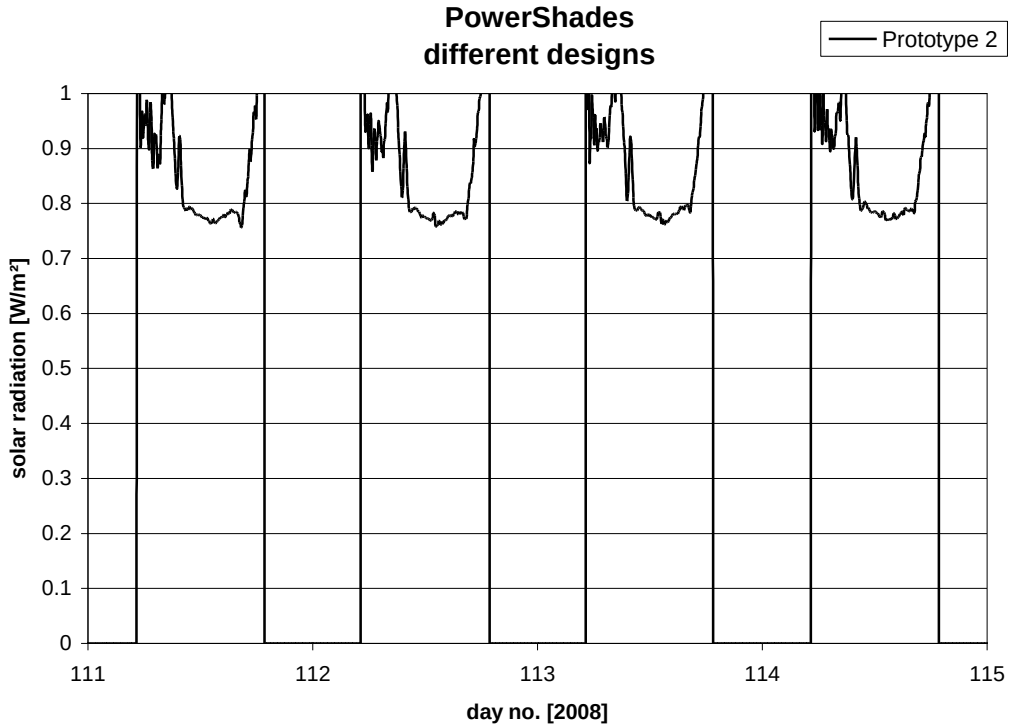

Figure 5.86. Difference between the measured solar radiation though Prototype 1 and 2 – 21-24/4, 2008.

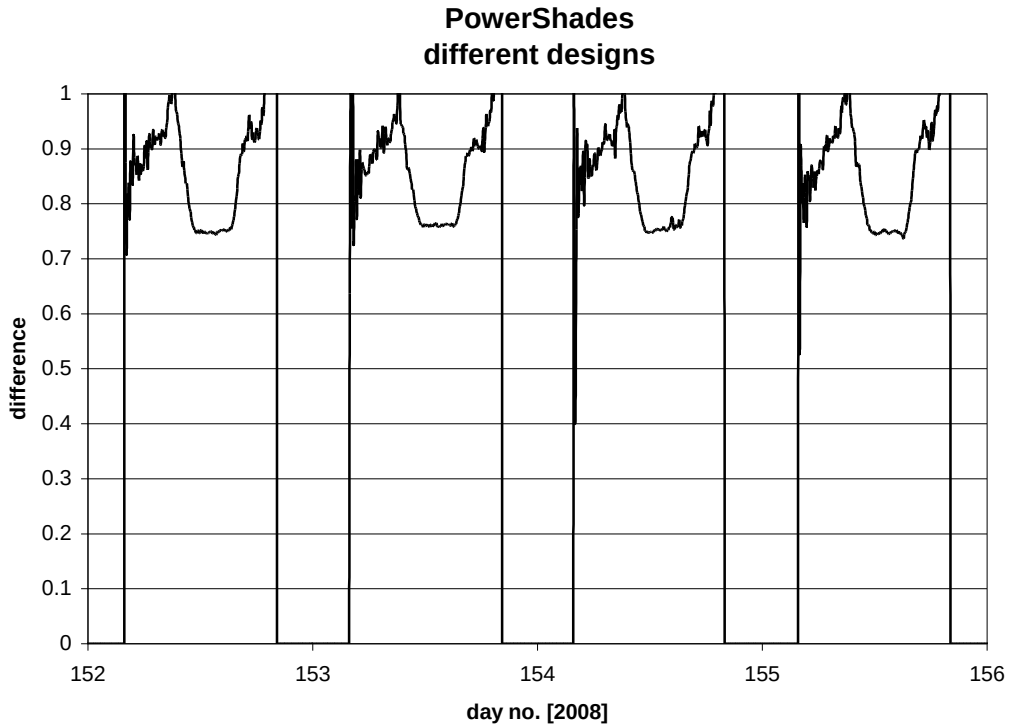

Figure 5.87.. Difference between the measured solar radiation though Prototype 1 and 2 – 1-4/6, 2008.

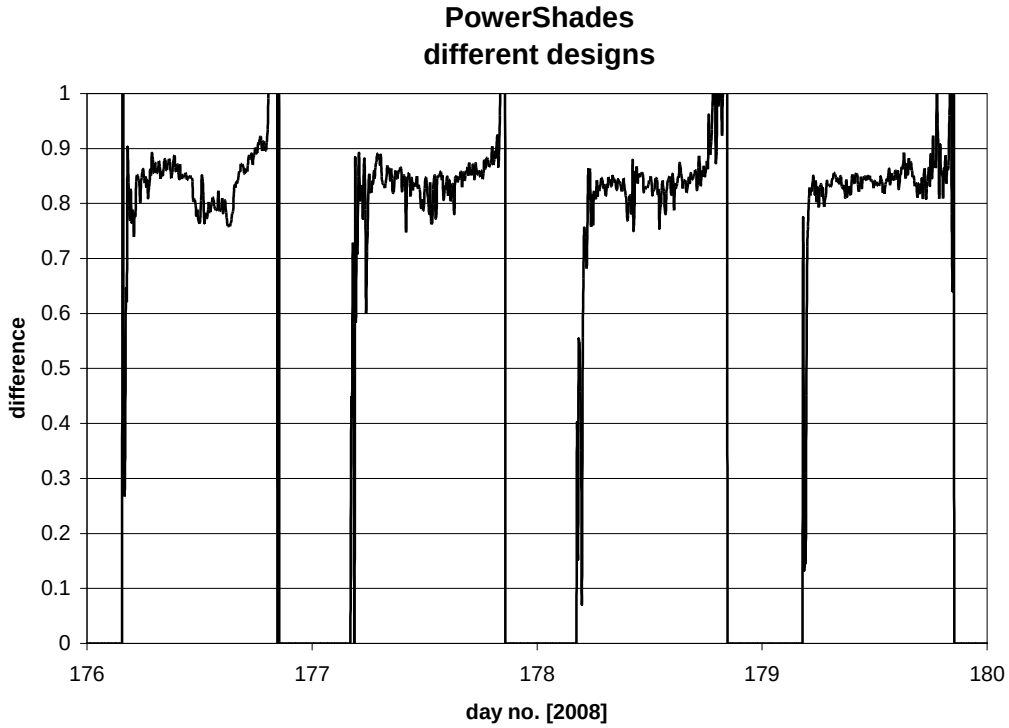

Figure 5.88. Difference between the measured solar radiation though Prototype 1 and 2 – 25-28/6, 2008.

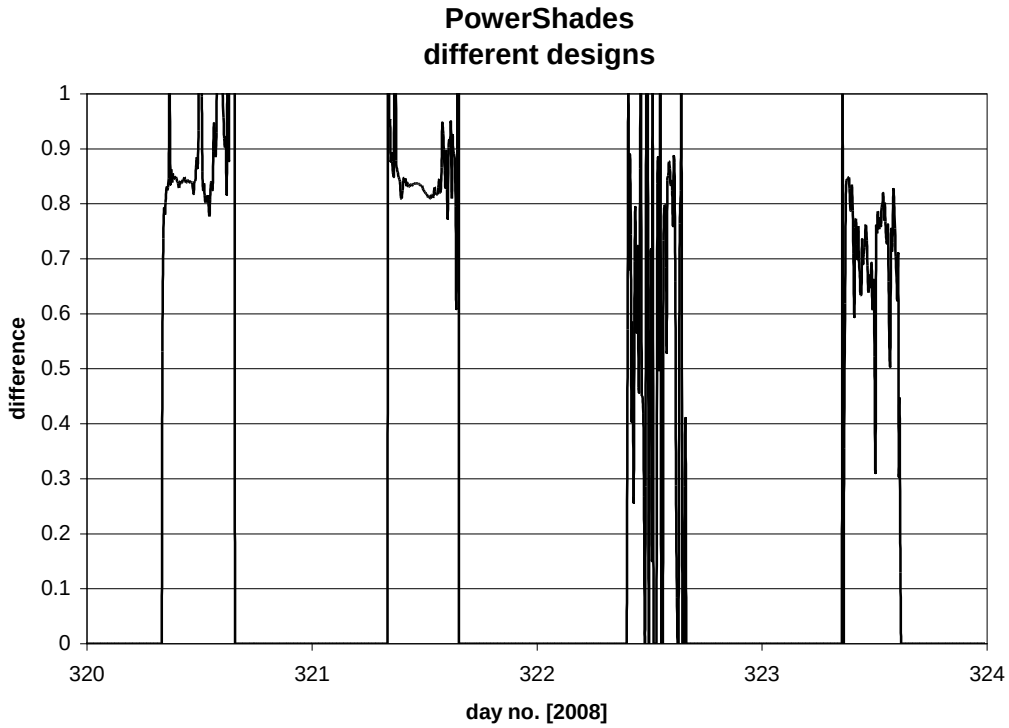

Figure 5.89. Difference between the measured solar radiation though Prototype 1 and 2 – 16-20/11, 2008.

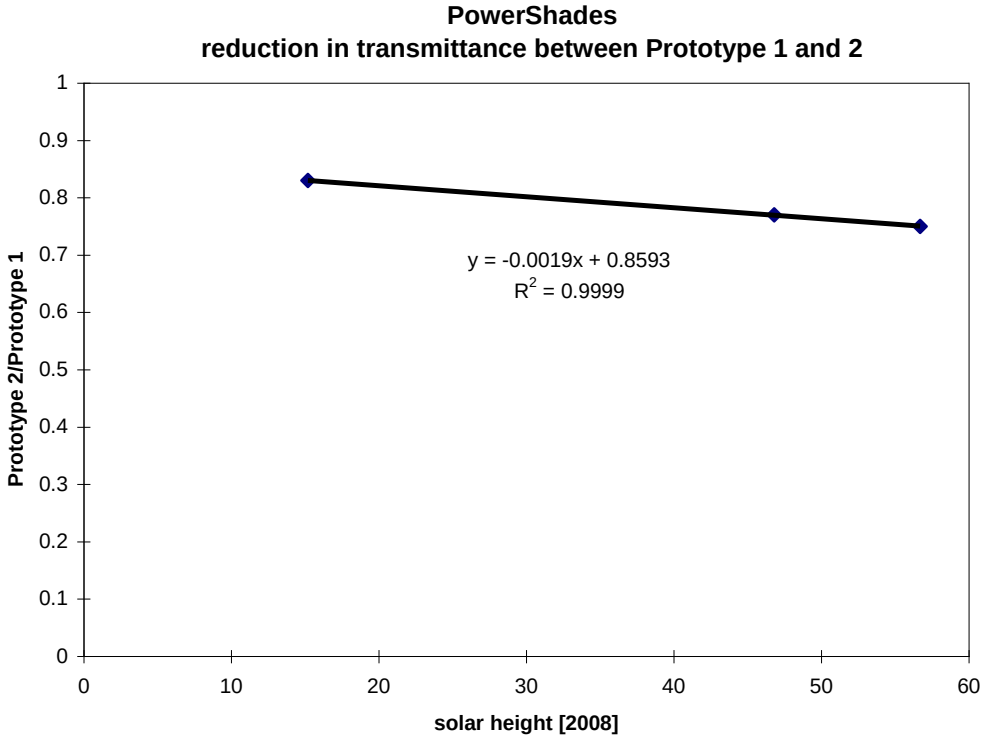

Figure 5.90. Difference between the measured solar radiation though Prototype 1 and 2 dependent on the solar height

5.2.3. Calibration of the rooms behind the Velfac and PowerShades windows

The rooms behind the Velfac and PowerShades windows have in the model been divided in 10 equally sized zones in such a way that they match the instrumentation with air temperature sensors in the real rooms – i.e. such that there is an air temperature sensor in the middle of each zone – see figure 5.91.

The materials of the rooms are those described in (Jensen, 2008a). The optical properties of the windows are those already described in the proceeding chapters - i.e. 121107-2 with stripes has been used as model for the PowerShade window.

For the chosen periods: winter, spring and summer 2008 the following graphs are shown:

- measured and calculated mean air temperature in room A
- measured and calculated mean air temperature in room B
- measured mean air temperature in room A and B
- calculated mean air temperature in room A and B
- measured and calculated temperature difference between room A and B
- surrounding air temperatures – see figure 5.91
- ambient temperature

these graphs should be seen in connection with the following already shown graphs:

- total solar radiation on the façade: figures 5.9-17
- solar radiation entering room A and B: figures 5.73-81

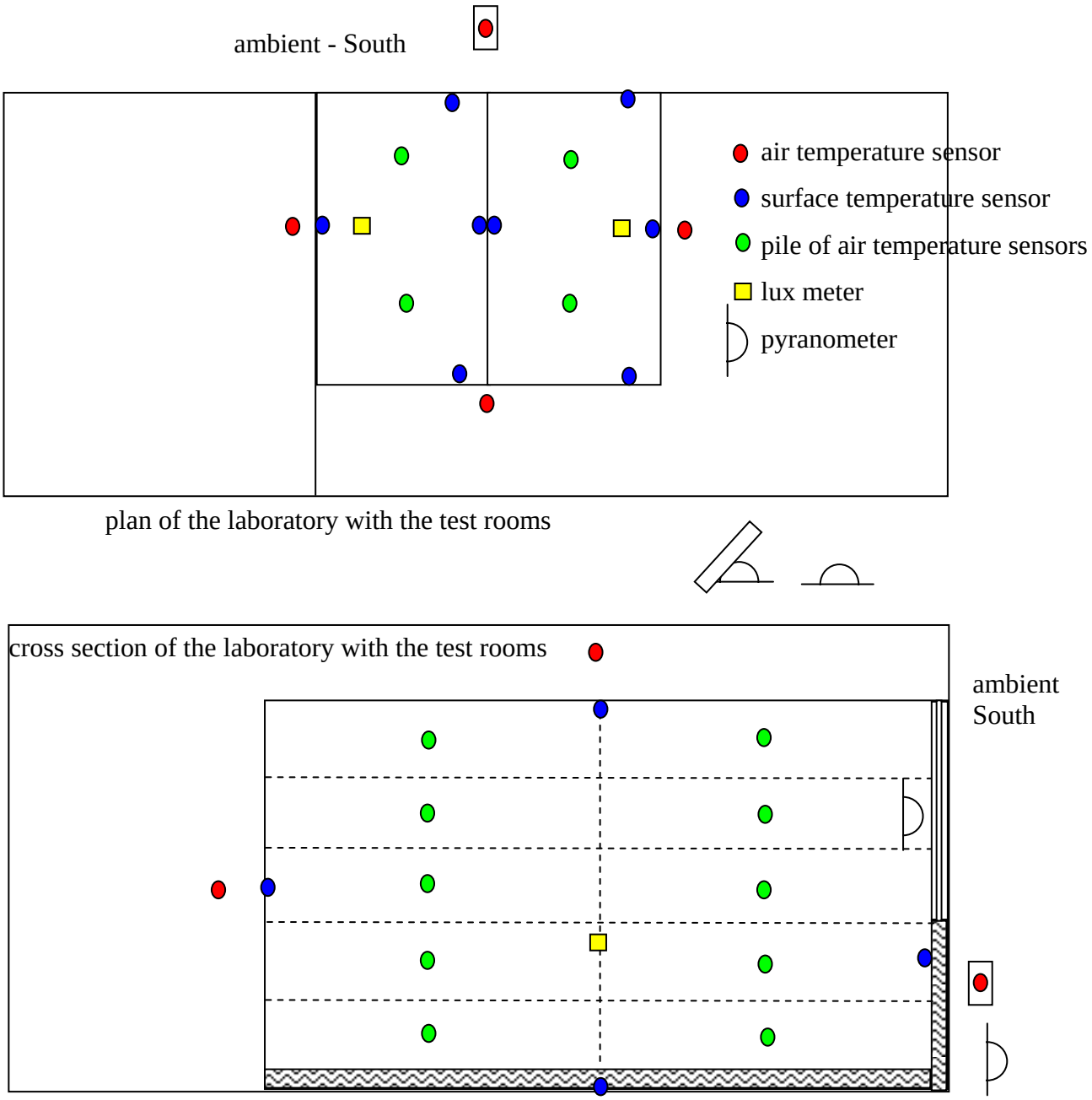

Figure 5.91. The sensors of the measuring system (Jensen, 2008a).

Comments on the absolute temperatures in figures 5.92-5.112

- the dynamical behaviour of the calculated mean air temperature is for both room very similar to the dynamical behaviour of the measured mean air temperature
- the calculated peak of the mean air temperature during sunshine is in both rooms nearly always lower than the measured peak temperatures
- the calculated temperature is during the night and periods with no or low solar radiation always higher that the corresponding measured temperature

- the calculated temperature declines slower than the measured temperatures after periods with solar radiation through the windows.

- the behaviour of the measured temperature in room A and B is very similar except that the day time peak values is – as expected – higher for room B than A during the spring and summer period. During the winter period the calculated temperature in room A has sometimes a higher peak that in room B. This latter is, however, more pronounced in the measurements and is due to an extra heat capacity in room B (an extra gypsum plate on the east wall in room B (Jensen, 2008a)). This extra heat capacity is also included in the model

- the air temperature of the laboratory to the east of room B (beside B in figures 5.97, 5.104 and 5.111) is very fluctuating. This is because this temperature is controlled by an electrical heater with a hysteresis (Jensen 2008a) with the temperature of beside A as set point. The control of this temperature failed from day 106 during the spring period. This has, however, no influence on the here performed comparisons, as the temperature is input to the calculations

Comments on the temperature differences in figures 5.96, 5.103 and 5. 110

Although very simple the test rooms are very complex from a modelling point of view. Although better defined than normal rooms most applied thermo physical properties have large uncertainty. It is further assumed that the test rooms are well sealed so that the infiltration is insignificant although this could not be determined (Jensen, 2008a). It's, therefore, not a surprise that the measured and calculated mean air temperatures aren't identical. But the agreement is actually very good for a first attempt.

The above was known from the start so the test rooms were erected with aim of being able to perform side by side experiments (Jensen et al, 1994) – i.e. the test rooms are almost identical (Jensen, 2008a) so that the main difference between the test rooms is the window which in fact is the interesting part of the tests. When using side by side experiments it is possible to eliminate most of the uncertainties of the identical parts of the test rooms. If instead of comparing absolute values for the air temperatures the measured difference in mean air temperature between the two rooms is compared with the calculated difference.

This comparison is done in figures 5.96, 5.103 and 5.110:

- the measurements shows that the measured temperature peak during solar radiation is 1.5 K higher in room B with the Velfac window compared to room A with Prototype 1. Remembering the previous chapter this difference would be 2 K if not the extra gypsum plate was present in room B.
- the measured and calculated difference aren't identical but the agreement is not that bad either
- there is most often calculated positive peaks when there is measured positive peaks
- the calculated peaks is smaller at clear sky conditions while the calculated peaks often is higher during overcast/cloudy/drifting cloud conditions
- the calculated difference declines slower than the measured difference after positive peaks
- the measured difference often becomes negative after positive peaks while the calculated difference most often stays above zero

5.2.3.1 Winter

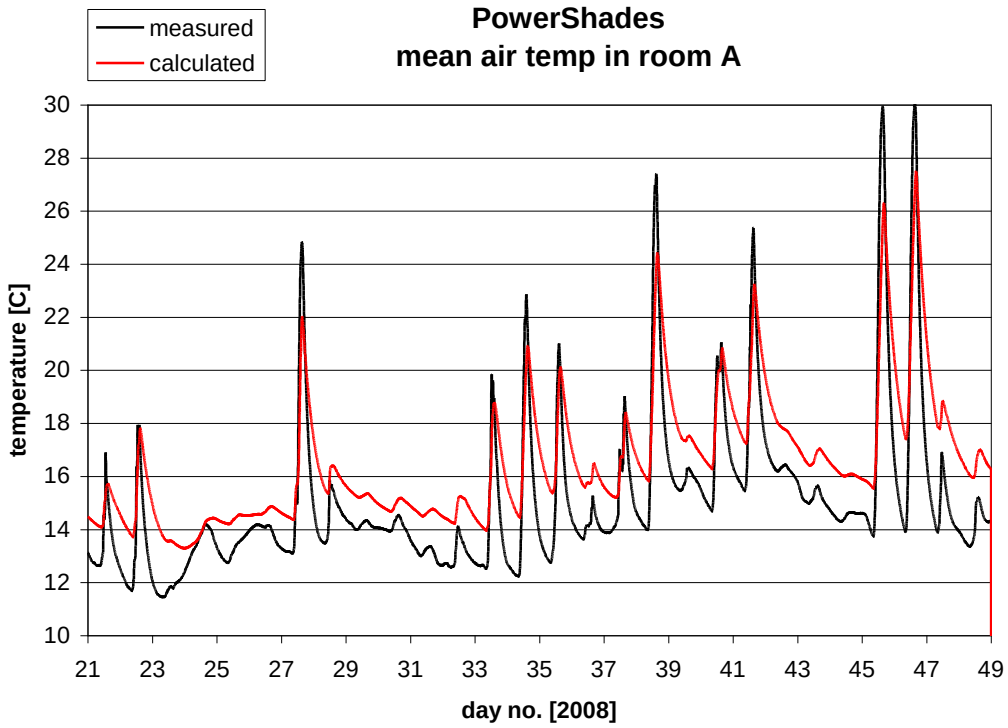

Figure 5.92. Measured and calculated mean air temperature in room A – 21/1-17/2, 2008.

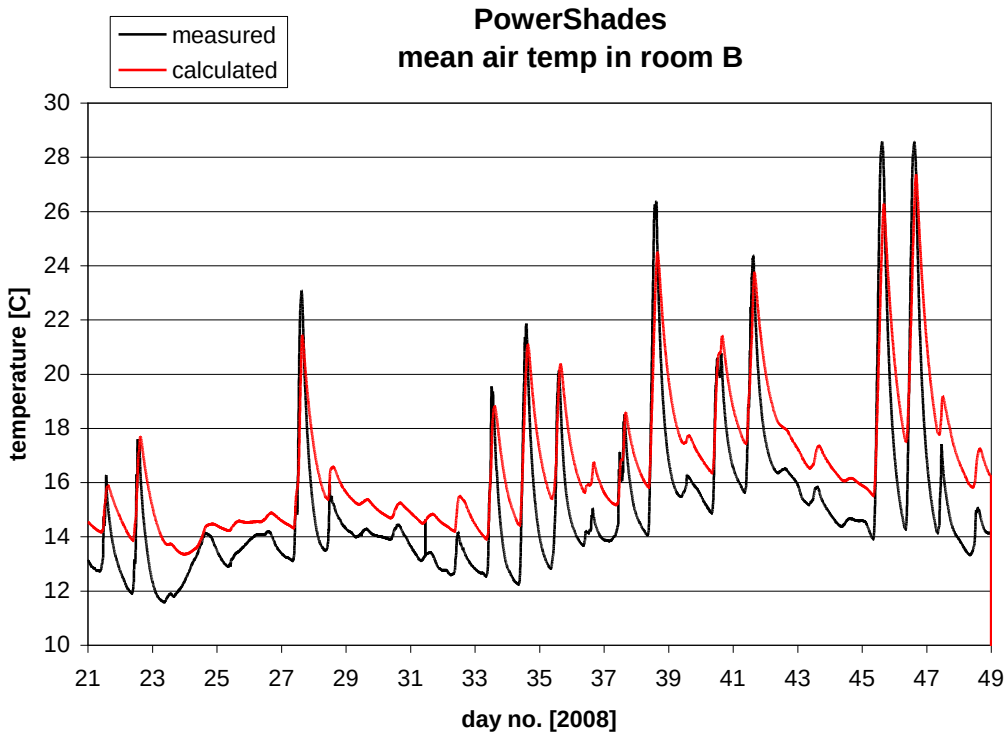

Figure 5.93. Measured and calculated mean air temperature in room A – 21/1-17/2, 2008.

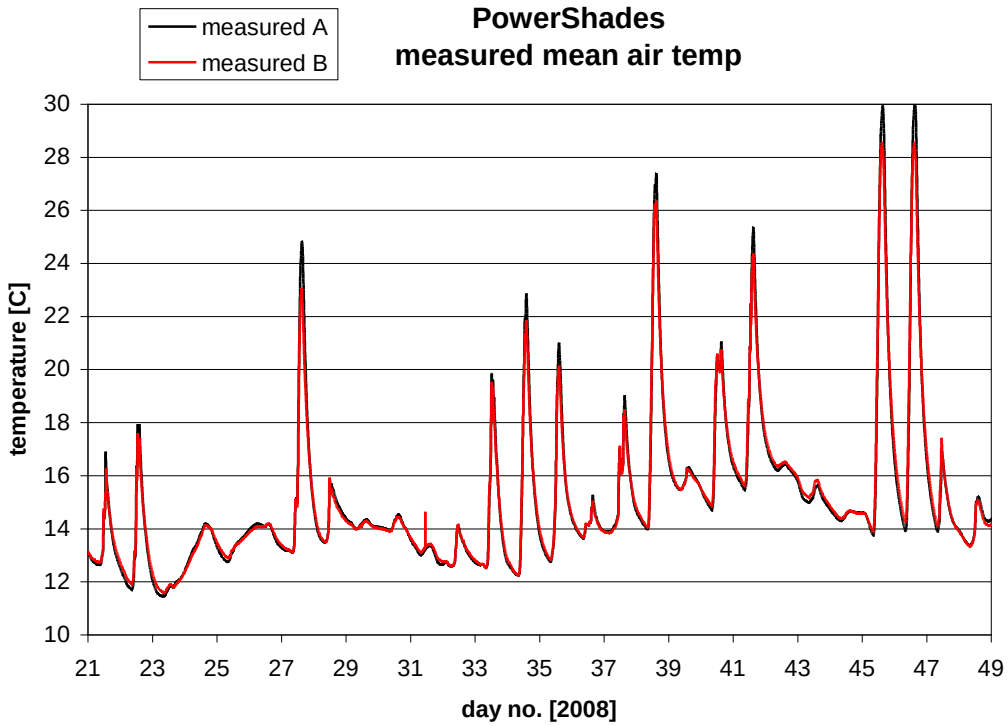

Figure 5.94. Measured mean air temperature in room A and B – 21/1-17/2, 2008.

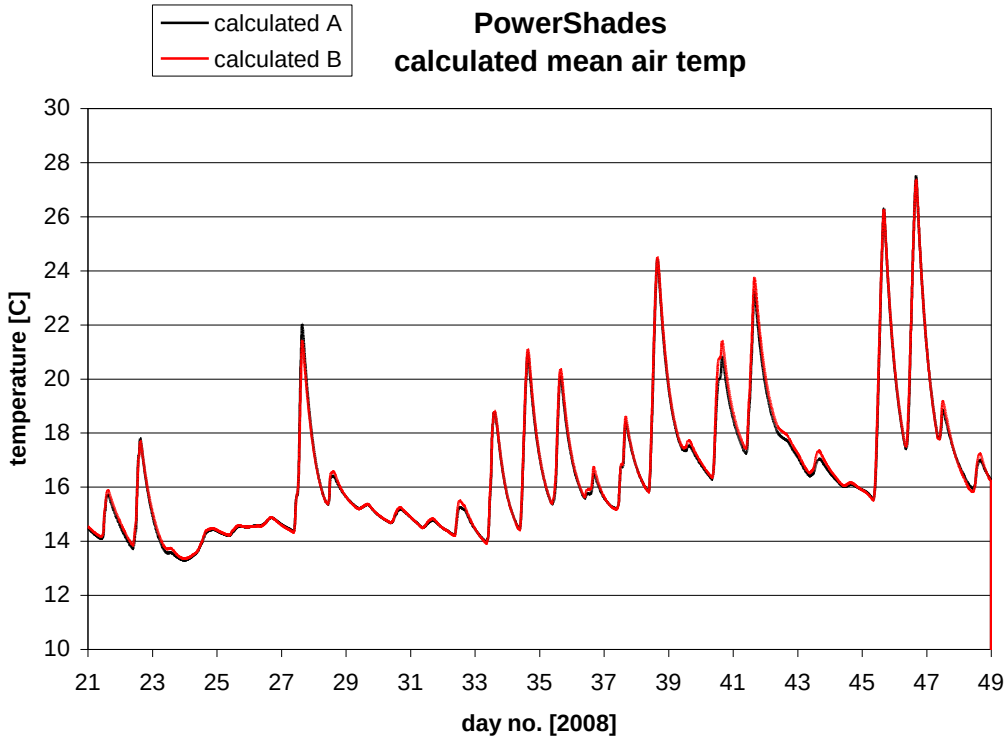

Figure 5.95. Calculated mean air temperature in room A and B – 21/1-17/2, 2008.

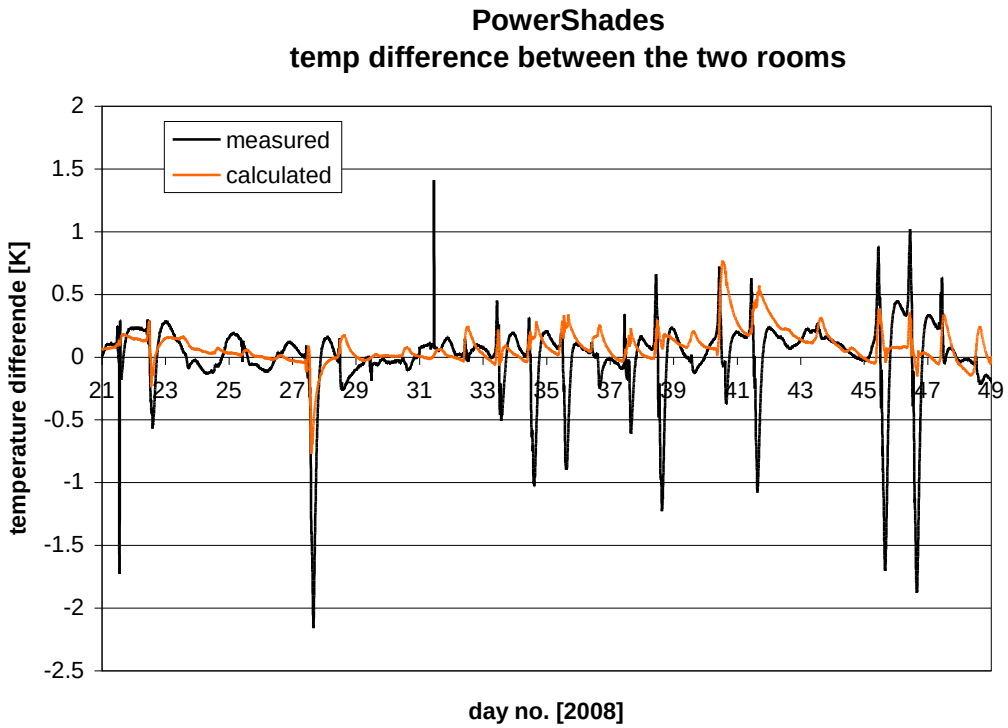

Figure 5.96. Measured and calculated temperature difference between room A and B – 21/1-17/2, 2008.

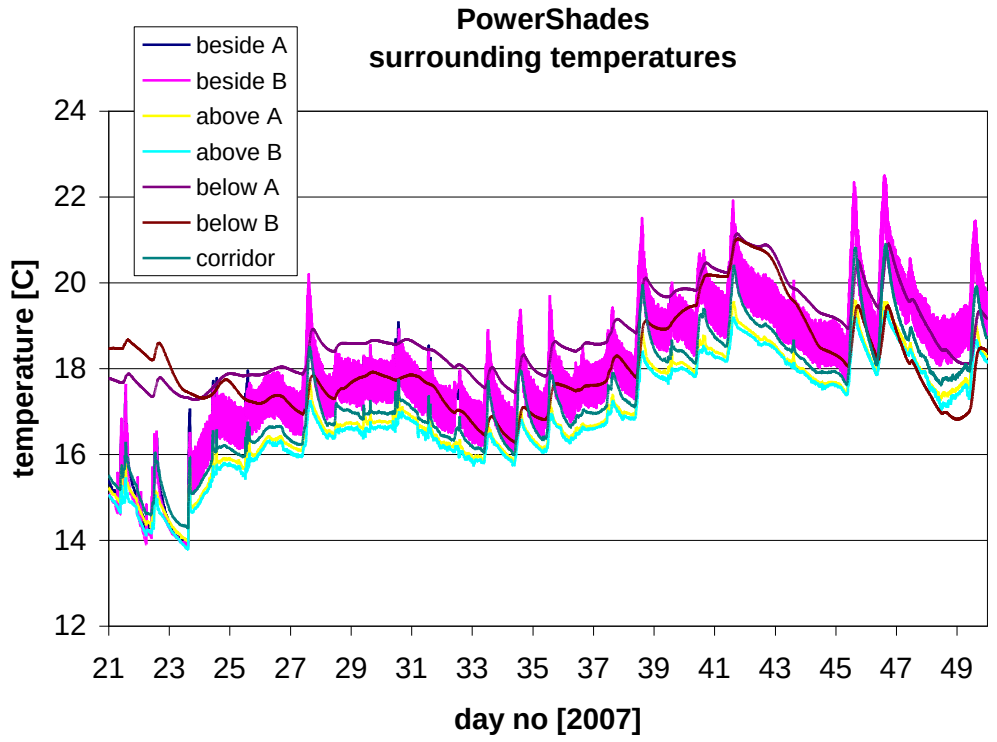

Figure 5.97. Surrounding temperatures – 21/1-17/2, 2008.

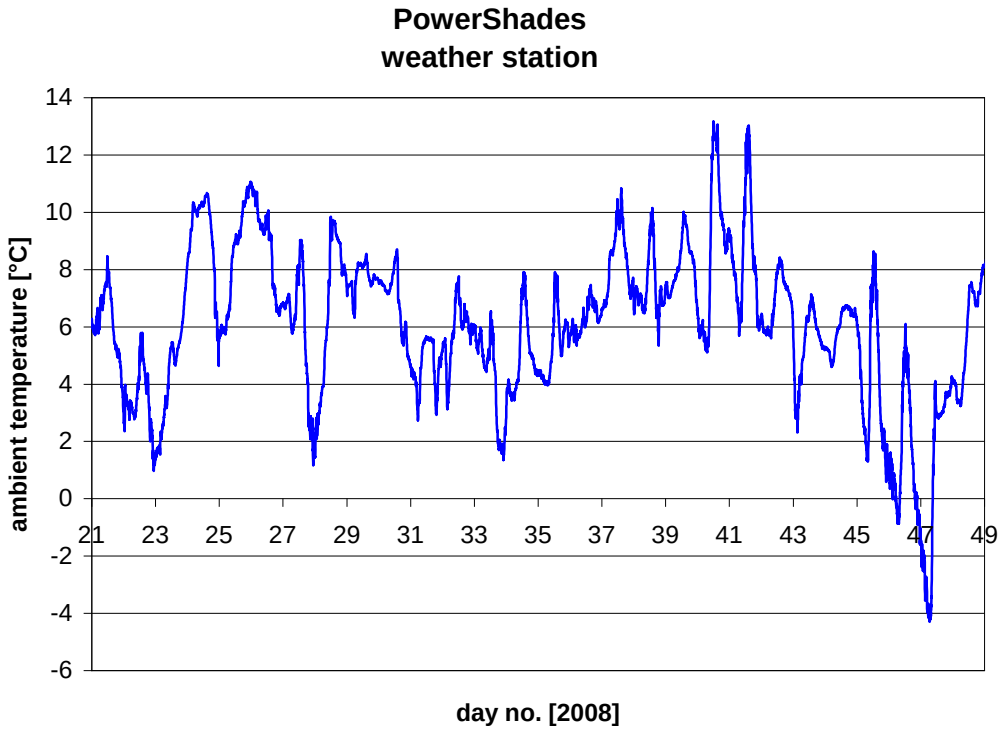

Figure 5.98. Ambient temperature – 21/1-17/2, 2008.

5.2.3.2 Spring

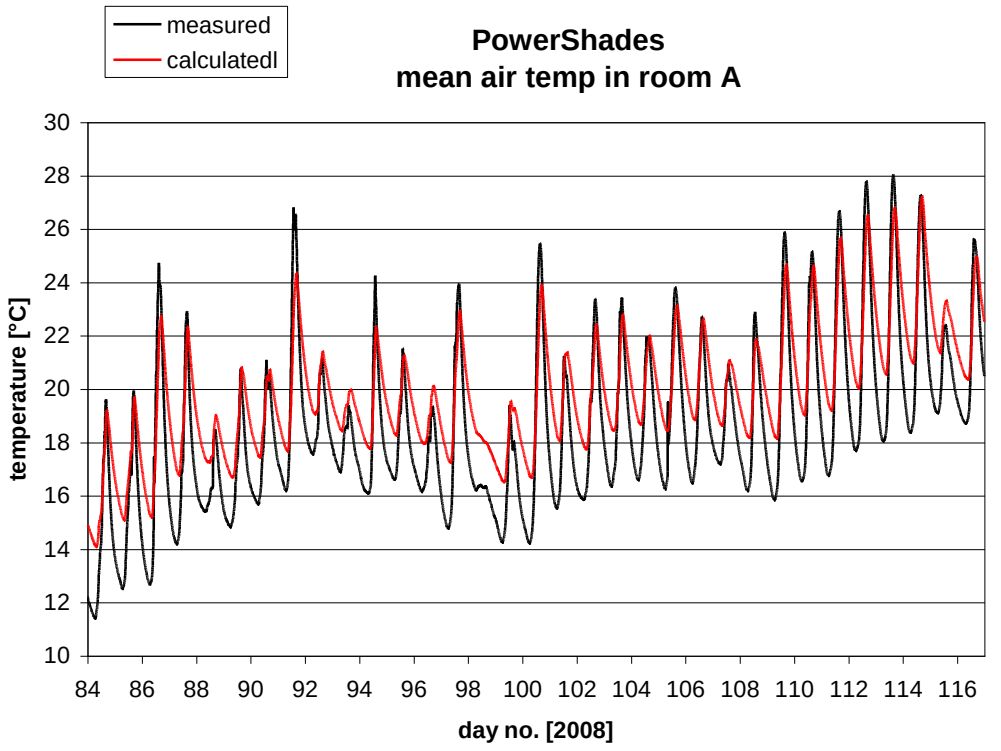

Figure 5.99. Measured and calculated mean air temperature in room A – 25/3-26/4, 2008.

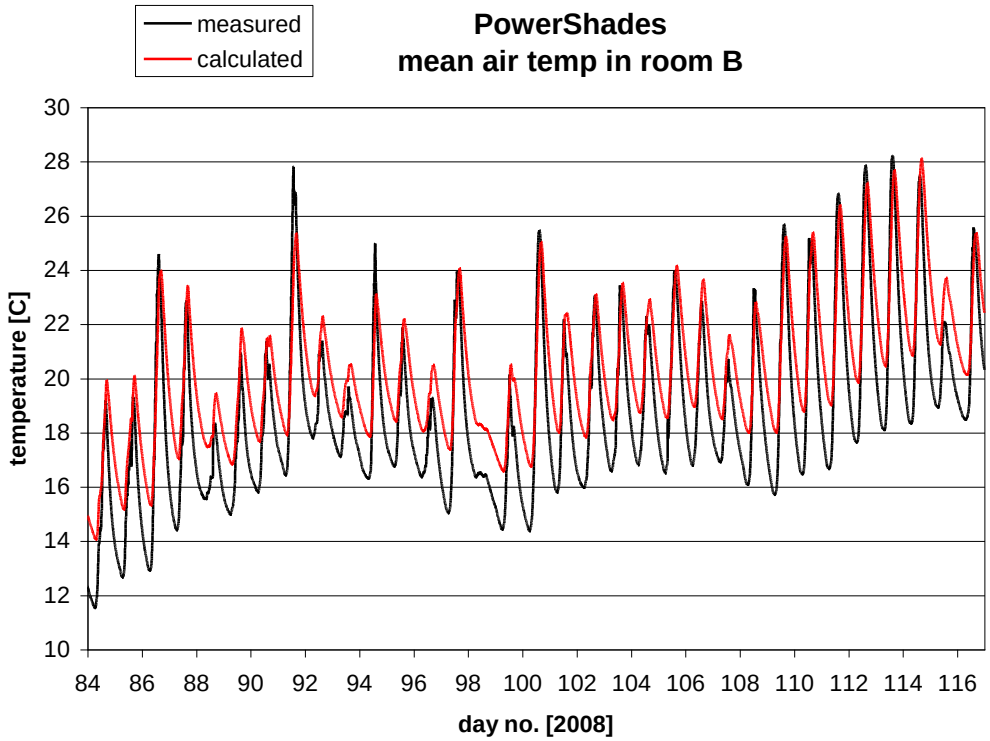

Figure 5.100. Measured and calculated mean air temperature in room A – 25/3-26/4, 2008.

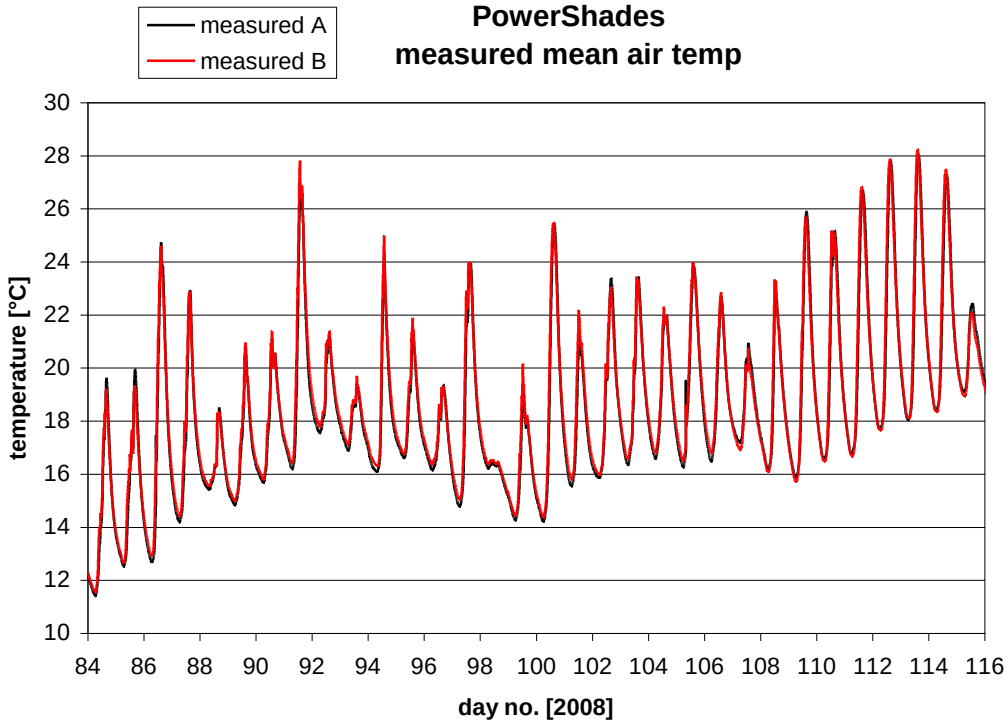

Figure 5.101. Measured mean air temperature in room A and B – 25/3-26/4, 2008.

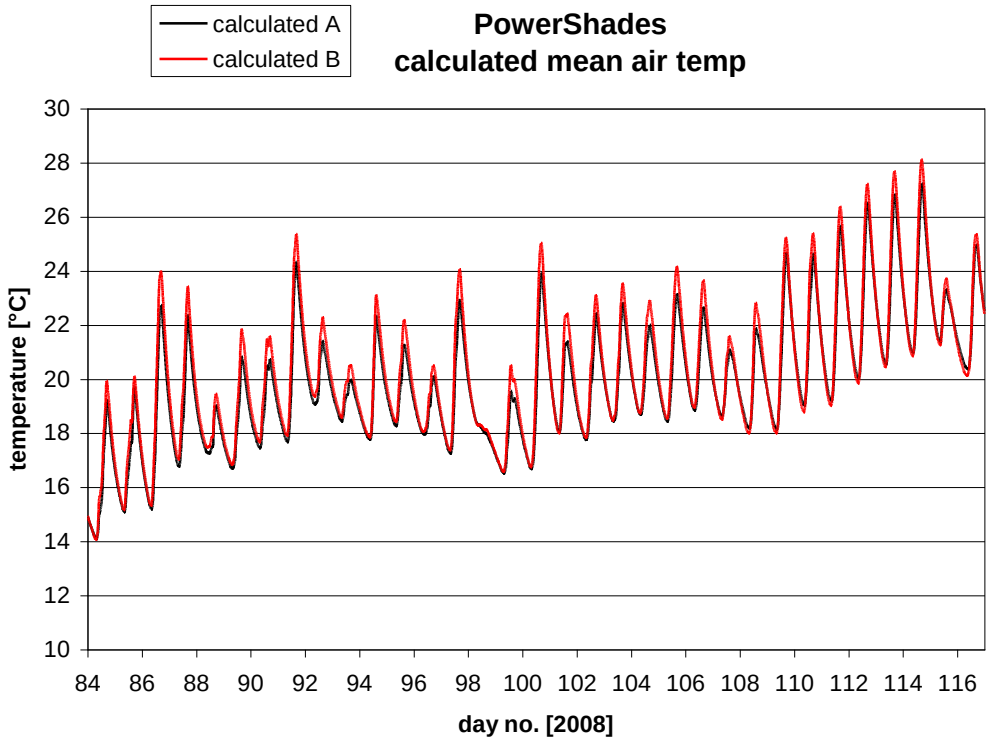

Figure 5.102. Calculated mean air temperature in room A and B – 25/3-26/4, 2008.

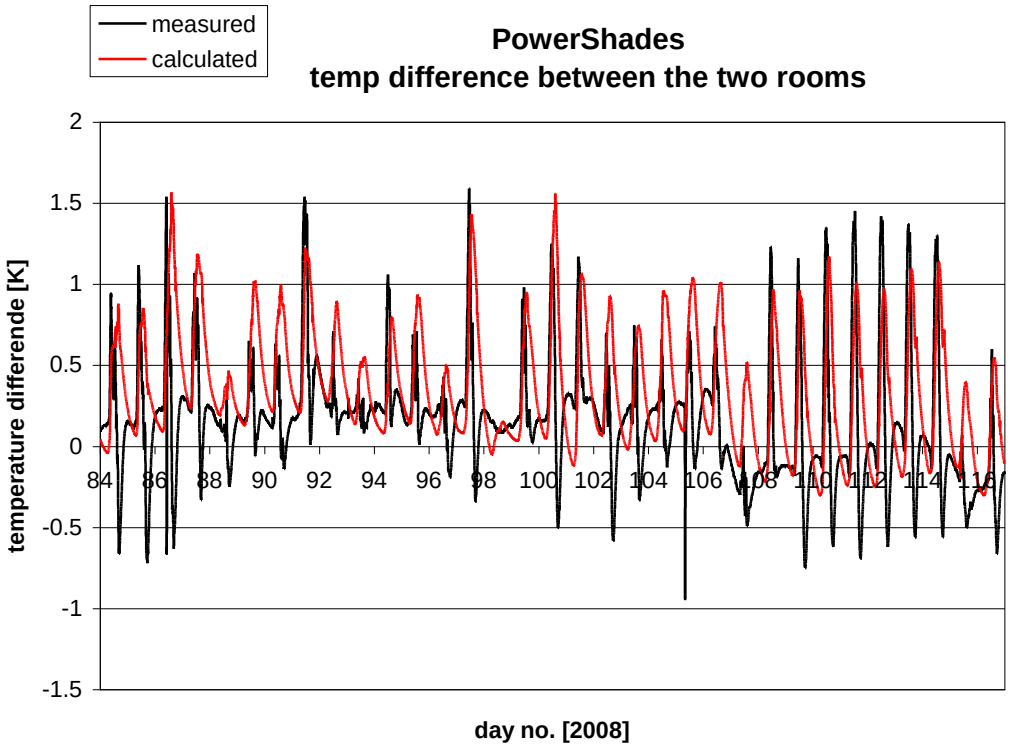

Figure 5.103. Measured and calculated temperature difference between room A and B – 25/3-26/4, 2008.

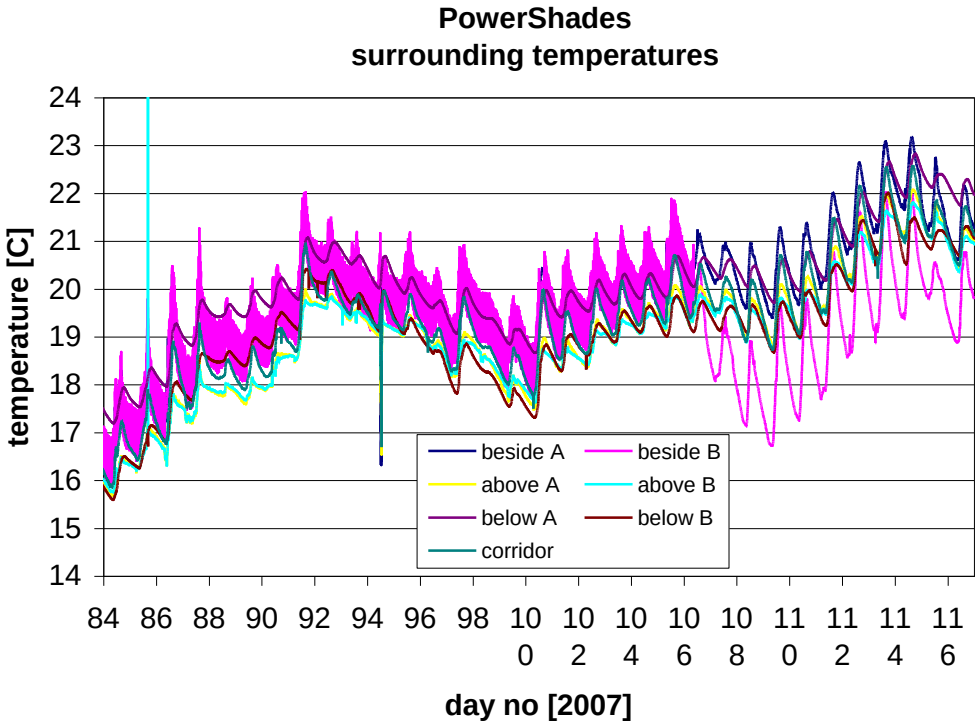

Figure 5.104. Surrounding temperatures – 25/3-26/4, 2008.

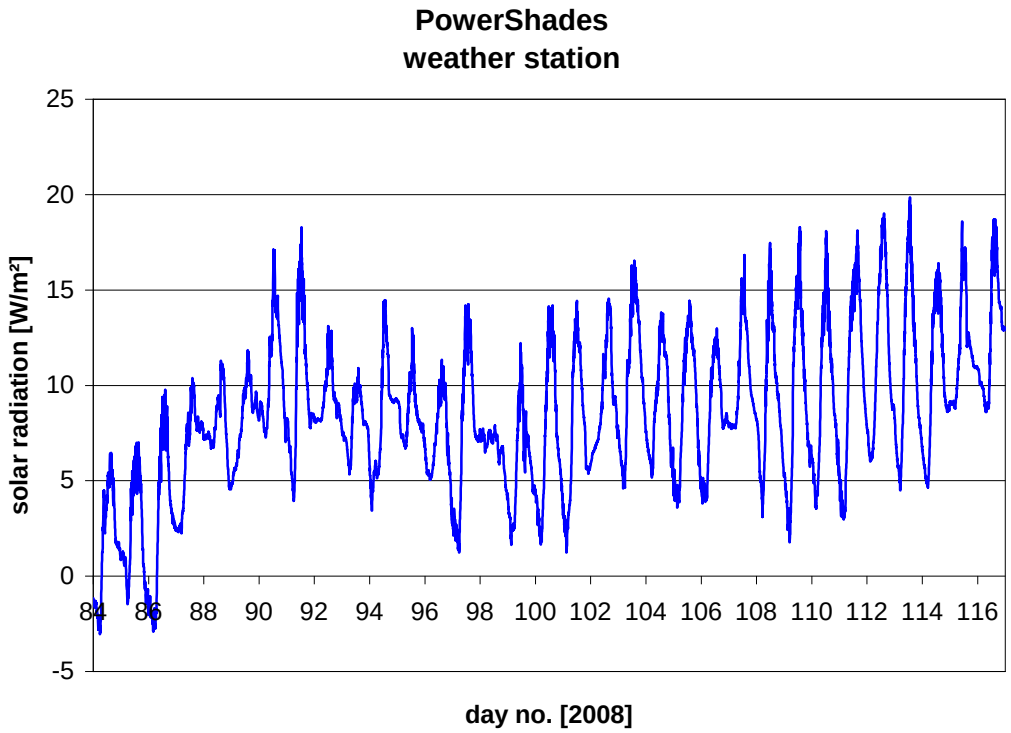

Figure 5.105. Ambient temperature – 25/3-26/4, 2008.

5.2.3.3 Summer

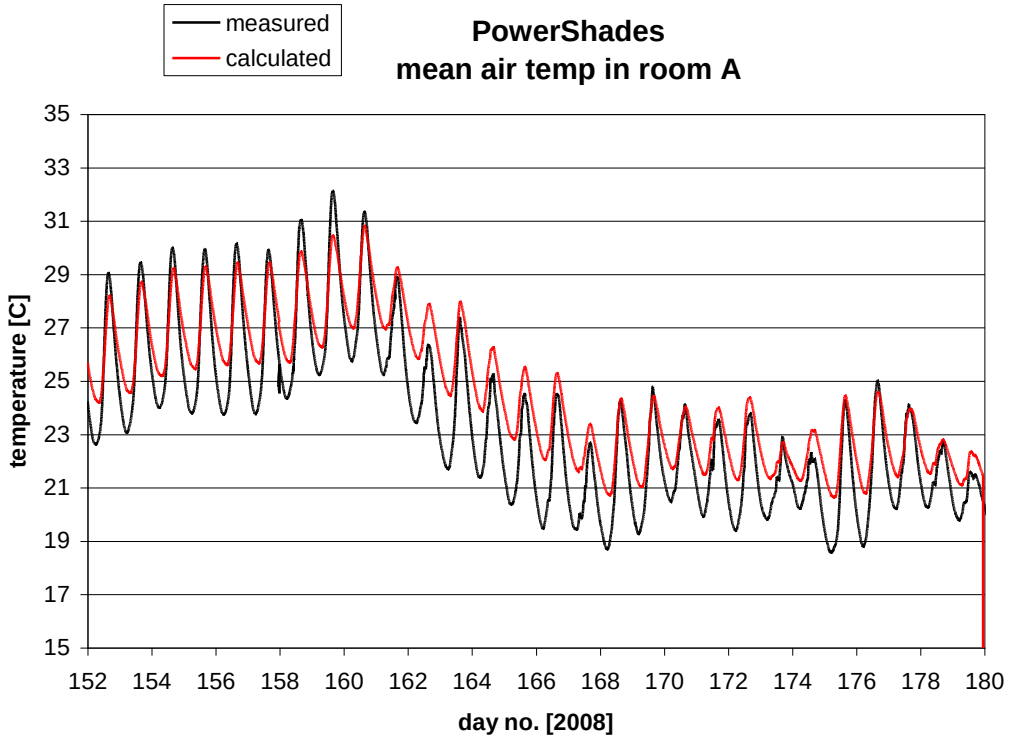

Figure 5.106. Measured and calculated mean air temperature in room A – 1-28/6, 2008.

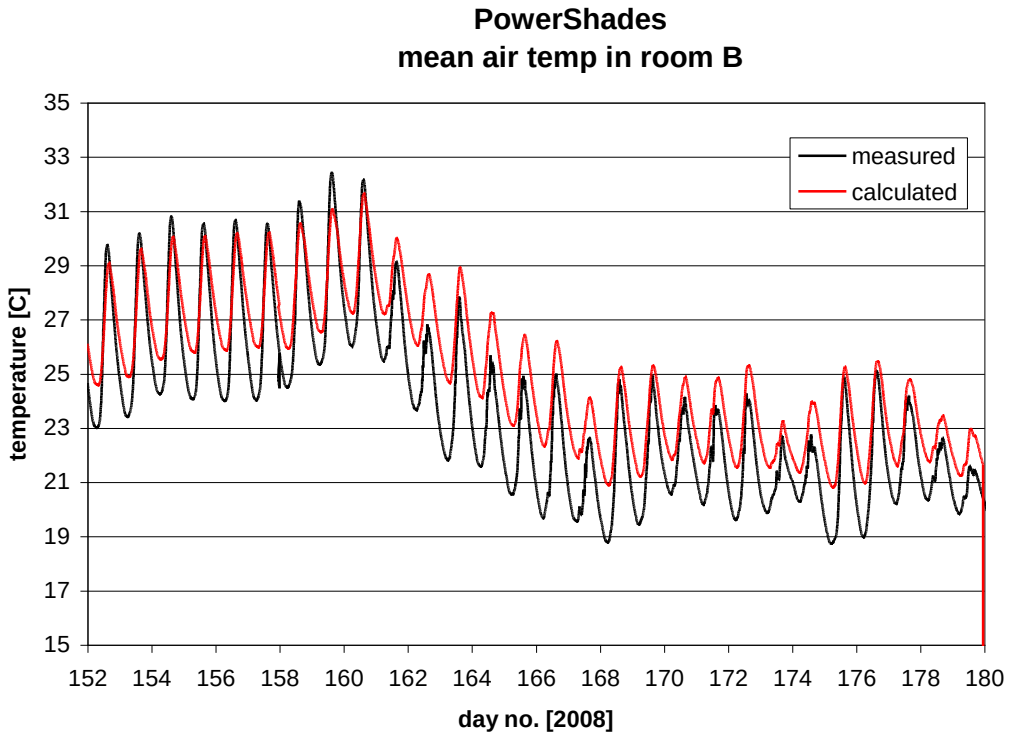

Figure 5.107. Measured and calculated mean air temperature in room A – 1-28/6, 2008.

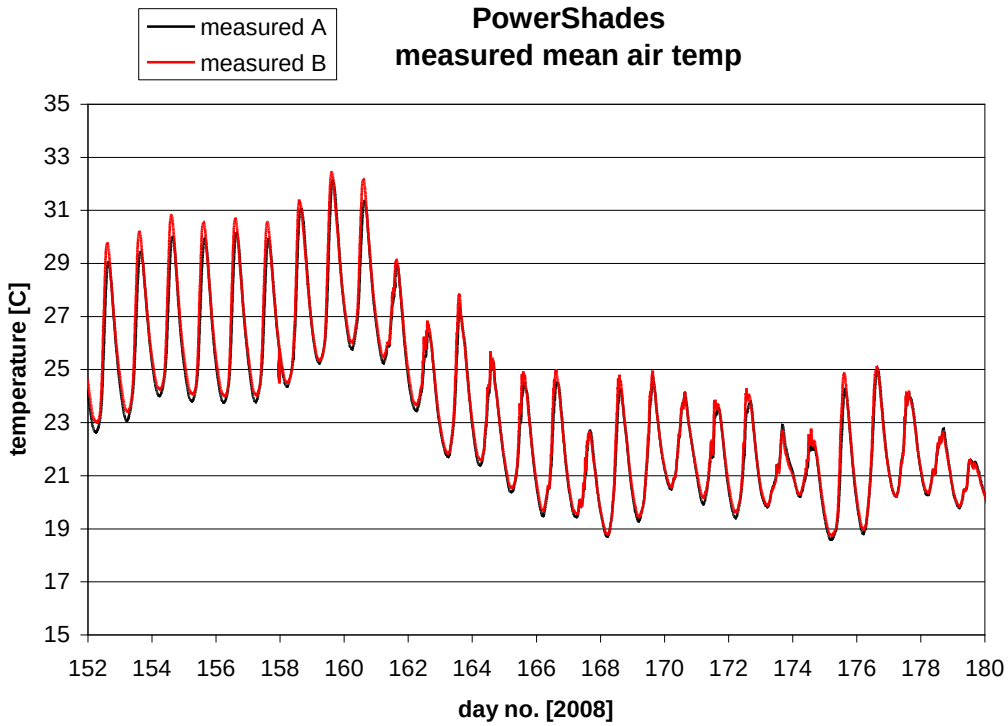

Figure 5.108. Measured mean air temperature in room A and B – 1-28/6, 2008.

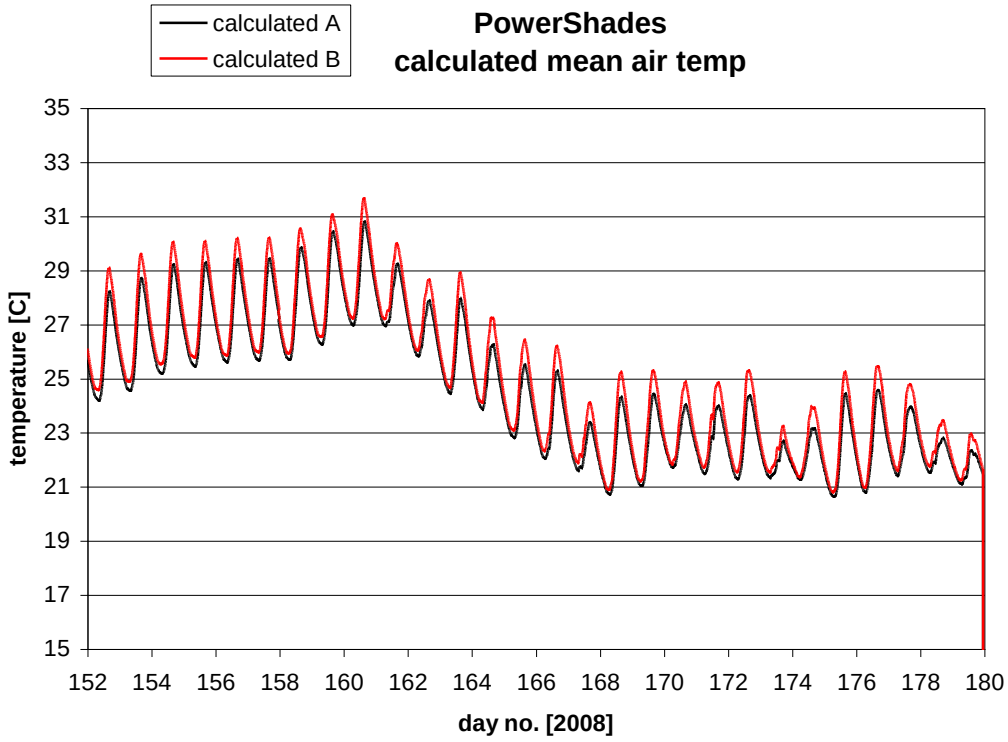

Figure 5.109. Calculated mean air temperature in room A and B – 1-28/6, 2008.

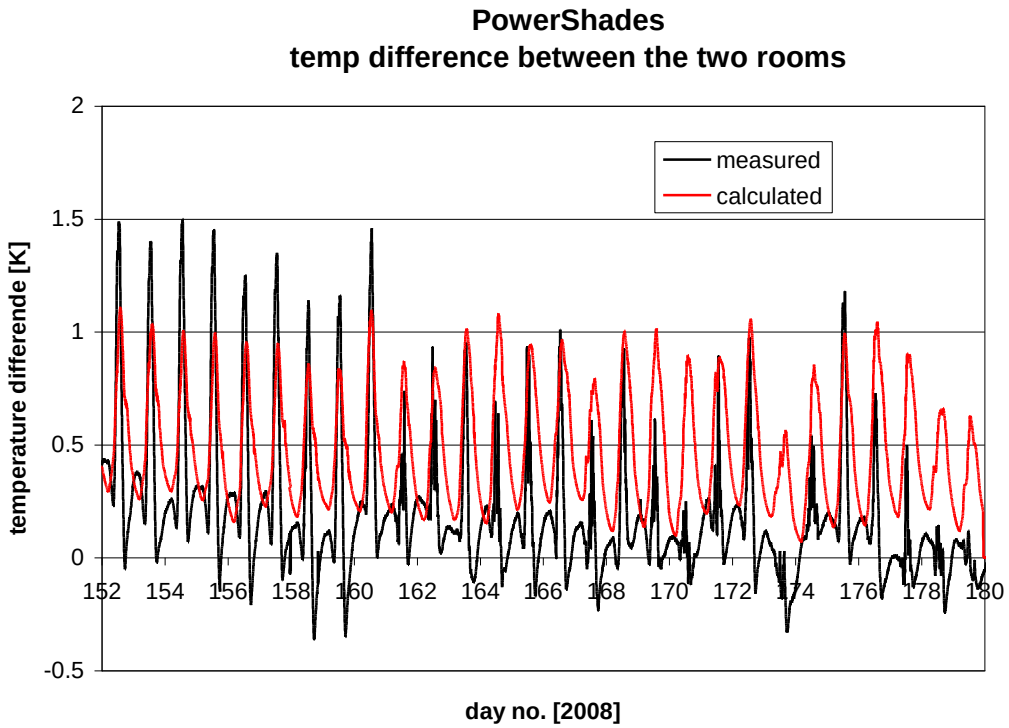

Figure 5.110. Measured and calculated temperature difference between room A and B – 1-28/6, 2008.

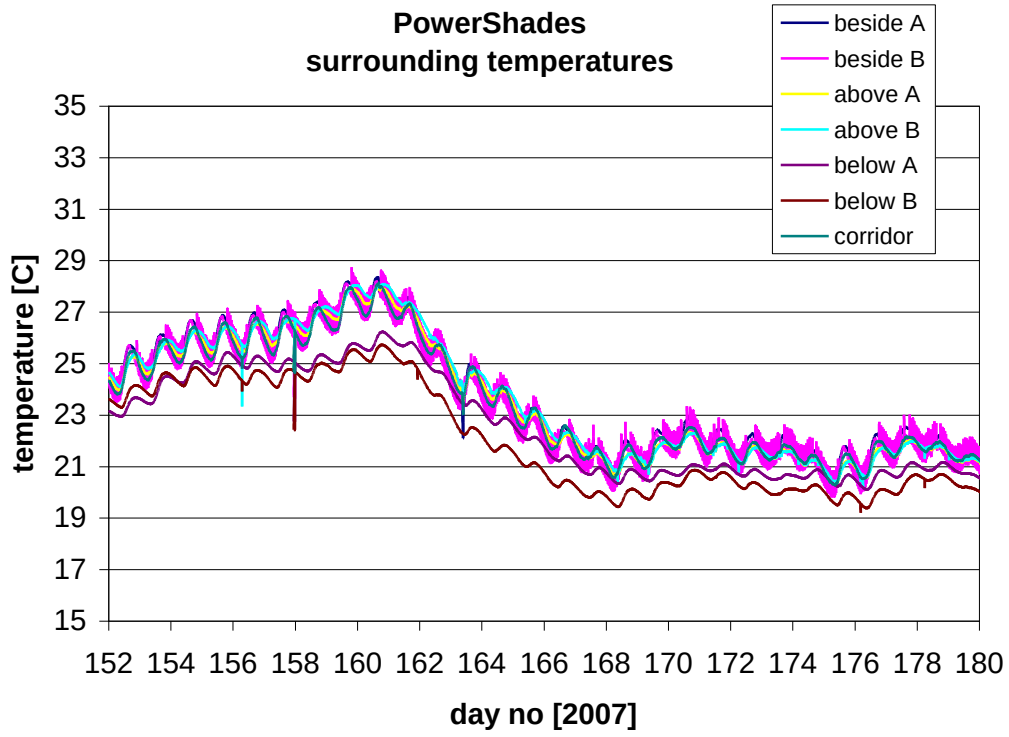

Figure 5.111. Surrounding temperatures – 1-28/6, 2008.

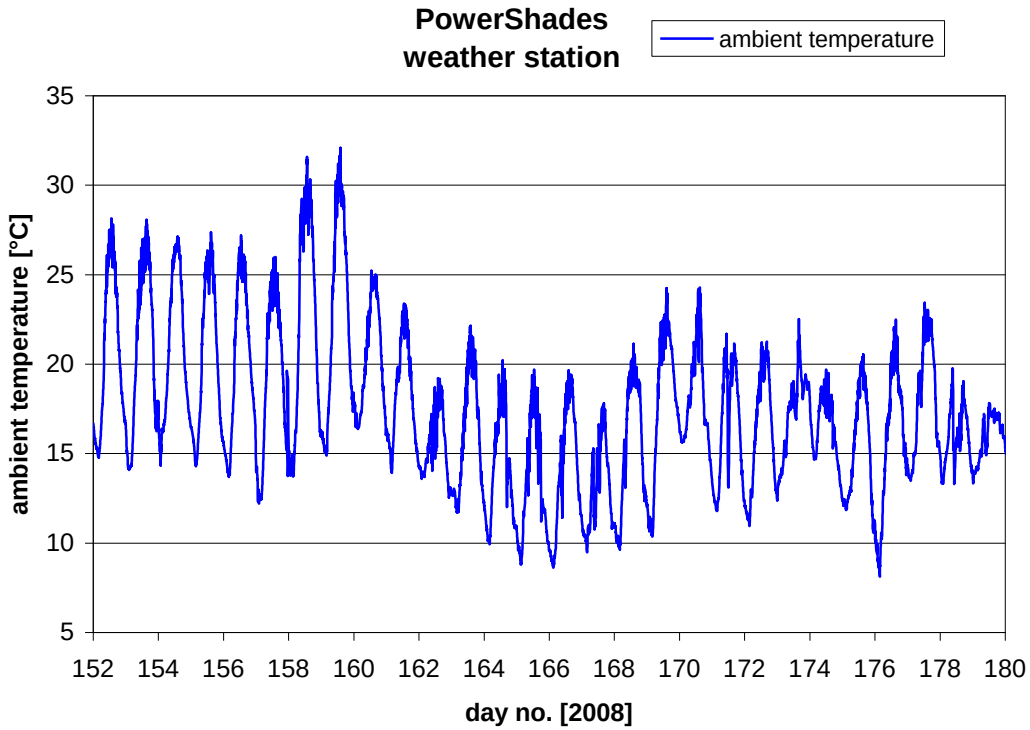

Figure 5.112. Ambient temperature – 1-28/6, 2008.

The model of the test rooms is as already mentioned very complex with large uncertainties on many parameters. It is therefore a non trivial task to calibrate the model of the test rooms.

When looking at e.g. figures 5.106-107 it is seen that although the dynamic is rather well represented by the model the amplitude of the calculated temperature swing is too small. And further the decline of the calculated temperature curve is slower than the measured curve. This suggests that:

- the thermal capacity of the test rooms are too high and/or
- the heat loss to ambient and/or the surrounding zones are wrong and/or
- there is infiltration in the test rooms
- ……

The above has been tested for the summer period.

- the heat capacity of the gypsum plates in both test rooms has been decreased with 50% compared to figures 5.106-110. See figures 5.114-118.
- the U-value of the window in test room A had been decreased and increased with 50% compared to figures 5.106-110. See figures 5.119-128.
- the U-value of the insulation in the internal walls and the ceiling of both test rooms have been decreased and increased with 50% compared to figures 5.106-110. See figures 5.129-138.
- infiltration has not been modelled, but the trend will be the same as when increasing the U-value of the windows

Figures 5.114-138 should be compared to figures 5.106-113. As figure 5.108 is not changed (only measured values) this figure is, therefore, not repeated in the following. A new figure is, however, introduced: figure 5.113 where only the first two days of figure 5.110 is shown in order also to be able to investigate the time shift of the calculated peak during clear sky conditions compared to the measured peak. For the reference case (figures 5.106-110) this is shown in figure 5.113

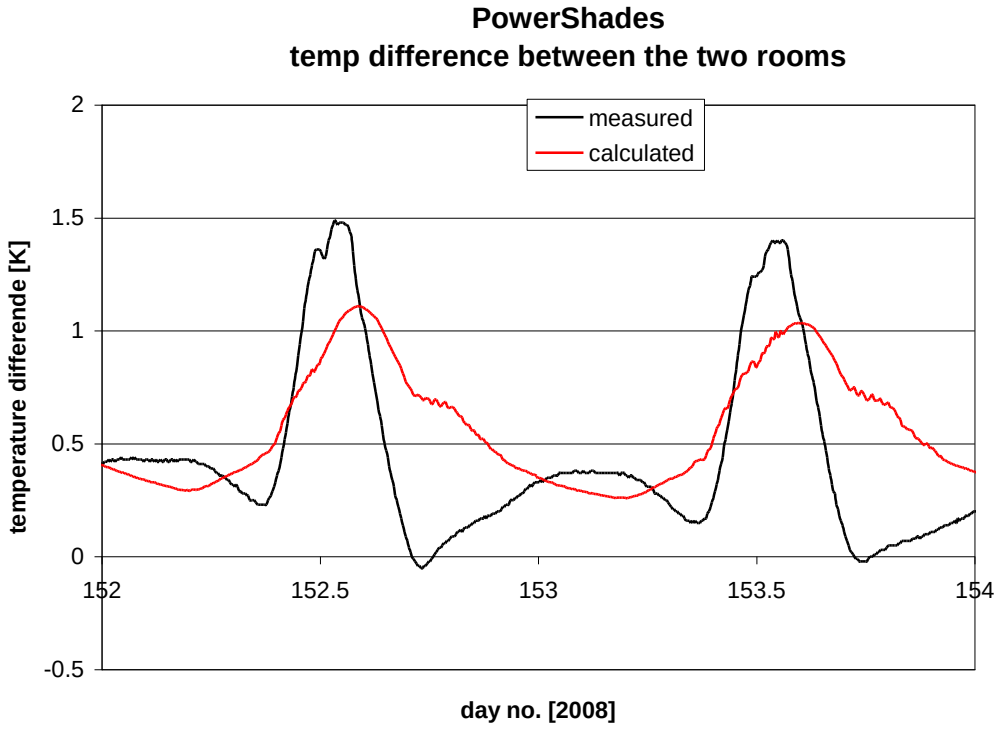

Figure 5.113. Measured and calculated temperature difference between room A and B – 1-2/6, 2008. Reference case.

Reduction of the heat capacity of the gypsum plates with 50% - figures 5.114-118

In figures 5.114-115 it is seen that the reduction of the heat capacity of the gypsum plates increases the amplitude of the calculated temperature swing. The daytime peak is now more in agreement with the measured peaks for the first 7 days, however, the increase in the daytime peak is also observed for days where the calculated peaks were above the measured peaks – day 161-175. The change doesn't really influence the slower calculated decline or the nighttime temperature level.

Concerning figure 5.117: there is now a better agreement in the peak level for day 156-161 while the peaks are now much too high during the days 163-179.

The off set has not been changed in figure 5.118.

Reduction of the U-value of the PowerShade window with 50% - figures 5.119-123

The reduction of the U-value of the PowerShade window lead in figures 5.119-120 to a less good agreement during daytime peak in the period 152-159, but a slightly better agreement

during 163-179. This is because the ambient temperature as seen in figure 5.112 has almost the same temperature level as the calculated test room temperature during the first period and a lower temperature level during the last period.

Although less good agreement for the absolute temperatures a very good agreement is obtained for the temperature difference between the two rooms as seen in figure 5.122 – at least for the first period until day 169. After this the daytime peaks becomes too large.

The off set has not been changed in figure 5.123.

Increase of the U-value of the PowerShade window with 50%

The increase of the U-value of the PowerShade window lead to a little bit better agreement in both daytime and night-time peaks in absolute temperatures - figures 5.124-125. However the amplitude of the calculated temperature differences is now far too low – figure 5.127. But the daytime peak of the temperature difference is now in phase as seen in figure 5.128.

Reduction of the U-value of the insulation in the internal walls and the ceiling window with 50% - figures 5.129-133

The reduction of the U-values of the internal surfaces lead to a better agreement for the daytime peak in figures 5.129-130 for the days 152-161 but a little worse for the rest of the period. The night-time temperatures increase a bit. This is because as seen in figure 5.104 that the surrounding temperatures is lower than the calculated test room temperatures during the first period and at more or less the same level during the last period.

Figure 5.132 shows that this leads to better daytime agreement for the temperature differences for the first part of the period but worse during the last part and to a too high level of the calculated night-time temperature difference during the night.

The off set has not been changed in figure 5.133.

Increase of the U-value of the insulation in the internal walls and the ceiling window with 50% - figures 5.134-138

The reduction of the U-values of the internal surfaces lead to a worse agreement for the daytime peak in figures 5.134-135 for the days 152-161 but quite good for the rest of the period. The night-time temperatures are hardly influenced.

The same picture is seen for the temperature differences as seen in figure 5.137.

The off set has not been changed in figure 5.138.

5.2.3.4 Reduction of the heat capacity of the gypsum plates with 50%

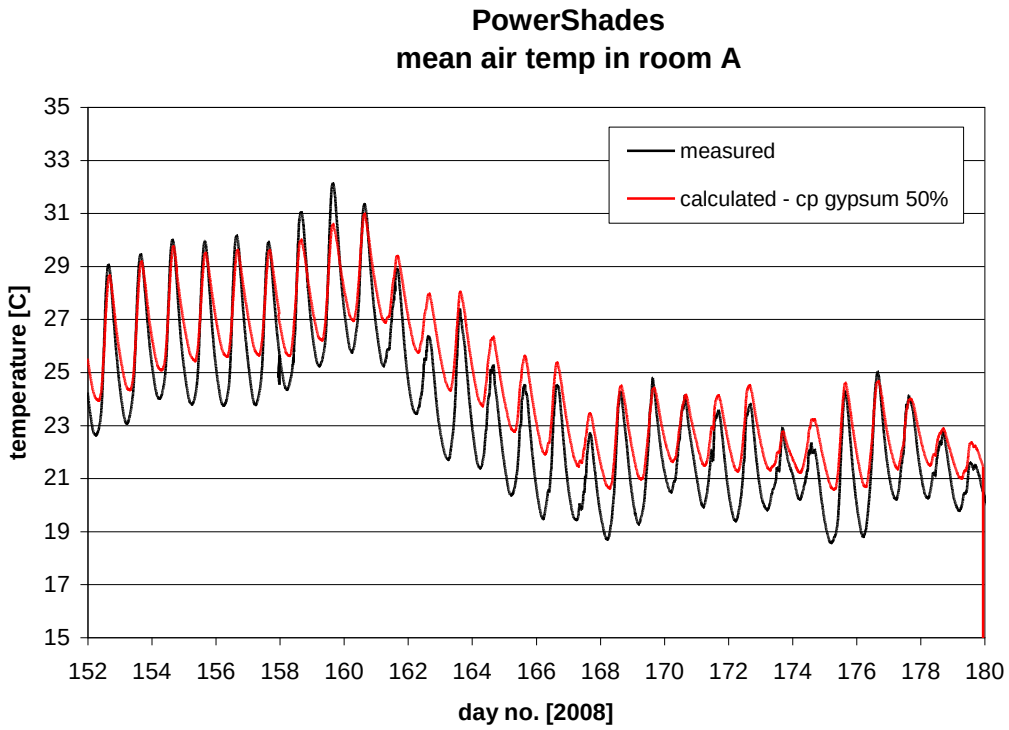

Figure 5.114. Measured and calculated mean air temperature in room A – 1-28/6, 2008. Reduction of the heat capacity of the gypsum plates with 50%.

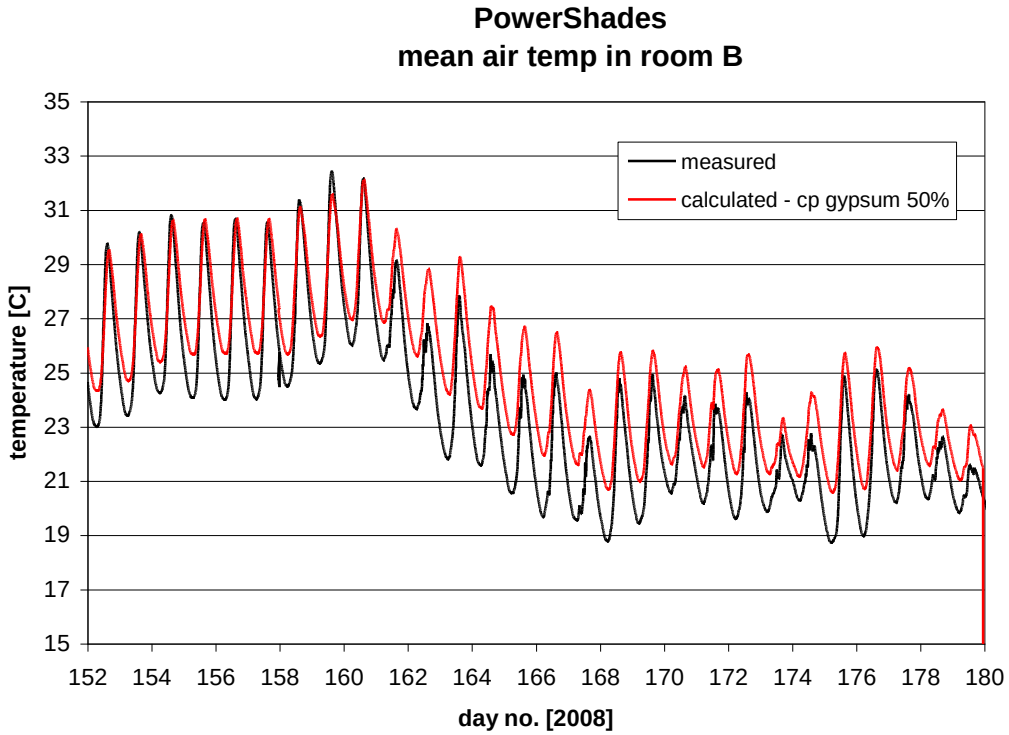

Figure 5.115. Measured and calculated mean air temperature in room A – 1-28/6, 2008. Reduction of the heat capacity of the gypsum plates with 50%.

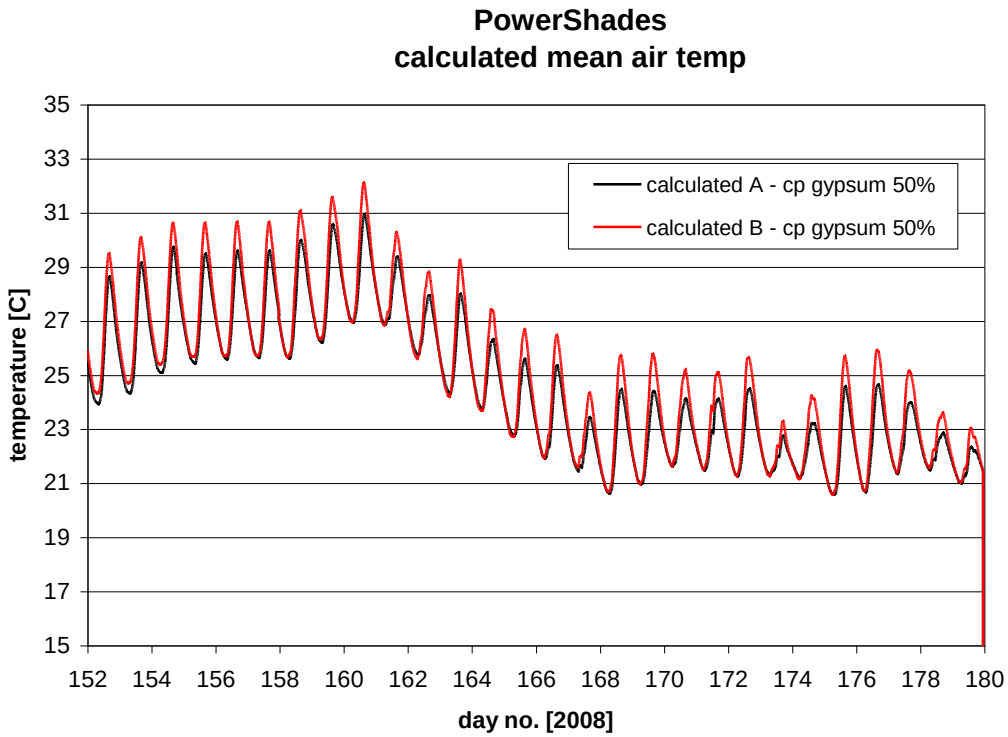

Figure 5.116. Calculated mean air temperature in room A and B – 1-28/6, 2008. Reduction of the heat capacity of the gypsum plates with 50%.

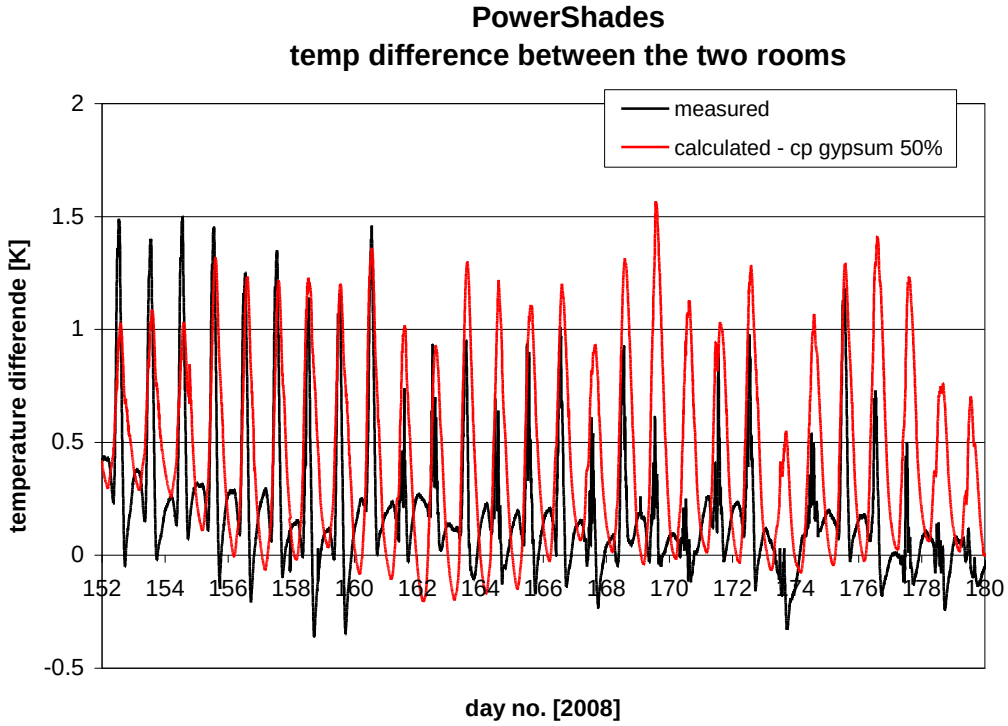

Figure 5.117. Measured and calculated temperature difference between room A and B – 1-28/6, 2008. Reduction of the heat capacity of the gypsum plates with 50%.

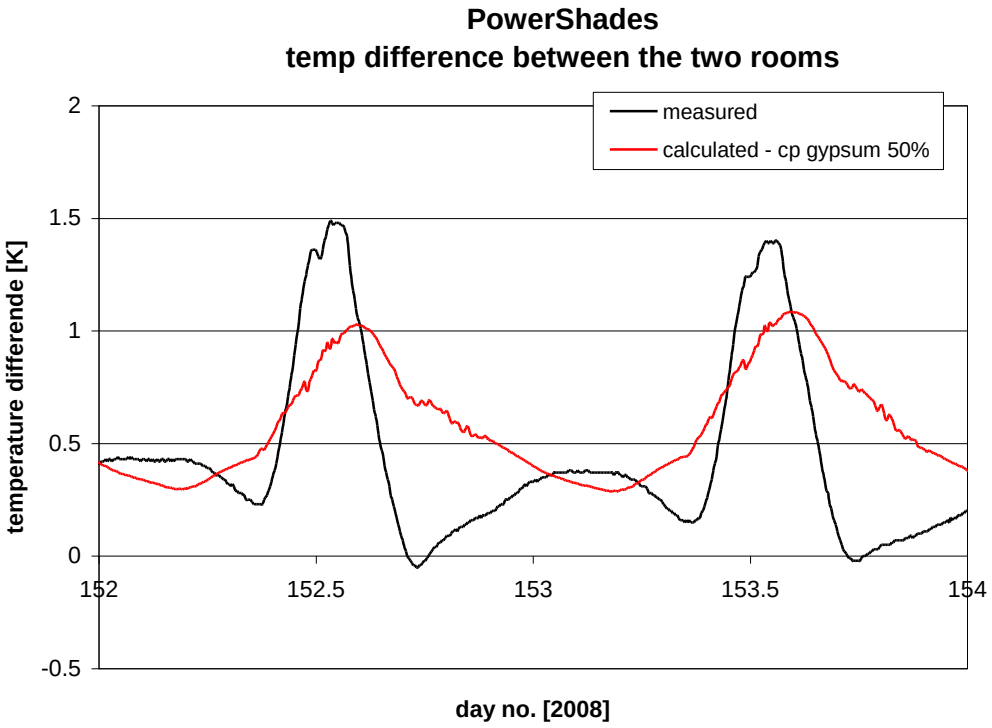

Figure 5.118. Measured and calculated temperature difference between room A and B – 1-2/6, 2008. Reduction of the heat capacity of the gypsum plates with 50%.

5.2.3.5 Reduction of the U-value of the PowerShade window with 50%

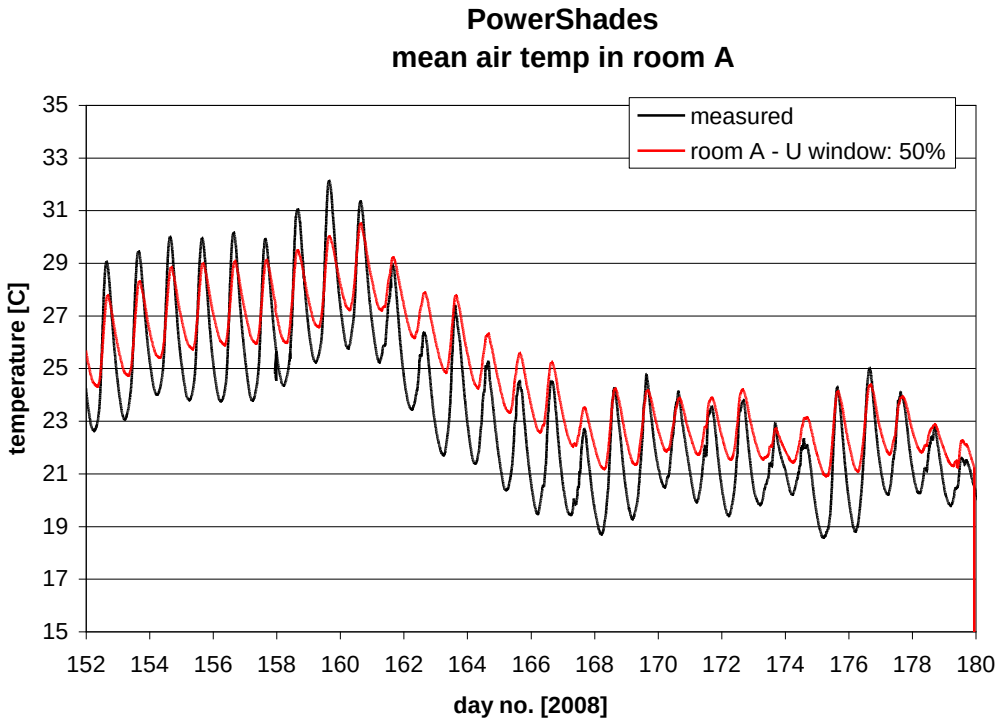

Figure 5.119. Measured and calculated mean air temperature in room A – 1-28/6, 2008. Reduction of the U-value of the PowerShade window with 50%.

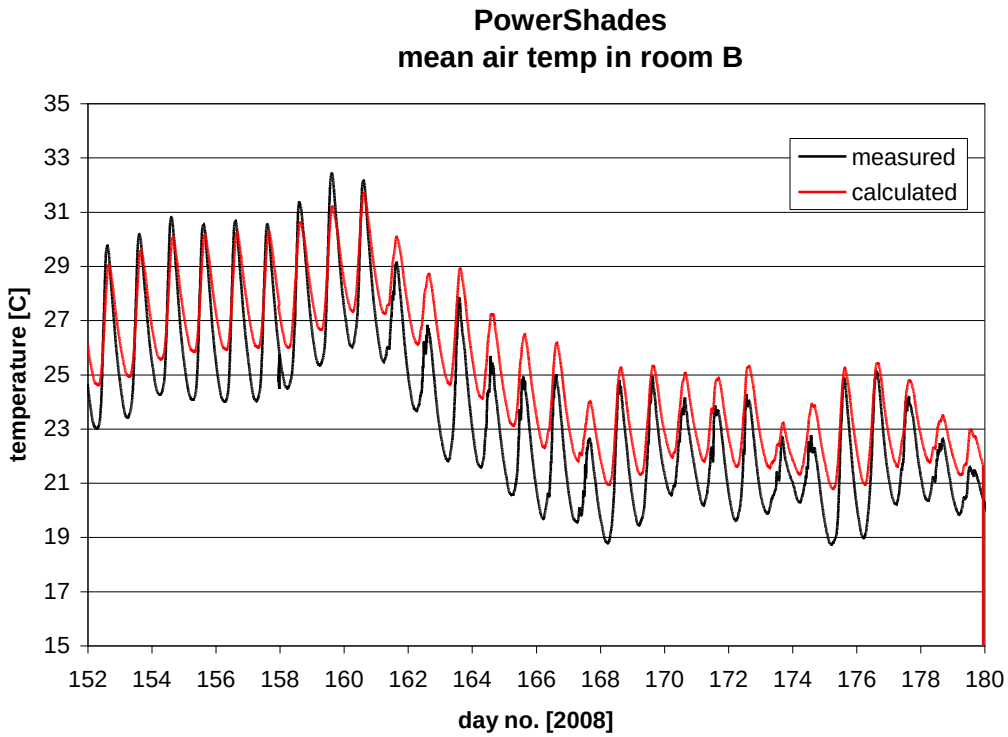

Figure 5.120. Measured and calculated mean air temperature in room A – 1-28/6, 2008. Reduction of the U-value of the PowerShade window with 50%.

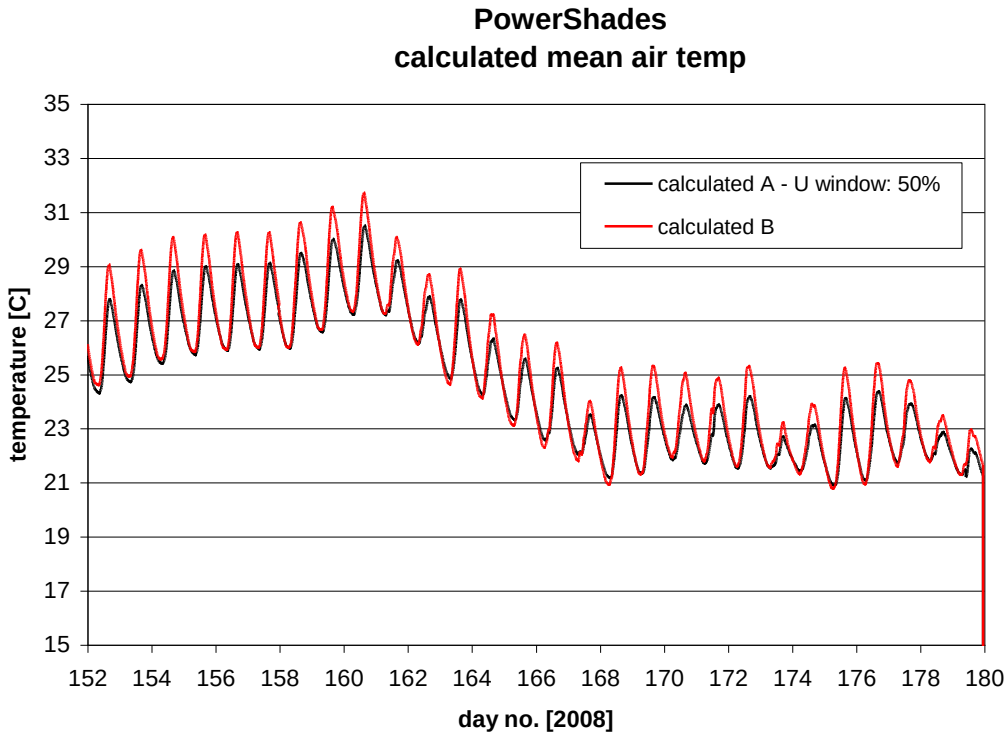

Figure 5.121. Calculated mean air temperature in room A and B – 1-28/6, 2008. Reduction of the U-value of the PowerShade window with 50%.

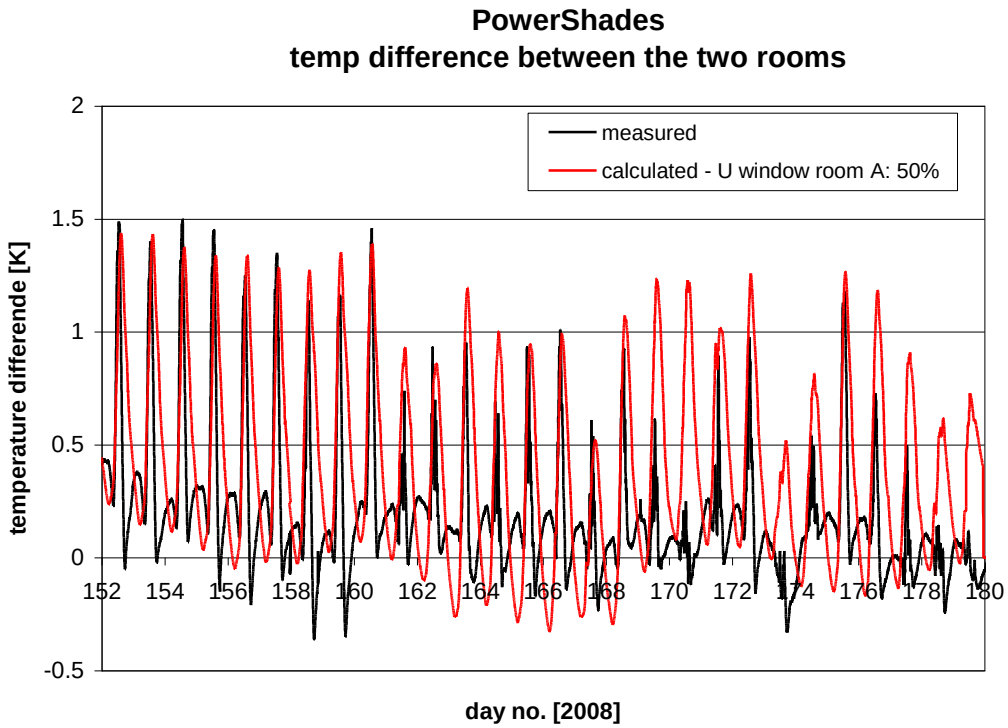

Figure 5.122. Measured and calculated temperature difference between room A and B – 1-28/6, 2008. Reduction of the U-value of the PowerShade window with 50%.

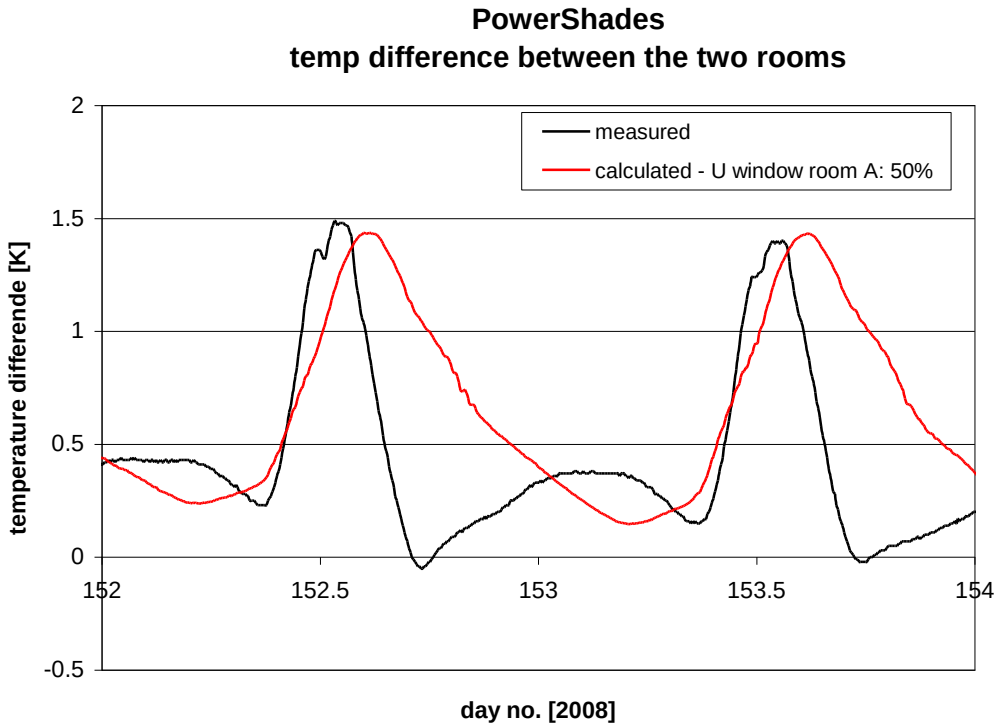

Figure 5.123. Measured and calculated temperature difference between room A and B – 1-2/6, 2008. Reduction of the U-value of the PowerShade window with 50%.

5.2.3.6 Increase of the U-value of the PowerShade window with 50%

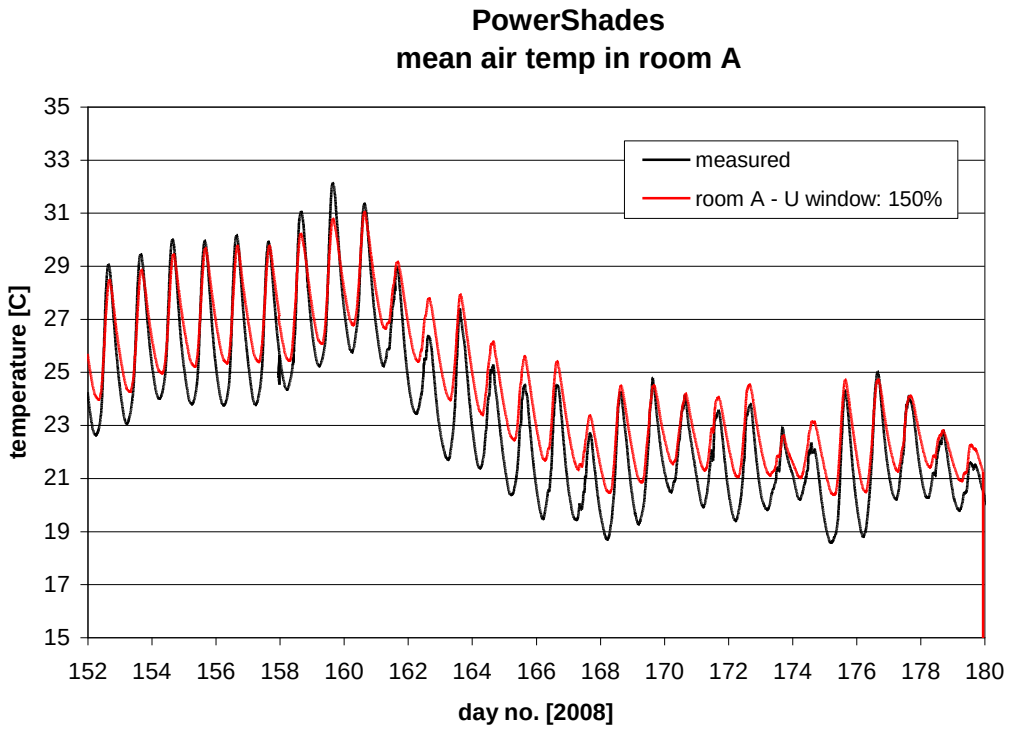

Figure 5.124. Measured and calculated mean air temperature in room A – 1-28/6, 2008. Increase of the U-value of the PowerShade window with 50%.

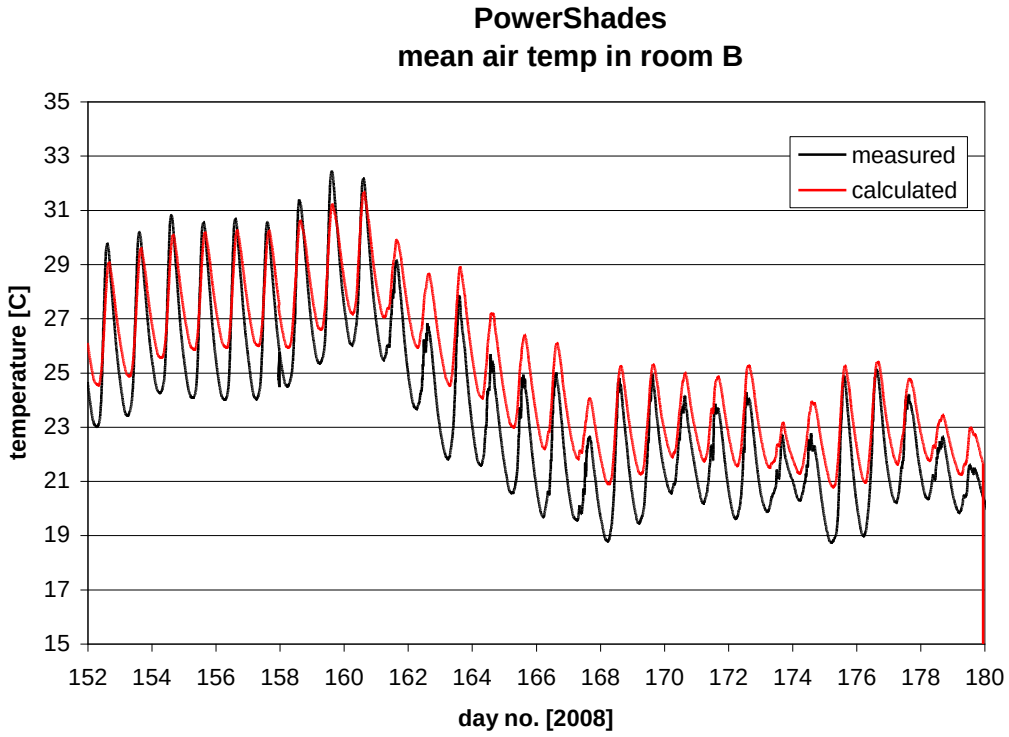

Figure 5.125. Measured and calculated mean air temperature in room A – 1-28/6, 2008. Increase of the U-value of the PowerShade window with 50%.

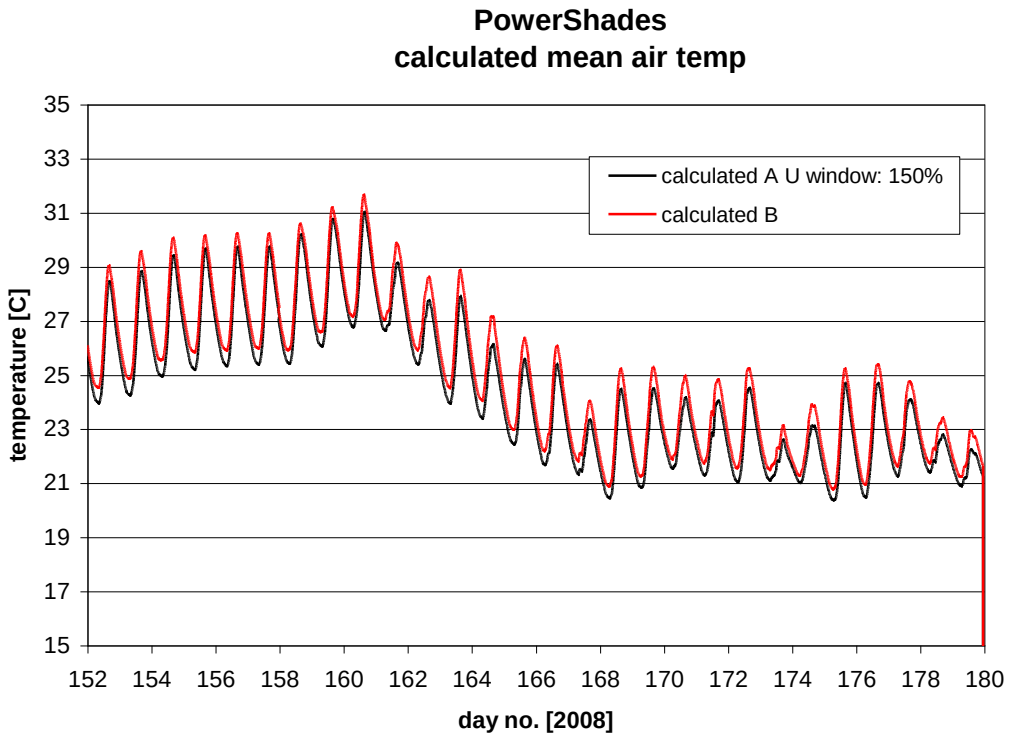

Figure 5.126. Calculated mean air temperature in room A and B – 1-28/6, 2008. Increase of the U-value of the PowerShade window with 50%.

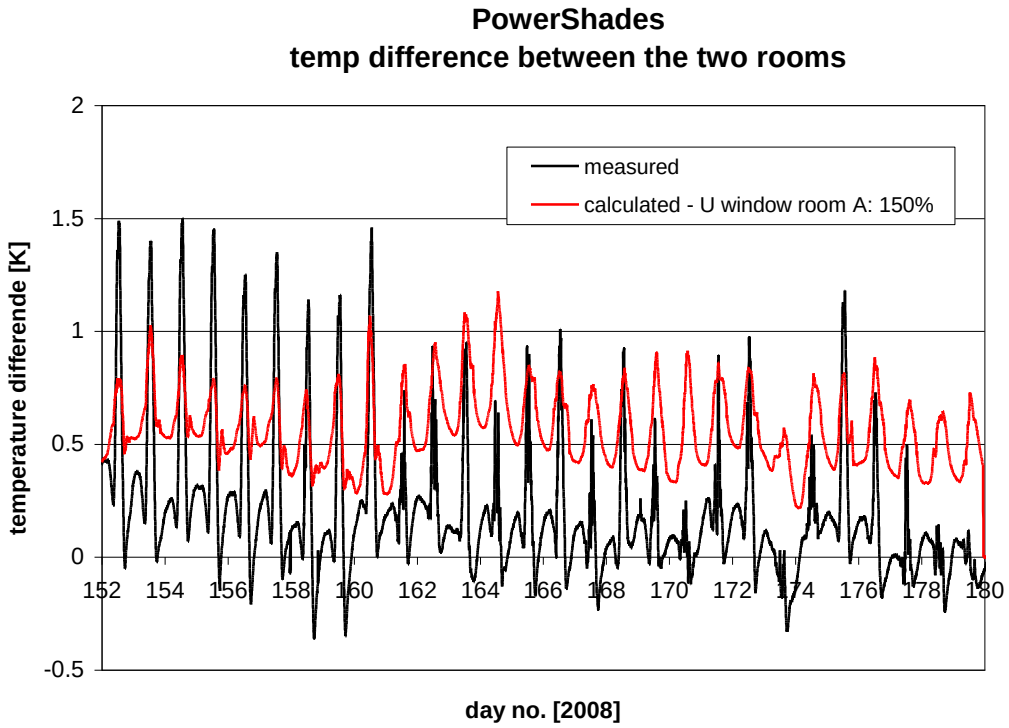

Figure 5.127. Measured and calculated temperature difference between room A and B – 1-28/6, 2008. Increase of the U-value of the PowerShade window with 50%.

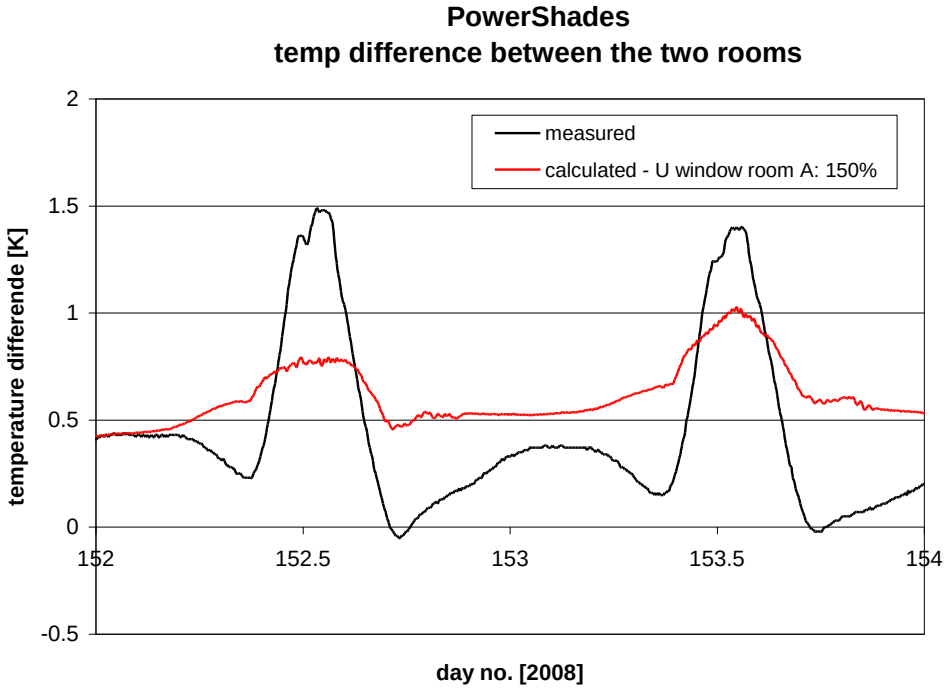

Figure 5.128. Measured and calculated temperature difference between room A and B – 1-2/6, 2008. Increase of the U-value of the PowerShade window with 50%.

5.2.3.7 Reduction of the U-value of the insulation in the internal walls and the ceiling with 50%

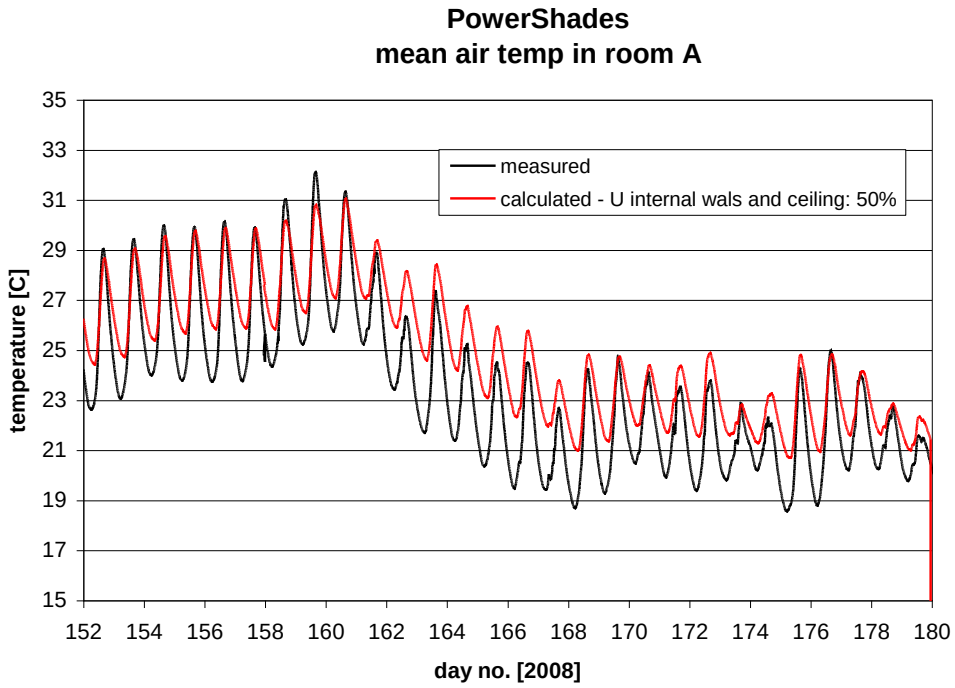

Figure 5.129. Measured and calculated mean air temperature in room A – 1-28/6, 2008. Reduction of the U-value of the insulation in the internal walls and the ceiling window with 50%.

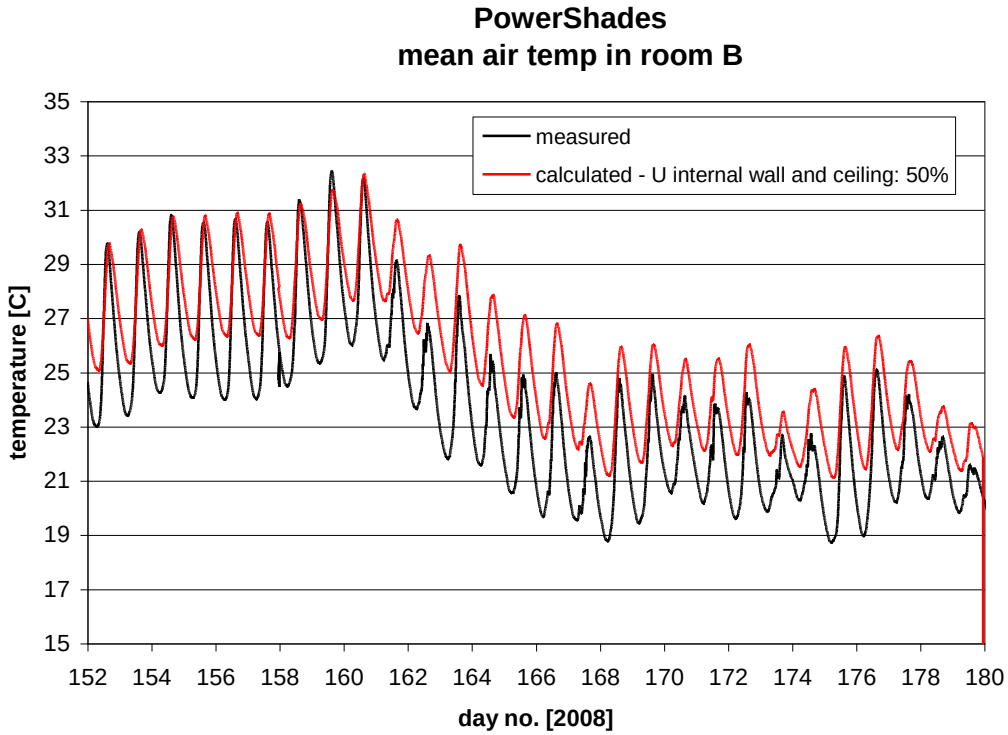

Figure 5.130. Measured and calculated mean air temperature in room A – 1-28/6, 2008. Reduction of the U-value of the insulation in the internal walls and the ceiling window with 50%.

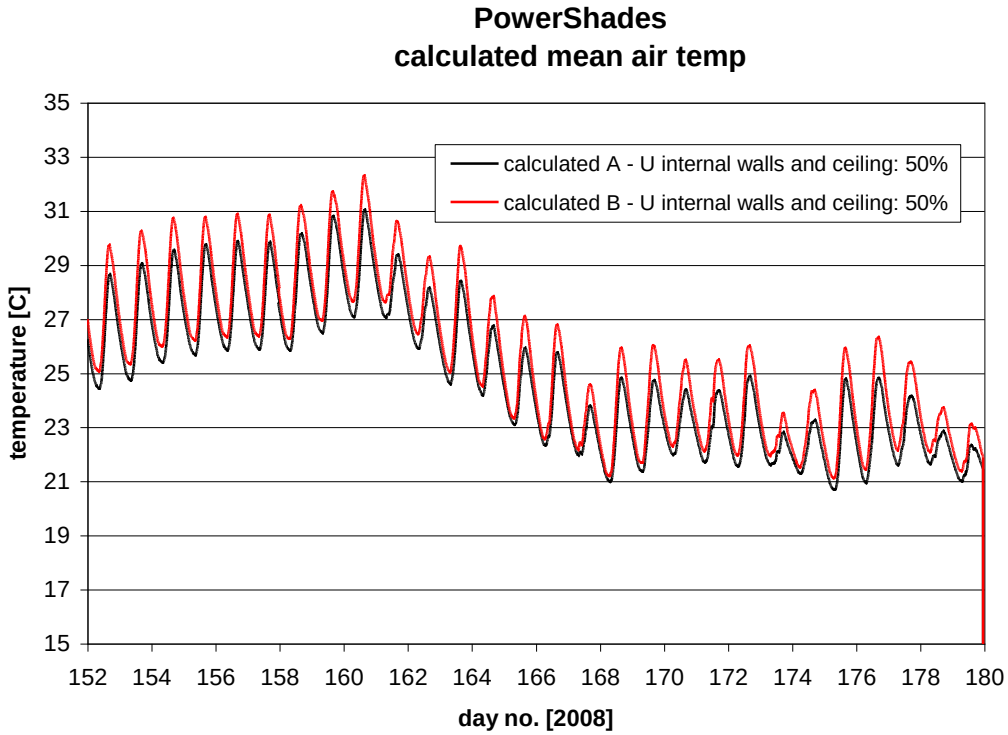

Figure 5.131. Calculated mean air temperature in room A and B – 1-28/6, 2008. Reduction of the U-value of the insulation in the internal walls and the ceiling window with 50%.

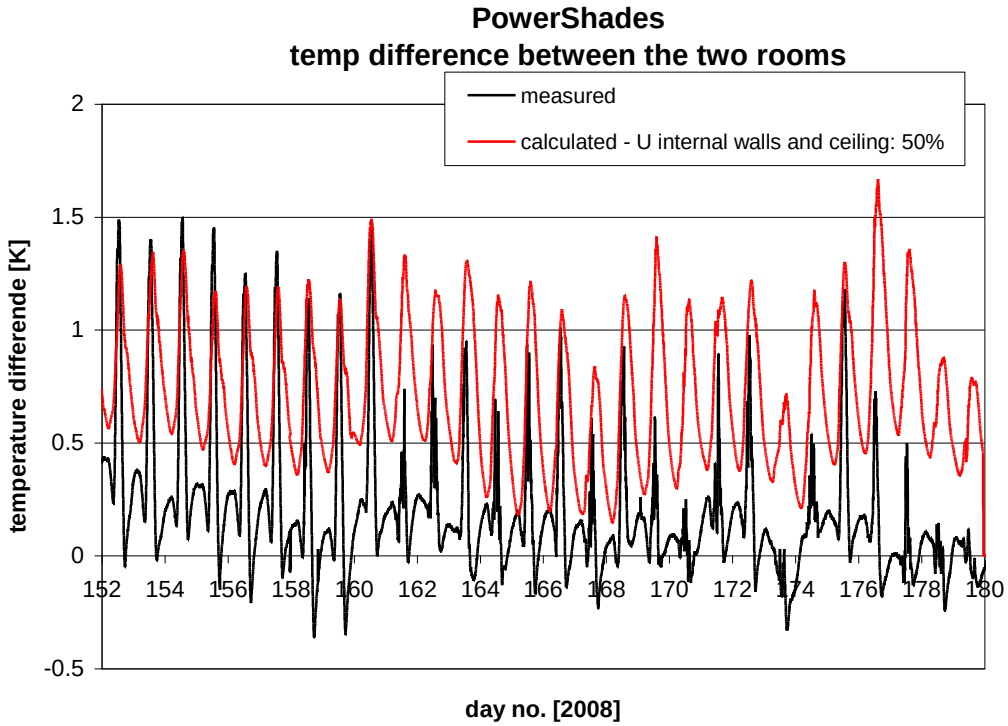

Figure 5.132. Measured and calculated temperature difference between room A and B – 1-28/6, 2008. Reduction of the U-value of the insulation in the internal walls and the ceiling window with 50%.

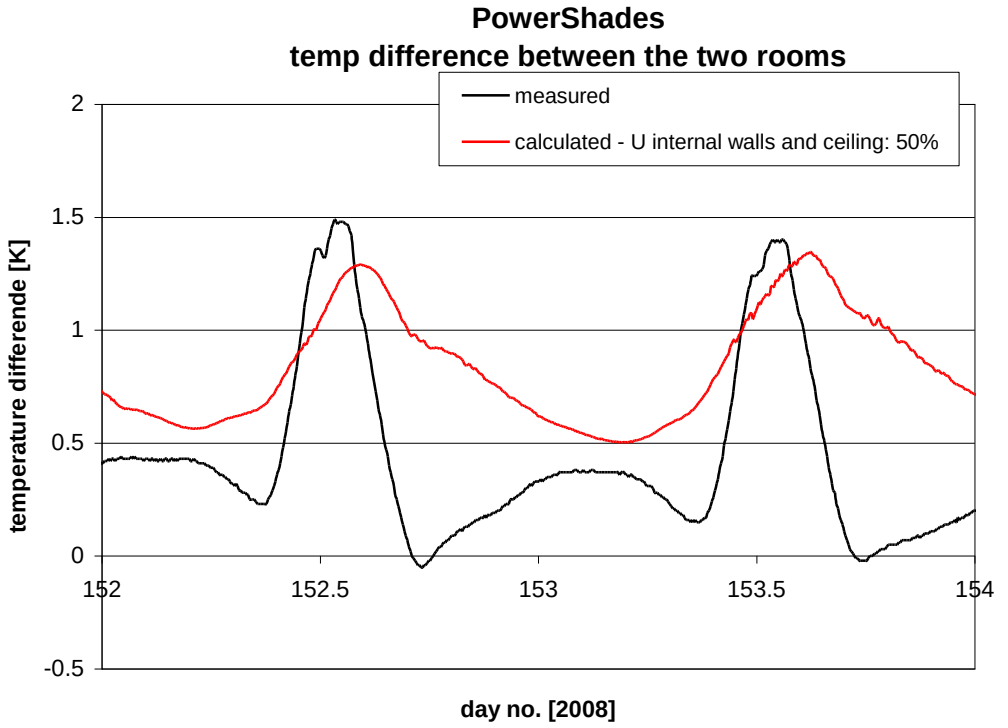

Figure 5.133. Measured and calculated temperature difference between room A and B – 1-2/6, 2008. Reduction of the U-value of the insulation in the internal walls and the ceiling window with 50%.

5.2.3.8 Increase of the U-value of the insulation in the internal walls and the ceiling with 50%

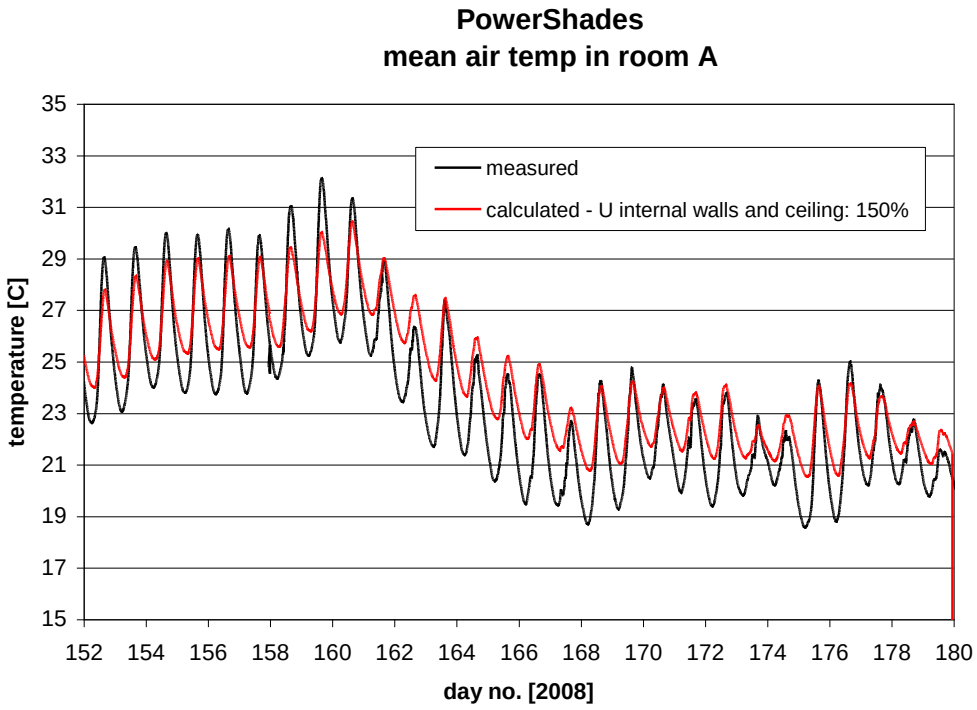

Figure 5.134. Measured and calculated mean air temperature in room A – 1-28/6, 2008. Increase of the U-value of the insulation in the internal walls and the ceiling window with 50%.

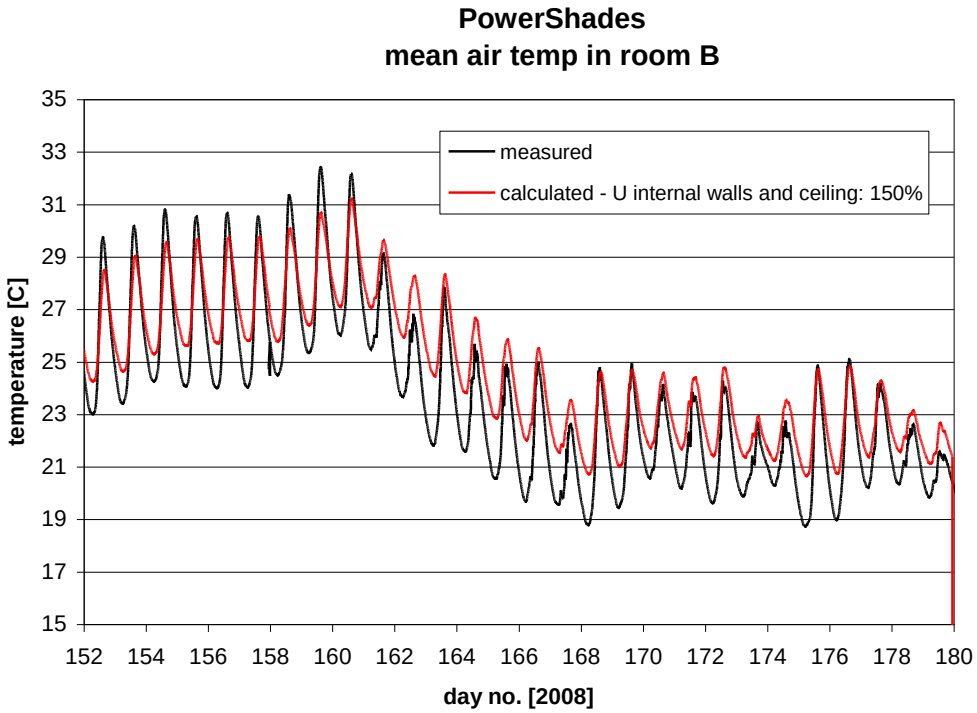

Figure 5.135. Measured and calculated mean air temperature in room A – 1-28/6, 2008. Increase of the U-value of the insulation in the internal walls and the ceiling window with 50%.

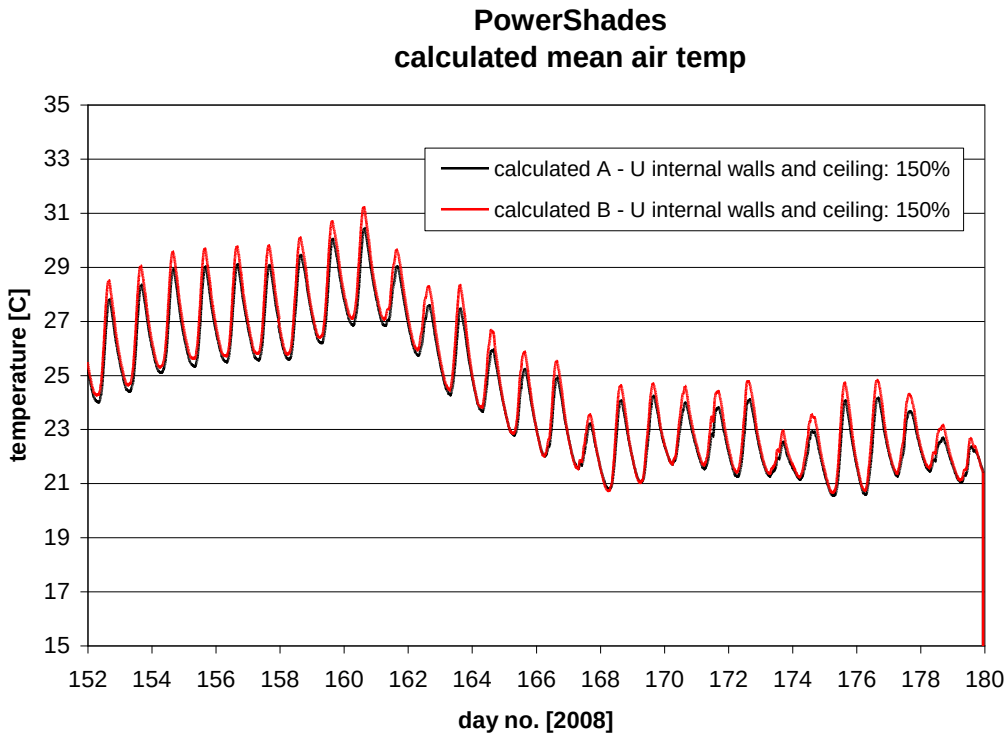

Figure 5.136. Calculated mean air temperature in room A and B – 1-28/6, 2008. Increase of the U-value of the insulation in the internal walls and the ceiling window with 50%.

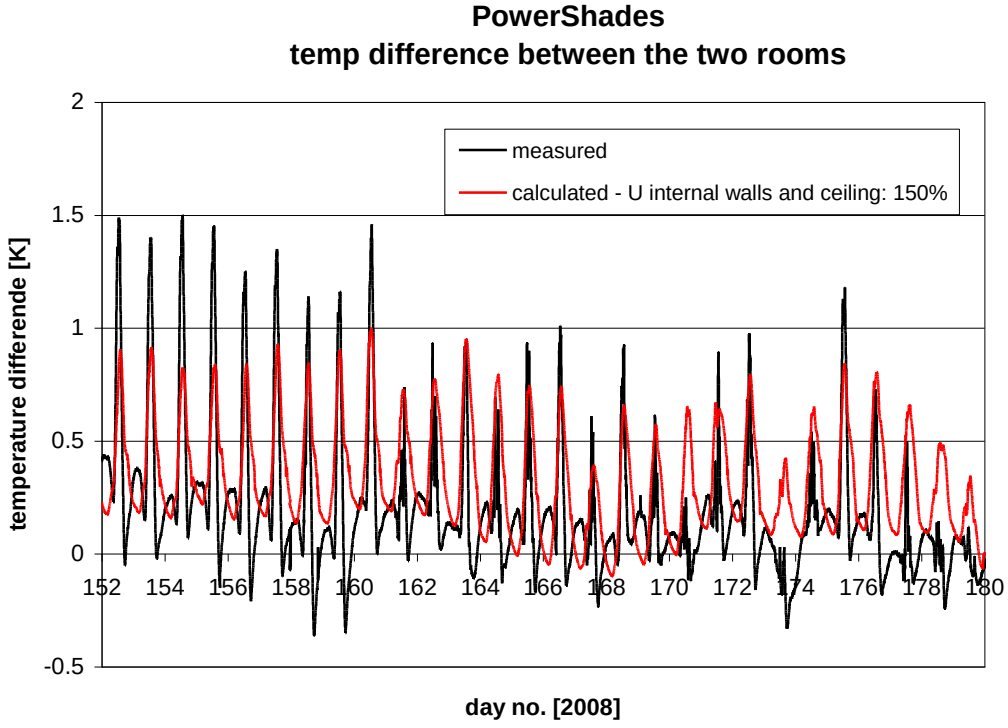

Figure 5.137. Measured and calculated temperature difference between room A and B – 1-28/6, 2008. Increase of the U-value of the insulation in the internal walls and the ceiling window with 50%.

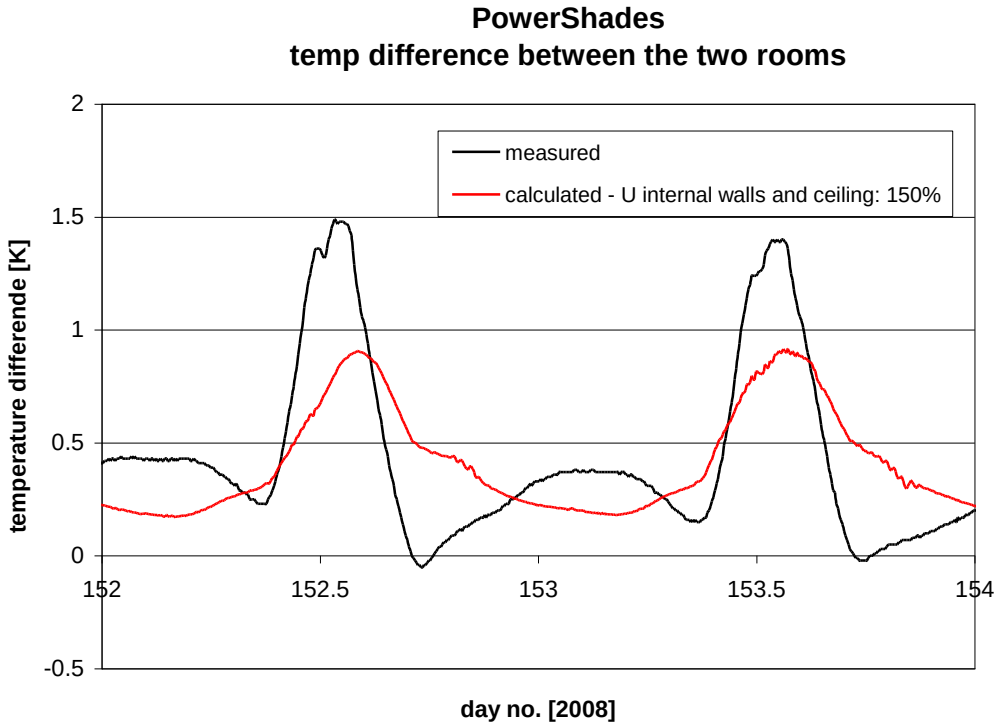

Figure 5.138. Measured and calculated temperature difference between room A and B – 1-2/6, 2008. Increase of the U-value of the insulation in the internal walls and the ceiling window with 50%.

5.2.3.9. Conclusions

In the previous graphs it is seen that the dynamics of the absolute mean air temperatures is rather well represented by the model, but the amplitude of the temperature swing is smaller leading to lower day time peaks during solar radiation and higher calculated temperatures during the night and periods without much solar radiation. As this goes for both rooms this suggests that the reason for the discrepancies is due to the input data to the rooms themselves. Not due to the optical properties of the windows as the measured solar radiation is in good agreement with the calculated solar radiation when using the new model of the Velfac window and the 121107-2 model for the PowerShades window.

A better agreement is often seen when comparing the measured and calculated temperature difference between the two rooms instead of the absolute air temperatures. This was anticipated because side by side comparison reduces the uncertainty of the non important parameters. The agreement could, however, be better.

Parameter variations have, therefore, been carried out for several of the main parameters of the two test rooms. Some changes lead to a better agreement concerning absolute temperatures but worse concerning temperature differences. And typically: if better agreement was obtained during the first part of the period worse agreement was obtained during the last part of the period and visa versa. This suggests that it is necessary to change several parameters simultaneously and most properly introduce new parameters in order to obtain reasonable agreement all over the chosen period and for all three periods. This is a non trivial task which

could take rather long time to carry out. There has unfortunately not been time for this in the present project. However, the calibration of the thermal model of the test rooms will be continued in the succeeding project.

Although a non perfect agreement was obtained when calibrating the model with respect to the mean air temperature confidence has been gained regarding the capability of the model to model the solar radiation coming into the rooms. The calibration exercise on the mean air temperatures of the rooms has revealed that the observed discrepancies most certainly are due to input problems to the model of the rooms and not due to the optical properties of the windows. It is, therefore, concluded that model 121107-2 for the PowerShades may be used to simulate the thermal performance of real buildings.

5.3. Conclusions from the calibration exercises

The performed calibration of the ESP-r model was performed in several steps:

- solar radiation hitting the facades
- the model of the Velfac window
- transmission of diffuse radiation through the PowerShades window
- transmission of direct radiation through the PowerShades window
- the mean air temperature in the two test rooms

and furthermore:

- the measured incoming radiation through Prototype 1 and the Velfac window has been compared
- the measured incoming radiation through Prototype 1 and 2 has been compared

The calculated solar radiation hitting the façade shows good agreement with the measured values when a reflection coefficient of 0.05 is applied. This is a low value but may be justified because the windows are facing a courtyard where several surfaces most of the time are shaded.

Good agreement between measured and calculated incoming solar radiation though the Velfac window were obtains when smaller modifications were introduced to the optical values from (Jensen, 2008a). The values at an incidence angle of 0° were left unchanged. These were given by the manufacture while the values at other incidence angles where calculated in (Jensen, 2008a). It is, therefore, assumed that the new model is more in agreement with reality that the model given in (Jensen, 2008a).

There is as yet no mathematical model for calculation of the transmittance of diffuse radiation through PowerShades. This value has to be obtained from measurements during overcast conditions. The validation exercise showed large uncertainty of this approach. And further - it will ease the development of models of different PowerShades if a mathematical model for determination of the transmittance of diffuse radiation through PowerShades is developed.

The calibration of the PowerShade model shows that the direct transmittance through PowerShades at large azimuths and large solar heights is overestimated. It is believed that this is due to a too imprecise calculation of the projected area of the holes in the PowerShades.

The handling of both diffuse and direct radiation through PowerShades will further be investigated and developed in the succeeding project.

The uncertainty in the model of PowerShades is clearly shown when comparing the transmitted solar radiation through Prototype 1 and 2. Although believed quite similar the measured results are very different. Why will be investigated in the succeeding project.

The modelling of the thermal performance of the two rooms behind the PowerShades and the Velfac window also need further attention in order to be able to explain the now observed discrepancies between measurements and calculations. However, it is believed that the observed discrepancies between the measured and calculated mean air temperatures are due to uncertainties in the description of the test rooms themselves and not in the description of the optical properties of the windows. So the derived model for the Velfac window and model 121107-2 for the PowerShades window is judged to be sufficiently accurate to be used in ESP-r models of real buildings.

The comparison between the Velfac window and the PowerShade windows showed that the PowerShades windows have the expected angular selective behaviour – i.e. that they screen off more direct solar radiation at high solar heights than at low solar heights. During wintertime when the solar heat most often is valuable Prorotype 1 has more or less the same solar transmittance as the Velfac window with a solar transmittance of 0.34, while Prorotype 1 only lets in half the amount of direct solar radiation during noon at summertime when the risk of overheating is at its max. PS4060 lets in only 14% of the amount of direct solar radiation as the Velfac window during noon at summertime but still in the order of 75% during the winter.

The difference in transmittance between Prototype 1 and PS4050 is also seen when comparing the difference in air temperature between room A and B during clear sky conditions. While a max difference of 3 K is obtained with PS4050 in room A this difference is 2 K with Prototype 1 in room A.

6. Performance in real buildings

The purpose of the calibration in the previous chapter was to investigate if the theoretical model of the PowerShades – ie the new module for ESP-r dealing with the angle selectivity of PowerShades correctly describes the real optical and thermo-physical performance of Power-Shades. After this has bee proven it is possible to apply the model in combination with real buildings in order to investigate the thermal behaviour of PowerShades in these buildings. The calibration procedure is not yet finalized, however, it seems that the model 121107-2 of the PowerShades are able to model the solar radiation entering through the window – maybe with a little to much solar radiation entering the room during the summer, which only means that the following results are conservative – i.e. that PowerShasde may actually decrease the cooling load more than shown in the following.

In order to investigate the thermal behaviour of PowerShades in a real building a building has been chosen which would have overheating problems if not main part of the solar radiation on the south façade is screened off. The building in the case study is the same building used in (Technological Institute, 2005) where PowerShades were investigated theoretically.

6.1. The Building of the case study

The building is designed by the world famous architects Henning Larsen. The building is the domicile of the bank Nordea. Figure 6.1 shows the north façade of the building. The figure shows the transparency of the building.

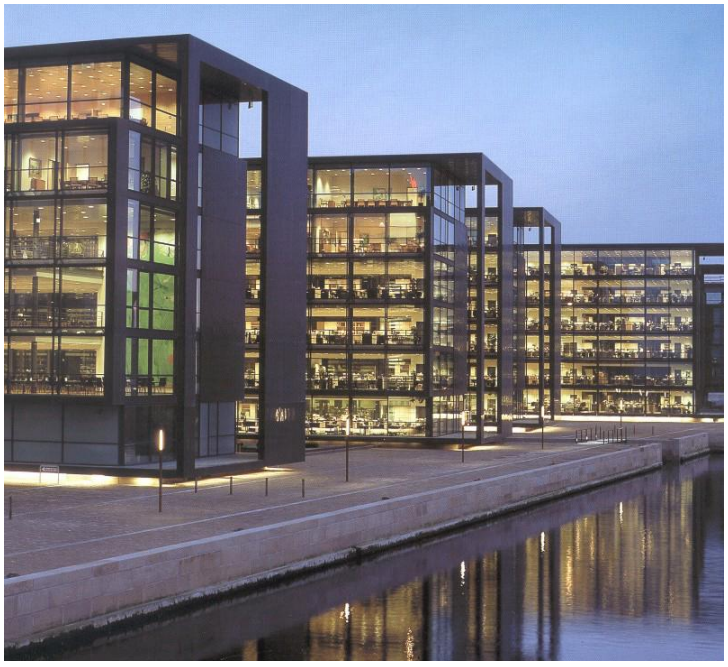

Figure 6.1. The north façades of the Nordea building.

Figure 6.2 shows one of the south facades of the building. 90% of the south and north facades is transparent so extensive solar screening is necessary in order to reduce the overheating problems and thereby reduce the cooling load and energy demand of the building. The glazing

of the facades themselves has solar screening coating reducing the g-value of the windows to 0,32 – ie rather similar to the original Velfac sun1/clear in the test rooms. The glazing in the Nordea building is Pilkington Suncool HP Clear. However, a g-value of 0,32 in the south facades is not enough to ensure a comfortable indoor climate in the building so external solar shading has been added as seen in figure 6.2.

Figure 6.2. One south façade of the Nordea building.

The external solar shading consists as shown in figure 6.3 and 6.4 of movable lamellas made of glass with silk screen printing. The lamellas follow the position of the sun (the solar height) over the day in such a way that all direct solar radiation hits the lamellas before hitting the windows.

Figure 6.3. The external solar shading consisting of glass lamellas with silk screen printing.

Due to the silk screen printing on glass there is still some outlook through the window even when the lamellas are closed as shown in figure 6.4.

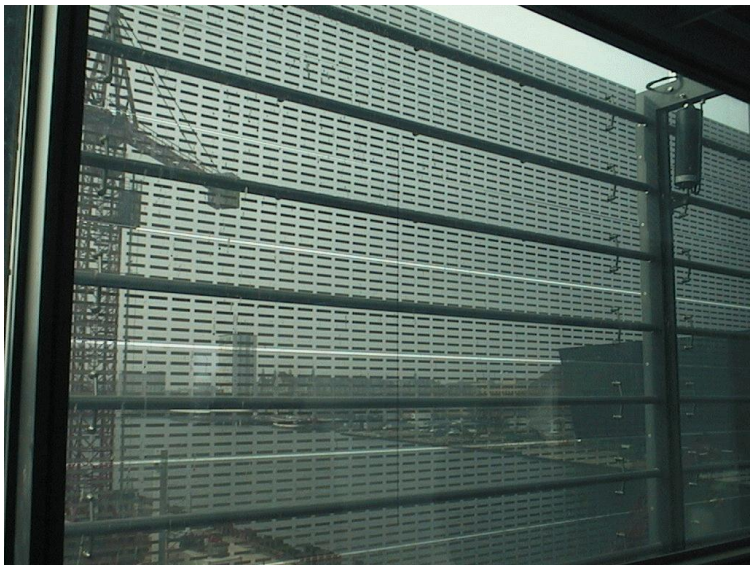

Figure 6.4. The external solar screening with closed lamellas.

The combination of solar screening glass and external solar shading gives an overall g-value of approx. 0.17 – which is very low.

An ESP-r model of one floor of the building was developed in (Technological Institute, 2005). This model will be applied in the present case study. The model is described in details in (Technological Institute, 2005) – please refer to this. Only some main characteristics will be outlined here.

The gross floor area of the chosen part of the building is 642 m². The floor contains one large office space, a staircase and toilets/depot as seen in figure 6.5. The windows of the south and north façade cover 90% of the facades. The vest façade is considered opaque while the east façade is the connection to the rest of the building complex.

Figure 6.5. Floor plan of the considered floor.

Different window configurations are as seen below applied for the south façade while the g-value for the north facing windows is 0.32. The U-value for all windows is 1.1 W/m²K. For more details on the constructions please refer to (Technological Institute, 2005).

Internal gains on weekdays for the period 9-17: persons: 10 W/m²
equipment: 24 W/m²
artificial lightning: 15 W/m²

Air change rate on weekdays for the period 9-17: 5 h^{-1}

Temperature set points: heating: 21°C
cooling: 24°C

Climate: the Danish Test Reference Year

6.3. Simulations

Simulations have been carried out with the above model with the following glazing/shading systems in the south façade:

- the present south façade with a g-value of 0.17
- the present Suncool window without external solar shading – g-value: 0.32
- the present windows and external solar shading have been replaced with windows with PowerShades like prototype 1. Both model 121107 and model 121107-2 has been applied
- the PowerShades PS5060 investigated theoretically in (Teknologisk Institute, 2005)

Three situations has been considered:
1) the air to the room is the ambient temperature
2) the air to the room is always 18°C in order to prevent draft
3) the air to the room is always 20°C in order to prevent draft.

The result of the simulations is presented in table 6.1.

Facade	Cooling demand					
	ambient air		18°C		20°C	
	kWh	%	kWh	%	kWh	%
Present, g-value: 0.17	2945	-	6106	-	8470	-
Suncool, g-value: 0.32	4731	61	9091	49	14439	70
PS5060	3095	5	6162	1	8846	4
Prototype 1, 121107	3923	33	7483	23	11414	35
Prototype 1, 121107-2	3400	15	6584	8	9753	15

Table 6.1. Absolute cooling demand and relative demand compared to the present situation. The column in % after the cooling demand in kWh states how much larger (in %) the cooling demand is compared to the present situation.

Table 6.1 shows that the cooling demand increases with increasing inlet temperature of the fresh air. This was expected as cooling of the fresh air in needed when the ambient temperature exceeds the wished inlet temperature. An inlet temperature of 18^{o}C is often used in order to eliminate the risk of draft.

For an inlet temperature of 18^{o}C Prototype 1 (121107-2) performs almost as well as the present rather complex solar screening system and much better that traditional sun screening glass. PowerShades with larger screening effect e.g. PS5060 will perform as well as the present solar screening system.

Table 6.1 further shows the importance of a correct model of the solar transmittance through the PowerShades. The cooling demand with 121107 is around 15 % higher than for 121107-2.

The simulations further shows that there is nearly no difference in the heating load between the four systems in table 6.1. The difference in electricity demand for artificial lightning should also be compared but is without the scope of this report.

The results given in table 6.1 apply only for that specific building under the modelled use of the building. The result will differ for different use of the building, different buildings and different weather conditions. It is thus necessary to perform calculations for each building where it is considered to utilize PowerShades.

Simulations is, however, a strong tool when investigating the impact of applying PowerShades on a specific building as it is much easier and cheaper to develop a model of a building than to carry out measurements in a building. Based on simulations it may further be possible to create curves or tables for quick evaluation of the performance of PowerShades in buildings.

One feature of the PowerShades which hasn't been dealt with in this report is the electricity production by the PowerShades. PowerShades are MicroShades coated with solar cells on the side facing the exterior. For a south facing façade it is estimated that Prototype 1 will have an annual electricity production of around 42 kWh/m². In the considered case the south facing window area is 110 m². This gives a total annual electricity production of 4.600 kWh. If the electricity is used in a refrigeration unit in the air condition system with an efficiency of 3 the electricity from the PowerShades has a cooling capacity of 13.800 kWh which is in the same order of magnitude as needed in table 1. PowerShades are thus not only able to reduce the cooling demand of a building but also to produce the necessary electricity for covering the remaining cooling demand.

7. Conclusion

Two test rooms for test of window systems - especially PowerShades (MicroShades) - have been erected at the Danish Technological Institut in Taastrup. The test rooms are heavily monitored making it possible to obtain high quality data sets for comparison of different windows systems with respect to both transmitted solar radiation, daylight and air temperatures in the rooms behind the window systems. The data sets may further be utilized for calibration of computer models of the window systems and the combination of rooms and window systems.

Windows with two different PowerShades has been tested in test room A, while the original Velfac window was maintained in room B. The window system in room B was, however, modified by mounting shading devices externally in front and internally behind it during some periods.

Measurements have been obtained for the whole of 2007-8 without much lack of data.

PowerShades lead to lower daylight factors than the original Velfac window with a light transmittance of 67%. PowerShades has a similar effect and magnitude as both the tested external and internal solar screening systems. But the look out is much better through the PowerShades than through traditional solar screening systems.

The two tested PowerShades let in 50% (Prototype 1) and 14% (PS4050) of the incoming solar radiation compared to the Velfac window at noon, high summer and clear sky conditions. The difference in peak air temperature in the test rooms during these periods is up to 2 and 3 K (respectively) lower in the test room with the PowerShades. During the winter the PowerShade window lets in the same amount or 25% less (respectively) than the Velfac window. It may, therefore, be concluded that the PowerShades have the desired angular selective effect – i.e. it screens off more direct solar radiation during the summer with often overheating problems than in the winter where the solar radiation often is valuable.

The function of PowerShades is similar to Venetian blinds, however, PowerShades are a microstructure of small holes embedded in a metal foil with a thickness of less than one mm. This means that PowerShades cannot be treated the same way as traditional windows as the transmission, absorption and reflection changes with the combinations of the two components of the incidence angle for the sun: horizontal and vertical incidence angle.

So a mathematical model describing PowerShades have been developed and have been embedded in the building simulation program ESP-r. The model of PowerShades is a matrix where the total direct transmission, the absorption in each layer of the window and the enhancement in incoming diffuse radiation due to the scattering of direct radiation in the PowerShades are listed for combinations of the horizontal and vertical incidence angle at steps of 5^{o}. It is at the moment not possible to calculate the transmittance for diffuse radiation – this value has to be determined based on measurements.

The model of PowerShades has been calibrated using data from the two test rooms. The calibration shows that there is a need for further work on the mathematically description of PowerShades: a method for determination of the transmittance of diffuse radiation based on calculations and a more precise method for determination of the transmittance of direct radiation which doesn't overestimate the transmittance at large azimuths and solar heights should be developed. This will be done in the succeeding project.

Based on the calibrations a new empiric model of Prototype 1 (model 121107-2) has been developed which is in better agreement with the measured solar radiation let in by Prototype 1. This model has been applied when calibrating the overall model of the test rooms.

Although very simple the test rooms are very complex from a modelling point of view. Although better defined than normal rooms most applied thermo physical properties have large uncertainty. It's, therefore, not a surprise that the measured and calculated mean air temperatures aren't identical. But the agreement is actually very good for a first attempt. Parametric studies were performed in order to obtain a better agreement between the measured and calculated mean air temperatures. There was not time for obtaining a good fit but the calibration exercises gained confidence in the 121107-2 model of Prototype 1 – i.e. the observed discrepancies between measured and calculated mean air temperatures are most certainly not due to the model of the PowerShade window but due to uncertainties in the description of the test room behind the windows. It was, therefore, decided that the model 121107-2 was applicable for use when calculating the performance of PowerShades in real building.

A model of a real building was developed in ESP-r. The building is a real building located in Copenhagen, the capital of Denmark. The building has without solar shading sever overheating problems. The real building has, therefore, south facing windows with a g-value of 0.32 (i.e. with solar screening film) and external movable lamellas which track the sun over the day. The overall g-value of the existing south facing system is 0.17, which is very low.

The simulations with the ESP-r model show that the cooling demand of the building with the existing windows but without the external solar shading will be increased with 50-70%. With PowerShades the cooling demand will dependent on the design of the PowerShades be increased with 1-15%. It is thus possible with PowerShades to obtain the same indoor climate as with the existing rather complex and expensive solar shading system. The look out is further believed to be improved. The PowerShades perform much better with regard to screening off unwanted solar radiation than traditional solar screening films. The simulations further show that it is very important to have the right model for the PowerShades.

Besides reducing the cooling demand PowerShades produce electricity – electricity which may be used in the cooling unit of an air condition system. Calculations for the considered case show that PowerShades may produce electricity in the same order of magnitude as needed in order to cover the remaining cooling demand.

The overall conclusion is that PowerShades may be a good choice in buildings with overheating problems – especially where the architect due to esthetical considerations don't want to apply external solar screening devices.

8. References

ESRU, 2001. Data Model Summary – ESP-r – Version 9 series. Energy Systems Research Unit, University of Strathclyde. December 2001.

Jensen et al, 1994. The PASSYS Project – Validation of Building Energy Simulation Programs – Part I and II. European Commission, Directorate-General XII for Science, Research and Development. February 1994. EUR 15115 EN.

Jensen, S.Ø., 2008a. Test rooms for test of PowerShades. Danish Technological Institute.

Jensen, S.Ø., 2008b. Energy and indoor climate conditions when having solar cells in transparent facades (in Danish). Danish Technological Institute.

Schultz, J.M., 2008. Measured transmittance for PhotoSolar PV-window at different incidence angles and rotation of the window (in Danish). Technological University of Denmark, Building Division.

Technological Institute, 2005. Transparent solar cells – the electricity producing solar shading of the future (in Danish). PEC Group, Technological Institute.